

University of Windsor

## Scholarship at UWindor

---

Electronic Theses and Dissertations

Theses, Dissertations, and Major Papers

---

1-1-1981

### The petrology and geochemistry of the Gamitagama Lake igneous complex, near Wawa, North Central Ontario.

Abdul G. Choudhry  
*University of Windsor*

Follow this and additional works at: <https://scholar.uwindsor.ca/etd>

---

#### Recommended Citation

Choudhry, Abdul G., "The petrology and geochemistry of the Gamitagama Lake igneous complex, near Wawa, North Central Ontario." (1981). *Electronic Theses and Dissertations*. 6756.  
<https://scholar.uwindsor.ca/etd/6756>

This online database contains the full-text of PhD dissertations and Masters' theses of University of Windsor students from 1954 forward. These documents are made available for personal study and research purposes only, in accordance with the Canadian Copyright Act and the Creative Commons license—CC BY-NC-ND (Attribution, Non-Commercial, No Derivative Works). Under this license, works must always be attributed to the copyright holder (original author), cannot be used for any commercial purposes, and may not be altered. Any other use would require the permission of the copyright holder. Students may inquire about withdrawing their dissertation and/or thesis from this database. For additional inquiries, please contact the repository administrator via email ([scholarship@uwindsor.ca](mailto:scholarship@uwindsor.ca)) or by telephone at 519-253-3000ext. 3208.

THE PETROLOGY AND GEOCHEMISTRY  
OF THE GAMITAGAMA LAKE IGNEOUS  
COMPLEX, NEAR WAWA, NORTH CENTRAL  
ONTARIO

by

ABDUL G. CHOUDHRY

A thesis submitted to the Faculty of the  
Graduate Studies of the University of  
Windsor in partial fulfillment of  
requirements for the degree of  
MASTER OF SCIENCE  
(GEOLOGY)  
1981

UMI Number: EC54739

## INFORMATION TO USERS

The quality of this reproduction is dependent upon the quality of the copy submitted. Broken or indistinct print, colored or poor quality illustrations and photographs, print bleed-through, substandard margins, and improper alignment can adversely affect reproduction.

In the unlikely event that the author did not send a complete manuscript and there are missing pages, these will be noted. Also, if unauthorized copyright material had to be removed, a note will indicate the deletion.

**UMI<sup>®</sup>**

---

UMI Microform EC54739  
Copyright 2010 by ProQuest LLC  
All rights reserved. This microform edition is protected against  
unauthorized copying under Title 17, United States Code.

---

ProQuest LLC  
789 East Eisenhower Parkway  
P.O. Box 1346  
Ann Arbor, MI 48106-1346

© ABDUL GHAFOOR CHOUDHRY 1981  
ALL RIGHTS RESERVED

II

**758504**

## ABSTRACT

The Gamitagama Lake Complex is a plug-shaped elliptical body of about 7x10 km in dimension, situated 40 km south of Wawa in Northern Ontario. Emplacement of the complex deformed and cross-folded the metavolcanic-metasedimentary rocks of the Shebandowan Greenstone Belt of the Superior Province. A contact metamorphic aureole of hornblende-hornfels facies occurs in the surrounding country rock and most of the xenoliths in the pluton are of pyroxene-hornfels facies metamorphism.

Four concentric intrusive phases can be recognized by differences in mode, degree of differentiation, and pattern of emplacement. They are: an olivine-bearing inner gabbroic series occurring at the core; a middle, less basic, outer gabbroic rock series; and an outer group of dioritic rocks composed of hornblende gabbro, diorite, quartz diorite, quartz monzodiorite and tonalite. The additional phases consist of leucocratic granodiorite and granite within the larger dioritic zone, and a discordant quartz-monzonite vertical dike cutting the dioritic and granitic rocks. In the olivine-bearing inner gabbroic series olivine gabbro and gabbro dominate, and troctolite, norite and andesine anorthosite are subordinate. In the outer gabbroic rocks gabbro and amphibole gabbro occur with lesser amounts of norite and pyroxene diorite. Late, minor fine-grained gabbroic rocks with porphyritic amphibole and phlogopite intrude the inner and outer gabbroic series.

Field relations, petrographic and geochemical studies suggest that mineral fractionation occurred near the surface and at depth in the magma source. In the inner gabbroic series olivine + plagioclase + titaniferous magnetite + clinopyroxene + orthopyroxene, and in the outer gabbroic series plagioclase + orthopyroxene + clinopyroxene + titaniferous magnetite fractionated out of the respective parent magmas at pressures less than 2 Kb to give calc-alkalic differentiation trends within each series.

The most basic phases of each discrete intrusive event are successively less basic in composition to indicate that fractionation was occurring in the source magma chamber at deeper levels. The late fine grained gabbroic intrusions in the complex have amphibole and phlogopite phenocrysts, which points to the original magma in the source chamber also following a calc-alkaline trend by fractionating amphibole and phlogopite at more than 10 Kb pressure (=35 km depth). The magma chamber differentiated from basic through intermediate to acidic in composition. Quartz monzonite owes its origin to a separate magma.

The metavolcanic-metasedimentary sequence in the surrounding areas of the complex represent an eugeosyncline-island arc-like series. These rocks in turn, are surrounded by a pre-existing granitic-metamorphic crust so that it is possible a 35 km thick crust existed at the time of Gamitagama Lake intrusion, and the tectonic regime in the Late Archean (2662 Ma) was not significantly different than that of the present day.

## ACKNOWLEDGMENTS

I am indebted to many people for their help and interest in this research project. I wish to acknowledge Dr. A. Turek for suggesting the problem. In particular, I would like to express my sincerest thanks to Professor T.E. Smith, who as thesis advisor, provided financial help, instruction in field mapping and stimulating discussions throughout this research work. I am particularly indebted to Dr. C.H. Huaug for his patient instruction in the techniques of X-Ray fluorescence analysis. Furthermore, I would like to thank Mr. I. Seddon of Ministry of Natural Resources, Wawa, who cordially granted me permission to collect samples from the Provincial Park. Last but not least, I would like to thank my wife, Azra, without whose moral support and patience, this work could not have been completed.

## TABLE OF CONTENTS

	Page
ABSTRACT	iv
ACKNOWLEDGEMENTS	vi
CHAPTER 1	
INTRODUCTION	1
1.1 PHYSIOGRAPHY	3
1.2 PREVIOUS WORK	5
1.3 PRESENT STUDY	9
CHAPTER 2	
GEOLOGICAL SETTING	11
CHAPTER 3	
FIELD RELATION	16
3.1 THE INNER GABBROIC ROCKS	20
3.1.1 Olivine Gabbro	21
3.1.2 Gabbro	23
3.1.3 Anorthosite	26
3.2 THE OUTER GABBROIC ROCKS	28
3.2.1 Gabbro	30
3.2.2 Amphibole Gabbro/Pyroxene Diorite	33
3.3 THE DIORITIC ROCKS	35
3.3.1 Diorite	36
3.3.2 Quartz Diorite	38
3.3.3 Quartz Monzodiorite	40
3.3.4 Tonalite	41
3.3.5 Other Satellitic Intrusions	44
3.4 THE GRANITIC ROCKS	44
3.4.1 Granodiorite	47
3.4.2 Granite	47
3.5 THE QUARTZ MONZONITE	48
3.6 CONCLUSION	49



## CHAPTER 4

PETROGRAPHY	52
4.1 INNER GABBROIC SERIES	55
4.1.1 Olivine Gabbro	55
4.1.1.1 Troctolite	55
4.1.1.2 Olivine gabbronorite	60
4.1.1.3 Amphibole olivine gabbronorite	66
4.1.2 Gabbro	69
4.1.2.1 Gabbronorite	69
4.1.2.2 Norite	75
4.1.3 Anorthosite	78
4.1.3.1 Andesine anorthosite	78
4.1.4 Paragenesis	84
4.2 OUTER GABBROIC SERIES	91
4.2.1 Gabbro	93
4.2.1.1 Norite	93
4.2.1.2 Gabbronorite	100
4.2.2 Amphibole Gabbro/Pyroxene Diorite	102
4.2.2.1 Amphibole gabbronorite	102
4.2.2.2 Pyroxene diorite	106
4.2.3 Paragenesis	112
4.3 DIORITIC ROCKS	118
4.3.1 Diorite	118
4.3.1.1 Hornblende gabbro	121
4.3.1.2 Diorite	124
4.3.2 Quartz Diorite	128
4.3.3 Quartz monzodiorite	130
4.3.4 Tonalite	133
4.3.5 Paragenesis	137
4.4 GRANITIC ROCKS	139
4.4.1 Granodiorite	139

4.4.2 Granite	143
4.4.3 Paragenesis	146
4.5 QUARTZ MONZONITE	147
4.5.1 Paragenesis	149
CHAPTER 5	
GEOCHEMISTRY	151
5.1 INNER GABBROIC SERIES	163
5.1.1 Major Element Variations	163
5.1.2 Trace Element Variations	168
5.2 OUTER GABBROIC SERIES	170
5.2.1 Major Element Variations	170
5.2.2 Trace Element Variations	171
5.3 DIORITIC ROCKS	172
5.4 GRANITIC ROCKS	174
5.5 QUARTZ MONZONITE	174
5.6 GENERAL CHEMICAL VARIATIONS IN VARIOUS ROCK GROUPS	179
5.7 OVERALL CHEMICAL VARIATIONS IN THE COMPLEX	190
CHAPTER 6	
PETROGENESIS	192
6.1 MINERALOGICAL FEATURES	193
6.1.1 Significance of Orthopyroxene	193
6.1.2 Abundance of Plagioclase	194
6.1.3 Amphibole and Phlogopite	195
6.1.4 Magnetite and Oxygen Fugacity	196

6.2 CHEMICAL FEATURES	197
6.2.1 Major Element	197
6.2.2 Trace Element	201
6.3 DISCUSSION	205
6.3.1 Proposed Parent Magma	208
6.3.2 Crystallization of the Inner Gabbroic Series	209
6.3.3 Crystallization of the Outer Gabbroic Series	210
6.3.4 Crystallization of the Dioritic Rocks	214
6.3.5 Crystallization of the Granitic Rocks	214
6.4 GENESIS OF PLUTONIC SERIES	215
6.5 EMPLACEMENT AND STRUCTURE OF THE COMPLEX	217
6.6 TECTONIC SETTING	219
CHAPTER 7	
CONCLUSION	221
REFERENCES CITED	223
APPENDIX A	236
APPENDIX B	238
APPENDIX C	240

## LIST OF FIGURES

### Figure

1.1	Map showing the location of the Gamitagama Lake Complex.	2
1.2	Physiographic map of the Gamitagama Lake Complex.	4
1.3	Areomagnetic map of the Gamitagama Lake Complex.	7
2.1	Regional geology of the area.	
3.1	Map showing location of different rock groups in the Gamitagama Lake Complex.	17
3.2	Geological map of the Gamitagama Lake Complex.	
4.1	Modal mineral proportions in rocks of the Inner Gabbroic Series.	56
4.2	Crystallization models for the gabbroic rocks.	87
4.3	Modal mineral proportions in rock of the Outer Gabbroic Series.	94
4.4	Modal mineral proportions in the dioritic Rocks.	119
4.5	Modal mineral proportions in the Granitic rocks and Quartz Monzonite Dike.	141
5.1	Plots of various oxides vs differentiation	

	index.	176
5.2	Plots of various oxides and indices vs solidification index.	180
5.3	Plots of Co, Cr, V, Ni and Ti vs mafic index.	184
5.4	Plot of sr vs (ppm) vs wt. % CaO.	186
5.5	Plot of Rb, Ba, Sr, Y, Nb, and Zr vs Felsic index.	188
6.1	Plot of SiO <sub>2</sub> vs alkalies.	199
6.2	Plots of SiO <sub>2</sub> and FeO vs FeO/MgO.	200
6.3	AFM diagram showing chemical trends of plutonic rocks from the gamitagama Lake complex and calc-alkaline suites of Guadalupe and Idaho.	202
6.4	Plot of felsic index vs mafic index.	202
6.5	Plot of CaO vs Na <sub>2</sub> O vs K <sub>2</sub> O showing increase in soda/potash ratio with each rock group.	203
6.6	Plot of Ba/Sr vs Sr(ppm).	203
6.7	Plot of K/Rb vs K(ppm).	206
6.8	Plots of Y, Rb, and Sr vs Ba.	207
6.9A	Liquidus diagram for a Medicine Lake Highlands high alumina basalt.	211
6.9B	Liquidus diagram for a Mt. Hood andesite.	211
6.10	Liquidus diagram for a Pariutin Lava.	212
6.11	The intrusive series of the Gamitagama Lake Complex and the proposed liquid line of descent	

	assuming a high alumina basalt as a parental magma in the magma chamber.	216
6.12	Schematic diagram illustrating the structure of the Gamitagama Lake Complex.	218

## LIST OF TABLES

Table	Page	
2.1	Table of formations	12
4.1	Classification of rock types encountered in the Gamitagama Lake Complex.	53
4.2	Modal mineral composition in the rock of the Inner Gabbroic Series.	54
4.3	Summary of petrographic observations in the Inner Gabbroic Series.	85
4.4	Modal mineral compositions in the rocks of the Outer Gabbroic Series.	92
4.5	Summary of petrographic observations in the Outer Gabbroic Series.	114
4.6	Modal mineral compositions of representative samples of the Dioritic Rock.	120
4.7	Modal mineral compositions of representative samples of the Granitic Rocks and Quartz Monzonite Dike.	140
5.1	Chemical composition and molecular weight percent norms of various rock groups in the Gamitagama Lake complex.	152
5.2	The calculated indices and ratios for the	

	analyzed rock samples.	161
5.3	Average chemical composition of various rock types encountered in the Gamitagama Lake Complex.	164
Table A-1	Modal Classification of non-feldspathoidal plutonic rock used by Ayres 1969.	237
Table C-1	Operating conditions for determination of major elements by X-ray fluorescence.	241
Table C-2	Operating conditions for determination of trace elements by X-ray fluorescence.	243



## LIST OF PHOTOGRAPHS

	Page
Photo 3.1. Gabbronorite of the Inner Gabbroic Series, about 300 m east of anorthosite body, containing bent, twisted and broken layers of pyroxene rich rock.	25
Photo 3.2. Spotted gabbronorite, about 200 m northwest of Picea Lake. The pyroxene is concentrated in spherical aggregates as much as 1 cm in diameter and 1-3 cm apart.	25
Photo 3.3. Irregular anorthositic dikes, about 1-15 cm in width, in the gabbronorite.	27
Photo 3.4. Anorthositic dikes brecciating the host gabbronorite.	27
Photo 3.5. Gabbronorite of the Outer Gabbroic Series showing weak asymmetric banding on the south side of a small lake near southern boundary of the complex.	29
Photo 3.6. Gabbronorite, south of Poikkimaki Lake, showing minor asymmetric banding in the upper half of the photo and band containing irregular, oriented inclusions of segregated pyroxene in the lower half.	29
Photo 3.7. The irregular inclusions of segregated pyroxene in the gabbronorite of the Outer Gabbroic Series. The inclusions, maximum 2 cm long, are randomly distributed in the rock. Location same as of photo 3.6	31
Photo 3.8. The irregular inclusion of the Inner Gabbroic Series in the gabbronorite of the Outer Gabbroic Series. The inclusion is comparatively coarser-grained and roughly parallel to the foliation of the host rock.	31
Photo 3.9. Road-cut in the northern satellitic intrusion on the Highway 17 showing intrusion breccia. Fine-grained equivalent of diorite is intruded by the quartz monzodiorite which in turn is brecciated by	

a number of 2-50 cm wide dikes of the granodiorite, granite, and pegmatite respectively.	37
Photo 3.10. Same intrusion breccia about 8 m north of photo 3.9.	37
Photo 3.11. The quartz diorite with abundant metavolcanic inclusions near the contact with metavolcanics on the gravel road leading to microwave tower from the Highway 17. The inclusions are oriented with their longer dimension parallel to the contact and dip subvertically away from the contact.	39
Photo 3.12. Tonalite of the Southern Satellitic Intrusion on the Highway 17 containing angular inclusions of metavolcanics and quartz diorite.	43
Photo 3.13. Tonalite containing rounded inclusions of a darker tonalite. Inclusions and the host rock are similar in all respects except for the colour index.	43
Photo 3.14. Quartz diorite, on gravel road near the contact with the granitic rocks about 100 m NW of microwave tower, showing intensive shearing and alteration.	45
Photo 3.15. The intensive shearing above (photo 3.14) changes to fine shear network away from the contact.	45
Photo 4.1a: Troctolite showing olivine partially rimed by clinopyroxene, orthopyroxene, and amphibole (dark).	58
Photo 4.1b. Same as above, crossed nicols.	58
Photo 4.2. Olivine gabbroite showing olivine with inclusions of plagioclase (white) and magnetite. Note the early separation of abundant titaniferous magnetite.	62

Photo 4.3. Olivine gabbronorite showing olivine with corona of orthopyroxene + amphibole + (amphibole + plagioclase) + plagioclase. Olivine inside the corona is partially replaced by orthopyroxene and trellis-like magnetite.	62
Photo 4.4. Olivine gabbronorite showing clinopyroxene with plagioclase, olivine, and titaniferrous magnetite inclusions. Note the multiple twinning in the clinopyroxene.	64
Photo 4.5. Olivine gabbronorite showing orthopyroxene with olivine, clinopyroxene (near left bottom), and plagioclase inclusions.	64
Photo 4.6a. Gabbronorite showing clinopyroxene which optically encloses plagioclase crystals.	72
Photo 4.6b. Clinopyroxene showing exsolved plates of orthopyroxene parallel to (100).	72
Photo 4.7. Gabbronorite showing clinopyroxene with acicular inclusions of oxide or mafic silicates oriented parallel to (100) and (001) directions.	74
Photo 4.8. Norite showing orthopyroxene with very thin lamellae of clinopyroxene exsolved parallel to (100).	74
Photo 4.9a. Andesine anorthosite showing oriented tabular crystals of plagioclase.	79
Photo 4.9b. Andesine anorthosite showing orthogonal mosaic texture of plagioclase.	79

Photo 4.10a. Core sample W155 showing euhedral to subhedral olivine crystals enclosed in plagioclase. Thin rims of orthopyroxene separate olivine crystals from plagioclase.	82
Photo 4.10b. Same as above, crossed nicols.	82
Photo 4.11. Fine-grained equivalent of norite showing central core of 100% sulphides and peripheral area where sulphides enclose plagioclase and orthopyroxene crystals.	97
Photo 4.12. Fine-grained equivalent of norite showing plagioclase xenocrysts with irregular recrystallized areas which are free from twinning, have similar optical orientation and are joined in a network.	97
Photo 4.13. Fine-grained equivalent of norite showing xenocrysts of plagioclase with sulphides inclusions.	99
Photo 4.14. Fine-grained equivalent of norite showing sulphide inclusions in orthopyroxene xenocrysts. Orthopyroxene crystals in bottom left corner represent the actual grain size of the rock.	99
Photo 4.15. Amphibole gabbronorite showing clinopyroxene with reaction rims of amphibole along margins and minute zones and patches along cleavage, parting, and fractures.	105
Photo 4.16. Amphibole gabbronorite showing amphibole which poikilitically encloses plagioclase, clinopyroxene and titaniferrous magnetite.	105

Photo 4.17a. Fine-grained pyroxene diorite showing subhedral phenocryst of amphibole.	109
Photo 4.18. Subhedral phenocryst of phlogopite in pyroxene diorite. Phlogopite often shows recrystallization to plagioclase, magnetite, orthopyroxene, and clinopyroxene.	109
Photo 4.19a. Hornblende gabbro showing clinopyroxene rimmed by amphibole. Clinopyroxene is partially replaced by uranalite.	122
Photo 4.19b. Same as above, crossed nicols.	122
Photo 4.20. Fine-grained equivalent of diorite showing subhedral to anhedral plagioclase, hornblende, quartz, aggregates of biotite, and magnetite.	126
Photo 4.21. Quartz monzodiorite showing flaky tremolite-actinolite amphibole which now represents the original clinopyroxene.	126
Photo 4.22. Coarse-grained tonalite showing biotite flakes with random orientation and inclusions of prismatic apatite and zircon.	135
Photo 4.23. Fine-grained tonalite showing subhedral to anhedral plagioclase, hornblende, quartz, aggregates of biotite, and magnetite.	135
Photo 4.24. Granite showing myrmekitic intergrowth at the boundaries of quartz and plagioclase which extends inside the microcline crystals.	144
Photo 4.25. Quartz monzonite showing hornblende with clinopyroxene core and inclusions of magnetite.	144

## CHAPTER 1

## INTRODUCTION

The Gamitagama Lake Complex is located in the Townships of Asselin, Tiernan, Stone and Barager, in the district of Algoma, about 40 km south of Wawa, Northern Ontario (Figure 1.1). It is elliptical in plan and underlies about 71 km<sup>2</sup> surface area in the Lake Superior Provincial Park. The access to the complex is by Highway 17 which passes through satellitic intrusions on the west side of the main intrusion. The old roads from Highway 17 leading inside the complex were built for logging haulage and mineral exploration purposes (Figure 1.2). In addition, there are roads leading from the Highway to Mijinemungshing Lake in the north and Old Woman Lake in the south of the complex. The northeastern and southeastern boundaries of the complex can be reached by boat through these lakes. Streams in the area are very small with many rapids and canoe travel is difficult.

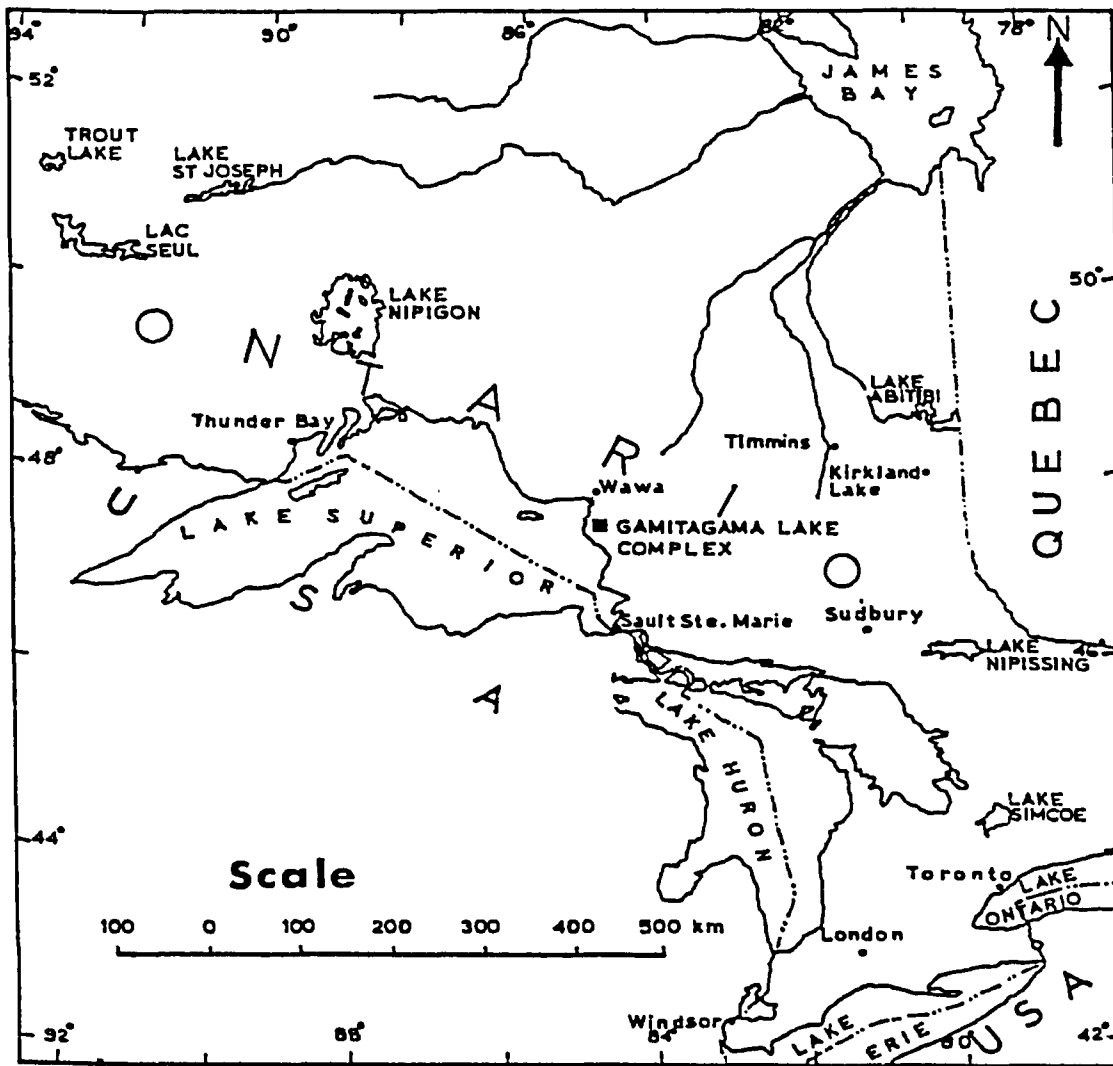


Figure 1.1. Map showing the location of the Gamitagama Lake Complex.

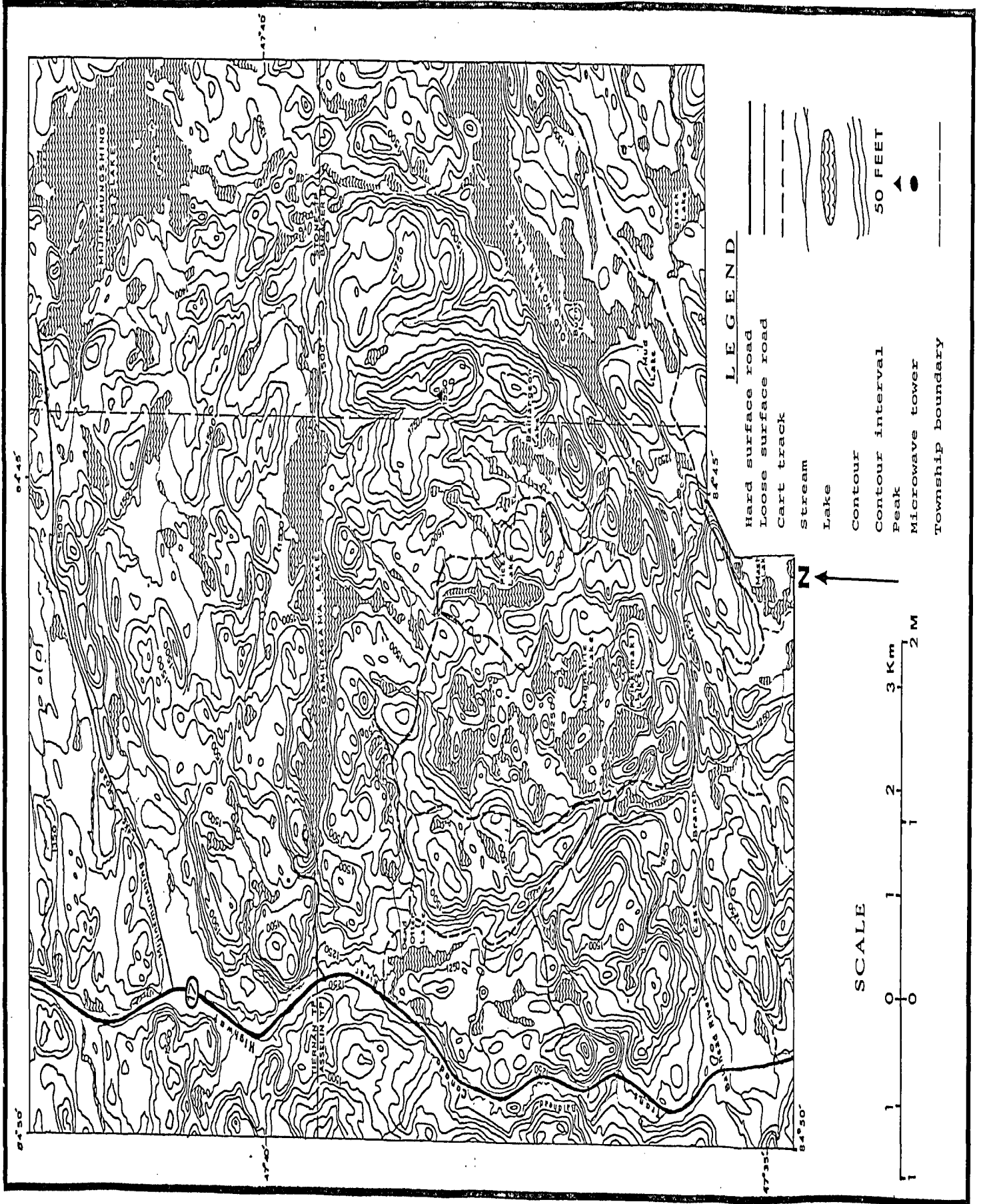
## 1.1 PHYSIOGRAPHY

The present landscape of the area is a result of stream erosion and superimposed glacial effects. The preglacial landscape was affected by glacial erosion which enlarged the already existing valleys. The glacial deposits of sand and gravel in the valleys are in sharp contrast to the thin soil covering outcrops at higher elevations. Eskers are present in the area, particularly north of Gamitagama Lake.

This area is one of the most rugged in Ontario (Figure 1.2). The highest elevation is approximately 595 m, occurring between Gamitagama and Old Woman Lakes, with maximum relief of 250 m. Crests of many hills have an elevation of 525 m and most probably represent erosion surfaces of the last ice age. Most of the bedrock topography is controlled by post-Pre-cambrian Faults. The area is characterized by forested hills and bluffs and cold, clear lakes and swamps nestled in the valleys. The lakes are drained by fast flowing streams, which usually occupy fault line valleys. In the southeastern parts of the complex many of the cliff faces and steep hills are being reduced by frost shattering, producing talus accumulation at their bases.



Figure 5.2: Physiographic map of the complex. (reproduced from topsheet 41 N/10, 41 N/11 issued by Survey and Mapping, Department of Energy, Mines and Resources, Ottawa).



## 1.2 PREVIOUS WORK

The earliest work in the surrounding area is reported back in the 19th century. Bell (1899) outlined the metavolcanic-metasedimentary belt in which the complex is located.

From 1900 to 1940 all geological and prospecting work was controlled by the Algoma Central Railway. After the creation of the Lake Superior Provincial Park, limited prospecting was allowed. During 1954 to 1955 the southern portion of the complex was staked for copper and nickel by Renner brothers and Falconbridge Nickel Mines Limited. The latter, after acquiring Renner property, carried out selective magnetic, electromagnatic, and geological surveys. The company put down 16 diamond drillholes with a total length of 7,580 feet. In 1959 the property was optioned by Empire Explorations Limited who, in 1960 carried out geological and electromagnetic surveys of the entire property. The Company also put down 16 diamond drillholes with an aggregate length of 4,265 feet. The plans, logs, cross-sections and sketches along with the results of the geophysical surveys of both (Falconbridge and Empire) exploration companies

have been deposited with Ontario Geological Survey's resident geologist in Sault Ste. Marie.

Couto Gold Mines Limited has claims in the center of the complex. The Company drilled 28 holes with an aggregate length of 3,249 feet in the years 1956 to 1961.

Ontario Geological Survey and Geological Survey of Canada published an aeromagnetic map of the area in 1963 (Map 2190 G; Figure 1.3).

Algoma Central Railway issued a series of maps of the area in 1964 which are as follows:

Geological Map	ACR 1964a
Pleistocene Geological Map	ACR 1964b
Photo-interpretation map	ACR 1964c
Photo-mosaic	ACR 1964d

Ayres et al. (1969) mapped the complex in detail. According to him the complex is calc-alkaline in nature and intruded the metavolcanic and metasedimentary sequences in the pre-Keweenawan time. It is rudely zoned outwards from an eccentric olivine gabbro and norite core through gabbro and norite, pyroxene diorite, biotite-hornblende diorite, tonalite, and trondhjemite to granodiorite, with quartz monzonite. Ayres mapped five units in the field which from oldest to youngest are: pyroxene gabbro and diorite; andesine anorthosite; biotite-hornblende diorite,



Figure 1.3. Areomagnetic map of the Gamitagama Lake Complex (from O.D.M. map 2190G).

tonalite, syendiorite, and trondhjemite; leucocratic grano diorite and quartz monzonite; and syenite and monzonite. Except for the last unit, contacts between rock types are generally gradational. The work on the complex was still in progress in 1966, at the time Ayres was writing his report. His suggestions about the origin of the complex are:

"The pyroxene-gabbro and diorite core appears to have formed by differentiation of a pipe-like body of tholeiitic magma. The biotite-hornblende diorite unit appears to be a hybrid unit formed by addition of a more sodic, hydrous, and siliceous magma. The leucocratic granodiorite and quartz monzonite represents a separate magma that was intruded into the partly consolidated biotite-hornblende diorite unit after consolidation of the pyroxene gabbro core".

The Ontario Geological Survey compilation maps 2220 and 2196, issued in 1970, include the complex and surrounding areas. According to both maps, the complex is Middle to Late Precambrian (Proterozoic) in age and may be intrusive equivalent of Keweenawan lavas or older. However, in both maps, it is indicated that the ages are comparative and uncertain.

Goodwin et al. (1972), while describing the different types of intrusive bodies in the supracrustal rocks of the Superior Province, classified the complex as gabbroic in nature. They noted that it

contained only minor ultramafic and anorthositic phases, but included an equal amount of diorite compared to gabbro, indicating that the original magma was calc-alkaline in nature.

### 1.3 PRESENT STUDY

The present study was undertaken to describe the petrography and geochemistry of the various rock types present in the Gamitagama Lake Igneous Complex, and to establish their mutual relationships. This information should indicate the mode and relative time of emplacement of the rock types and should serve to define the processes involved in producing the variation in the rock suites. Comparisons are made between this complex and other similar, well described complexes, particularly the gabbroic complexes of the Peninsular Ranges in Southern California. These show the similarities and differences in the evolution of the Archean Crust of Northern Ontario and the Mesozoic crust of California. Such comparisons may be used to elucidate the tectonic environments in which the igneous activity took place.

For this purpose approximately 4 weeks were spent in the field. Traverses were made systematically and

representative samples were collected of all rock types in the area. Mineralogy and mineral paragenesis were established by optical examination of 80 thin sections. Selected rock samples were analyzed for major (74 samples) and trace elements (60 samples). The results and conclusions of all the above work are summarized in this report.

## CHAPTER 2

## GEOLOGICAL SETTING

The Gamitagama Lake complex outcrops in a typical Archean Greenstone Belt, the Shebandowan (Wawa) Belt of the Superior Province. The sequence of geological events has been described by Ayres, (1969). His work shows that there are four groups of rock units in the area: pre-Keweenawan, Keweenawan, Paleozoic, and Cenozoic, which are separated by major breaks in the sequence of events (Table 2.1; Figure 2.1, back pocket). Turek et al (1978), in a study of radiometric ages, showed that the pre-Keweenawan rocks are Archean in age and generally confirmed the age relationships proposed by Ayres (1969).

The oldest rocks in the area, the pre-keweenawan metavolcanics, are three distinct formations. These, from oldest to youngest, are: the 1600 m thick lower mafic metavolcanics, the 550 m thick felsic metavolcanics, and the 1465 m thick upper mafic metavolcanics. They occur mostly in the northern parts of the map area. The metavolcanics interfinger southwestward and possibly eastward with 3,100 m thick metasediments.



TABLE 2.1

**TABLE OF FORMATIONS**  
(Modified after Ayres, L.D., 1969)

<b>CENOZOIC:</b>		
<u>Pleistocene:</u>		
Drift, sand and gr. vel.		
	Unconformity	
<b>PALEOZOIC:</b>		
<u>Lower and Middle Cambrian</u>		
Jacobsville Sandstone.		
	Fault Contact	
<b>PRECAMBRIAN</b>		
<b>KEWEENAWAN:</b>		
<u>Upper-Middle to Upper Keweenaw:</u>		
Alkalic syenite.		
	Intrusive Contact	
Diabase and granophyre.		
	Intrusive Contact?	
<u>Middle Keweenaw:</u>		
Basalt, conglomerate, and rhyolite.		
	Unconformity	
<b>ARCHEAN-</b>		
	Unmetamorphosed Ultramafic dikes.	
Gamitagama Lake Complex	Leucocratic Quartz Monzonite.	
	Intrusive Contact	
	Leucocratic Granodiorite and Granite (in the complex).	= Quartz monzonite, granodiorite, and granite stocks.
	Intrusive Contact	
	Diorite, quartz diorite, monzodiorite, and tonalite.	
	Intrusive Contact	
	Outer-- Gabbro-norite, amphibole gabbro-norite, and pyroxene diorite.	
	Intrusive Contact	
	Inner-- Olivine gabbro-norite, gabbro-norite, and anorthosite.	
	Intrusive Contact?	
	Batholithic trondhjemite, granodiorite, quartz monzonite, granite, and syenite.	= Ryan Migmatite: Metasediment plus batholithic granitic rocks.
	Intrusive Contact	
	Gargantua Harbour Granodiorite.	
	Intrusive Contact	
Rabbit Blanket Lake Trondhjemite.	= Mijinemungshing Lake Trondhjemite.	
Intrusive Contact		
Upper mafic metavolcanic formation.		
Felsic metavolcanic formation.	= Metasedimentary formation.	
Lower mafic metavolcanic formation.		

The mafic metavolcanics are dominantly massive flows and balloon to loaf shaped pillows, while the felsic metavolcanics are commonly pyroclastic ashflows and tuffs. The metasediments are mostly interbedded metagreywacke and metasilstone, showing graded bedding and cross-bedding, with rare pebble and cobble conglomerates. Iron formations, containing thickly laminated metachert layers, occur in the metavolcanic-metasedimentary sequence. Neither the base nor the top of this stratified sequence is exposed.

Approximately half of the map area is underlain by pre-Keweenaw intrusive rocks. Emplacement of the intrusions began during volcanism and continued until late in the tectonic cycle. The only definitely established pre-tectonic intrusions are the Mijinemungshing Lake and the Rabbit Blanket Lake trondhjemitic plutons, bordering the metavolcanic-metasedimentary sequence in the northeast and north respectively. These plutons, and the metavolcanic-metasedimentary sequence were isoclinally folded and subjected to progressive regional metamorphism.

The composite Southern Batholith, considered to be syntectonic to post tectonic in age, is exposed to the southwest of the stratified sequence. Within this batholith, Ayres (1969) recognized the older Gargantua

Harbour Granodiorite and younger Ryan Migmatite. The migmatite is exposed in the west and comprises equal parts of metasediments and granitic rocks. Granitic intrusions, coeval with the migmatite, are exposed to the east of the granodiorite.

The Gamitagama Lake Complex is a post-orogenic, differentiated, gabbroic pluton. The rock types present in the complex range from troctolite to granite in composition. The emplacement of leucocratic granodiorite and granite in the complex was accompanied by the intrusions of eight elliptical stocks of similar composition in the surrounding metavolcanic-metasedimentary sequence. The last phase of Gamitagama Complex involves the intrusion of leucocratic quartz monzonite. A sequence of ultramafic dykes represent the last event recorded in the pre-Keweenawan.

In a study of the radiometric ages of these rocks (Turek et al 1980), a U-Pb zircon age obtained for the upper mafic metavolcanic indicates that the volcanic rocks and related metasediments are at least 2715 Ma old. The trondhjemite plutons have been dated as 2645 Ma old by Rb-Sr and 2663 Ma by U-Pb. The Gamitagama Lake Complex gives a 2640 Ma Rb-Sr age and a 2662 Ma U-Pb age. Post-tectonic potassic plutons yield 2565

Ma Rb-Sr age. For the southern Batholith's migmatite the Rb-Sr age is 2560 Ma and corresponding U-Pb age is 2608 Ma. This does not agree with Ayres (1969) work and is a somewhat younger age for migmatite than is general for the Superior Province and may be caused by younger tectonic uplift of this crustal block.

The pre-Keweenawan rocks are overlain unconformably by up to 675 m of Middle Keweenawan basalt, conglomerate, and rhyolite. There are one northeast-trending and two northwest-trending sets of diabase dykes. Many of the dykes are younger than the Middle Keweenawan volcanic rocks. The Jacobsville Sandstone, 200 m thick, is Lower to Middle Cambrian in age.

The last movement on most of the faults in the area is Keweenawan or younger. Cenozoic deposits, mostly gravel and sand, are wide spread but are mostly thin.

## CHAPTER 3

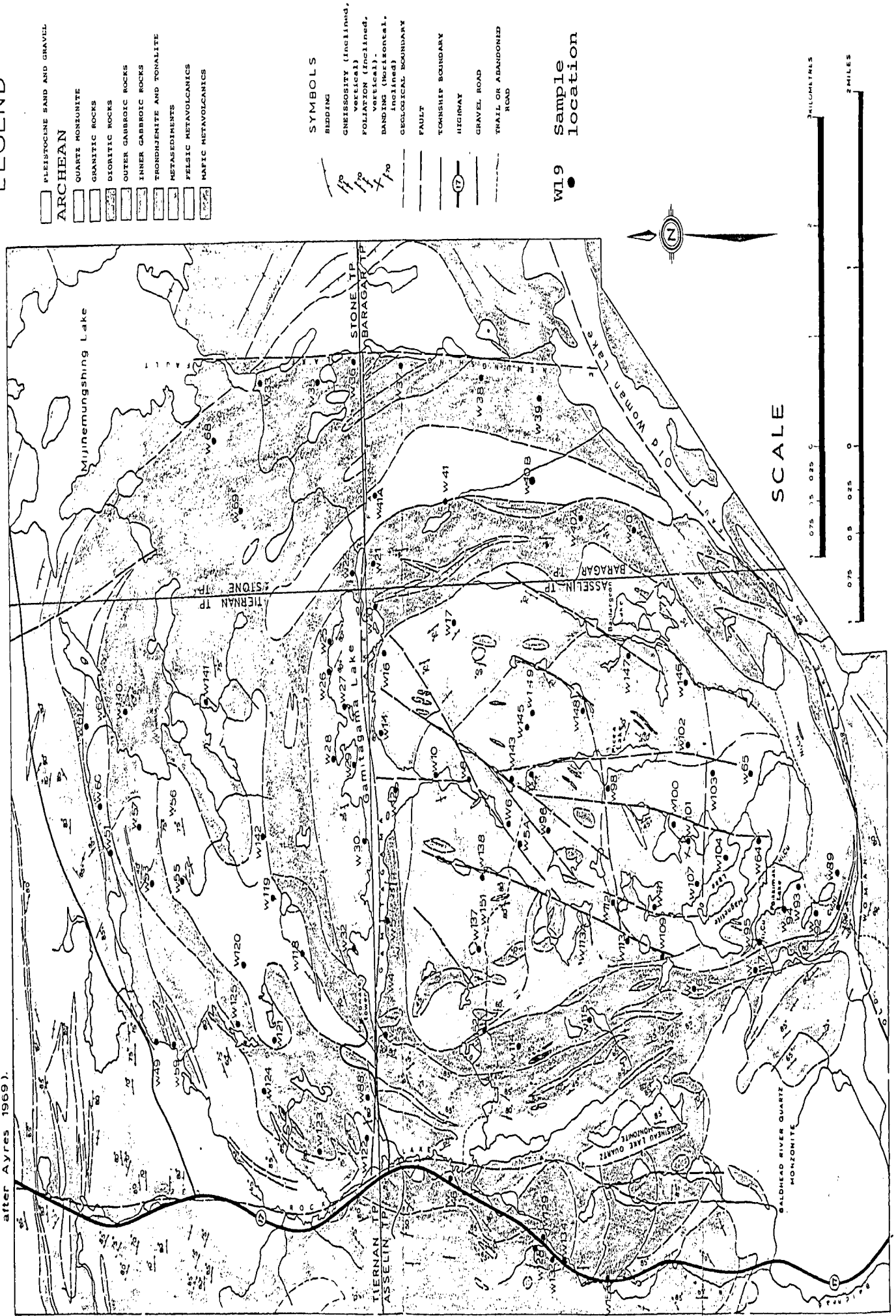
## FIELD RELATIONS

The Gamitagama Lake Complex ranges in composition from basic through intermediate to acidic and consists of 5 distinct rock groups. Each group consists of mineralogically and texturally related rocks and occupies a specific area in the complex (Figure 3.1).

Almost all the basic rocks, mostly gabbroic in composition, outcrop south of Gamitagama Lake except for a small fault-separated part in the north. These basic rocks may be divided into two distinct groups, an "inner gabbroic series" and an "outer gabbroic series".

The rocks of inner gabbroic series occupy about 25% (19 km<sup>2</sup>) of the total area of the complex. Outcrops of outer gabbroic series surround the area underlain by these rocks. The boundary between these two very similar looking rock series is difficult to delineate in the field and is marked with the help of petrography, air photos and an aeromagnetic map. Fine-grained dikes of the outer gabbroic series intrude the inner gabbroic rocks but are rare.

FIGURE 31: MAP SHOWING THE LOCATION OF THE DIFFERENT ROCK GROUPS IN THE GAMITAGAMA LAKE COMPLEX (Modified after Ayres 1969).



**LEGEND**

- PLEISTOCENE SAND AND GRAVEL
- ARCHEAN
- QUARTZ MONZONITE
- GRANITIC ROCKS
- DIORITIC ROCKS
- OUTER GABBROIC ROCKS
- INNER GABBROIC ROCKS
- TROXENITE AND TONALITE
- METASEDIMENTS
- FELSIC METAVOLCANICS
- MAFIC METAVOLCANICS

**SYMBOLS**

- BEDDING
- GNEISSOSITY (inclined, vertical)
- FOLIATION (inclined, vertical)
- BANDING (horizontal, inclined)
- GEOLOGICAL BOUNDARY
- FAULT
- TOWNSHIP BOUNDARY
- HIGHWAY
- GRAVEL ROAD
- TRAIL OR ABANDONED ROAD

W19 ● sample location



**SCALE**



There are numerous inclusions and roof-pendants of metavolcanics scattered throughout the inner gabbroic rocks.

The rocks of outer gabbroic series underlie about 13% (10 km<sup>2</sup>) of the total area of the complex and form a complete annular outcrop around the inner gabbroic series. These rocks are bounded in the north, east, and west by dioritic rocks and to the south by metavolcanics. The boundary with the dioritic rocks appears gradational as the pyroxenes of the outer gabbroic rocks are uralitized near the contact. The southern contact with the metavolcanics is sharp but at places a 15 to 30 m wide zone of dioritic rocks separate the two. Inclusions and roof-pendants of metavolcanics occur scattered throughout these rocks. Huge xenoliths of the inner gabbroic series (Cu-Ni showings in the south and small olivine-bearing outcrops north of Baillargeon Lake) occur oriented parallel to the inner boundary.

A series of criss-crossing faults, restricted to the gabbroic rocks, trend approximately east to west, northeast to southwest, and north to south (Figure 3.1). The east-west trending faults are the oldest while the north-south trending ones are the youngest.

The intermediate rocks, mostly dioritic in composition, occupy about 47% (35 km<sup>2</sup>) of the total area of the complex. They encircle the outer gabbroic rocks to the north, east, and west, forming an incomplete annular outcrop. Contact between the dioritic and metavolcanic rocks is subvertical and generally sharp. The boundary at places is marked by the local development of intrusion breccia where the dioritic rocks intruded the metavolcanic rocks. Inclusions and roof pendants of volcanic rocks are abundant in the dioritic rocks, but there are very few inclusions and roof pendants of the outer gabbroic series present.

The acidic rocks include "granitic rocks" and "quartz monzonite" which are two distinct rock groups. The former (leucocratic granodiorite and quartz monzonite of Ayres, 1969) underlies about 10% (7.5 km<sup>2</sup>) of the total area of the complex. It forms a discontinuous annular outcrop in the center of dioritic rocks. Dikes and apophyses of granitic rocks, about 20 cm to 150 m in thickness, with sharp margins, occur in the dioritic and gabbroic rocks.

The quartz monzonite (syenite and monzonite of Ayres 1969) occupies 3% (2 km<sup>2</sup>) of the total area of the complex near its northern boundary. It forms a roughly east-west trending, 500 m wide, vertical dike,



which cross-cuts the dioritic and granitic rocks and has an assimilation zone at the contacts. There are inclusions of dioritic and metavolcanic rocks in this dike, which also show evidence of assimilation.

A contact metamorphic aureole in the meta-volcanic-metasedimentary sequence around the complex, approximately 300 to 3000 m wide, has been superimposed on the regional metamorphism (Ayres, 1969). Most roof pendants and inclusions in the plutonic rocks of the complex and country rocks immediately adjacent to the complex are in the Pyroxene-hornfels facies; the remainder of the aureole is in the hornblende-hornfels facies.

### 3.1 THE INNER GABBROIC SERIES

The inner gabbroic series consist of 3 rock types recognizable in the field. All these rock types are coarser-grained than those of the outer gabbroic series and contain plagioclase, olivine and/or pyroxene with minor to substantial amounts of amphibole and opaque minerals. The rock types show a more or less continuous variation in mineralogy and because of the gradational nature of this variation,

only a few rock types are mappable in the field. These include olivine gabbro, gabbro and anorthosite.

### 3.1.1 OLIVINE GABBRO

The olivine gabbro outcrops in the areas of the lowest relief and underlies 6% (4.5 km<sup>2</sup>) of the total area of the complex around Magnetite Lake (Figure 3.2; back pocket). This unit further contains 3 rock types which are coarse-grained with variable grain-size and colour index. Mineralogical variations are reflected in the colour of weathered surfaces of the outcrops. Troctolite, colour index about 30, contains plagioclase and olivine and is light-brown on both fresh and weathered surfaces. Layering occurs in a small troctolite outcrop between two small lakes NE of Magnetite Lake. It is comprised of tabular bands, 10 to 50 cm thick, alternating with 5 to 10 mm thick laminations. The thick bands have a colour index of about 25 and consist of plagioclase and olivine with minor opaques. The thin laminations, colour index around 45, contain plagioclase, olivine, pyroxene and opaques rarely exceed 10 meters in length and lense out in the thick bands. Both plagioclase and olivine show a strong

preferred orientation parallel to the lamination boundary which has an almost horizontal attitude dipping a few degrees toward NNE. The troctolite grades upwards into olivine gabbro with the increase in pyroxene towards higher elevations in the north and west.

The dark grey olivine gabbro, colour index about 35, is comprised of plagioclase, olivine, and pyroxene. It occurs in rusty, brownish grey outcrops west of Picea Lake and rarely may show a rude foliation defined by the parallel to subparallel arrangement of plagioclase crystals. This foliation dips 30 NE near the southwestern end of Picea Lake (Figure 3.2).

Southeast of Magnetite Lake the troctolite grades into amphibole olivine gabbro by increase in the percentage of amphibole (more than 5%). The amphibole olivine gabbro is made up of plagioclase, olivine, pyroxene and amphibole, with a colour index of about 60. The rock is massive dark-grey when fresh, and dark greyish-green when weathered. The amphibole commonly forms rounded poikilitic crystals up to 1 cm in diameter.

### 3.1.2. GABBRO

The olivine gabbro grades upwards into gabbro with the disappearance of olivine and further increase in elevation in the north and west. Across Picea Lake, towards the east, olivine gabbro abruptly changes into anorthositic gabbro. This is probably due to a north-south trending fault which passes through the lake. In fact, the original systematic distribution of lithologies appears to be disturbed by the movements along those criss-crossing faults (Figure 3.2).

The gabbro underlies about 8% (6.5 km<sup>2</sup>) of the total area of the complex. It is coarse-grained and has a colour index varying from 10 in minor leucocratic sections to 40 in typical rock. The light grey to grey coloured rock consists of plagioclase, pyroxenes and opaques and weathers to rusty reddish-grey on the surface.

Symmetric banding due to variations in the proportions of felsic and mafic constituents has been noted in a few outcrops near Picea Lake. These bands vary from 2 to 35 cm in thickness and are defined by concentrations of pyroxene and plagioclase in adjacent

bands. In some bands pyroxene or plagioclase exceed 90% and these are layered internally on a mm and cm scale. The contacts of those bands are sharp and there is no gradation in mineral proportions between them. The dip of the banding varies in different outcrops. Near the southeastern end of Picea Lake the banding dips toward southeast at about  $35^{\circ}$ , while near the northeastern end the dip is almost  $25^{\circ}$  to the east. At a number of places for instance, on the logging haulage road about 300 m east of the anorthosite body, the gabbro contains bent, twisted, and broken layers of pyroxene rich rock with a colour index of about 95 (Photo 3.1). Ayres (1969) reported an almost imperceptible, approximately horizontal, layering caused by slight differences in both pyroxene content and grain size in several outcrops.

The gabbro is well foliated at many localities because of parallel to subparallel arrangements of tabular plagioclase and prismatic pyroxene crystals. The foliation has a highly variable attitude in different outcrops. Neither the banding nor the foliation show any systematic pattern of regional variation (Figure 3.2).

In many outcrops, particularly northwest of Picea Lake, the gabbro is spotted due to concentrations of

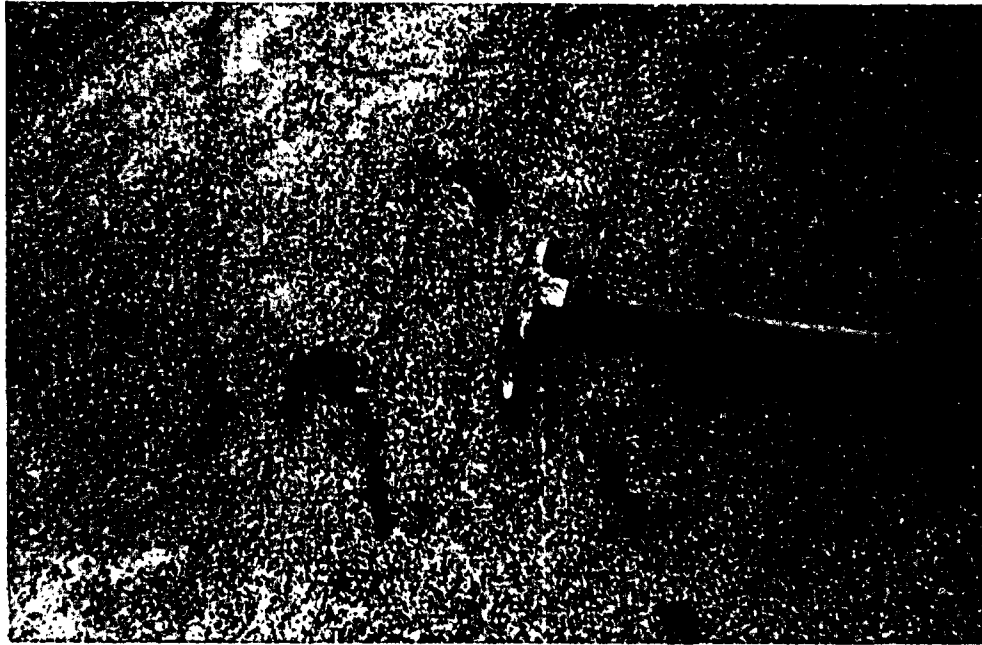


Photo 3.1. Gabbronorite of the Inner Gabbroic Series, about 300m east of anorthosite body, containing bent, twisted and broken layers of pyroxene rich rock.

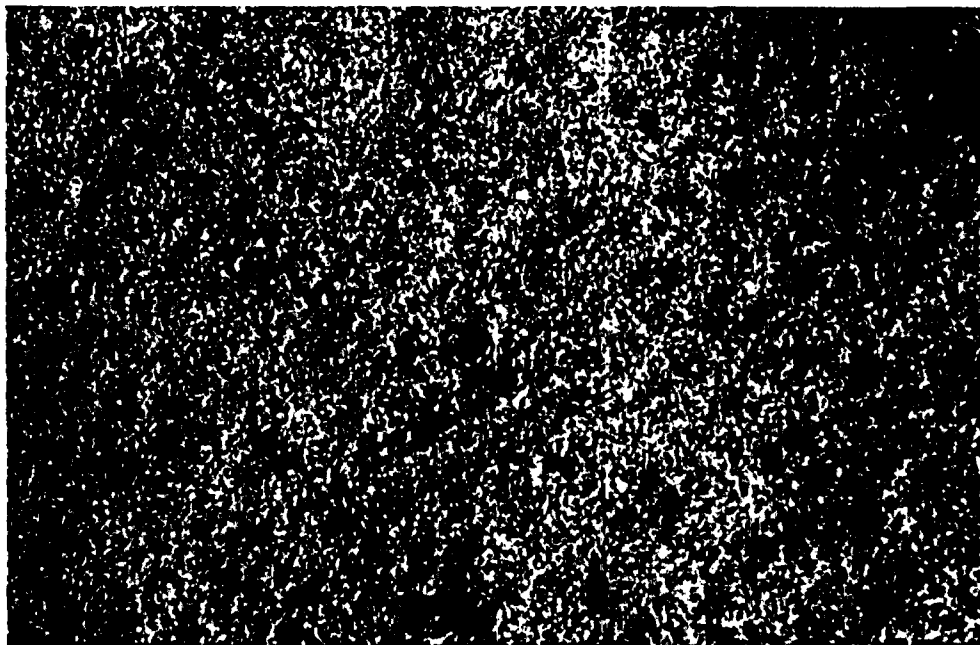


Photo 3.2. Spotted gabbronorite, about 200m northwest of Picea Lake. The pyroxene is concentrated in spherical aggregates as much as 1 cm in diameter and 1-3 cm apart.

pyroxene in spherical aggregates as much as 1 cm in diameter and 1 to 3 cm apart (Photo 3.2). Ayres (1969) reported these spherical aggregates of mafic minerals to be up to 2.5 cm in diameter and 2 to 15 cm apart.

### 3.1.3 ANORTHOSITE

The anorthositic gabbro in the north and east of Picea Lake grades outwards (away from olivine gabbro and gabbro) into anorthosite.

The anorthosite occupies about 1% ( $< 1 \text{ km}^2$ ) of the total area of the complex. It underlies a small fault-bounded area to the north and occurs as a few small outcrops to the east of Picea Lake.

The rock is coarse-grained, greyish-white when fresh and weathers to a light rusty-brown colour. It consists of plagioclase, pyroxene and/or opaques and has a colour index between 1 to 5. In the fault-bounded body, the amount of pyroxene decreases toward northeast. The rock shows a weak foliation when pyroxene is present. This foliation dips at about  $75^\circ$  towards NW (Figure 3.2).

The anorthosite outcrops east of Picea Lake have a colour index of about 5. A weakly developed

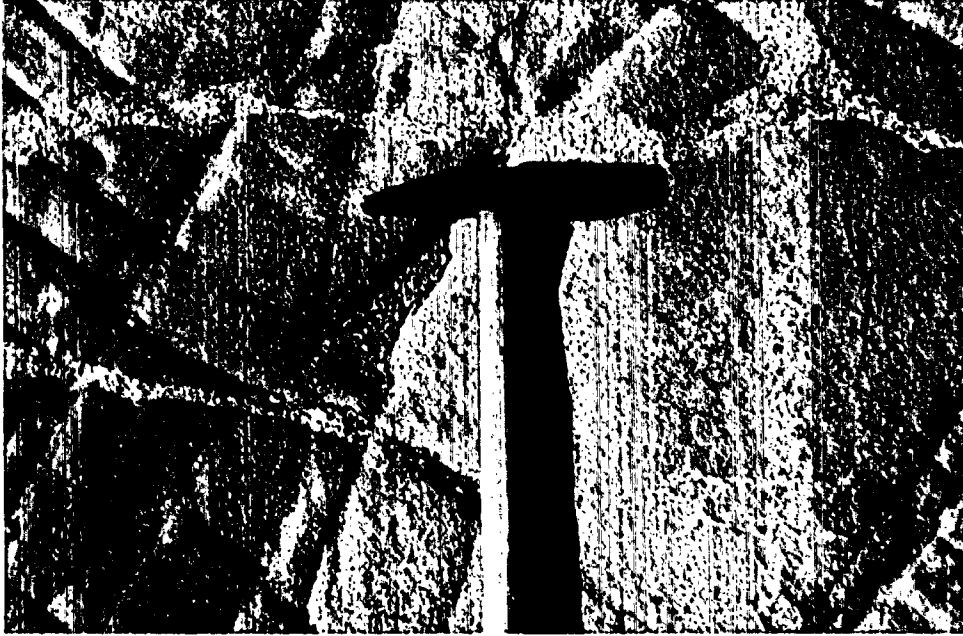


Photo 3.3: Irregular anorthositic dikes, about 1-15 cm in width, in the gabbronorite.

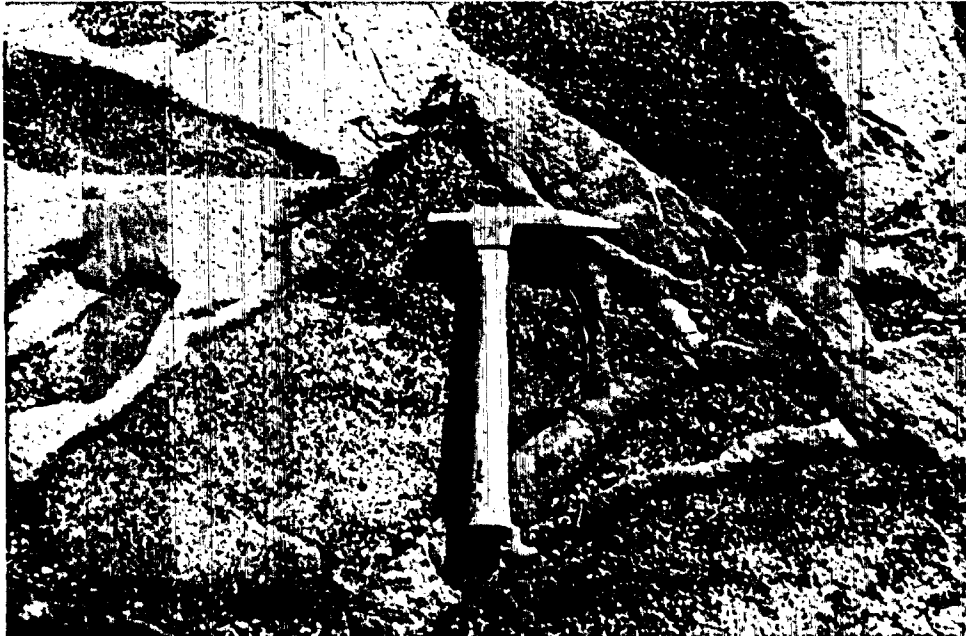


Photo 3.4: Anorthositic dikes brecciating the host gabbronorite.



foliation, which is occasionally difficult to make out, appears to have a variable attitude, dipping from  $56^{\circ}$  northwest to  $75^{\circ}$  southeast.

Anorthosite dikes ranging from 1 mm to 15 cm in thickness occur in the gabbro, sometimes brecciating the host rock (Photo 3.3 & 3.4). Mostly they are local in extent, but a few can be traced for up to 100 m. They are fine to medium-grained and consist of almost 100% of plagioclase.

### 3.2 THE OUTER GABBROIC SERIES

The outer gabbroic series consists of two recognizable rock types in the field. These rocks are generally medium but may be coarse-grained and contain plagioclase and pyroxene, with variable, and sometimes substantial proportions of amphibole, brown mica and opaques. The rock types show a more or less continuous variation in mineralogy, and because of the gradational nature of this variation, only two rock types are mappable in the field. These include gabbro and amphibole gabbro/pyroxene diorite.

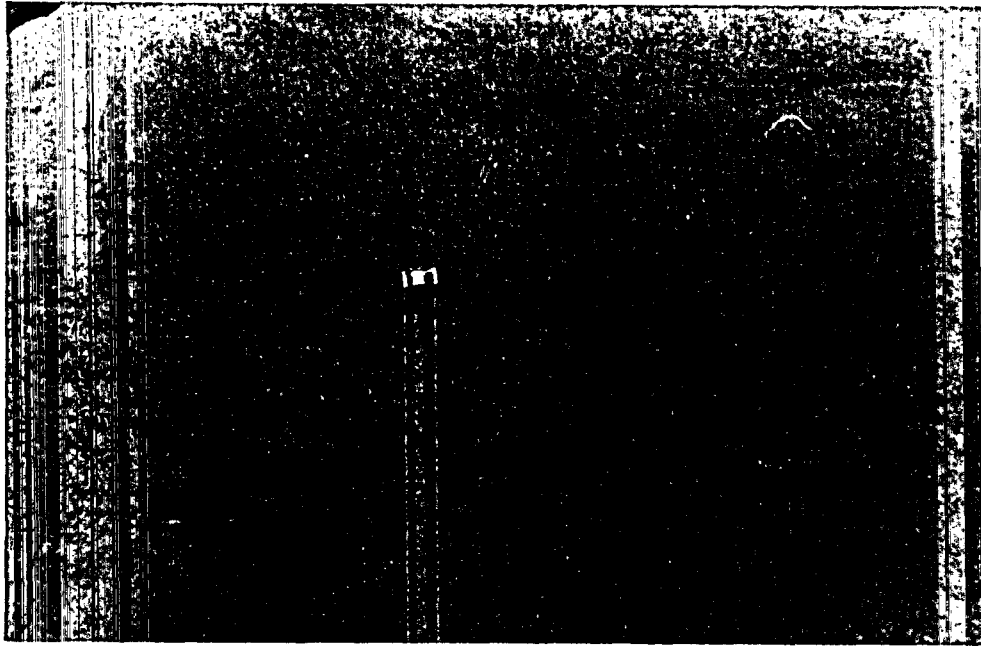


Photo 3.5: Gabbro-norite of the Outer Gabbroic Series showing weak asymmetric banding on the south side of a small lake near southern boundary of the complex.

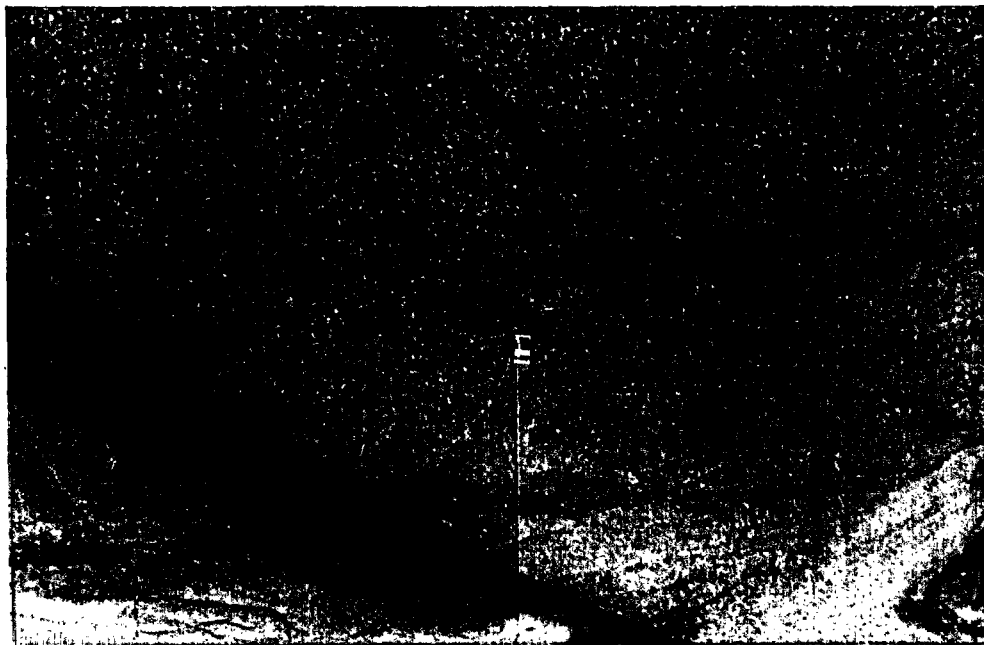


Photo 3.6: Gabbro-norite, south of Poikkimaki Lake, showing minor asymmetric banding in the upper half of the photo and band containing irregular, oriented inclusions of segregated pyroxene in the lower half.

### 3.2.1 GABBRO

The gabbro underlies about 10% (7 km<sup>2</sup>) of the total area of the complex, and mainly occupies the southern and eastern marginal areas. It is medium-grained, greyish-brown when fresh and weathers to rusty-brown on the surface. The colour index varies from 30 to 45 at different outcrops. The commonly well foliated rock consists of tabular plagioclase, prismatic pyroxene, with minor and variable amounts of opaques and amphibole.

Weak asymmetric banding, maximum 30 cm in thickness, occurs in the south and southeast of Poikkimaki Lake (Photos 3.5 & 3.6). In these bands pyroxene is concentrated at the base and plagioclase is concentrated towards the top. The bands consist of about 60% pyroxene and 35% plagioclase at the base and grade upwards to the lighter parts which contain about 70% to 80% plagioclase and 20% to 25% pyroxene. The bands extend for 10 to 20 m laterally and strike roughly parallel to the outer contact with the dioritic and metavolcanic rocks. The dip of these bands is towards the inner contact and varies from 50° N to 70° NW.

At scattered localities within the gabbro, there is well developed foliation due to the parallel align-

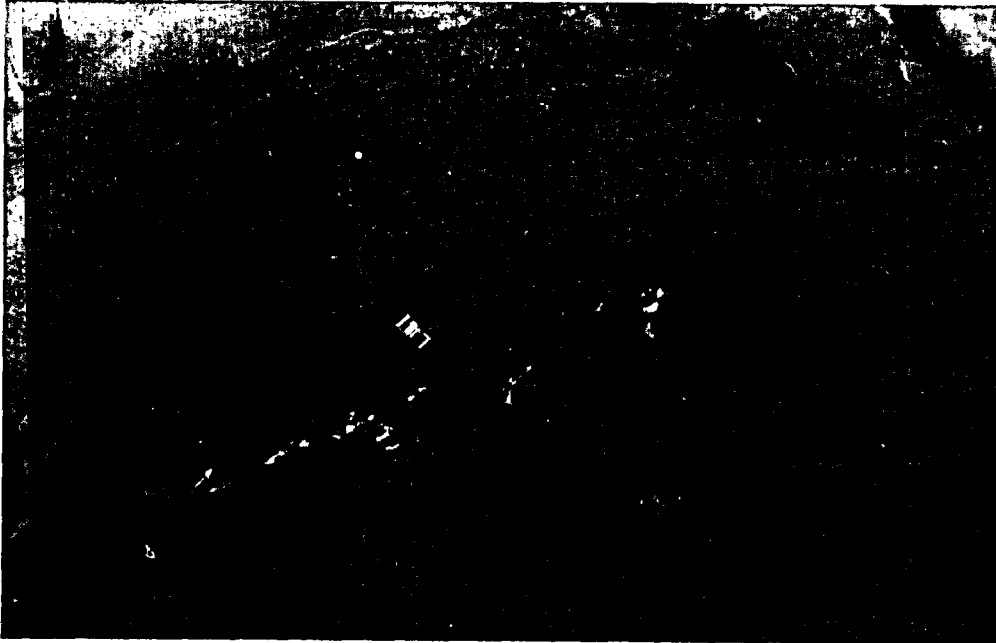


Photo 3.7: The irregular inclusions of segregated pyroxene in the gabbronorite of the Outer Gabbroic Series. The inclusions, maximum 2 cm long, are randomly distributed in the rock. Location same as of photo 3.6.

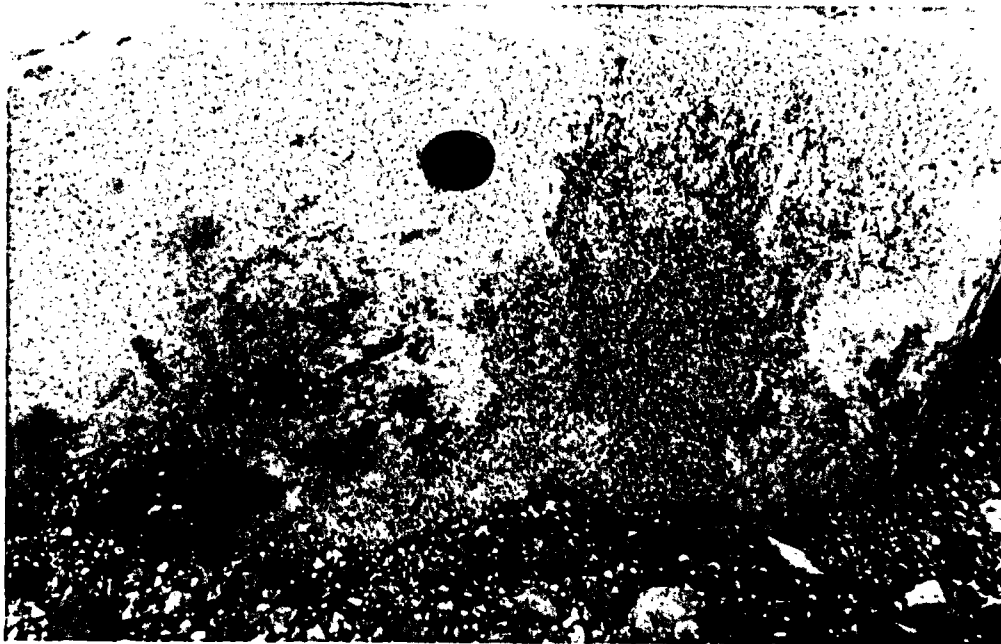


Photo 3.8: The irregular inclusion of the Inner Gabbroic Series in the gabbronorite of the Outer Gabbroic Series. The inclusion is comparatively coarser-grained and roughly parallel to the foliation of the host rock.

ment of tabular plagioclase and prismatic pyroxenes crystals. The strike of the foliation in most outcrops is approximately parallel to the outer boundary with the diorite and it dips at angles varying from vertical to  $60^{\circ}$  towards the inner boundary with the inner gabbroic rocks.

At a few places, particularly southeast of Poikkimaki Lake, the gabbro contains irregular, segregated oriented mafic inclusions in 3 to 30 cm wide bands (Photo 3.6 & 3.7). These inclusions consist of angular aggregates of pyroxene and are up to 2 cm in length. The attitude of their orientation is similar to the nearby banding described above.

Xenoliths or roof pendants of olivine-bearing rocks of the inner gabbroic series, each less than  $0.01 \text{ km}^2$  in area, crop out north of Baillargeon Lake near the boundary between Asselin and Barager Townships. Numerous smaller xenoliths of the inner gabbroic series are also present in the outcrops near the southern boundary and are distinguished from the host rock by coarser grain size (Photo 3.8) colour of the weathered surfaces, occurrence of sulphide mineralization, and thin section studies. These xenoliths show a strong tendency to occur with their

longer dimensions roughly parallel to the outer boundary of the host rock (Figure 3.2).

### 3.2.2 AMPHIBOLE GABBRO/PYROXENE DIORITE

There is an increase in amphibole and brown mica in the rocks of this unit and the gabbro grades northwards into amphibole gabbro. Ayres (1969) delineated the pyroxene diorite as a mappable unit. Later petrographic studies of samples collected from this unit reveal that the unit is mostly amphibole gabbro except for small areas north and south of Gamitagama Lake, near its eastern end, where the rock is dominantly pyroxene diorite. The pyroxene diorite differs from amphibole gabbro in the anorthite content of plagioclase which is less than 50% in the case of the former.

The amphibole gabbro/pyroxene diorite unit underlies about 4% (about 3 km<sup>2</sup>) of the total area of the complex. This unit occupies a narrow strip (maximum 400 m wide) in the north and west of the inner gabbroic series (Figure 3.2; back pocket). Around an unnamed lake, about 1 mile north of Magnetite Lake, this strip widens to form an embayment in the inner

gabbroic series. Some of the outcrops in this embayment, particularly on the west of the unnamed lake, consist of fine-grained rock which contains euhedral to anhedral phenocrysts of amphibole up to 3 x 2 cm in dimension. Fine-grained dikes of pyroxene diorite, 5 to 20 cm in width and local in extent, intrude the anorthositic outcrops of the inner gabbroic series east of Picea Lake. These dikes contain micro-phenocrysts of brown mica up to 1 mm long.

The amphibole gabbro/pyroxene diorite consists of plagioclase, pyroxene, amphibole and/or brown mica with minor amounts of opaques. In hand specimens the pyroxenes are of finer grain-size compared to plagioclase and amphibole. The colour index at different outcrops varies from 35 to 45. The brownish-grey rock weathers to a dark rusty-grey on the surface.

A well developed foliation is present at a number of localities in these rocks. It is defined by a parallel to subparallel alignment of mafic minerals and has an attitude similar to the above gabbro. In outcrops of the western strip the foliation has an almost north-south strike and variable, vertical to 60°, easterly dip. Along the northern side of Gamitagama Lake the foliation has an approximate NW-SE strike and dips 80° to 45° towards SW. An average

strike is roughly parallel to the outer boundary with the dioritic rocks and dips towards the inner gabbroic rocks.

A xenolith of the inner gabbroic series, about 0.03 km<sup>2</sup> in area, occurs around the NW corner of the unnamed lake. This xenolith has its longer dimension parallel to outer boundary of the host rock.

### 3.3 THE DIORITIC ROCKS

The dioritic part of the complex is a heterogeneous body made up of 4 recognizable rock types. All of these rock types contain plagioclase, hornblende, and biotite together with variable and sometimes substantial proportions of several other minerals. Pyroxene, quartz, and potash feldspar may all be present separately or together. The satellitic intrusions (on Highway 17), are comprised of quartz monzodiorite and tonalite. In the main complex the rock types show a continuous gradational variation from hornblende gabbro through diorite, quartz diorite, and quartz monzodiorite to tonalite.



### 3.3.1. DIORITE:

The diorite underlies about 6% (4.5 km<sup>2</sup>) of the total area of the complex. It is exposed in a 600 m wide maximum north-south trending strip, stretching from the western end of Old Woman Lake to the eastern end of Gamitagama Lake (Figure 3.2).

The diorite is a coarse-grained rock with the colour index varying from 25 to 50. The colour of the rock varies from grey to dark-grey or greenish-grey on both fresh and weathered surfaces. It consists of tabular plagioclase, prismatic hornblende, and minor biotite. Later petrographic studies indicated that in the southern half of this strip, the plagioclase is labradorite in composition and hence the rock is, in fact, hornblende gabbro.

The diorite unit is mostly massive but a weak foliation is noted at a few outcrops. This foliation has an average north-south strike and 70° to 80° westerly dip. Huge metavolcanic xenoliths, some of them 100 m x 1500 m in dimension, occur oriented parallel or at a slight angle, to the inner boundary of the host rock.

A fine-grained equivalent of diorite occurs near the southern end of the northern satellitic intrusion



Photo 3.9: Road-cut in the northern satellitic intrusion on the Highway 17 showing intrusion breccia. Fine-grained equivalent of diorite is intruded by the quartz monzodiorite which in turn is brecciated by a number of 2-50 cm wide dikes of the granodiorite, granite, and pegmatite respectively.



photo 3.10: Same intrusion breccia about 8 m north of photo 3.9.

on Highway 17. It is a massive, dark-grey rock which consists of plagioclase and hornblende and has a colour index of about 40. The outcrop is brecciated by the later intrusive rocks (Photo 3.9 & 3.10). No metavolcanic or gabbroic inclusions were observed in this rock.

### 3.3.2. QUARTZ DIORITE

The diorite, with increase in quartz grades into quartz diorite around the eastern end of Gamitagama Lake. The quartz diorite is a major rock type in the dioritic rocks. It underlies about 37% (28 km<sup>2</sup>) of the total area of the complex. A narrow area south of Gamitagama Lake is fault-separated from the main northern body and extends southwest, then south in the form of a strip (maximum 500 m wide) forming the western margin of the main complex. It also occupies the area north of Old Woman Lake, forming the eastern margin of the complex (Figure 3.2).

The quartz diorite is a coarse-grained rock, with a colour index which varies from 25 to 35. It is grey to greenish-grey on both fresh and weathered surfaces and consists of plagioclase, hornblende, biotite, and quartz. The rock is mostly massive, but shows a weak



Photo 3.11: The quartz diorite with abundant metavolcanic inclusions near the contact with metavolcanics on the gravel road leading to microwave tower from the Highway 17. The inclusions are oriented with their longer dimension parallel to the contact and dip subvertically away from the contact.

foliation at a few localities near the outer boundary with the metavolcanics. This foliation, in Asselin Township, has a strike roughly parallel to the north-eastern boundary and dips towards the inner contact with the outer gabbroic rocks.

Rare inclusions of the outer gabbroic series are present in the quartz diorite. A huge xenolith of the series, about 400 x 150 m in dimensions, occurs south of the quartz monzonite dike near the northern boundary of the complex. The longer dimension of the xenolith is roughly parallel to the outer boundary with the metavolcanics. Metvolcanic inclusions or xenoliths have a very strong orientation with their longer dimensions parallel to the outer boundary of the host rock (Photo 3.11; Figure 3.2).

### 3.3.3 QUARTZ MONZODIORITE

There is an increase in the amount of quartz and alkali feldspar about 1 km north of Old Woman Lake, near the eastern margin of the complex, and quartz diorite grades in to quartz monzodiorite. This rock also occupies most of the southern satellitic intrusion on Highway 17. In the southern most outcrop of this intrusion, quartz monzodiorite intrudes and

brecciates a small area of fine-grained rock which is equivalent to diorite in composition. This intrusion breccia is in turn brecciated by a number of small dikes, 2 to 50 cm in width (Photos 3.9, 3.10). These dikes have the composition of grandiorite, granite and pegmatite in decreasing age respectively.

The quartz monzodiorite is a medium-grained (in the northern satellitic intrusion) to coarse-grained rock (eastern margin of complex). It consists of plagioclase, hornblende, biotite, alkali-feldspar and quartz. The coarse-grained rock is massive and contains only a few metavolcanic inclusions. The medium-grained rock shows a weak foliation due to a sub-parallel arrangement of plagioclase, hornblende and biotite grains. This foliation has an average N20°E strike and dips at about 80° to the east. The metavolcanic and "fine-grained diorite" inclusions are oriented with their longer dimension parallel to the above foliation in this rock but very rarely do they show a random orientation.

#### 3.3.4 TONALITE

The quartz diorite, with the further increase in quartz, grades into tonalite near the southern most end of Mijinemungshing Lake. The tonalite also

occurs in the southern satellitic intrusion on the Highway 17. The total area underlain by this rock is less than 1% of the total area of the complex.

The tonalite south of Mijinemungshing Lake is a coarse-grained, massive rock with the colour index varying from 15 to 30. It consists of plagioclase, hornblende, biotite, quartz and epidote. The rock is light-grey to light-greenish grey on both fresh and weathered surfaces. A few volcanic inclusions with random orientation occur at a few tonalite outcrops. The medium-grained tonalite of the satellitic intrusion has a colour index of about 30. It consists of plagioclase, hornblende, biotite, and quartz. The rock is light-grey in colour on both fresh and weathered surfaces. It rarely has a foliation which strikes approximately parallel to the longer dimension of the intrusion and dips between 55° SW and vertical (Figure 3.2).

The tonalite contains inclusions of quartz diorite and metavolcanics. These inclusions are angular in shape and do not show any systematic orientation (Photo 3.12). Rounded inclusions of a darker tonalite (about 1 m across and a little richer in hornblende and biotite) occur in the tonalite outcrop on the highway (Photo 3.13).



Photo 3.12: Tonalite of the Southern Satelitic Intrusion on the Highway 17 containing angular inclusions of metavolcanics and quartz diorite.



Photo 3.13: Tonalite containing rounded inclusions of a darker tonalite. Inclusions and the host rock are similar in all respects except for the colour index.



### 3.3.5 OTHER SATELLITIC INTRUSIONS

Ayres (1969) described the occurrence of many small satellitic intrusions west of the main intrusion and Highway 17 (Figure 3.2) as follows:

"These intrusions are highly variable in composition and are dominantly intrusion breccias composed of mafic metavolcanic and metasedimentary country rock, at least four mafic plutonic phases, and several leucocratic plutonic phases; each plutonic phase, except the earliest, intrudes and contains rounded inclusions of earlier plutonic rocks. In order of decreasing age, the identified plutonic phases are: (1) gabbro and hornblende gabbro, (2) hornblende diorite, (3) quartz-bearing diorite, (4) tonalite and trondhjemite, (5) leucocratic, calcic granodiorite, granodiorite, and quartz monzonite, and (6) pegmatite. Pyroxene rich phases are rare".

The first intrusive phase is probably of the outer gabbroic series while phases 2 to 4 belong to the dioritic rocks. All the rest of the phases probably belong to the granitic rocks.

### 3.4 GRANITIC ROCKS

The granitic rocks of the complex form irregularly-shaped, discontinuous bodies which are

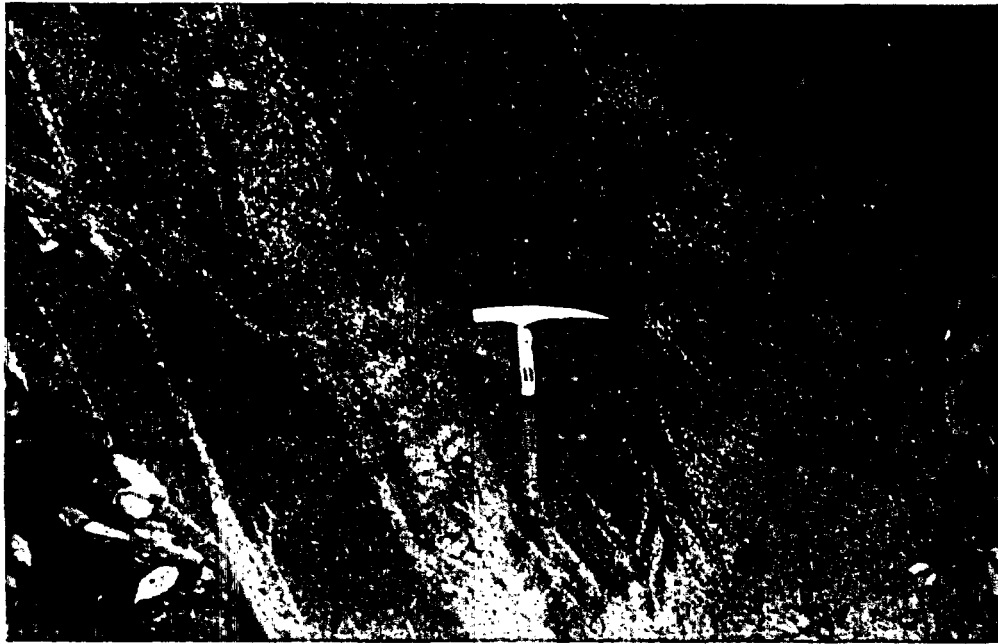


Photo 3.14: Quartz diorite, on gravel road near the contact with the granitic rocks about 100 m NW of microwave tower, showing intensive shearing and alteration.



Photo 3.15: The intensive shearing above (photo 3.14) changes to fine shear network away from the contact.

systematically distributed on the north and east sides of the complex. These bodies are mainly confined within the dioritic rocks but small, rounded to lense-shaped and narrow dike like bodies also intrude the inner and outer gabbroic rocks. Medium-grained dikes, 15 cm to 150 m wide with sharp contacts, occur in both the dioritic and gabbroic rocks. A narrow zone of the gabbroic rocks, about 2 to 5 m wide, adjacent to these granitic bodies, shows sericitization and uralitization of plagioclase and pyroxenes respectively. In the dioritic rocks a zone of hydrothermal alteration, about 2 to 15 m wide, occurs along the contact with granitic rocks. This zone consists of a fine network of shear-fractures along which plagioclase is strongly sericitized and hornblende is altered to chlorite (Photo 3.14 & 3.15).

Ayres (1969) described the occurrence of pegmatite dikes, containing crystals of oligoclase up to 2.5 cm long, microcline quartz and minor biotite. These dikes are associated with and locally form a marginal phase of the granitic dikes. He further noted that pegmatites are rare in the larger granitic bodies and those parts of the complex where granitic rocks are not present.

The granitic rocks consist of two recognizable rock types which occupy specific areas in the complex. These include granodiorite and granite. The occurrence of a fault in between, masks the exact relationship between the two.

#### 3.4.1 GRANODIORITE

The granodiorite underlies a small outcrop on Highway 17, about 800 m south of the boundary between Tiernan and Asselin Townships (Figure 3.2). It is intrusive and in sharp contact with the dioritic rocks. The medium-grained rock has a maximum colour index of about 15 and consists of plagioclase, alkali feldspars, hornblende, biotite and quartz. The rock is foliated due to the parallel to subparallel alignment of its constituent minerals. This foliation has a NE to SW strike and dips  $85^{\circ}$  NW. The few meta-volcanic inclusions that were observed in this rock do not show any specific orientation.

#### 3.4.2 GRANITE

The granite underlies about 10% (7.5 km<sup>2</sup>) of the total area of the complex. It is a medium to coarse-

grained rock which has a colour index of less than 10. The colour of the rock varies from light-grey to pink on both fresh and weathered surfaces. It consists of plagioclase, alkali feldspar, quartz and biotite with minor hornblende. Rarely, alkali feldspar forms up to 0.75 cm long phenocrysts.

The granite is a massive to weakly foliated rock. In some foliated outcrops in the east and northwest of the complex the strike of the foliation is parallel to the nearest contact with the dioritic rocks. East of boundary between Asselin and Baragar townships, this foliation has a north to south strike and dips to the west at an average of  $80^{\circ}$ . In the north of the complex the foliation has NE to SW trend and the dip varies between  $75^{\circ}$  NW to vertical. The few metavolcanic inclusions present in the granite have a random orientation.

### 3.5. QUARTZ MONZONITE

The quartz monzonite, which forms an up to 500 m wide dike near the northern margin of the complex, is in sharp contact with the granitic and dioritic rocks. The white to pink coloured rock weathers to light-grey and greyish brick-red in colour respectively. In hand

specimens it consists of alkali feldspars, plagioclase, amphibole, biotite and quartz. The colour index of the rock seldom exceeds 10.

The quartz monzonite is a coarse-grained rock and occasionally contains phenocrysts of microcline. These phenocrysts, when present, make up 10 to 15% of the rock. It is mostly a massive rock except near the margins where it shows a weak foliation developed due to the planar orientation of its constituent minerals. This vertical flow foliation strikes parallel to the contacts of the dike.

The assimilation zone around the inclusions and at the contacts of the rock is 1 to 3 cm wide. This zone is fine-grained and light grey to light greenish-gray in colour. Feldspar, quartz and minor muscovite were recognized in this zone.

### 3.6 CONCLUSION

The field observations and relations suggest the following sequence of events, which is similar to, but not identical with that deduced by Ayres (1969).

Basic magma intruded the metavolcanic-metasedimentary sequence, further deforming and cross-folding the already deformed and cross-folded country rock

near the complex. Crystallization and fractionation of this magma resulted in the formation of the inner gabbroic rocks.

The xenoliths and inclusions of the inner gabbroic series in the outer gabbroic series and fine-grained dikes of the latter in the former suggest that the two series were formed from two separate intrusions of basic magma. Moreover, the inner gabbroic rocks were already consolidated, cool and behaved rigidly at the time of the second intrusion, giving rise to most of the block faulting in the inner gabbroic rocks.

The rare inclusions of the outer gabbroic series in the dioritic rocks indicate that the latter intruded after the consolidation of the former. In addition, the block faulting in the inner gabbroic rocks may have been extended in the outer gabbroic rocks by this intrusive episode.

The sharp contacts and apophyses of granitic rocks in the dioritic and gabbroic rocks indicate that the granitic rocks were formed by the consolidation of a separate magma which intruded the already existing intrusive rocks.

Intrusion of monzonitic magma in the dioritic and granitic rocks is indicated by its cross-cutting rela-

tionship and reaction zones at the dike contacts.  
This conclusion is further supported by the presence  
of dioritic and metavolcanic inclusions in the quartz  
monzonite.



**CHAPTER 4****PETROGRAPHY**

Detailed examination of thin sections was undertaken to: (1) further distinguish the rock types in the field mappable units on the basis of their mineralogy, mode, and texture, (2) determine possible paragenetic trends in each rock group and genetic relationship of various groups, and (3) detect mineralogical differences that are undetectable in hand specimens. For this purpose 20 specimens of the inner gabbroic rocks, 18 specimens of the outer gabbroic rocks, 17 specimens of the dioritic rocks, 8 samples of the granitic rocks and 4 samples of quartz monzonite were used for detailed studies of modal analysis. Anorthite % in plagioclase were determined by measurements on flat stage using the Carlsbad-albite method for basic and intermediate rocks and the Michel Levy's method for the acidic rocks.

The field units are further classified and properly named following the IUGS classification of Streckeisen (1976 Appendix A). The petrographic studies indicate that there is no true gabbro in the

Table 4.1: Classification of rock types encountered in the Gamitagama lake Complex.

1. INNER GABBROIC SERIES

i. OLIVINE GABBRO

- a. Troctolite
- b. Olivine Gabbronorite
- c. Amphibole Olivine Gabbronorite

ii. GABBRO

- a. Gabbronorite
- b. Norite

iii. ANORTHOSITE

- a. Andesine Anorthosite

2. OUTER GABBROIC SERIES

i. GABBRO

- a. Norite
- b. Gabbronorite

ii. AMPHIBOLE GABBRO-PYROXENE DIORITE

- a. Amphibole Gabbronorite
- b. Pyroxene Diorite

3. DIORITIC ROCKS

i. DIORITE

- a. Hornblende Gabbro
- b. Diorite

ii. QUARTZ DIORITE

iii. QUARTZ MONZODIORITE

iv. TONALITE

4. GRANITIC ROCKS

i. GRANODIORITE

ii. GRANITE

5. QUARTZ MONZONITE

Table 4.2: Modal mineral compositions in the rocks of the Inner Gabbroic Series.

INNER GABBROIC ROCKS													
Rock Name	Troctolite			Olivine Gabbronorite				AOGN**			Gabbronorite		
	W100	W101	W104	W111	W103	W98	W64	W65	W112	W147	W151	W146	
Sample No.	W100	W101	W104	W111	W103	W98	W64	W65	W112	W147	W151	W146	
Plagioclase	72.3	70.8	58.1	60.3	50.9	54.2	40.7	36.1	71.1	54.4	56.4	59.6	
Olivine	22.7	23.1	21.4	12.2	10.7	9.9	26.5	14.5	-	-	-	-	
Corona	-	-	-	6.2	8.4	8.3	-	-	-	-	-	-	
Clinopyroxene	3.5	3.1	3.4	9.6	10.1	8.9	2.5	12.8	16.8	17.3	21.1	18.7	
Orthopyroxene	0.6	0.9	3.9	6.9	17.4	15.3	3.5	14.5	8.3	21.4	11.1	16.6	
Amphibole	0.4	0.6	1.4	4.1	0.3	0.5	24.3	21.0	1.0	tr	0.8	1.5	
Mica	tr*	tr	-	-	0.2	-	2.0	0.2	-	tr	tr	-	
Opauques	0.3	1.3	11.8	0.7	1.4	2.1	0.3	0.8	2.1	5.7	10.5	3.6	
Apatite	tr	tr	tr	tr	0.6	0.7	tr	tr	0.7	1.2	tr	tr	
An# in Plag.	74	74-72	70	66-64	65	65-62	66-62	64	64	58	56	54	

INNER GABBROIC ROCKS (CONT'D)									
Rock Name	Norite			Andesine Anorthosite		Inclusions			
	W149	W96	W144	W138	W148	W143	W155	W156	
Sample No.	W149	W96	W144	W138	W148	W143	W155	W156	
Plagioclase	66.7	80.5	68.9	71.4	83.7	88.7	44.9	64.3	
Olivine	-	-	-	-	-	-	30.1	-	
Clinopyroxene	2.3	1.7	0.3	4.6	tr	-	10.6	20.1	
Orthopyroxene	26.2	10.7	22.0	19.4	6.9	2.8	5.2	10.3	
Amphibole	0.5	tr	tr	-	1.6	3.2	2.1	tr	
Mica	tr	-	tr	-	0.3	-	0.1	tr	
Opauques	4.2	5.5	7.2	4.1	6.4	5.2	7.0	5.0	
Apatite	tr	1.5	1.4	0.4	1.0	tr	tr	tr	
An# in Plag.	52	54	52	50	48	46	68	62	

\* Trace

\*\* Amphibole Olivine Gabbronorite

complex and the rocks classified in the field under this name are norite and/or gabbronorite (Table 4.1).

#### 4.1 INNER GABBROIC ROCKS

The modal mineral compositions of the inner gabbroic rocks are presented in Table 4.2. The modal compositions, are plotted after Streckeisen (1976) in Figure 4.1.

##### 4.1.1 OLIVINE GABBRO

###### 4.1.1.1 TROCTOLITE:

The troctolite is a coarse-grained, hypidiorhmic granular rock with a maximum 2.5x1.5 mm in grain size. It consists of about 70 to 73% plagioclase, 20 to 24% olivine, 3 to 4% clinopyroxene, less than 1% orthopyroxene, and minor, variable amounts of opaques and amphibole. It has a heterogeneous distribution of its constituent minerals and the rock is banded in part. The bands are defined by variation of mineral proportions and mineral species present and range in thickness from 11 to 51 cm.

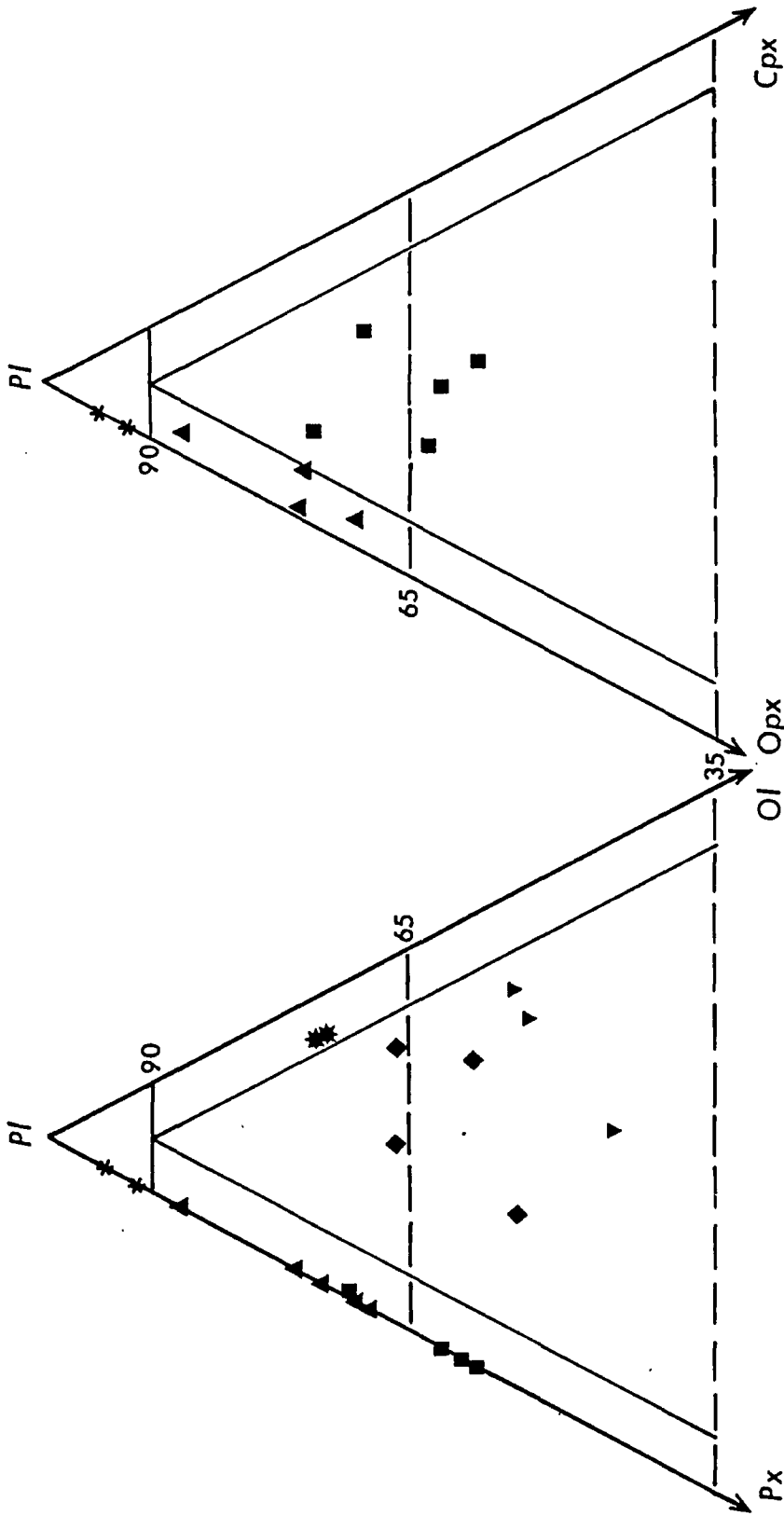


Figure 4.1 Modal mineral proportions in rocks of the Inner Gabbroic Series.

- (\*) Troctolite
- (◆) Olivine Gabbronorite
- (▼) Amphibole Olivine Gabbronorite
- (■) Gabbronorite
- (▲) Norite
- (\*) Andesine Anorthosite

Field boundaries according to Streckeisen (1976).

Thick bands, within this banding, contain about 75 to 80% plagioclase, 19 to 24% olivine and minor opaques. The thin laminations which alternate with the thick bands consist of 55 to 60% plagioclase, 15 to 20% olivine, 10 to 15% clinopyroxene, 4 to 5% orthopyroxene, 0 to 5% amphibole, and minor variable amounts of opaques.

Unzoned plagioclase (An<sub>72-74</sub>) forms euhedral to subhedral tabular crystals most of which are 2x1 mm in dimensions. Twinning is common on the albite and Carlsbad-albite laws but rare on the pericline law. Inclusion of prismatic apatite maximum 0.1x0.3 mm are rare. Alteration of plagioclase to saussurite in places, maximum 0.2 mm in diameter, is common.

The olivine, about 1x0.7 mm in maximum dimension, forms isolated subhedral to anhedral grains. Some of the grains have a strongly embayed outline indicating magmatic resorption. Inclusions of lath-shaped plagioclase, maximum 0.1x0.2 mm in dimension, occur enclosed in olivine. Many of the olivine crystals are partially to completely enclosed by 0.1 mm wide reaction rims of clinopyroxene. In some cases multiple rims of consecutively occurring clinopyroxene, orthopyroxene, and hornblende enclose or partially



Photo 4.1a: Troctolite showing olivine partially rimmed by clinopyroxene, orthopyroxene, and amphibole (dark). Plane light, field of view 1.5X1 mm

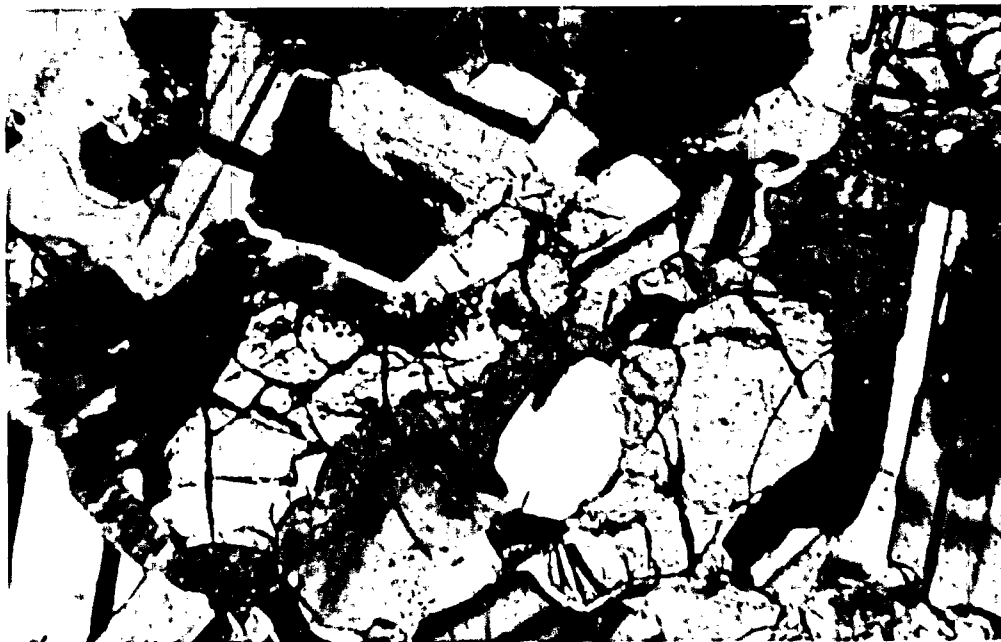


Photo 4.1b: Same as above, crossed nicols.

surround olivine grains (Photo 4.1a & 4.1b). In other cases one or more of these rims may be absent. Apparently, reaction of olivine with the magma was not complete upon final consolidation of the rock or further reaction between olivine and interstitial liquid was stopped by the surrounding rims. Olivine is generally fresh except for thin margins along internal fractures filled with opaque material and an iddingsite-like mineral.

Subhedral to anhedral titaniferous magnetite, about 1 mm in diameter, occupies the interstices between plagioclase and olivine and is commonly enclosed by amphibole reaction rims.

Anhedral clinopyroxene, maximum 0.5x0.2 mm, occupies interstitial positions and forms reaction rims around olivine. It has a neutral body colour and may be enclosed in partial to complete amphibole reaction rims. Neutral to pink pleochroic orthopyroxene is mostly restricted to 0.1 mm wide reaction rims around olivine. Interstitial anhedral grains are rare but when present are optically similar to the orthopyroxene of reaction rims. Amphibole, pleochroic from light yellowish-brown to dark reddish-brown, forms partial to complete reaction rims around both



orthopyroxene and clinopyroxene. Occasional flakes of phlogopite, about 0.1x0.2 mm in dimension are associated with the amphibole.

#### 4.1.1.2 OLIVINE GABBRONORITE:

The transition from troctolite to olivine gabbronorite is gradual and marked by decrease in modal olivine and plagioclase and relative increase in pyroxenes (Figure 4.1).

The olivine gabbronorite is a coarse-grained, hypidiomorphic granular rock and has a heterogeneous mineral distribution. It has a maximum 3x2 mm grain size and consists of 50 to 60% plagioclase, 10 to 21% olivine, 3 to 10% clinopyroxene, 4 to 17% orthopyroxene, 0 to 12% opaques, 0 to 8% symplectic corona and variable minor amounts of amphibole and mica.

Subhedral to anhedral plagioclase crystals ( $An_{62-70}$ ) reach a maximum of 3x2 mm in grain size. Twinning is common on the albite and Carlsbad-albite laws but is rare on the pericline law. A weak normal zoning, cores slightly more calcic than rims, is present in a few grains. Inclusions of subhedral opaque minerals, about 0.1 mm in diameter, are rare but when present occur near the crystal boundaries.

Protoclastic texture is indicated by bends and kinks in the twin lamellae. Alteration of plagioclase to saussurite occurs in rare patches which are maximum 0.1 mm in diameter.

Anhedral olivine, maximum 2x1.5 mm in dimension, commonly has an irregular embayed outlines showing effects of magmatic resorption. Aggregates of sub-hedral to anhedral olivine, about 0.5 mm in diameter, and pyroxenes may reach to 3 mm in diameter. Inclusions of 0.05x0.1 mm plagioclase laths (An<sub>72-74</sub>) and 0.2x0.1 mm anhedral opaque minerals are found in a few olivine crystals (Photo 4.2). Alteration to iddingsite-like secondary opaque mineral along internal cracks is common.

Symplectic coronas have developed along boundaries between olivine and plagioclase (Photo 4.3). The coronas typically are 0.1 to 0.2 mm wide and comprise two to three zones. The observed assemblage is olivine + orthopyroxene + amphibole + (intergrowth of amphibole and plagioclase/spinel) + plagioclase. The zone nearest to olivine consists of bladed grains of orthopyroxene with their longer dimension parallel to olivine margin. The next zone is a band of fine-grained, bluish-green amphibole oriented perpendicular to orthopyroxene. Occasionally, when orthopyroxene



Photo 4.2: Olivine gabbronorite showing olivine with inclusions of plagioclase (white) and magnetite. Note the early separation of abundant titaniferrous magnetite. Plane light, field of view 1.5X1 mm.



Photo 4.3: Olivine gabbronorite showing olivine with corona of orthopyroxene + amphibole + (amphibole+plagioclase) + plagioclase. Olivine inside the corona is partially replced by orthopyroxene and trellis-like magnetite. Plane light, field of view 0.75X0.5 mm.

is absent, the margin of amphibole in contact with olivine is marked by a thin bleached zone showing no colour or pleochroism. The outer zone of the corona is symplectite and consists of wormy intergrowth of green amphibole and plagioclase or in a few cases, spinel. Several examples were observed where olivine in the corona cores is partially or completely replaced by orthopyroxene or tremolite-actinolite containing a trellis-like intergrowth of magnetite.

Subhedral to anhedral clinopyroxene, about 2x1 mm in maximum dimension, has neutral to faint brownish body colour. It shows simple twinning parallel to (100) and rare multiple, parallel to (001) twinning (Photo 4.4). Larger crystals of clinopyroxene poikilolitically enclose plagioclase laths (0.3x0.2 mm), anhedral olivine (0.3x0.1 mm), and opaque crystals (0.1 mm). Thin plates and larger blebs of orthopyroxene are exsolved from the clinopyroxene parallel to (100) and (001) respectively. The multiple twinning differs from exsolution in the regularity and extinction of lamellae. In the former case, the twin lamellae in the same crystal are variable in width and have different extinction positions. In the latter, the exsolving plates are regularly spaced and show an even

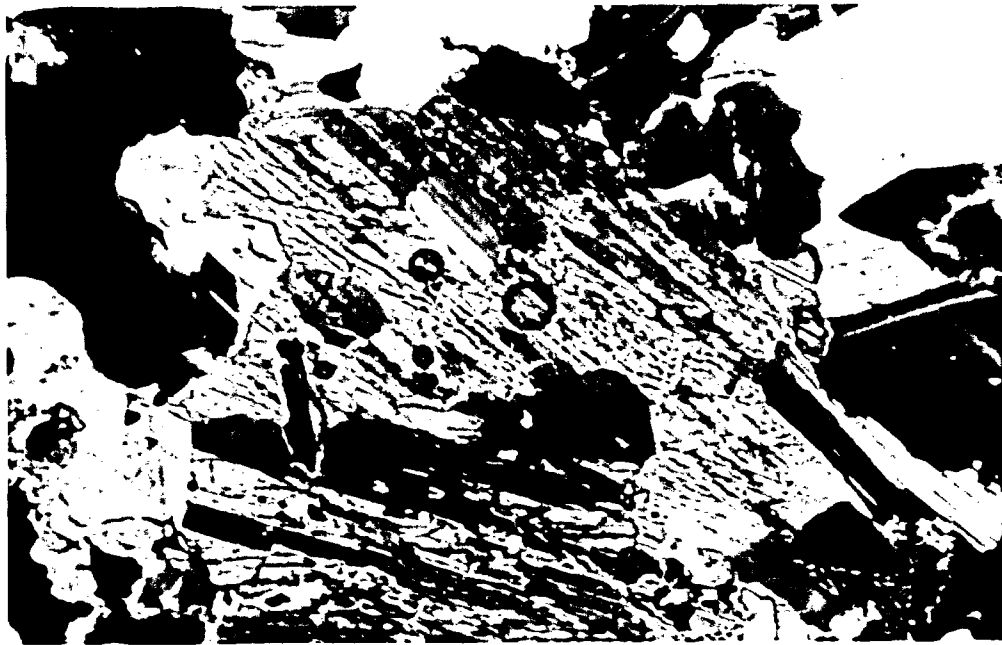


Photo 4.4: Olivine gabbronorite showing clinopyroxene with plagioclase, olivine, and titaniferrous magnetite inclusions. Note the multiple twinning in the clinopyroxene. Crossed nicols, field of view 1.5X1 mm.



Photo 4.5: Olivine gabbronorite showing orthopyroxene with olivine, clinopyroxene (near left bottom), and plagioclase inclusions. Crossed nicols, field of view 1.5X1 mm.

extinction. Reaction rims of amphibole around clinopyroxene are less than 0.2 mm wide.

Besides occurring as reaction rims around olivine and clinopyroxene, orthopyroxene forms discrete, rarely subhedral to anhedral crystals less than 3x2 mm in dimension. It is moderately pleochroic, from neutral to pink, and poikilitically encloses subhedral plagioclase (0.2x0.1 mm), anhedral olivine (0.2x0.3 mm) and subhedral to anhedral titaniferous magnetite less than 0.1 mm in diameter (Photo 4.5). Smaller orthopyroxene grains occupy the interstitial positions. Partial to complete, maximum 0.2 mm wide, reaction rims of amphibole around orthopyroxene are often present.

Euhedral to subhedral prismatic apatite, maximum 0.5x1 mm in dimension, occur together with plagioclase and mafic minerals. Smaller prismatic crystals, about 0.1x0.4 mm, occupy interstitial positions and often occur enclosed in opaques.

Anhedral titaniferous magnetite\*, about 0.1 mm in diameter, occupy interstitial positions between plagioclase and mafic minerals. Amphibole, pleochroic

\*Determined by XRD and XRF

from light yellowish-brown to dark reddish-brown, forms partial to complete reaction rims around mafic minerals and magnetite. Phlogopite flakes, about 0.2x0.1 mm in dimension, and pleochroic from light brownish-yellow to dark brownish-red, are occasionally associated with amphibole or form partial reaction rims around titaniferous magnetite.

Plagioclase and clinopyroxene exhibit a distinct clouded appearance extending from the crystal cores to about 0.05 to 0.1 mm inside from margins. The clouding, under high power objective, appears to be caused by minute inclusions of oxide or mafic silicates, probably exsolved or diffused into the crystals while temperature was high but below solvus. The clear outer edges of crystals indicated that these margins are late additions to the primary crystals.

#### 4.1.1.3 AMPHIBOLE OLIVINE GABBRONORITE:

The transition of olivine gabbronorite and troctolite to amphibole olivine gabbronorite occurs by decrease in modal plagioclase and increase in modal amphibole.

The amphibole olivine gabbronorite is a coarse grained (maximum 10x8 mm) hypidiomorphic granular

rock, and has a heterogeneous mineral distribution. The plagioclase crystals occur in clumps surrounded by mafic aggregates showing synneusis texture. It consists of 36 to 41% plagioclase, 14 to 27% olivine, 2 to 13% clinopyroxene, 3 to 15% orthopyroxene, 21 to 24% amphibole, and variable, minor amounts of phlogopite and magnetite.

Plagioclase ( $An_{62-66}$ ) occurs as anhedral to subhedral tabular crystals which are about 3x2 mm in maximum dimension. Twinning on the albite and Carlsbad-albite laws is common, but is rare on the pericline law. Weak, normal zoning is present in a few grains. Alteration to saussurite and occasionally to carbonate occurs in small irregular patches, about 1 mm in diameter, inside the plagioclase crystals.

Anhedral olivine crystals, maximum 1.5x1 mm, are generally enclosed in the amphibole and show strong effects of magmatic resorption. A thin, about 0.05 mm wide, orthopyroxene rim commonly separates the rare subhedral olivine and enclosing amphibole. Inclusions of plagioclase laths ( $An_{72-74}$ ), about 0.1x0.05 mm in dimensions, occur enclosed in olivine. Alteration to serpentine and secondary magnetite is common along internal cracks.



Clinopyroxene, maximum 2.5x2 mm in size, forms anhedral to subhedral crystals and is neutral to slightly brownish in colour. It poikilitically encloses 0.2x0.1 mm plagioclase laths and about 0.1 mm in diameter anhedral olivine crystals. Amphibole forms partial to complete, reaction rims around clinopyroxene about 0.1 mm wide.

Orthopyroxene, about 2.75x2.5 mm in dimension, forms anhedral crystals. It is pleochroic from neutral to pink and poikilitically encloses about 0.3x0.2 mm plagioclase laths, 0.2 mm in diameter anhedral olivine and 0.3x0.15 mm large subhedral clinopyroxene crystals. Smaller grains of anhedral orthopyroxene occupy the interstitial positions. Exsolution of clinopyroxene in very thin lamellae parallel to (100) is restricted to a few larger crystals. The reaction rims of amphibole around hypersthene are variable, maximum 0.5 mm, in width.

Anhedral titaniferous magnetite, maximum about 0.5x0.2 mm, occupy interstitial positions. Amphibole and phlogopite form reaction rims around it.

Amphibole, pleochroic from light yellowish-brown to dark reddish-brown, has an interstitial habit apart from its reaction rims around olivine and pyroxens. These interstitial grains become large at places and

join each other to poikilitically enclose plagioclase, olivine, and pyroxene crystals. Such amphiboles sometimes reach up to 1 cm in diameter.

Anhedral phlogopite flakes, maximum 1.5x1 mm, are pleochroic from light-yellow to dark brownish-red and occur associated with amphibole.

#### 4.1.2 GABBRO

The gabbro unit is further divided into two rock types, gabbronorite and norite, on the basis of modal proportions of the constituent pyroxenes (Table 4.1 and 2; Figure 4.1).

##### 4.1.2.1 GABBRONORITE:

The transition from olivine gabbronorite to gabbronorite is marked by gradual decrease of modal olivine to less than 5% and by the occurrence of clinopyroxene as the major primary phase. In addition, orthopyroxene changes habit from anhedral, interstitial crystals to subhedral, prismatic crystals.

The gabbronorite is a heterogeneous, coarse grained, hypidiomorphic granular rock with maximum

grain size of 7x5 mm. Occasionally it shows an orthogonal mosaic texture containing randomly oriented subhedral plagioclase laths. It consists of 54 to 71% plagioclase, 16 to 21% clinopyroxene, 11 to 22% orthopyroxene, 2 to 11% opaque minerals, with variable, minor amounts of amphibole, phlogopite and apatite.

Plagioclase ( $An_{64-54}$ ) forms, about 3x2 mm in size, euhedral to subhedral interlocking crystals. Twinning is common on the albite law, less common on the Carlsbad-albite law and uncommon on the pericline law. Weak normal zoning (less than 5% An) is observed in a few plagioclase crystals. Protoclastic texture is rare and indicated by bends and kinks in the lamellae. Alteration to saussurite and occasionally to carbonate in small patches, about 0.2 mm in diameter, is rare.

Euhedral to subhedral clinopyroxene, maximum about 4x3 mm in maximum dimension, is neutral to pale-brown. Simple twinning parallel to (100) is common in clinopyroxene. Exsolution of orthopyroxene, in the form of thin plates parallel to (100) is present in most of the clinopyroxene crystals (Photo 4.6a & 4.6b). Reaction rims of amphibole, less than 1 mm wide, are rare.

Orthopyroxene, up to 7x5 mm in dimension, shows characteristic neutral to pink pleochroism. It forms subhedral to anhedral prismatic crystals. Inclusions of subhedral to anhedral opaque grains, about 0.1 mm in diameter, are often present near the crystal boundaries in orthopyroxene. A few crystals of orthopyroxene contain regularly oriented, rectangular opaque plates arranged parallel to (001). Exsolution of very thin clinopyroxene lamellae occur parallel to (100). Amphibole occasionally forms reaction rims around orthopyroxene. Alteration to tremolite-actinolite amphibole is often present, in traces, at orthopyroxene crystal boundaries.

Apatite is of two generations. Large subhedral to anhedral crystals, about 1.5x1 mm in size, occur together with the major mineral phases. Smaller prismatic crystals of 0.05x0.3 mm occupy interstitial position and occasionally occur enclosed in opaques.

Opaque minerals, up to 1x0.5 mm, mainly titaniferous magnetite with some chalcopyrite, occur interstitially. Reaction rims of amphibole, which is pleochroic from light yellowish-brown to dark reddish-brown, occur around titaniferous magnetite. Phlogopite flakes, up to 0.5x0.2 mm, are pleochroic from light-yellow to dark brownish-red and often occur



Photo 4.6a: Gabbro showing clinopyroxene which optically encloses plagioclase crystals. Plane light, field of view 3x2 mm.

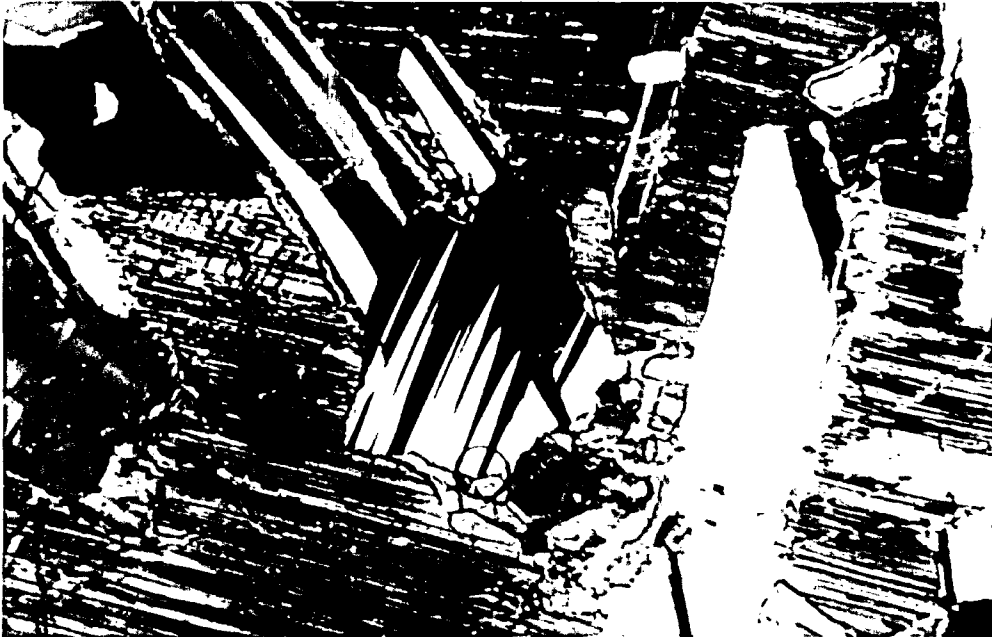


Photo 4.6b: Clinopyroxene showing exsolved plates of orthopyroxene parallel to (100). Crossed nicols, same as above.

associated with amphibole. It may form partial to complete, less than 0.1 mm wide reaction rims directly around titaniferous magnetite.

Plagioclase and clinopyroxene of the gabbro-norite, like those of the olivine gabbro-norite, also exhibit clouded appearance caused by minute accicular inclusions of oxides or mafic silicates. These inclusions (Photo 4.7) appear to be oriented parallel to (100) and (001) directions of host plagioclase and clinopyroxene. The clear outer edges of the host crystals indicate that these margins are a late addition to the primary crystals.

In the layered gabbro-norite the felsic layers consist of about 90% plagioclase, 5% pyroxenes, and traces of titaniferous magnetite. The mafic layers contain about 60% clinopyroxene, 30% orthopyroxene, 5% titaniferous magnetite, and 5% plagioclase. The two pyroxenes occur in variable proportions with their longer dimensions parallel to felsic layers. Both plagioclase and pyroxenes have similar characteristics and grain size to those described above in the unlayered rock.

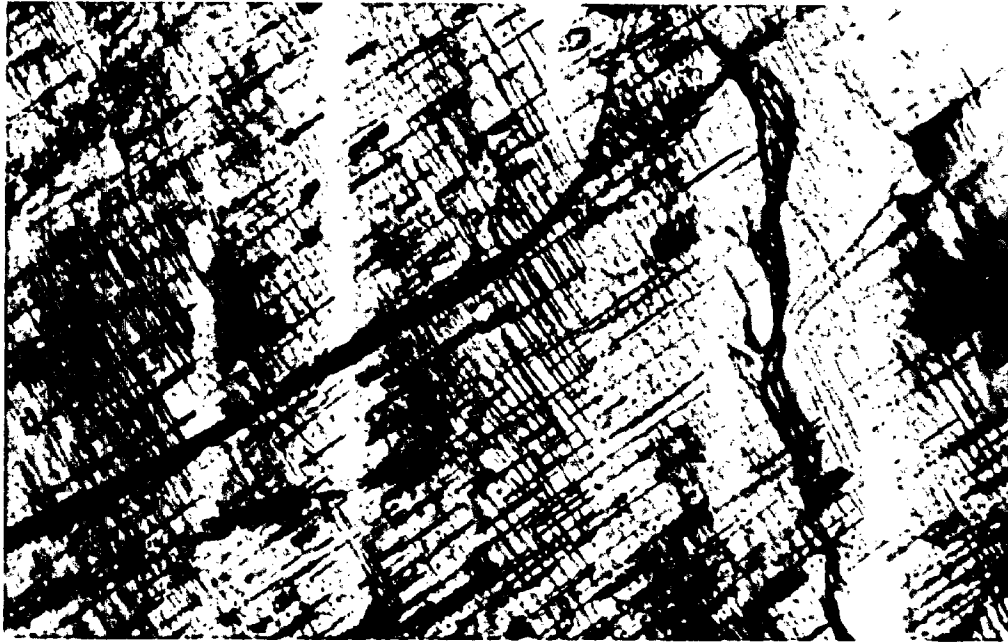


Photo 4.7: Gabbronorite showing clinopyroxene with accicular inclusions of oxide or mafic silicates oriented parallel to (100) and (001) directions. Plane light, field of view 0.75X0.5 mm.

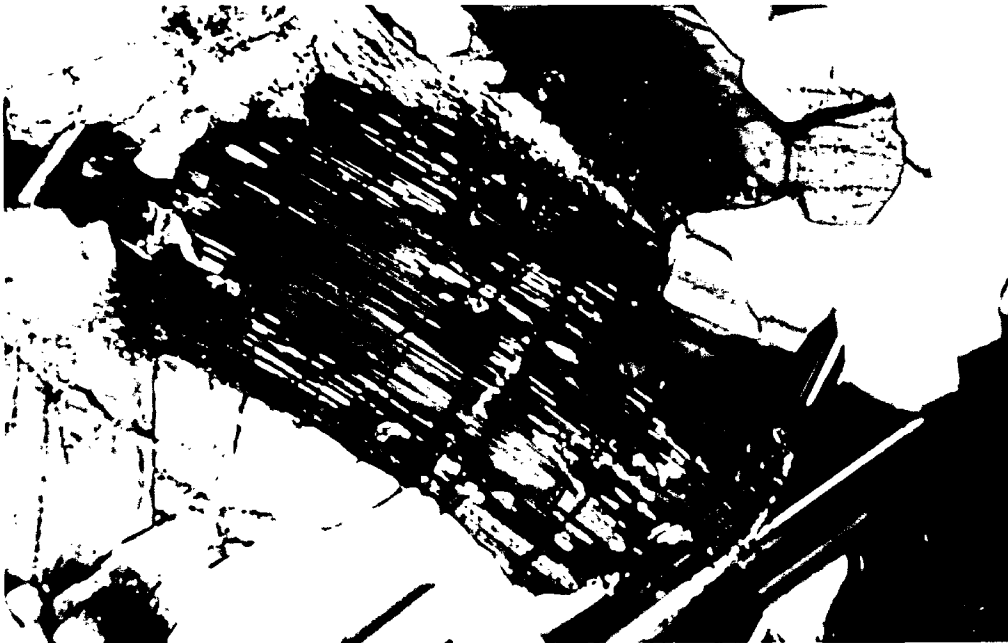


Photo 4.8: Norite showing orthopyroxene with very thin lamellae of clinopyroxene exsolved parallel to (100). Crossed nicols, Field of view 3X2 mm.

#### 4.1.2.2 NORITE:

The transition from gabbronorite to norite is marked by the increase in modal orthopyroxene and gradual decrease in clinopyroxene to less than 5% (Figure 4.1; Table 4.2).

The norite is a heterogeneous, coarse grained, hypidiomorphic granular rock with a maximum grain size of 5x3 mm. It rarely shows subophitic texture in which clinopyroxene partially encloses plagioclase laths. The norite consists of 66 to 81% plagioclase, 1 to 5% clinopyroxene, 10 to 26% orthopyroxene, and 4 to 8% opaque minerals with minor variable amounts of amphibole, phlogopite and apatite.

Plagioclase ( $An_{50-54}$ ) forms euhedral to subhedral crystals, about 3x2 mm in maximum dimensions. It occurs as a mosaic texture of interlocking crystals. Twinning is common on the albite law, less common on the Carlsbad albite law, and uncommon on the pericline law. Weak normal zoning, with cores slightly more calcic than margins, was observed in a few crystals. Inclusions of prismatic apatite, about 0.3x0.2 mm, and subhedral to anhedral titaniferous magnetite, about 0.2 mm in diameter, are occasionally



present. Alteration to saussurite and carbonate occurs in small irregular patches, about 1x1.5 mm in dimension.

Orthopyroxene, which shows a neutral to pink pleochronism, forms euhedral to subhedral rectangular crystals about 5x2 mm in dimensions. Subhedral to anhedral opaque inclusions, about 0.2 mm in diameter, most often occur near the margins of the orthopyroxene crystals. Inclusions of anhedral clinopyroxene, less than 0.2 mm in diameter, are rare. Exsolution of clinopyroxene in very thin lamellae parallel to (100) of orthopyroxene occur in many crystals (Figure 4.8). Protoclastic texture is indicated by bends and kinks in crystals showing wavy extinction.

Clinopyroxene, neutral in colour and about 3x1.5 mm in maximum dimension, occurs in subhedral to anhedral crystals. Inclusions of minute, regularly oriented, rectangular opaque plates occur parallel to (001). Exsolution of thin orthopyroxene plates parallel to (100) is almost always present but broad plates parallel to (001) are rare. Partial to complete reaction rims of amphibole around clinopyroxene, less than 0.1 mm wide, are rare.

Titaniferous magnetite forms about 1x0.75 mm large, subhedral to anhedral crystals which occupy

interstitial positions. Amphibole, pleochroic from light yellowish-brown to dark reddish-brown, forms reaction rims around titaniferous magnetite individually or together with light-yellow to dark brownish-red pleochroic phlogopite.

Small prismatic apatite crystals, about 0.4x0.05 mm in dimension, occupy interstitial positions together with titaniferous magnetite. Occasionally these apatite crystals occur enclosed in titaniferous magnetite.

In the layered norite felsic layers contain about 91% plagioclase, 9% hypersthene and minor amounts of titaniferous magnetite and clinopyroxene. The plagioclase forms interlocking mosaic texture in these bands (Photo 4.9a). Euhedral orthopyroxene occurs tightly packed with plagioclase and has a random orientation. Subhedral to anhedral titaniferous magnetite occupies interstitial positions.

The mafic layers consist of about 81% orthopyroxene, 8% plagioclase, 10% titaniferous magnetite, and 2% clinopyroxene. Subhedral orthopyroxene and clinopyroxenes are linked into chains parallel to layering. Magnetite has an interstitial habit with longer dimension parallel to the layering.

The contact between the layers is sharp or nearly so and no gradation from one layer to an other layer was observed.

#### 4.1.3 ANORTHOSITE

##### 4.1.3.1 ANDESINE ANORTHOSITE:

The transition from norite to andesine anorthosite occurs by the disappearance of clinopyroxene, gradual decrease in orthopyroxene to less than 10% and by decrease in the An% of plagioclase to less than 50.

The andesine anorthosite is a coarse grained, hypidiomorphic granular rock with a maximum grain size of about 3x2 mm. It has a heterogeneous distribution of its constituent minerals. The rock consists of 83 to 88% plagioclase, 0 to 7% orthopyroxene, 5 to 6% titaniferous magnetite, and variable, minor amounts of amphibole and phlogopite.

Subhedral plagioclase (An<sub>46</sub> to 48) occurs in interlocking crystals, maximum 3x2 mm, and producing an orthogonal mosaic texture (Photo 4.9b). Twinning on the albite law is common but is rare on the Carlsbad-albite and percline laws. Plagioclase rarely shows slight (about 2% An) normal zoning. Inclusions

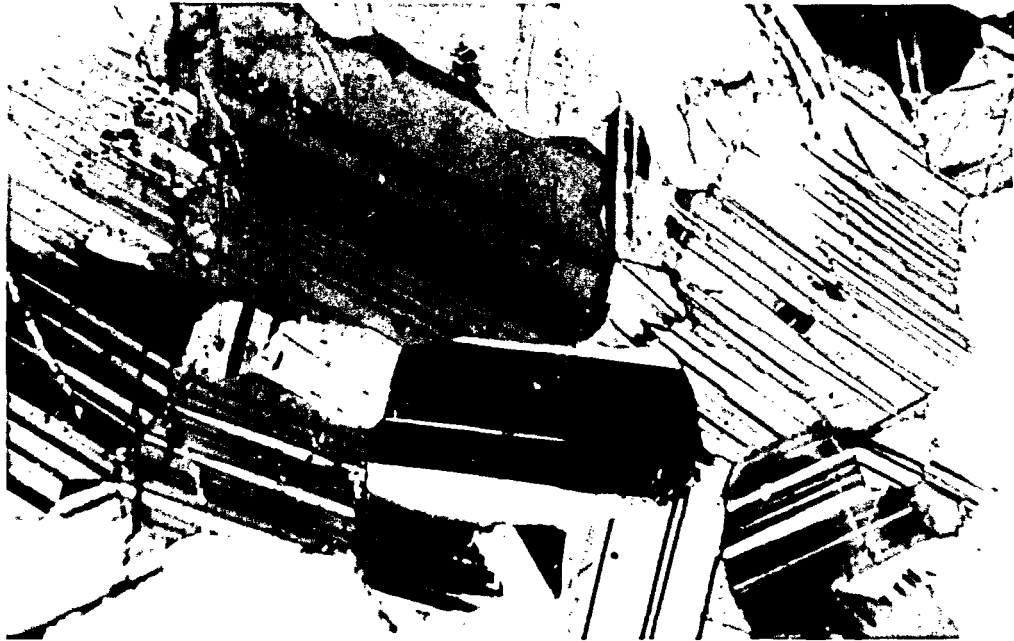


Photo 4.9a: Andesine anorthosite showing oriented tabular crystals of plagioclase. Crossed nicols, field of view 3X2 mm.

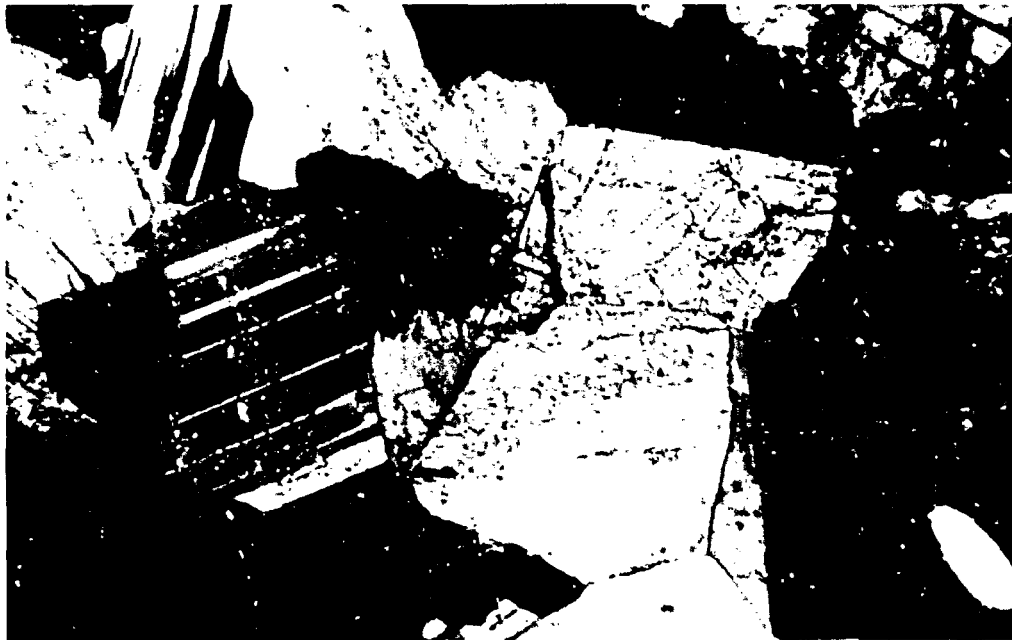


Photo 4.9b: Andesine anorthosite showing orthogonal mosaic texture of plagioclase. Crossed nicols, field of view 3X2 mm.

of regularly oriented fine acicular opaques or mafic silicates occur oriented parallel to (100) and (001) planes of plagioclase crystals. Alteration to saussurite and carbonate patches, about 0.1 mm in diameter, are occasionally present.

Orthopyroxene, maximum  $1 \times 0.5$  mm, pleochroic from neutral to pink, forms subhedral to anhedral crystals which have random orientation. Exsolution of very fine lamellae of clinopyroxene parallel to (100) is common. Alteration to tremolite-actinolite is rare and restricted to crystal boundaries.

Apatite, about  $0.3 \times 0.05$  mm in dimensions, forms prismatic crystals and is often associated with and included in subhedral to anhedral titaniferous magnetite. The latter occupies the interstitial positions between plagioclase and orthopyroxene crystals. Amphibole, pleochroic from light yellowish-brown to dark-brown, forms reaction rims around magnetite. It also occurs in  $0.2 \times 0.1$  mm anhedral crystals separately or together with light-yellow to dark brownish-red pleochroic phlogopite. Separate reaction rims less than 0.1 mm wide of phlogopite around magnetite are rare.

The samples W155 and W156 (Table 4.2) are of coarse grained, hypidiomorphic granular rocks of the

inner gabbroic series and were collected from the drill cores of Cu-Ni showings near the southern boundary of the complex.

The core sample W155 in hand specimen contains 2 to 3 cm wide segregated sulphide layers. The modal mineral composition of the rock consists of about 50% plagioclase, 30% olivine, 11% clinopyroxene, 5% orthopyroxene, 6% sulphides and minor variable amounts of titaniferous magnetite, amphibole, and mica.

Olivine, 2x1.5 mm in maximum dimension, forms euhedral to anhedral crystals and occurs enclosed in plagioclase. A thin, less than 0.1 mm wide, orthopyroxene rim around olivine usually separates it from enclosing plagioclase (Photo 4.10a & 4.10b). Olivine is generally fresh except for thin margins along internal fractures, filled with opaque material and iddingsite-like mineral.

Plagioclase (An<sub>70</sub>) forms subhedral to anhedral crystals maximum 3x2 mm in maximum dimension. It shows twinning on the albite and Carlsbad-albite laws and often enclose olivine crystals. Alteration to saussurite is rare.

Both clinopyroxene and orthopyroxene form 0.75x0.5 mm anhedral crystals, and occupy interstitial positions between plagioclase and olivine. Anhedral

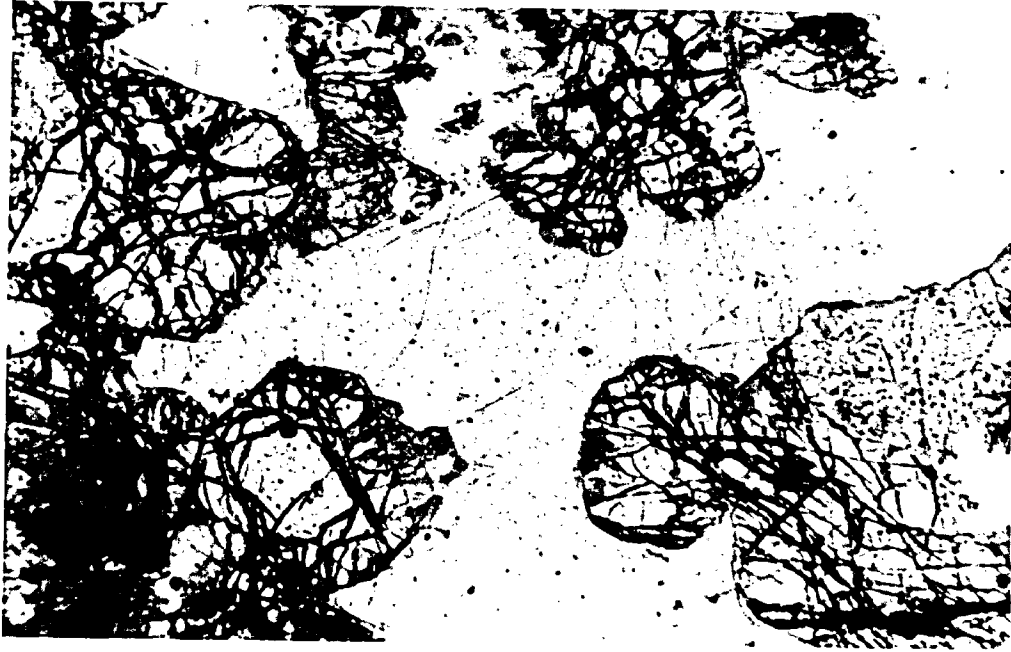


Photo 4.10a: Core sample W155 showing euhedral to subhedral olivine crystals enclosed in plagioclase. Thin rims of orthopyroxene separate olivine crystals from plagioclase. Plane light, field of view 3X2 mm.

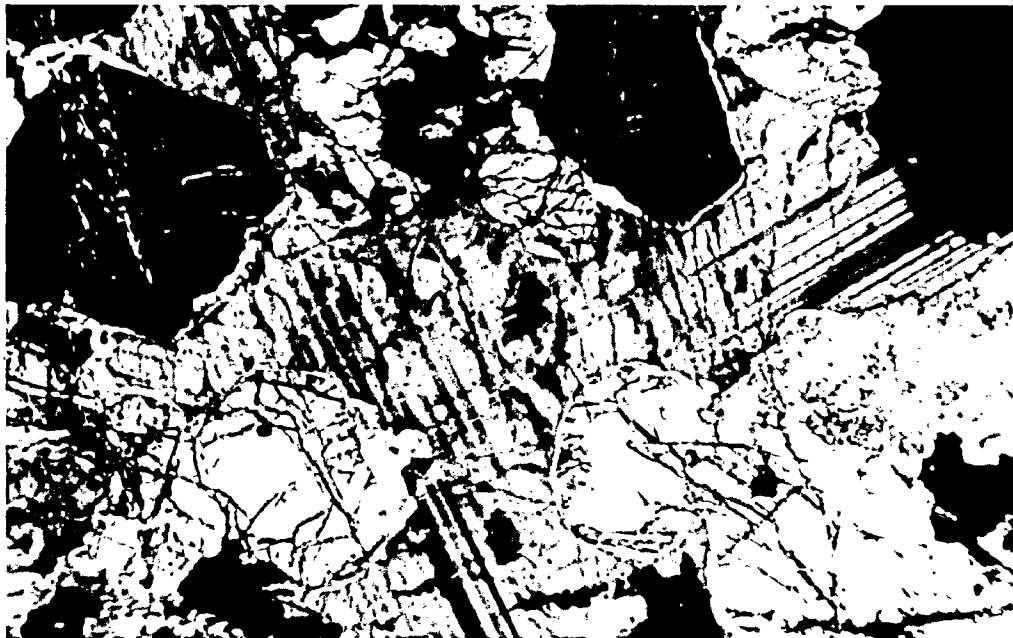


Photo 4.10b: Same as above, crossed nicols.

titaniferous magnetite (maximum 0.2 mm in diameter) is commonly associated with the pyroxenes. Amphibole, pleochroic from light yellowish-brown to dark reddish-brown form partial to complete reaction rims around titaniferous magnetite and pyroxenes. AnhedraI phlogopite, pleochroic from light brownish-yellow to dark brownish-red also occurs associated with amphibole.

Sulphides occupy interstitial positions between plagioclase and olivine and form layers parallel to the longer dimensions of these silicates. Pyroxenes and titaniferous magnetite were not observed sharing interstitial positions with the sulphides.

The sample W157 is also from the same drill core. It consists of 64% plagioclase, 20% clinopyroxene, 10% orthopyroxene, 3% sulphides and 2% titaniferous magnetite. Sulphides occupy interstitial positions individually or together with titaniferous magnetite. The rock, in modal mineralogy and petrographic characteristics, is similar to the previously described gabbro-norite.



#### 4.1.4 PARAGENESIS:

One of the most interesting textural features of the inner gabbroic rocks is the numerous well developed reaction relations between the mafic phases. The entire discontinuous reaction series of Bowen is represented by these reaction rims. The reaction relationships indicate a strong fractionation and disequilibrium between crystals and the melt. Relatively rapid cooling or a quick deposition of the crystals, away from the melt, may have prevented the completion of large scale reaction of the entire crystals and the liquid.

To summarize, the following reaction relationships were observed in the inner gabbroic series:

1. Olivine commonly has single or multiple reaction rims of clinopyroxene, orthopyroxene and amphibole.
2. Clinopyroxene encloses olivine and occurs enclosed in orthopyroxene and/or amphibole reaction rims.
3. Orthopyroxene encloses olivine, clinopyroxene and magnetite and itself occurs enclosed in amphibole reaction rims.

Table 4.3: Summary of petrographic observations in the Inner Gabbroic Series.

<u>ROCK TYPE</u>	<u>PHASE CHANGES</u>	<u>RATIO CHANGES</u>	<u>FORM CHANGES-REACTION RIMS</u>	<u>TEXTURE-STRUCTURE</u>	<u>CUMULUS TEXTURE</u>
Andesine Anorthosite	Disappearance of Opx.	Decrease in Opx. Increase in Plag.	Subhedral Plag. Subhedral to anhedral Opx and Ti. Magnetite. Amphibole rims Opx and Ti. Magnetite	Interlocking mosaic texture of Plag.	Cumulus Plag, Opx, and Ti. Magnetite. Intercumulus Amphibole. Adcumulate
Norite	Disappearance of Cpx.	Decrease in Cpx. Increase in Plag. Increase and then decrease in Opx.	Subhedral to anhedral Cpx and Ti. Magnetite. Subhedral to euhedral Opx. Amphibole rims Pyroxene and Ti. Magnetite	Rarely banded. Clumping of Pyroxene into chains	Cumulus Plag, Cpx, Opx, and Ti. Magnetite. Intercumulus Amphibole. Adcumulate
Gabronorite	Disappearance of Olivine	Increase in Cpx, Opx, and Ti. Magnetite	Subhedral to euhedral Plag and Cpx. Subhedral to anhedral Opx and Ti. Magne- tite. Amphibole rims Cpx, Opx and Ti. Magnetite	Rarely banded. Mosaic texture of Plag. Clumping of Pyroxene into chains and spheri- cal aggregates	Cumulus Plag, Cpx, Opx, and Ti. Magnetite. Intercumulus Amphibole. Adcumulate
Olivine Gabronorite and Amphibole Olivine Gabronorite	Appearance of Pyroxene	Decrease in Olivine and increase in Pyroxene and Plag.	Subhedral to anhedral Plag and Olivine. Pyroxenes rim Olivine and Amphibole rims Pyroxene and Olivine in early stages. Cpx becomes subhedral in late stages	Cpx poikilitically encloses Plag and Olivine. Opx poikilitically encloses Plag, Olivine and Cpx.	Cumulus Plag, Olivine, Cpx, and Ti. Magnetite. Intercumulus Opx and Amphibole. Orthocumulate
Troctolite	Plag, Olivine and Ti. Magne- tite form the major phases	Plag dominates the rock	Subhedral Plag and Olivine. Rare reaction rims of Cpx, Opx, and Amphibole	Rarely banded. Mosaic texture of Plag. Olivine embayed	Cumulus Plag, Olivine, and Ti. Magnetite. Intercumulus Cpx, Opx, and Amphibole. Adcumulate

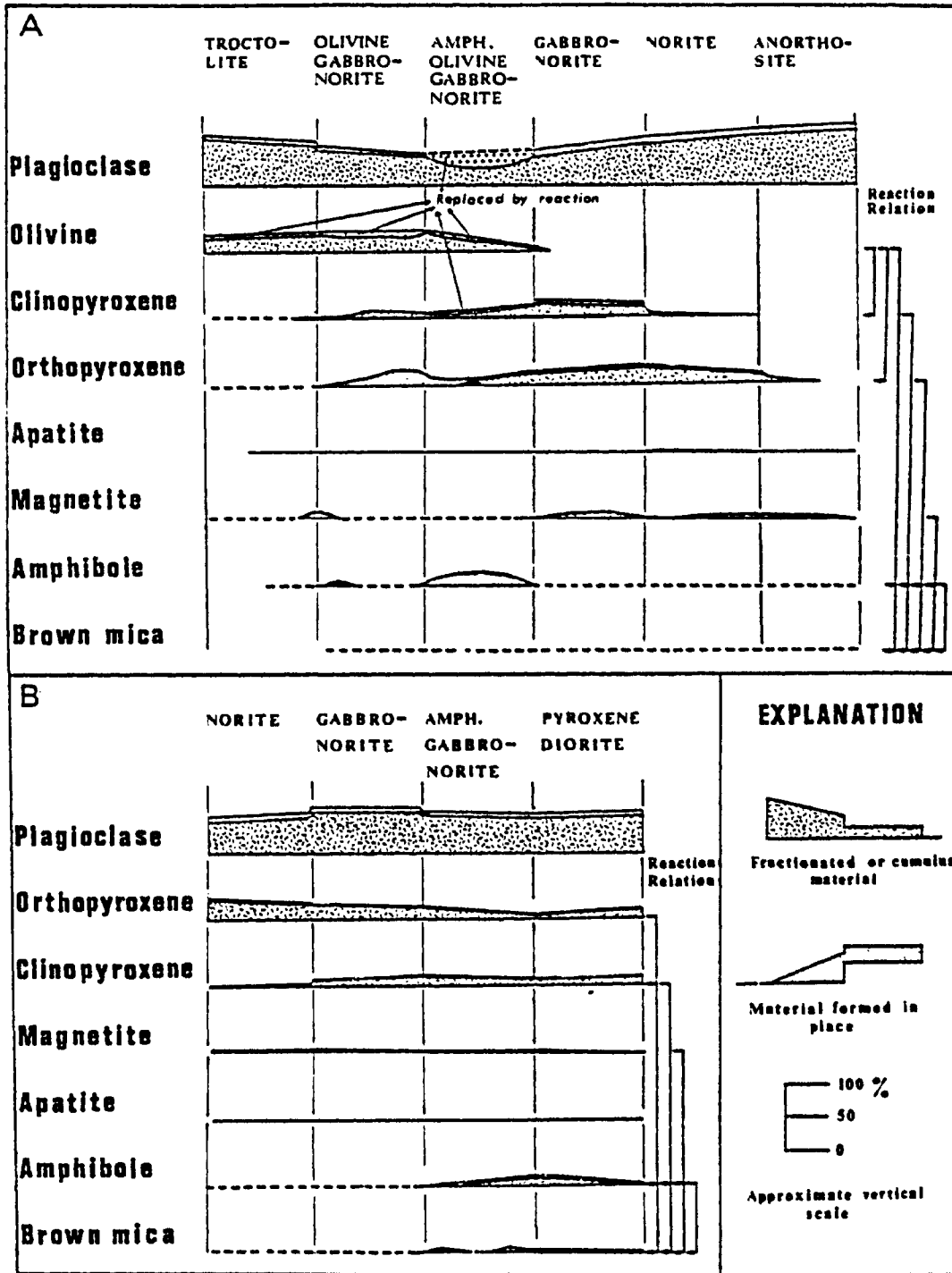
4. Amphibole partially or completely rims titaniferous magnetite.
5. Phlogopite partially rims or occurs associated with amphibole.

On the basis of petrographic interpretation, the following order and stages of crystallization are inferred:

- (a) Early magmatic—crystallization of olivine and plagioclase, sulphides, apatite and titaniferous magnetite.
- (b) Intermediate magmatic—reaction and crystallization of clinopyroxene and orthopyroxene; continuation of plagioclase crystallization.
- (c) Late magmatic—reaction of hornblende and phlogopite; exsolution of clinopyroxene and orthopyroxene.

Jackson (1967) suggested three types of changes which separate the compositionally bounded horizons of differentiated intrusive rocks. These include the changes in mineral phases, changes in mineral ratios and changes in mineral form or habit. Table 4.3 presents such changes in rocks of the inner gabbroic series. The changes in phases and ratios of phases from troctolite upward towards higher elevations (Figure 4.2) are:

Figure 4-2: Crystallization modals for the gabbroic rocks. A. Inner gabbroic series. B. Outer gabbroic Series. Order of mineral fractionation is from top to bottom, or from left to right. Stages of frectionation are represented by successive rock types (after Irvine, 1974).



- (a) appearance of pyroxenes in troctolite.
- (b) increase in the pyroxenes and decrease in olivine in the olivine gabbro-norite.
- (c) disappearance of olivine and further increase in clinopyroxene in the gabbro-norite.
- (d) decrease in clinopyroxene, relative increase in orthopyroxene and finally disappearance of clinopyroxene in norite;
- (e) gradual decrease in orthopyroxene and its disappearance in andesine anorthosite.

Changes in the form of mineral phases in these rocks are best illustrated by the pyroxenes. The clinopyroxene has an anhedral to subhedral outline in the olivine gabbro-norite which changes from subhedral to euhedral in the gabbro-norite. The clinopyroxene again becomes subhedral in the norite. The orthopyroxene is anhedral in the olivine gabbro-norite, anhedral to subhedral in the gabbro-norite, euhedral in norite and again changes to subhedral in the andesine anorthosite. Apart from these changes, An% in plagioclase continuously decreases with each rock type from troctolite to andesine anorthosite.

The mineralogical banding observed in the field due to variations in the contents of mafic and felsic components, is horizontal or dips at a few degrees

to the NE, in the olivine gabbro unit. This unit occupies the largest and probably the most stable of the fault separated blocks in the area underlain by the inner gabbroic rocks (Figure 3.2). The banding and foliations in the other blocks have variable attitudes probably due to different types and amounts of movement along fault planes. The original (before block-faulting) horizontal layering and igneous lamination due to alignment of the mafic minerals in the inner gabbroic rocks indicate that they are cumulates. In addition clumping of mafic minerals into chains and rounded aggregates, and lack of zoning and presence of interlocking mosaic textures of the plagioclase in these rocks also suggest a cumulate origin.

The order of crystallization, above discussed, changes in mineral phases, ratios, and forms and their banding and laminations confirm that the inner gabbroic rocks were formed by the in situ differentiation of the parental basaltic magma.

Since the inner gabbroic rocks, in general are cumulates, an attempt has been made to relate them by fractional crystallization modal. On the basis of terminology modified after Jackson (1967; 1971), Wager (1967), and Wager et al (1960), the inner gabbroic

rocks, are divided into adcumulates, mesocumulates and orthocumulates.

The troctolite (Table 4.3; Figure 4.2) has an interlocking mosaic texture of subhedral plagioclase and olivine is embayed indicating post-cumulation growth and resorption respectively. The titaniferous magnetite in this rock is also a cumulus phase. Olivine, in the thin lamination of banded troctolite, has reaction rims which are intercumulus phases. The rock contains less than 5% intercumulus material and is classified as adcumulate.

In the olivine gabbro-norite and amphibole olivine gabbro-norite, the early formed rocks have plagioclase and olivine as cumulus phases. Intercumulus phases—clinopyroxene, orthopyroxene and amphibole form reaction rims and enclose the cumulus phases. In the late formed rocks clinopyroxene also becomes a cumulus phase. Intercumulus phases poikilitically enclose the cumulus phases. Both rock types contain more than 5% intercumulus material and are considered orthocumulates.

The average gabbro-norite and norite have cumulus plagioclase, clinopyroxene, orthopyroxene, and titaniferous magnetite. The first two phases contain regularly oriented, acicular, opaque, or mafic

silicate inclusions which are usually not present near the crystal margins. The absence of these inclusions and presence of mosaic texture of plagioclase indicate an adcumulus growth of cumulus phases. Amphibole in minor amounts occurs as intercumulus phase. The gabbro-norite and norite are interpreted as adcumulates.

In the andesine anorthosite plagioclase, orthopyroxene and titaniferous magnetite are cumulus phases. The plagioclase shows characteristic mosaic adjustment. Presence of titaniferous magnetite indicates that anorthosite is not a flotation cumulate. The reaction rims of amphibole and phlogopite and the absence of protoclastic texture suggests that the process of filter pressing was not involved. Plagioclase has the same characteristics as in the gabbro-norite and norite, and shows interlocking mosaic texture which indicates adcumulus growth. The rock is classified as an adcumulate.

#### 4.2 OUTER GABBROIC ROCKS

The outer gabbroic rocks, like the inner gabbroic rocks, also show a systematic variation when their modal mineral compositions (Table 4.4) are projected



Table 4.4: Modal mineral compositions in the rocks of the Outer Gabbroic Series.

OUTER GABBROIC ROCKS

Rock Name	Norite		Gabbronorite			Amphibole Gabbronorite			
	W94	W95	W154*	W30	W90	W92	W32	W17	W12
Plagioclase	52.6	59.2	50.3	68.1	52.6	66.3	57.7	67.3	60.6
Orthopyroxene	29.3	24.5	25.2	14.3	24.9	16.8	12.6	6.3	5.9
Clinopyroxene	3.4	4.3	-	10.2	16.1	12.6	18.9	8.2	9.5
Amphibole	2.7	2.6	tr	0.2	1.2	3.2	8.2	12.8	17.8
Mica	tr	-	2.1	-	tr	0.7	tr	0.8	4.5
Opauques	1.7	5.2	20.9	6.3	5.2	tr	2.1	3.3	1.3
Apatite	0.8	tr	tr	0.9	-	0.3	0.3	1.2	0.4
Quartz	9.5	4.2	-	-	-	-	-	-	-
An# in Plag.	54-50	52-50	54-52	52	52-50	52-50	53	50	52-49

OUTER GABBROIC ROCKS (CONT'D)

Rock Name	Amphibole Gabbronorite (Cont'd)		Pyroxene Diorite						
	W27	W113	W152	W29	W16	W25	W57	W113A*	W145*
Plagioclase	56.0	62.8	57.6	58.3	61.5	64.5	50.1	45.1	51.3
Orthopyroxene	16.9	12.3	12.7	10.5	14.0	10.2	7.7	14.4	12.6
Clinopyroxene	13.9	12.6	11.3	19.4	17.3	14.4	20.3	21.3	19.4
Amphibole	5.2	5.7	12.5	1.7	2.4	3.8	3.8	10.1	-
Mica	4.3	tr	2.9	5.6	1.6	0.5	14.8	-	8.5
Opauques	3.6	5.7	2.4	4.4	2.9	6.1	2.5	8.0	7.6
Apatite	0.1	0.8	0.5	tr	0.3	0.5	0.8	tr	0.6
An# in Plag	52-50	50	50	46	44-42	44	46-42	44	42

\* Fine grained rock.

on a triangular plot with plagioclase, orthopyroxene, and clinopyroxene at the apices (Figure 4.3).

In the outer gabbroic rocks there is a general increase in clinopyroxene, amphibole, and phlogopite and the gradation is towards successively less basic rocks.

#### 4.2.1 GABBRO

The gabbro unit, in outer gabbroic series, consists of two rock types, norite and gabbronorite (Table 4.1).

##### 4.2.1.1 NORITE:

The norite is a coarse-grained, maximum 2x1 mm in dimensions, hypidiomorphic-granular rock. It is characterized by a heterogeneous distribution of its constituent minerals and consists of 50 to 60% plagioclase, 25 to 30% orthopyroxene, 3 to 5% clinopyroxene, 1 to 6% titaniferous magnetite, and variable, minor amounts of amphibole, phlogopite and apatite.

Plagioclase (An<sub>50-54</sub>) forms euhedral to subhedral lath-shaped to tabular crystals reaching a maximum 2x1 mm in dimension. Twinning is common on the albite and

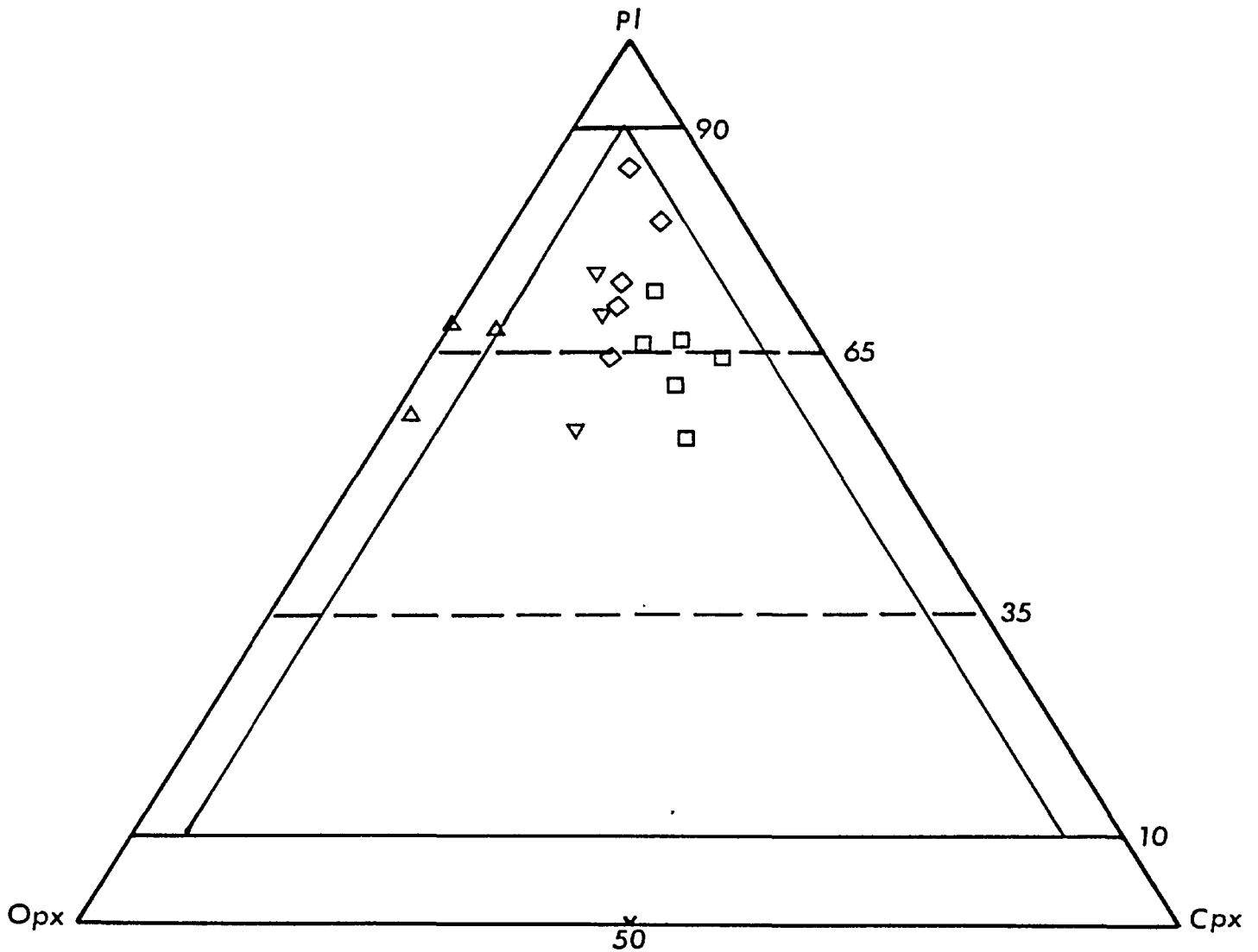


Figure 4.3 Modal mineral proportions in rocks of the Outer Gabbroic Series.

( $\Delta$ ) Norite

( $\nabla$ ) Gabbronorite

( $\diamond$ ) Amphibole Gabbronorite

( $\square$ ) Pyroxene Diorite

Field boundaries according to Streckeisen (1976).

Carlsbad-albite laws but uncommon on the pericline law. A slight normal zoning,  $An_{48}-An_{54}$ , is noted in a number of plagioclase crystals. Inclusions of other minerals were not observed but fine sericitization of plagioclase, in patches about 0.2 mm in diameter, is present.

Orthopyroxene forms euhedral to subhedral prismatic crystals, maximum 1.5x1 mm in dimensions, and shows neutral to pink pleochroism. Twinning parallel to (100), which was not observed in the orthopyroxene of inner gabbroic rocks, is present in a number of orthopyroxene crystals. Very thin, straight plates of clinopyroxene exsolve parallel to (100) plane of orthopyroxene. Amphibole rarely forms partial to complete reaction rims around orthopyroxene.

Clinopyroxene, neutral in colour, forms anhedral crystals up to 1.5x0.75 mm in dimensions. Twinning parallel to (100) is present in a few crystals. Clinopyroxene poikilitically encloses about 0.2 mm anhedral crystals of orthopyroxene. Subophitic to ophitic texture results rarely when clinopyroxene, partially to completely, encloses plagioclase crystals. Amphibole, occasionally forms less than 0.1 mm wide reaction rims around clinopyroxene.

Prismatic apatite, about 0.3x0.1 mm, is commonly associated with titaniferous magnetite in the interstices between major mineral phases. The latter forms anhedral crystals of about 0.5 mm in diameter. Light yellowish-brown to dark reddish-brown, pleochroic amphibole forms partial to complete reaction rims, less than 0.1 mm wide, around titaniferous magnetite and pyroxenes.

Fine-grained equivalent of norite (W.154, Table 4.4; a core sample from southern Cu-Ni showings, Figure 3.2) is a holocrystalline, aphanitic rock and consists of about 50% plagioclase, 25% orthopyroxene, 20% sulphides, 5% titaniferous magnetite, and about 2% phlogopite. It has a maximum grain size of 0.3x0.2 mm and contains large, complete to broken xenocrysts of plagioclase and orthopyroxene of the inner gabbroic rocks up to 3x2 mm.

Plagioclase (An<sub>52</sub>) forms subhedral to anhedral tabular crystals of about 0.5x0.3 mm in dimension. It shows twinning on the albite and Carlsbad-albite laws and is generally fresh except for a slight sericitization along fractures.

Orthopyroxene forms anhedral crystals up to 0.2x0.1 mm in maximum dimensions, and is interstitial

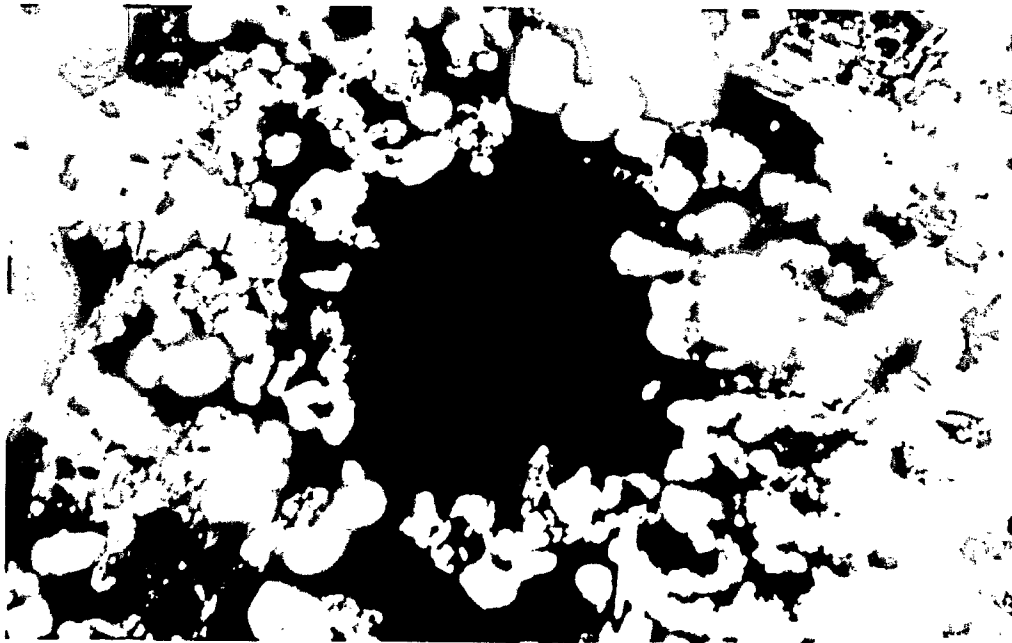


Photo 4.11: Fine-grained equivalent of norite showing central core of 100% sulphides and peripheral area where sulphides enclose plagioclase and orthopyroxene crystals. Crossed nicols, field of view 3X2 mm.

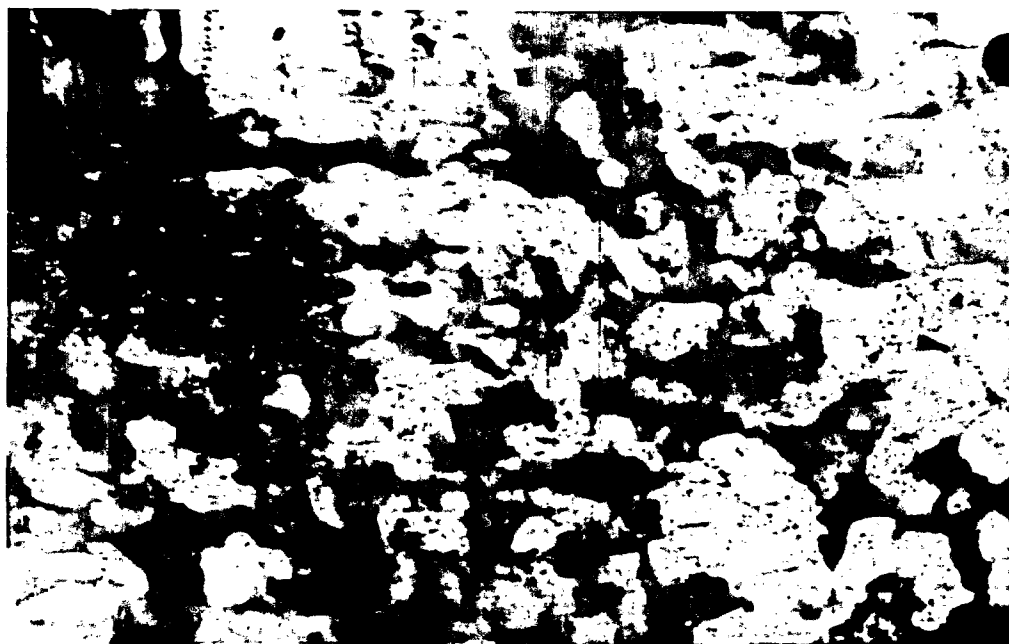


Photo 4.12: Fine-grained equivalent of norite showing plagioclase xenocrysts with irregular recrystallized areas which are free from twinning, have similar optical orientation and are joined in a network. Crossed nicols, field of view 1.5X1 mm.

to plagioclase in habit. It is pleochroic from neutral to pink and does not show any twinning or exsolution.

The sulphides form rounded (globular in hand specimen) aggregates. These aggregates have inner cores of 100% sulphides which grade outwards to peripheral areas in which sulphides enclose plagioclase and orthopyroxene crystals (Photo 4.11). The margins of these peripheral areas near sulphide aggregates, which contain only interstitial sulphides, may join to form a network enclosing irregular areas of host rock.

Titaniferous magnetite forms minute (less than 0.1 mm) anhedral crystals which occupy interstitial places. Phlogopite, pleochroic from light-yellow to dark brownish-red, forms partial to complete reaction rims, less than 0.1 mm wide, around titaniferous magnetite and sulphides.

The coarse-grained plagioclase and orthopyroxene xenocrysts are in sharp contrast to fine grained plagioclase and orthopyroxene of the host rock. The plagioclase of xenocrysts, about 3x2 mm in maximum dimension, have twinning on the albite and Carlsbad-albite laws. It is in various stages of recrystallization which is taking place in triangular to

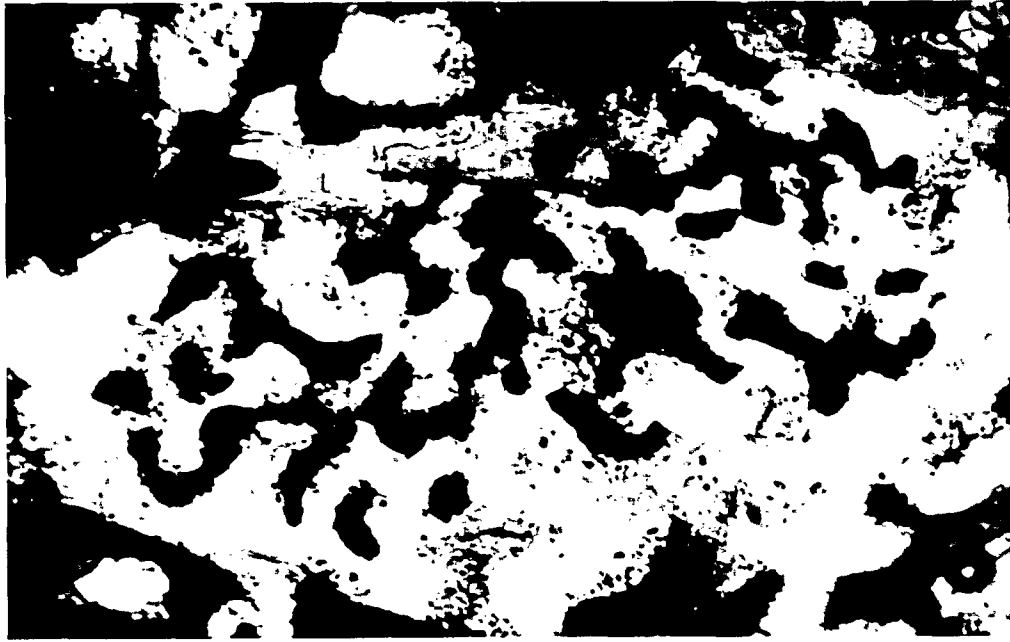


Photo 4.13: Fine-grained equivalent of norite showing xenocrysts of plagioclase with sulphides inclusions. Crossed nicols, field of view 3X2 mm.

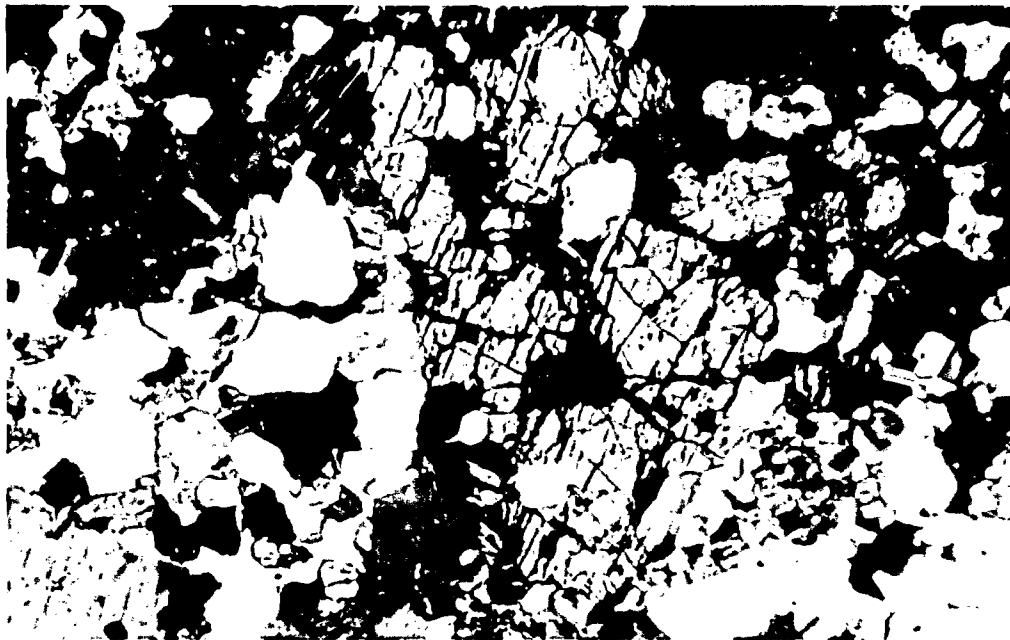


Photo 4.14: Fine-grained equivalent of norite showing sulphide inclusions in orthopyroxene xenocrysts. Orthopyroxene crystals in bottom left corner represent the actual grain size of the rock. Plane light, field of view 3X2 mm.



rounded or rectangular areas less than 0.1 mm (Photo 4.12). The recrystallized areas are free from twinning, have similar optical orientation and often join to form a network in the host plagioclase. Orthopyroxene xenocrysts, 2.5x1 mm in maximum dimension, have typical neutral to pink pleochroism. Exsolution of clinopyroxene in very thin lamellae parallel to (100), occurs in the orthopyroxene.

Both plagioclase and orthopyroxene have irregular sulphide inclusions less than 0.1 mm in diameter (Photo 4.13 and 4.14). Longer dimensions of these inclusions are at right angle to each other which suggest that the sulphide liquid was squeezed into the xenocrysts along cleavage.

#### 4.2.1.2 GABBRONORITE:

The norite grades into the gabbronorite with increase in modal clinopyroxene.

The gabbronorite is a coarse grained, maximum 2x1 mm in grain size, hypidiomorphic-granular rock and its constituent minerals are heterogeneously distributed. It consists of 52 to 68% plagioclase, 14 to 25% orthopyroxene, 10 to 16% clinopyroxene, 0 to 6%

titaniferous magnetite, 1 to 3% amphibole, and minor, variable amounts of phlogopite and apatite.

Plagioclase ( $An_{52-50}$ ) forms euhedral to subhedral, tabular crystals which reach a maximum 2x1 mm in dimensions. It is twinned on the albite and Carlsbad-albite laws. Weak normal zoning ( $An_{55}$  to  $An_{48}$ ), often occurs in a number of plagioclase crystals. Alteration to saussurite is rare in irregular patches of maximum 0.2x0.1 mm in diameter.

Orthopyroxene forms euhedral to subhedral prismatic crystals which are 1x0.75 mm in maximum dimensions. Twinning parallel to (100) is present in a few crystals. Exsolution of clinopyroxene in very thin lamellae occurs parallel to (100) plane of the orthopyroxene. Amphibole forms partial to complete reaction rims around orthopyroxene.

Clinopyroxene, neutral to pale brown in colour forms subhedral to anhedral crystals 1.5x1 mm in maximum dimensions. Twinning parallel to (100) occurs in a few crystals. Ophitic to sub-ophitic textures result when clinopyroxene partially to completely encloses 0.05x0.2 mm plagioclase crystals. Amphibole forms partial to complete reaction rims around clinopyroxene.

Prismatic apatite, 0.3x0.1 mm, occupies interstitial positions together with anhedral to subhedral titaniferous magnetite. The latter is about 0.4 mm in diameter and contains partial to complete reaction rims of amphibole.

Anhedral amphibole, occurs as reaction rims (less than 0.1 mm wide) around other minerals, and occupies interstitial positions together with apatite and titaniferous magnetite. It shows light yellowish-brown to dark reddish-brown pleochroism and forms up to 0.2x0.1 mm crystals. Rarely minute phlogopite flakes, less than 0.1 mm in diameter, are associated with amphibole.

#### 4.2.2 AMPHIBOLE GABBRO-PYROXENE DIORITE

The amphibole gabbro-pyroxene diorite unit consists of two rock types - amphibole gabbronorite and pyroxene diorite.

##### 4.2.2.1 AMPHIBOLE GABBRONORITE:

The gabbronorite grades into the amphibole gabbronorite with increase in the amphibole and phlogopite to more than 5%.

gabbronorite with increase in the amphibole and phlogopite to more than 5%.

The amphibole gabbronorite is a coarse-grained (maximum 3x2 mm), hypidiomorphic-granular rock. The distribution of minerals making up this rock is heterogenous. It consists of 56 to 68% plagioclase, 6 to 17% orthopyroxene, 8 to 19% clinopyroxene, 5 to 18% amphibole, and 1 to 16% titaniferous magnetite, with minor amounts of phlogopite and apatite.

Euhedral to subhedral plagioclase ( $An_{50}$  to  $52$ ) forms tabular crystals (maximum 2x1 mm in dimensions). Twinning on the albite law is common and is less common on the Carlsbad-albite and pericline laws. Normal to discontinuous zoning (generally less than 10% An), mostly restricted to larger subhedral plagioclase crystals, is particularly common in rocks containing abundant amphibole. Protoclastic texture is indicated by some of the subhedral plagioclase crystals having bends and kinks in twin lamellae. Alteration to saussurite and carbonate is rare, but when present occurs in small patches of about 0.2 mm in diameter.

Euhedral to subhedral orthopyroxene, about 1.5x1 mm in dimensions, occurs in prismatic crystals.

Inclusions of anhedral plagioclase (maximum 0.3x0.2 mm), and titaniferous magnetite (less than 0.1 mm in diameter), occur poikilitically enclosed in a few larger orthopyroxene crystals. Amphibole commonly forms partial to complete reaction rims around orthopyroxene. In the absence of these reaction rims, the margins of orthopyroxene crystals are altered to colourless, fibrous actinolite-tremolite amphibole (less than 0.1 mm in width).

Pale brown, euhedral to subhedral clinopyroxene forms stubby to prismatic crystals up to 1.5x1 mm in dimensions. Simple twinning parallel to (100) and malacolite parting parallel to (001) are present in most clinopyroxene crystals. Amphibole commonly forms reaction rims (0.1 to 0.2 mm in width) around clinopyroxene. In addition, optically similar amphibole commonly forms thin zones and patches along clinopyroxene cleavage, parting and fractures (Photo 4.15). This occurrence suggests interstitial liquid was squeezed into fractures and zones of weakness in the clinopyroxene, causing the development of reaction relations similar to those rimming margins of grains.

Subhedral to anhedral amphibole (maximum 3x2 mm), is pleochroic from light yellowish-brown to dark



Photo 4.15: Amphibole gabbro showing clinopyroxene with reaction rims of amphibole along margins and minute zones and patches along cleavage, parting, and fractures. Plane light, field of view 1.5X1 mm.

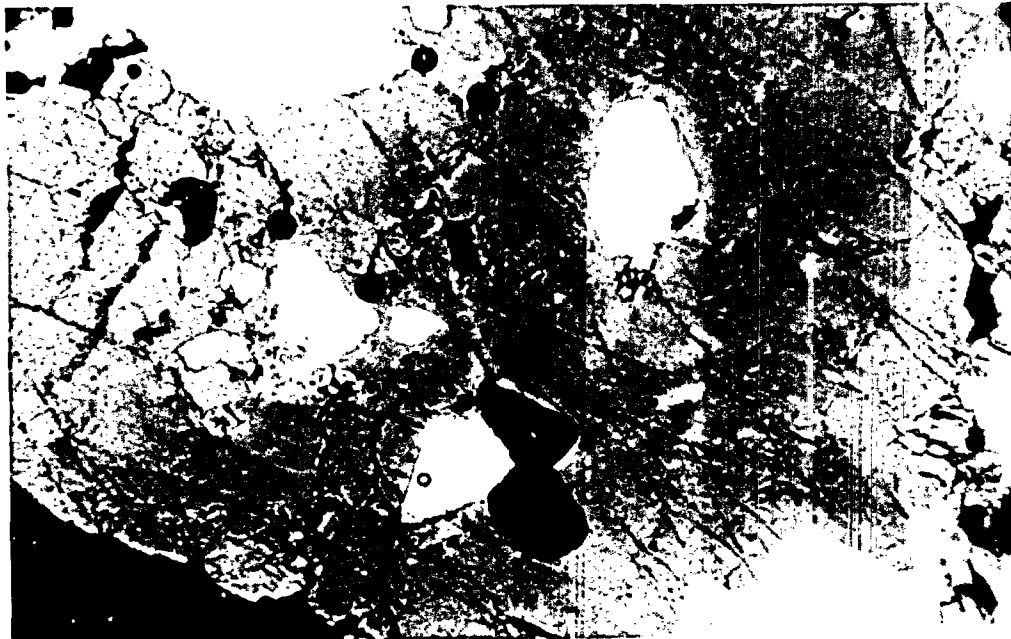


Photo 4.16: Amphibole gabbro showing amphibole which poikilitically encloses plagioclase, clinopyroxene and titaniferrous magnetite. Plane light, field of view 1.5X1 mm.

reddish-green. It forms discrete crystals and reaction rims around other ferromagnesian. Twinning parallel to (100) is present in a few crystals. It often poikilitically encloses plagioclase, orthopyroxene, and clinopyroxene crystals (all anhedral and less than 0.4x0.3 mm; Photo 4.16).

Prismatic apatite, 0.3x0.1 mm, occupies the interstitial positions together with subhedral to anhedral titaniferous magnetite which is 0.5x0.2 mm in maximum dimension. Phlogopite, pleochroic from light-yellow to dark brownish-red, forms partial to complete reaction rims, less than 0.1 mm wide, around magnetite and also occur associated with amphibole.

#### 4.2.2.2 PYROXENE DIORITE:

With decrease in An% of plagioclase to below 50 and increase in amphibole and/or phlogopite relative to pyroxenes, the amphibole gabbrograde grades into pyroxene diorite.

The pyroxene diorite is a medium to coarse-grained, (maximum 3x2 mm) hypidiomorphic granular rock, and has a heterogeneous distribution of its constituent minerals. It consists of 50 to 65% plagioclase, 7 to 14% orthopyroxene, 15 to 20%

clinopyroxene, 1 to 4% amphibole, 1 to 15% phlogopite, and 2 to 6% titaniferous magnetite with minor apatite.

Euhedral to subhedral plagioclase ( $An_{42}$  to  $46$ ) forms tabular crystals. Twinning is most common on the albite law but uncommon on the Carlsbad-albite and pericline laws. Normal discontinuous zoning (generally less than 8% An) is mostly restricted to larger subhedral crystals. Alteration of plagioclase to saussurite and carbonate is rare, but when present occurs in small patches of about 0.2 mm in diameter.

Orthopyroxene, about 1.5x1 mm, forms euhedral to subhedral prismatic crystals. Exsolution of clinopyroxene in very thin lamellae parallel to (100) is rare. Alteration to fine grained fibrous tremolite-actinolite and then to green amphibole, is restricted to crystal margins of orthopyroxene and was observed in only one specimen.

Euhedral to subhedral clinopyroxene, about 1.5x1 mm in maximum dimension, occasionally occurs linked into chains and clumps. Twinning parallel to (100) is uncommon. Reaction rims and reaction alteration to amphibole, similar to that noted in the amphibole gabbro-norite, often occurs around and inside most of the clinopyroxene crystals. Partial reaction rims of phlogopite around clinopyroxene are rare.



Amphibole, pleochroic from light yellowish-brown to dark reddish-green, forms subhedral to anhedral crystals up to 3x2 mm in dimensions. Occasionally it shows simple twinning parallel to (100). Anhedral inclusions of plagioclase, clinopyroxene and subhedral to anhedral inclusions of titaniferous magnetite, all less than 0.5x0.3 mm in size, often occur enclosed in larger amphibole crystals. Phlogopite forms partial reaction rims, less than 0.1 mm wide around amphibole.

Phlogopite (maximum 1x1 mm), forms anhedral to rarely subhedral crystals. It is pleochroic from light brownish-yellow to dark brownish-red and contains minute oriented inclusions of oxide or mafic silicate. Small irregular titaniferous magnetite inclusions, less than 0.1 mm in diameter, also occur enclosed in phlogopite.

Prismatic apatite, about 0.4x0.1 mm and subhedral to anhedral titaniferous magnetite, about 0.75x0.5 mm, occupy the interstitial positions. Occasionally apatite crystals are enclosed in titaniferous magnetite.

Fine-grained equivalents W113A and W145 are porphyritic-aphinitic rocks. The former consists of about 45% plagioclase, 14% orthopyroxene, 21%

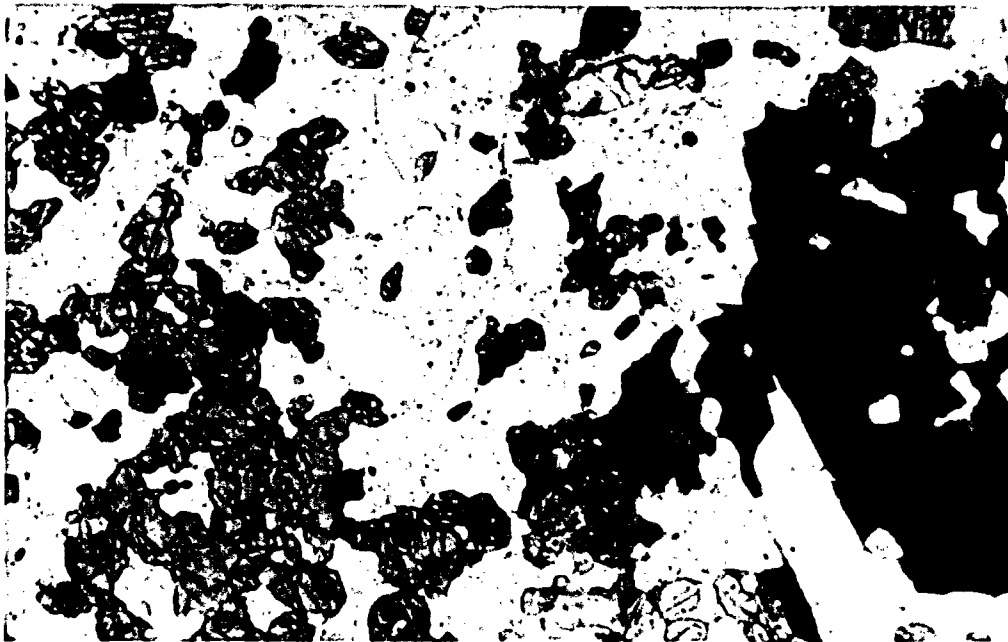


Photo 4.17a: Fine-grained pyroxene diorite showing subhedral phenocryst of amphibole, Plane light, field of view 3X2 mm.

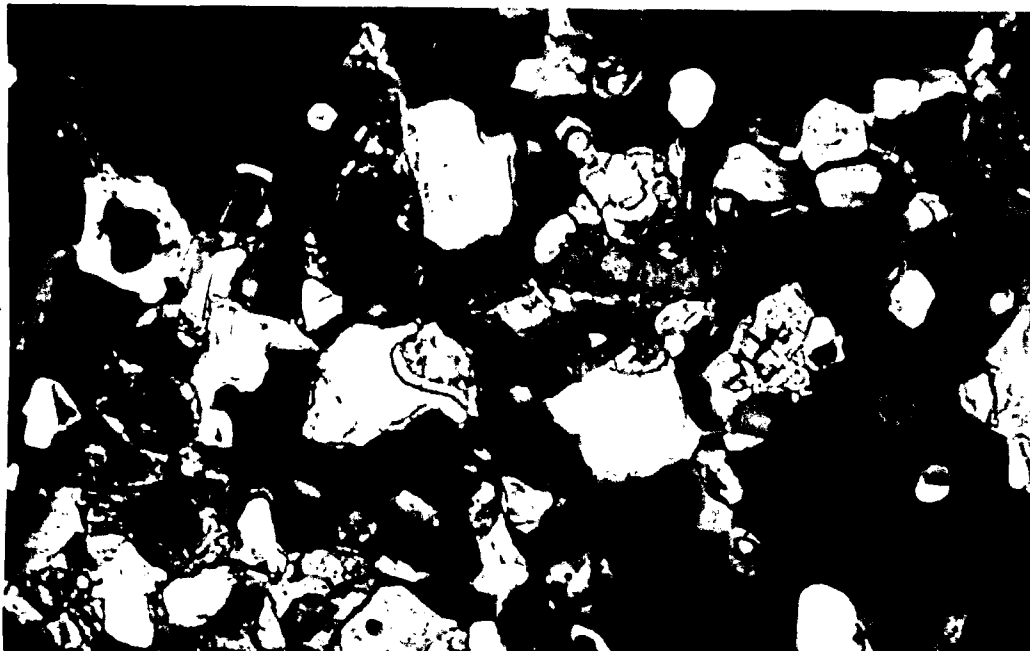


Photo 4.17b: Same sample as above. Amphibole shows recrystallization to plagioclase + clinopyroxene + orthopyroxene + magnetite. Plane light, field of view 1.5X1 mm.

clinopyroxene, 10% amphibole and 8% titaniferous magnetite.

Plagioclase ( $An_{48}$  to  $50$ ) forms anhedral to subhedral crystals 0.3x0.2 mm in maximum dimension. Twinning is present only on the albite law. Plagioclase is generally fresh without any inclusions or alterations.

Both orthopyroxene and clinopyroxene form anhedral crystals, less than 0.2x0.1 mm in size which do not contain any twinning or inclusions. Amphibole forms up to 3x2 mm (in hand specimen up to 3x2 cm) subhedral to anhedral crystals (Photo 4.17a). It is pleochroic from light yellowish-brown to dark reddish-green and occasionally shows twinning parallel to 100. Most of phenocrysts show recrystallization to plagioclase, orthopyroxene, clinopyroxene and magnetite all less than 0.1 mm in diameter (Photo 4.17b).

Titaniferous magnetite forms anhedral crystals less than 0.1 mm in diameter. Apatite forms minute prismatic crystals and occupies interstitial positions together with titaniferous magnetite.

Fine-grain equivalent W145 consists of about 51% plagioclase, 12% orthopyroxene, 19% clinopyroxene, 9%

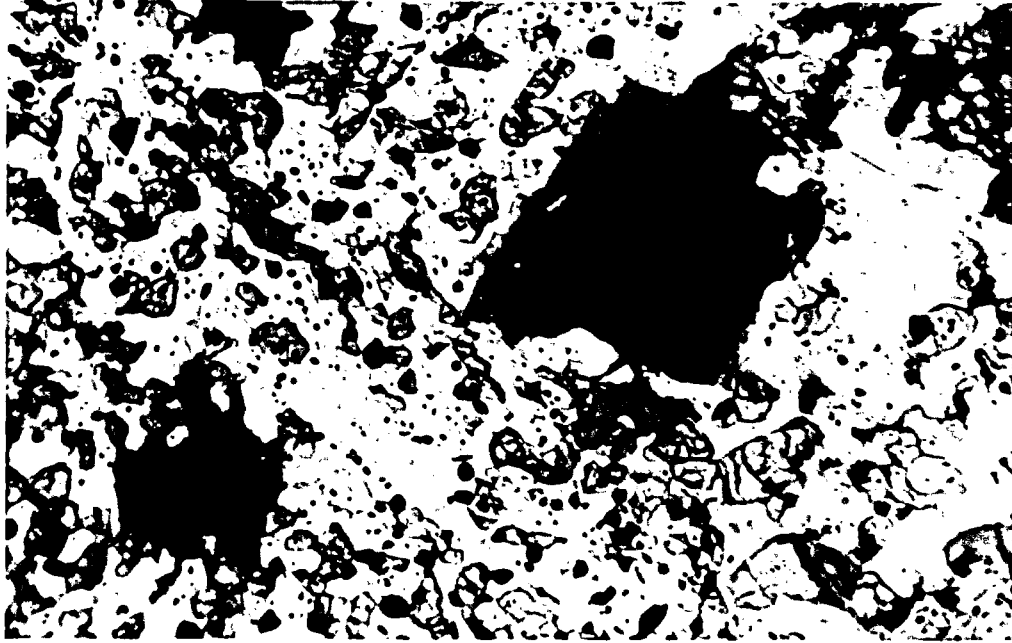


Photo 4.18: Subhedral phenocryst of phlogopite in pyroxene diorite. Phlogopite often shows recrystallization to plagioclase, magnetite, orthopyroxene, and clinopyroxene. Plane light, field of view 3X2 mm.

phlogopite, and 8% titaniferous magnetite with minor amounts of apatite.

Plagioclase ( $An_{42}$ ) forms subhedral to anhedral crystals up to 0.5x0.4 mm in maximum dimension. Twinning is common on the albite and Carlsbad-albite laws. It contains minute anhedral inclusions of titaniferous magnetite and apatite. Occasionally anhedral pyroxenes also occur as inclusions.

Pyroxenes form anhedral crystals less than 0.1 mm in diameter. Orthopyroxene is neutral to pink pleochroic, while clinopyroxene shows light-green to light-brown pleochroism. Both pyroxenes contain minute titaniferous magnetite as inclusions.

Phlogopite forms up to 1x0.5 mm subhedral microphenocrysts and contains plagioclase + titaniferous magnetite + orthopyroxene + clinopyroxene and apatite as inclusions all less than 0.1 mm in diameter (Photo 4.18). Minute prismatic crystals of apatite also occur in interstitial positions together with anhedral titaniferous magnetite.

#### 4.2.3 PARAGENESIS

The reaction relationships and textural observations in the outer gabbroic rocks (Table 4.5) are summarized as below:

- (1) Orthopyroxene and clinopyroxene subophitically enclose plagioclase.
- (2) Clinopyroxene rims and encloses orthopyroxene.
- (3) Amphibole forms reaction rims around pyroxenes and titaniferous magnetite. It often poikilitically encloses plagioclase, clinopyroxene and/or orthopyroxene and titaniferous magnetite.
- (4) Phlogopite forms partial reaction rims around pyroxenes, amphibole, and titaniferous magnetite.

On the basis of petrographic interpretations (Figure 4.2), the following order and stages of crystallization are concluded:

- (a) Early magmatic -- crystallization of plagioclase, orthopyroxene apatite and titaniferous magnetite.
- (b) Intermediate magmatic -- reaction and crystallization of clinopyroxene and amphibole, continuation of plagioclase, orthopyroxene and titaniferous magnetite crystallization.
- (c) Late magmatic -- reaction and crystallization of phlogopite, exsolution in orthopyroxene.

Table 4.5. Summary of petrographic observations in the Outer Gabbroic Series.

<u>ROCK TYPE</u>	<u>PHASE CHANGES</u>	<u>RATIO CHANGES</u>	<u>FORM CHANGES REACTION RIMS</u>	<u>TEXTURE-STRUCTURE</u>	<u>CUMULUS TEXTURE</u>
Pyroxene Diorite		Increase in Cpx, Amphibole, and Phlogopite	Euhedral to subhedral Plag, Opx, Cpx, and subhedral to anhedral Amphi- bole and Phlogo- pite	Amphibole poikiliti- cally encloses Plag, Opx, Cpx, and Ti.Mag- netite. Clumping of Pyroxene	Cumulus Plag, Opx, Cpx, and Ti.Magnetite. Intercumulus amphibole and Phlogopite. Orthocumulate to Adcumulate.
Amphibole Gabbronorite	Appearance of Phlogopite	Decrease in Opx. Increase in Cpx and Amphibole	Euhedral to subhedral Plag, Opx, Cpx. Sub- hedral to an- hedral Amphibole and Ti-Magnetite. Phlogopite rims Pyroxenes, Amphi- bole, and Ti.Mag- netite	Amphibole poikiliti- cally encloses Plag, Opx, Cpx, and Ti. Magnetite. Clumping of Pyroxene	Cumulus Plag, Opx, Cpx, and Ti. Magnetite. Intercumulus Amphibole and Phlogopite. Mesocumulate to Orthocumulate
Gabbronorite	Appearance of Amphibole	Decrease in Opx. Increase in Cpx.	Euhedral to subhedral Plag, Opx, Cpx. Subhedral to anhedral Ti. Mag- netite. Amphibole rims Pyroxene and Ti. Magnetite	Rarely banded. Clumping of Pyroxene into aggregates	Cumulus Plag, Opx, Cpx, and Ti. Magnetite. Intercumulus Amphibole. Adcumulate
Norite	Plag, Opx, Cpx, and Ti. Magne- tite form major phases.	Plag dominates the rock	Euhedral to subhedral Plag and Opx. Subhedral to anhedral Ti.- Magnetite. Cpx rims Opx	Cpx encloses Plag ophitically to subophitically	Cumulus Plag, Opx, and Ti. Magnetite. Intercumulus Cpx. Adcumulate

The earliest formed rock, norite has subhedral to euhedral orthopyroxene and anhedral to subhedral clinopyroxene. The changes in phases, phase ratios and phase forms are marked by:

- (i) Increase in the clinopyroxene compared to orthopyroxene in the gabbro-norite; clinopyroxene becomes euhedral.
- (ii) Appearance of amphibole as a primary phase and its increase in the amphibole gabbro-norite with a general increase in clinopyroxene; amphibole shows anhedral to subhedral outlines.
- (iii) Appearance of phlogopite as a primary phase in pyroxene diorite along with a general increase in clinopyroxene.

Apart from these changes, plagioclase is most calcic in the norite and varies successively with each rock type to least calcic in the pyroxene diorite.

The banding due to variations in the felsic and mafic components, and the clumping of mafic minerals into chains and aggregates observed in the field suggest a cumulate origin for the outer gabbroic rock series. The order of crystallization discussed above, changes in mineral phases, ratios and forms, and occurrence of a fine-grained equivalent of the



earliest rock (norite) all suggest an in situ differentiation of the parent magma.

The outer gabbroic rocks are like the inner gabbroic rocks are interpreted by a fractional crystallization model. The norite, in the outer gabbroic rocks, has euhedral to subhedral plagioclase and orthopyroxene and subhedral to anhedral titaniferous magnetite. All three minerals represent cumulus phases. Intercumulus clinopyroxene, which rims and encloses orthopyroxene, is less than 5%. The norite is classified as an adcumulate rock.

The average gabbronorite contains euhedral to subhedral plagioclase, orthopyroxene, clinopyroxene and subhedral to anhedral titaniferous magnetite as cumulus phases. Anhedral amphibole which rims the mafic cumulus phases is less than 5%. It is concluded that the rock is an adcumulate.

The average amphibole gabbronorite contains euhedral to subhedral plagioclase, orthopyroxene, clinopyroxene and subhedral to anhedral titaniferous magnetite as cumulus phases in the early stages. Anhedral amphibole and phlogopite which rim the mafic cumulate phase are the intercumulus phases. During the late stages amphibole also becomes a cumulus phase

and shows a subhedral outline. The intercumulus phases exceed 5% and the rock varies from a mesocumulate to an orthocumulate.

In the pyroxene diorite, euhedral to anhedral plagioclase, orthopyroxene, clinopyroxene and subhedral to anhedral titaniferous magnetite are the cumulus phases. Anhedral amphibole poikilitically encloses the cumulus phases and rarely rims the mafic cumulus phases together with phlogopite. In a few cases amphibole with subhedral outlines also becomes cumulus phase, while in others only the cumulus phases are observed without any intercumulus phases. The rock shows a wide range in the cumulus and intercumulus phases, and hence varies from an orthocumulate to an adcumulate.

Fine-grained porphyritic rocks represent separate and comparatively homogeneous intrusions. Petrographic relations indicate that amphibole phenocrysts represent the first crystalline phase in specimen W113A. Plagioclase, orthopyroxene, clinopyroxene and titaniferous magnetite followed one another after amphibole respectively. In specimen W145, phlogopite is the earliest mineral and plagioclase, orthopyroxene, clinopyroxene and titaniferous magnetite followed one another respectively.

#### 4.4 DIORITIC ROCKS

The modal mineral compositions and modal plot of the dioritic rocks are presented in Table 4.6 and Figure 4.4 respectively. The modal plot reveals a systematic gradational trend from the hornblende gabbro through diorite and quartz diorite to quartz monzodiorite and tonalite. In general, all the dioritic rocks show the effects of deformation and recrystallization which become more pronounced near the granitic intrusions. These effects include tectonic deformation and recrystallization of plagioclase, and uraltitization and recrystallization of clinopyroxene.

##### 4.2.1 DIORITE

The diorite unit includes two rock types namely hornblende gabbro and diorite. The former grades into the latter with decrease in modal clinopyroxene and An% of plagioclase to below 50.

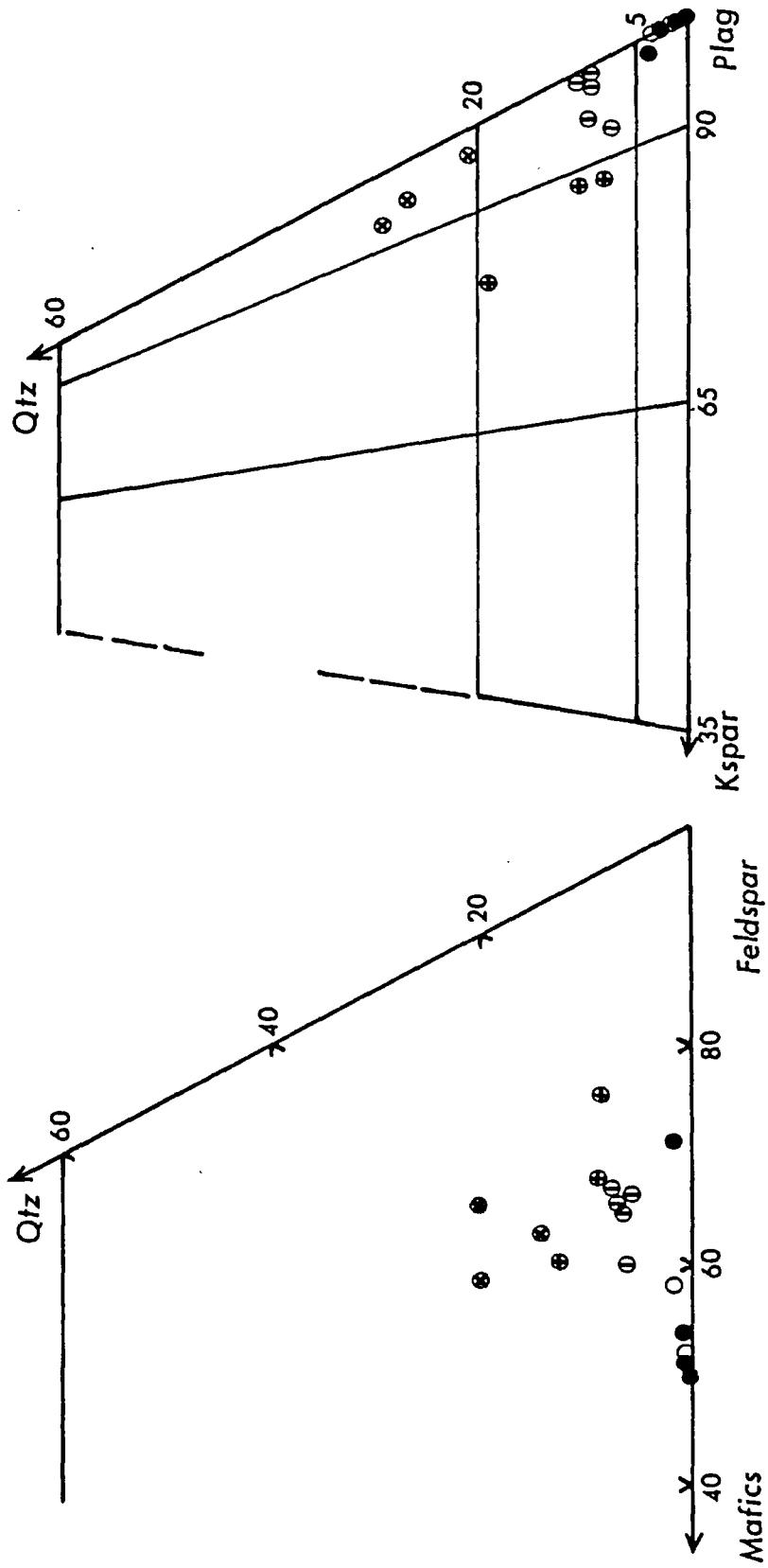


Figure 4.4 Modal mineral proportions in the Dioritic Rocks.

- (○) Hornblende Gabbro
- (●) Diorite
- (⊙) Quartz Diorite
- (⊕) Quartz Monzodiorite
- (⊗) Tonalite

Field boundaries according to Streckeisen (1976).

Table 4.6: Modal mineral compositions of representative samples of the Dioritic Rocks.

DIORITIC ROCKS

Rock Name	Hornblende Gabbro		Diorite				Quartz Diorite		
	W40	W40A	W21	W132*	W20	W22	W55	W115	W88
Plagioclase	57.1	51.6	52.9	51.2	70.6	50.3	62.7	63.8	61.1
K-Feldspar	-	-	0.7	-	tr	-	0.6	tr	0.4
Quartz	1.7	0.9	2.1	0.8	1.9	-	5.4	7.2	6.7
Clinopyroxene	9.5	6.3	1.5	-	tr	1.3	0.5	1.8	tr
Hornblende	18.6	25.3	26.8	32.6	14.5	30.5	12.7	12.7	13.1
sec Amphibole	5.4	6.4	8.1	0.6	7.8	0.3	7.3	2.7	4.1
Biotite	5.7	8.2	7.2	10.8	3.8	-	8.3	6.9	10.6
Chlorite	-	-	-	-	tr	7.1	2.3	2.6	1.8
Epidote	-	-	-	-	tr	2.6	tr	tr	-
Opaque	0.5	0.1	tr	3.5	tr	7.2	0.5	1.2	1.3
Apatite	1.4	1.0	0.5	0.3	1.2	0.6	tr	0.9	0.6
Sphene	tr	tr	0.2	tr	tr	tr	tr	tr	tr
An% in Plag.	53	54-49	46-42	45	40	38	38-32	38	38

DIORITE ROCKS (CONT'D)

Rock Name	Quartz Diorite (Cont'd)			Quartz Monzodiorite and			Tonalite		
	W117	W124	W140	W129	W128	W134	W153*	W33	W35
Plagioclase	59.3	56.2	59.9	63.6	61.1	43.8	45.3	52.3	53.9
K-Feldspar	2.8	0.6	4.1	8.1	9.2	10.2	2.5	2.9	1.7
Quartz	6.8	6.3	5.2	8.6	7.6	12.5	20.5	20.2	14.3
Clinopyroxene	tr	1.2	tr	-	2.3	1.6	-	-	-
Hornblende	13.4	20.1	14.6	7.2	9.7	12.7	19.2	2.1	17.6
sec Amphibole	3.8	3.4	1.7	3.7	1.5	4.3	-	-	-
Biotite	12.5	8.2	10.6	8.2	7.8	12.6	10.2	10.3	9.5
Chlorite	-	tr	-	-	-	tr	-	-	tr
Epidote	tr	1.2	tr	tr	tr	1.2	1.5	11.4	1.5
Opaque	0.3	1.5	2.6	tr	tr	tr	tr	0.7	1.1
Apatite	1.0	1.2	1.2	0.5	0.7	0.9	0.5	tr	0.2
Sphene	tr	tr	tr	tr	tr	tr	tr	tr	0.1
An% in Plag	36	36	34	40-34	36	32	34	24	28

\*Fine to medium grained rock.

4.3.1.1 HORNBLLENDE GABBRO:

The hornblende gabbro is a coarse grained, micro-porphyrific granular rock with maximum grain size of 4x3 mm. It has a heterogeneous distribution of its constituent minerals.

The hornblende gabbro consists of 51 to 57% plagioclase, 6 to 10% clinopyroxene, 18 to 25% amphibole, 5 to 8% biotite, and minor variable amounts of quartz, potash feldspars, magnetite, apatite and sphene (Table 4.6).

Plagioclase (An<sub>54-49</sub>) occurs in euhedral to subhedral tabular crystals, 3x2 mm in maximum dimensions. Twinning is common on the albite and Carlsbad-albite laws but rare on the pericline law. Patchy normal to oscillatory zoning (less than 10% An) is mostly present in larger microphenocrysts. Inclusions of prismatic apatite, 0.2x0.05 mm, occur in a few plagioclase crystals. Alteration to saussurite is common in small areas of about 0.2 mm in diameter. Tectonic deformation and recrystallization of plagioclase is rare.

Clinopyroxene, maximum 3x2 mm in dimension, forms euhedral to subhedral stubby crystals. Inclusions of



Photo 4.19a: Hornblende gabbro showing clinopyroxene rimmed by amphibole. Clinopyroxene is partially replaced by uralite. Plane light, field of view 3X2 mm.

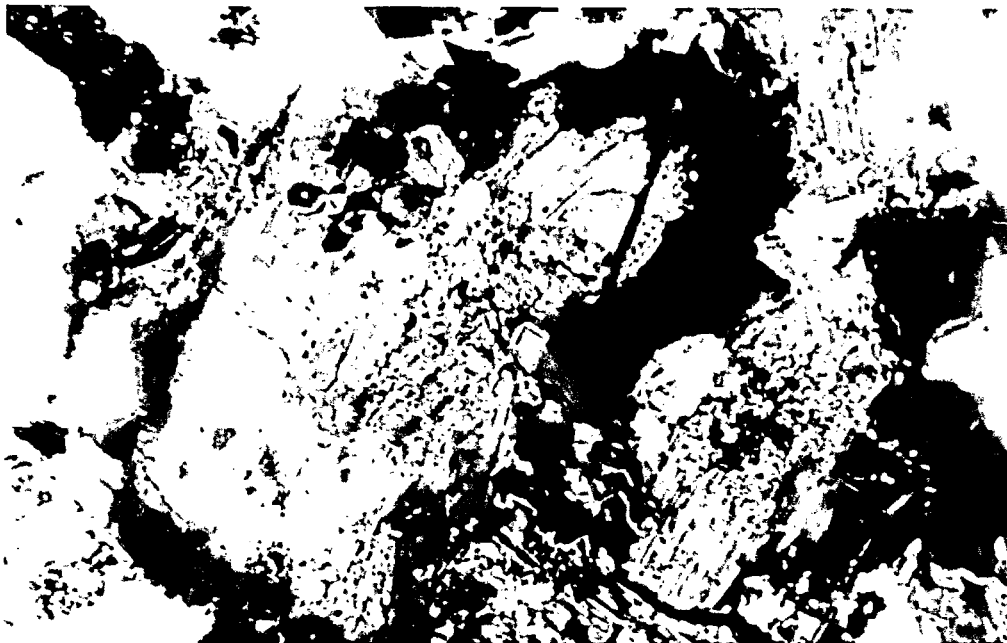


Photo 4.19b: Same as above, crossed nicols.

subhedral plagioclase, less than 0.2 mm in diameter, occur in a few crystals. Hornblende forms reaction rims less than 0.2 mm wide around clinopyroxene (Photo 4-19 a & 4.19b). Most of the clinopyroxene crystals are in advanced stages of alteration to fine grained, flaky uralite which is a pleochroic pale-yellow to yellowish-green tremolite-actinolite amphibole.

Hornblende, 3x3 mm in maximum dimensions, forms euhedral to anhedral prismatic crystals. It ranges in colour from dark-brown to dark-green and is readily distinguished from the reddish-brown variety in the gabbroic rocks. Simple twinning parallel to (100) is present in a few crystals. Hornblende poikilitically encloses subhedral plagioclase (0.5x0.3 mm), subhedral clinopyroxene (0.5x0.4 mm), and prismatic crystals of apatite (0.1x0.05 mm). Occasionally plagioclase (0.5x0.3 mm) and subhedral to anhedral magnetite (0.2x0.2 mm), individually or together, occur as inclusions in hornblende. Alteration to biotite on crystal margins is rare.

Biotite, 2x1 mm in maximum dimension, is pleochroic from yellowish-brown to dark-brown. It occurs in tabular to lamellar aggregates and usually occupies the area round anhedral magnetite (0.3x0.2 mm).



Inclusions of minute prismatic apatite are common. Alteration of biotite to chlorite is rare and restricted to the crystal margins.

Anhedral microcline and quartz, both less than 0.3x0.2 mm, individually occupy the interstitial positions between major mineral phases. Prismatic apatite occurs as inclusions in both minerals. Euhedral to subhedral sphene, 0.2x0.1 mm in size, is sometimes associated with quartz and microcline in the interstices.

#### 4.3.1.2 DIORITE:

The diorite is a coarse grained (maximum 5x3 mm), hypidiomorphic granular to microporphyritic rock. It has a heterogeneous distribution of its constituent minerals.

The diorite consists of 50 to 70% plagioclase, 22 to 35% amphibole, 3 to 11% biotite, 0 to 7% magnetite, 1 to 2% quartz and minor, variable amounts of potash feldspar, apatite, chlorite, epidote and sphene (Table 4.6).

Euhedral to subhedral plagioclase (An<sub>46-38</sub>) forms tabular crystals 3.5x3 mm in maximum dimensions.

Twinning is common on the albite and Carlsbad-albite laws and is uncommon on the pericline law. Normal zoning (plagioclase  $An_{50}-An_{38}$ ) has a patchy habit. Inclusions of prismatic apatite (0.1x0.05 mm) occur in plagioclase. Saussuritization is common in small patches of 0.5x0.3 mm in the altered specimen. Tectonic deformation and recrystallization of plagioclase often occurs along shear planes.

Clinopyroxene, less than 0.5 mm in diameter, forms the cores of a few hornblende crystals. Commonly, clinopyroxene cores have been altered to uralite which is a neutral to yellowish-brown pleochroic tremolite-actinolite amphibole.

Hornblende forms euhedral to anhedral prismatic crystals (maximum 3x2 mm). Twinning parallel to (100) is often present in a number of grains. It poikilitically encloses subhedral plagioclase (0.5x0.3 mm), anhedral clinopyroxene (0.3 mm in diameter) and prismatic apatite (0.1x0.05 mm). Alteration to chlorite and epidote in minute areas, less than 0.1 mm in diameter, is commonly restricted to crystal margins.

Biotite (maximum 2x1 mm), forms lamellar aggregates. It is pleochroic from light-brown to dark-brown. Prismatic apatite (0.1x0.05 mm), and rarely

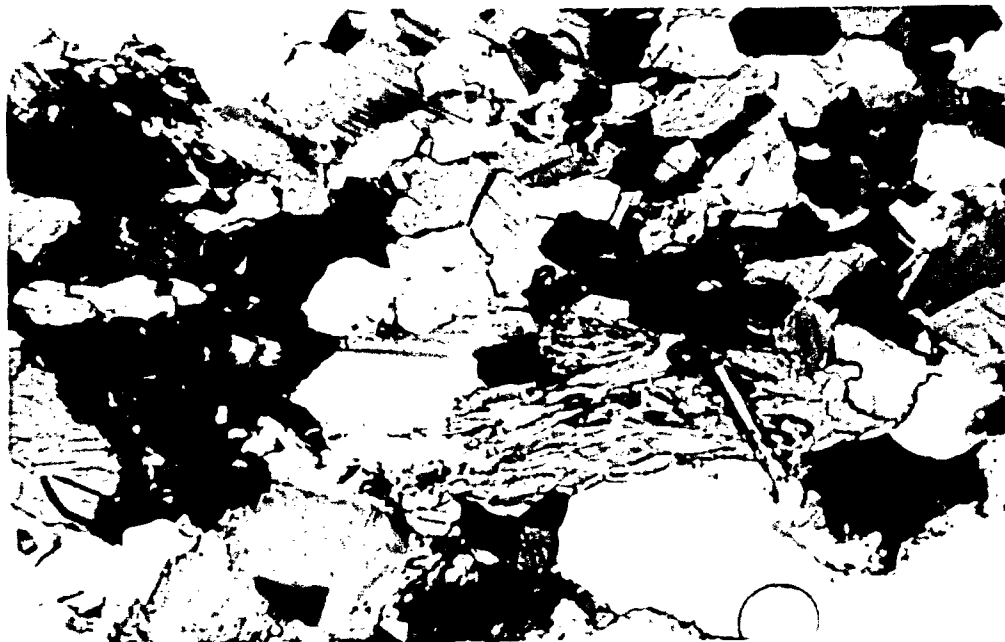


Photo 4.20: Fine-grained equivalent of diorite showing subhedral to anhedral plagioclase, hornblende, quartz, aggregates of biotite, and magnetite. Crossed nicols, field of view 1.5X1 mm.

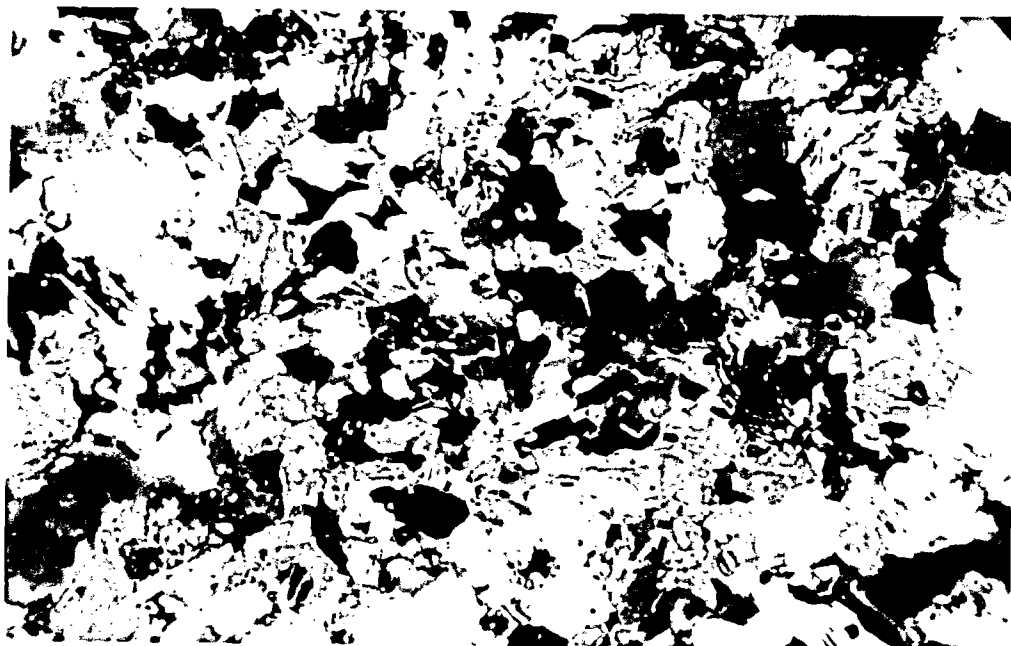


Photo 4.21: Quartz monzodiorite showing flaky tremolite-actinolite amphibole which now represents the original clinopyroxene. Crossed nicols, field of view 1.5X1 mm.

minute subhedral zircon with dark pleochroic haloes, occur as inclusion in biotite. Biotite is often partially to completely altered to chlorite in specimens collected near the granitic rocks. Minute, anhedral epidote is commonly associated with chlorite as an alteration product.

Subhedral to anhedral magnetite, 0.5x0.3 mm in maximum dimension, occupies the interstitial positions together with quartz, microcline and apatite. Occasionally, it encloses the prismatic apatite.

Anhedral quartz and microcline, both less than 1x0.2 mm in dimension, individually occupy the interstitial positions. Prismatic apatite occurs as inclusions in both minerals. Subhedral to anhedral sphene (maximum 0.5x0.2 mm), is occasionally associated with the quartz and microcline.

The fine grained equivalent of diorite (W132, Table 4.6) consists of 51% plagioclase, 33% hornblende, 11% biotite, 3.5% magnetite and minor, variable amounts of apatite, quartz and sphene (Photo 4.20).

The plagioclase ( $An_{45}$ ) forms subhedral to anhedral, zoned ( $An_{50-45}$ ) equant crystals about 1x1 mm in maximum dimension. Subhedral to anhedral hornblende, forms crystals 0.75x0.5 mm maximum dimensions,

some of which appear like recrystallized pyroxenes in colour and form. Biotite forms anhedral (0.3x0.2 mm) flakes and occurs in small (2x1 mm) aggregates. Anhedral quartz and magnetite, both less than 0.2 mm in diameter, individually or together occupy interstices between plagioclase, hornblende, and biotite.

#### 4.3.2 QUARTZ DIORITE

The diorite grades into quartz diorite with an increase in quartz to more than 5% (Figure 4.4).

The quartz diorite is coarse grained, micro-porphyrific, granular to hypidiomorphic granular rock. It has a heterogeneous distribution of its constituent minerals.

The quartz diorite consists of 56 to 64% plagioclase, 15 to 24% amphiboles, 7 to 13% biotite, 5 to 7% quartz, 0 to 3% magnetite and variable, minor amounts of potash feldspar, apatite, sphene and chlorite (Table 4.6).

Plagioclase ( $An_{38-34}$ ) forms euhedral to subhedral rectangular crystals about 5x4 mm in maximum dimensions. Twinning is common on the albite, Carlsbad-albite, and pericline laws. Patchy normal to oscillatory, zoning ( $An_{50}$  to  $An_{36}$ ) occurs mostly in the

larger grains. Inclusions of prismatic apatite (0.1x0.05 mm) and anhedral magnetite (0.3x0.2 mm) are present in a few plagioclase crystals. Tectonic deformation and recrystallization of plagioclase is observed in samples collected near the granitic rocks. Saussuritization of plagioclase in patches up to 0.3x0.2 mm occurs near crystal margins.

Hornblende forms subhedral to rarely anhedral prismatic crystals (maximum 4x2 mm) and shows yellow-green through olive-green to dark-green pleochroism. Some of the hornblende crystals have 0.5x0.3 mm cores of pyroxene which are in advanced stages of alteration to uralite. Inclusions of minute prismatic apatite, subhedral plagioclase (0.7x0.4 mm), magnetite (0.2 mm in diameter) and rare anhedral clinopyroxene (0.3x0.2 mm) occur in hornblende. Alteration to chlorite and/or epidote is rare and restricted to the crystal margins.

Biotite (maximum 1x1 mm) is pleochroic from yellowish-brown to dark-brown and forms randomly oriented lamellar aggregates. Prismatic apatite and rare zircon with pleochroic haloes, occur as inclusions in biotite. Alteration to chlorite is rare and occurs only in specimens collected near the contact with the granitic rocks.

Magnetite (maximum 0.4x0.2 mm), forms subhedral to anhedral grains and occupies the interstitial positions. Occasionally apatite forms inclusions in or occurs associated with, the magnetite.

Anhedral quartz, 1 mm in maximum diameter, and microcline (maximum 0.2x0.1 mm) occupy interstitial positions independently or side by side. Both contain inclusions of prismatic apatite. Euhedral to anhedral sphene (maximum 0.2x0.1 mm) is often associated with the quartz and microcline in interstices between major mineral phases.

#### 4.3.3 QUARTZ MONZODIORITE

The quartz diorite grades into the quartz monzodiorite as alkali-feldspars increase in proportion (Table 4.6; Figure 4.4).

The quartz monzodiorite is a coarse-grained hypidiomorphic granular rock. It is 5x2 mm in maximum grain size and has a heterogeneous distribution of its constituent minerals. It consists of 43 to 63% plagioclase, 1 to 3% clinopyroxene, 11 to 17% amphibole, 7 to 12% biotite, about 8 to 10% microcline, and 7 to 12% quartz with minor and variable amounts of magnetite, apatite and sphene.

Plagioclase ( $An_{32-40}$ ) forms euhedral to anhedral microporphyratic crystals 5x2 mm in maximum dimension. Twinning on the albite and Carlsbad-albite laws is common. Strong normal to oscillatory patchy zoning ( $An_{42}$  to  $An_{32}$ ) is present in most of the microphenocrysts. Inclusions of prismatic apatite occur in plagioclase. Alteration to saussurite and occasionally to carbonate, in patches less than 0.1 mm in size, occurs in the more calcic rims of the zoned plagioclase.

Clinopyroxene (maximum 5x2 mm), occurs as subhedral microphenocrysts. Twinning parallel to (100) and normal zoning are present in a few crystals. The 0.2x0.1 mm mafic inclusions inside pyroxene crystals have very thin reaction rims of hornblende and are now replaced by biotite and epidote. Reaction rims of green hornblende around pyroxene are 0.1 to 0.05 mm wide. In a few cases the clinopyroxene inside hornblende reaction rims is completely represented by recrystallized flaky tremolite-actinolite amphibole (Photo 4.21). Inclusions of euhedral apatite, less than 0.05 mm in diameter, are rare.

Hornblende forms subhedral to anhedral prismatic crystals 3x2 mm in maximum dimensions. It is pleochroic from pale-brown through olive-green to



dark-green. It rarely shows twinning parallel to (100) and often contains anhedral inclusions of clinopyroxene (maximum 0.4x0.2 mm) and minute magnetite. Alteration to epidote, less than 0.1 mm in diameter, is restricted to the crystal margins.

Biotite occurs in randomly oriented lamellar aggregates (maximum 1x0.75 mm). It is pleochroic from light-yellowish brown to dark-brown. Inclusions of apatite and zircon are common. The latter usually has dark coloured pleochroic haloes in biotite. Alteration to chlorite is only present in altered rocks.

Microcline forms anhedral crystals (maximum 1x0.5 mm) and occupies interstices between major mineral phases. It often contains minute inclusions of prismatic apatite. Quartz forms anhedral strained crystals (maximum 1x0.5 mm) and occupies interstices together with microcline. Myrmekitic intergrowth of oligoclase and quartz, up to a maximum of 0.1 mm in diameter, occur at the contacts of the two minerals.

Sphene, maximum 0.2x0.1 mm, forms euhedral to subhedral crystals and occupies interstitial positions together with anhedral secondary magnetite.

Inclusions of previously described fine-grained diorite in the quartz monzodiorite form interlocking

aggregates of hornblende and biotite. Plagioclase in these inclusions forms polygonal interlocking small crystals (less than 0.1 mm) in diameter which have boundaries like 'triple junctions' at 120 degrees. These inclusions are stretched into layers and streaks in between the hornblende and plagioclase microphenocrysts.

#### 4.3.4 TONALITE:

The quartz diorite grades into tonalite with further increase in quartz (Figure 4.4).

The tonalite is a coarse-grained, maximum 3x2 mm, microporphyritic granular to hypidiomorphic granular rock. It consists of 52 to 54% plagioclase, 2 to 8% hornblende, 9 to 10% biotite, 14 to 20% quartz, 1 to 11% epidote, 1 to 3% microcline and minor, variable amounts of apatite, sphene and magnetite.

Plagioclase ( $An_{24-28}$ ) forms subhedral to anhedral microphenocrysts up to a maximum of 3x2 mm in dimensions. Twinning on the albite and Carlsbad-albite laws is common, but rare on the pericline law. A moderate normal to oscillatory zoning ( $An_{40}$  to  $An_{30}$ ) is present in most of plagioclase crystals. Inclusions of prismatic apatite, 0.1x.05 mm in size, occur in

plagioclase. Tectonic deformation and recrystallization is common along the microphenocrysts margins. Alteration to saussurite occurs in small patches of maximum 0.2x0.1 mm in the plagioclase crystals.

Hornblende forms subhedral to anhedral crystals approximately 1x0.5 mm in maximum dimensions. It is pleochroic from light-green through olive-green to dark blueish-green. Twinning parallel to (100) is present in a few hornblende crystals. Prismatic apatite and anhedral minute magnetite crystals occur as inclusions in hornblende. Alteration to chlorite and epidote in small areas, less than 0.1 mm in diameter, is rare and restricted to crystal margins.

Biotite (maximum 0.75x0.5 mm), forms both individual flakes and flake aggregates (Photo 4.22). In aggregates, the flakes have random orientation. Inclusions of prismatic crystals of apatite and zircon occur in biotite. Alteration of biotite to chlorite is rare. Subhedral to anhedral crystals of epidote (maximum 1.5x1 mm) were observed in one specimen (W33). The epidote has developed at the expense of hornblende which is present only in trace amounts. Inclusions of quartz (0.2x0.1 mm), biotite (0.1x0.05 mm) and rare subhedral sphene (0.2x0.1 mm) occur in the epidote crystals.

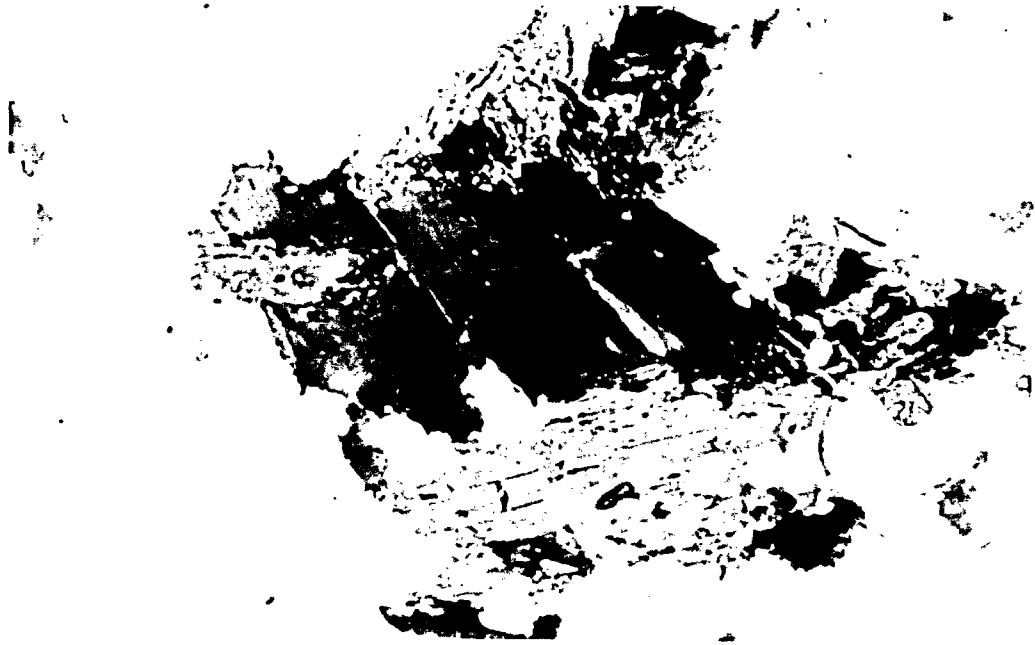


Photo 4.22: Coarse-grained tonalite showing biotite flakes with random orientation and inclusions of prismatic apatite and zircon. Plane light, field of view 1.5X1 mm.

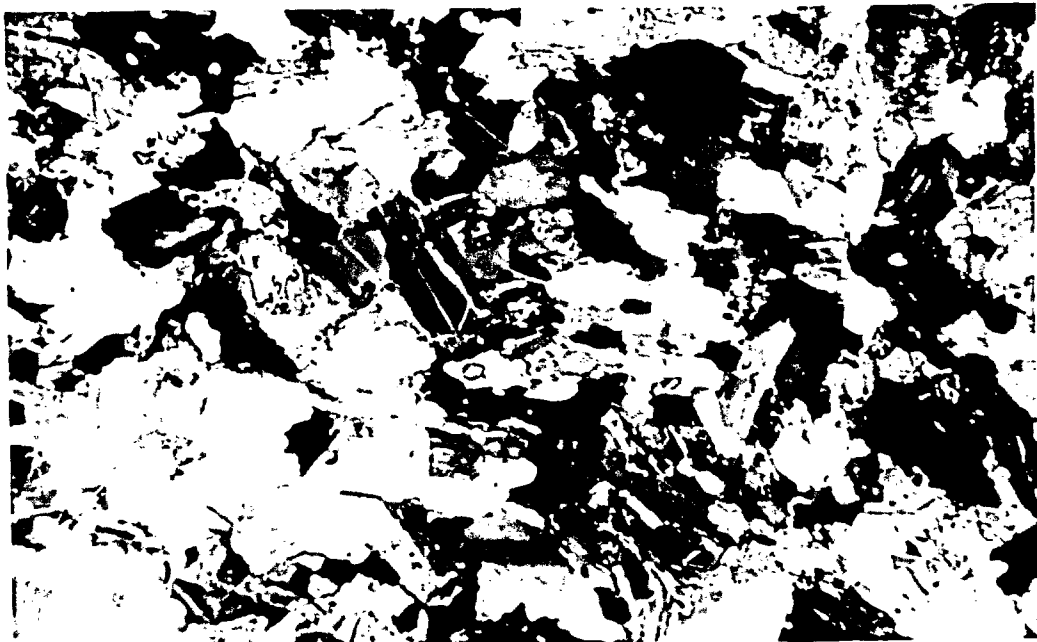


Photo 4.23: Fine-grained tonalite showing subhedral to anhedral plagioclase, hornblende, quartz, aggregates of biotite, and magnetite. Crossed nicols, field of view 1.5X1 mm.

Quartz forms anhedral crystals (maximum 2x1 mm) which occupy the interstitial positions. It shows an undulating extinction and contains prismatic apatite as inclusions. Subhedral sphene and anhedral microcline (0.2x0.1 mm) occur in interstitial positions together with quartz.

The tonalite of the southern satellitic intrusion (W153) is a fine to medium grained rock with a maximum grain size of 1x0.75 mm (Photo 4.23). It consists of about 54% plagioclase, 18% amphibole, 10% biotite, 14% quartz and less than 2% k-felspar with minor amounts of magnetite, sphene and epidote (Table 4.6).

Plagioclase forms subhedral to anhedral equant crystals (maximum 1x0,75 mm) most of which show oscillatory zoning ( $An_{40}$  to  $An_{34}$ ). Hornblende forms subhedral to anhedral prismatic crystals (maximum 0.75x0.5 mm) and contains minute apatite inclusions. Anhedral biotite occurs in randomly oriented crystals (0.5x0.3 mm) which occasionally form irregular aggregates of 3x2 mm in size. Anhedral quartz, magnetite and sphene are all less than 0.2x0.1 mm and occupy the interstitial positions between the major mineral phases. Epidote, less than 0.1 mm in diameter, is an alteration product of hornblende.

## 4.3.5 PARAGENESIS:

The petrographic studies of dioritic rocks reveal the following textural and reaction relationships:

- (1) Clinopyroxene encloses plagioclase crystals.
- (2) Hornblende rims and/or encloses clinopyroxene.
- (3) Biotite forms individual flakes, or aggregates of flakes.
- (4) Quartz and microcline are restricted to interstitial positions.

The interpretation of these textural relationships suggest the following order and stages of crystallization.

- (a) Early magmatic—crystallization of plagioclase and clinopyroxene.
- (b) Intermediate magmatic—reaction and crystallization of hornblende, crystallization of biotite and continuation of plagioclase crystallization.
- (c) Late magmatic—crystallization of quartz and microcline.

There exists a general, gradual change in the shape and size of plagioclase phenocrysts from maximum size euhedral crystals in the amphibole gabbro to minimum size anhedral crystals in the tonalite. In addition, plagioclase shows gradation from most calcic in the hornblende gabbro to most sodic in tonalite. Although there is a general increase in the amounts of quartz and microcline from the amphibole gabbro to the quartz monzodiorite and tonalite, both mineral phases do not show any change in the crystal form.

In the field, apart from satellitic intrusions, the quartz monzodiorite, tonalite and most of the quartz diorite occupy areas north of the Gamitagama Lake fault and west of the Mijinemungshing Lake fault near the eastern margin of the complex (Figure 3.2). The former area is a downthrown block, and the latter is fault-bounded on three sides while on the fourth it is separated by the granitic intrusion from the other dioritic rocks. Both of the areas represent higher levels of the dioritic intrusion.

The field relations discussed above and changes in the mineral ratios and forms suggest in situ differentiation of the parent magma. The sinking of early formed plagioclase and clinopyroxene to the lower levels and subsequent upwards movement of the

magma gave rise to a systematic variation of rock types, basic at lower levels and acidic at higher levels.

In the fine-grained equivalent of the diorite, plagioclase and pyroxene (now recrystallized to amphibole) are the early phases. Hornblende, biotite, microcline, and quartz followed one after the other, in the intermediate and late stages.

In the fine grained equivalent of the tonalite plagioclase is the earliest phase to crystallize. Hornblende closely followed the plagioclase. Biotite and quartz are the intermediate and late stage mineral phases respectively.

#### 4.4 GRANITIC ROCKS

The granitic rocks are two closely related rock types, namely granodiorite and granite. The modal mineral compositions and modal plot of granitic rocks are given in Table 4.7 and Figure 4.5 respectively.

##### 4.4.1 GRANODIORITE:

The granodiorite is a coarse grained (maximum 2x2 mm), hypidiomorphic granular rock. It consists of about 47% plagioclase, 18% microcline, 19% quartz, 4%



Table 4.7: Modal mineral compositions of representative samples of the Granitic Rocks and Quartz Monzonite Dike.

		GRANITIC ROCKS									
Rock Name	Sample No.	Grano-diorite		Granite							
		W46	W46	W141	W142	W408	W118	W121	W55G	W41A	
Plagioclase		47.2	40.2	35.8	40.2	39.5	38.2	41.7	40.3	42.6	
K-feldspars		17.8	23.7	24.2	23.7	24.8	25.1	26.9	26.2	18.2	
Quartz		19.3	31.6	32.3	31.6	27.9	30.6	27.6	20.6	29.5	
Hornblende		4.2	1.5	1.8	1.5	2.7	0.8	0.7	0.5	3.9	
Biotite		10.5	1.9	5.2	1.9	4.7	4.1	2.6	3.1	3.9	
Apatite		0.5	0.4	0.2	0.4	0.2	0.1	0.3	0.2	0.3	
Opauques		0.4	0.3	0.3	0.3	0.1	0.5	0.1	tr	1.3	
Zircon		tr	tr	tr	tr	tr	0.1	tr	tr	tr	
Sphene		tr	tr	0.1	tr	tr	tr	0.1	tr	0.1	
An% in Plag.	19-14		16	18	16	16	15	14	16-10	13	

		QUARTZ MONZONITE DIKE				
Sample No.	Sample No.	W62	W60	W51	W50	
		Plagioclase	35.2	40.9	39.7	39.5
K-feldspars	49.3	44.5	48.3	46.6		
Quartz	4.8	5.7	6.4	5.2		
Hornblende	2.6	1.7	1.2	1.4		
Biotite	5.2	6.4	3.5	6.5		
Apatite	0.5	0.2	0.2	0.5		
Opauques	0.3	0.5	0.6	0.4		
Zircons	tr	0.1	tr	tr		
Sphene	tr	tr	tr	0.1		
An% in Plag.	15-10	15	12	11		

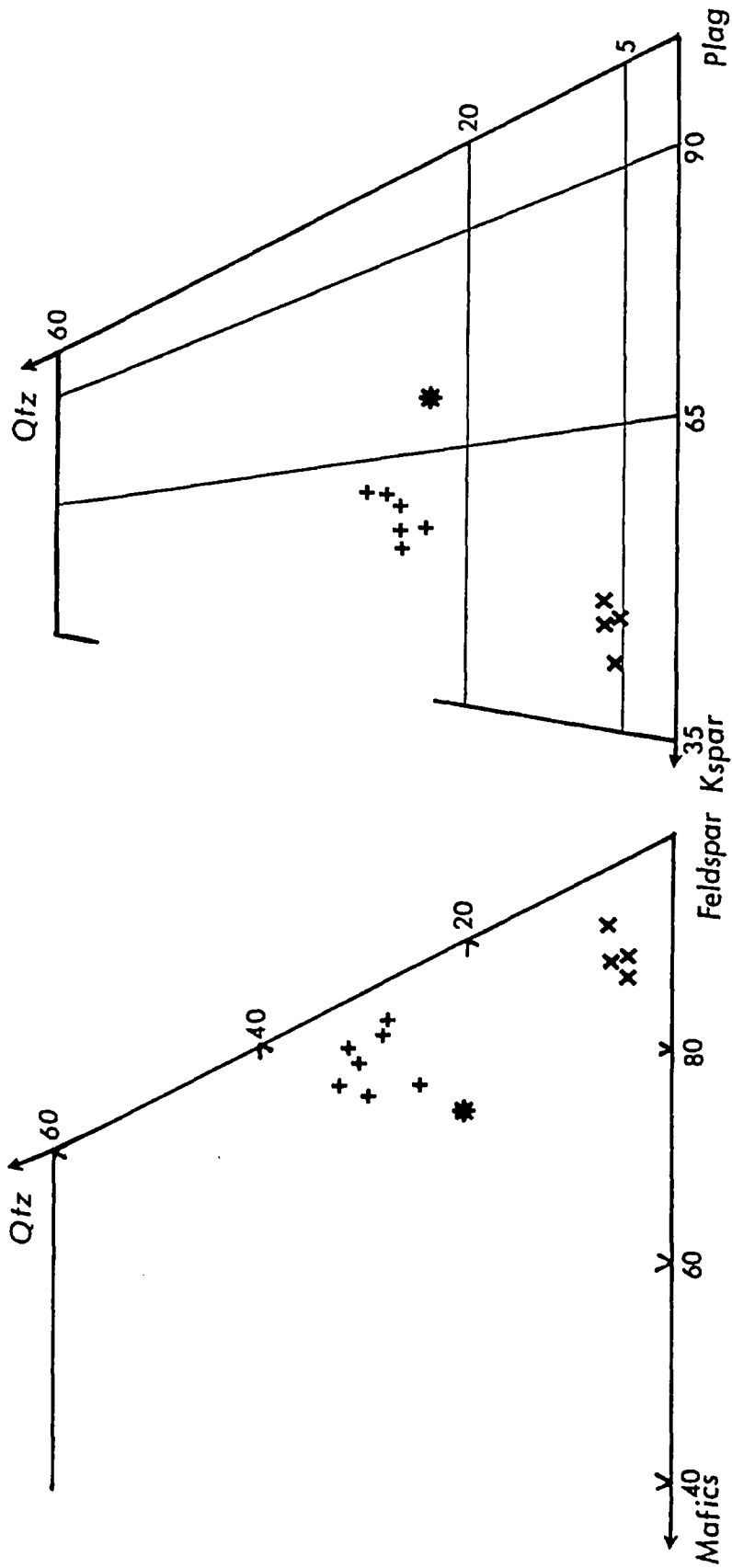


Figure 4.5 Modal mineral proportions in the Granitic Rocks and Quartz Monzonite Dike.

(\*) Granodiorite

(+) Granite

(x) Quartz Monzonite

Field boundaries according to Streckeisen (1976).

hornblende, 10% biotite and minor amounts of magnetite and apatite.

Plagioclase ( $An_{19-14}$ ) forms subhedral to anhedral crystals (maximum 2x1 mm), which show twinning on the albite and carlsbad-albite laws. Strong oscillatory patchy zoning ( $An_{20}$  to  $An_{14}$ ) is common in plagioclase. Alteration to aggregates of sericite with rare epidote in patches, maximum 0.1 mm in diameter, is mostly restricted to the most calcic zones of the plagioclase.

Microcline occurs in subhedral to euhedral crystals (maximum 2x2 mm). Some of the anhedral crystals occupy the interstitial positions. Carlsbad twinning was observed in a few crystals. Inclusions of anhedral plagioclase (0.2x0.1 mm) and minute prismatic apatite are occasionally present in microcline grains.

Hornblende, pleochroic from light pale-green to dark-green, forms subhedral crystals (maximum 1x0.5 mm). Biotite flakes often surround the hornblende crystals. Twinning parallel to (100) is rare. Alteration to chlorite sometimes occur in thin areas near crystal margins.

Biotite occurs in aggregates of randomly oriented flakes (maximum 1x0.5 mm) and is pleochroic from light

yellowish-green to dark-green. Inclusions in biotite of minute prismatic apatite and zircon with pleochroic haloes are fairly common. Alteration to chlorite and anhedral epidote, up to a maximum of 0.1 mm in diameter, occurs at the junction of the hornblende and biotite crystal boundary.

Anhedral quartz (maximum 2x1 mm), occupies interstitial positions and has undulating extinction. Inclusions of other minerals were not observed in the quartz.

The magnetite occurs in anhedral rounded grains less than 0.1 mm in diameter. It occupies interstitial positions together with quartz and also occurs as inclusion in hornblende.

#### 4.4.2 GRANITE:

The granite is a coarse-grained (maximum 4x2 mm), hypidiomorphic granular rock. It has a heterogeneous distribution of its constituent minerals.

The Granite consist of 35 to 43% plagioclase, 18 to 27% microcline, 27 to 32% quartz, 0.5 to 3% hornblende, 2 to 5% biotite and minor amounts of magnetite, apatite, sphene, and zircon.



Photo 4.24: Granite showing myrmekitic intergrowth at the boundaries of quartz and plagioclase which extends inside the microcline crystals. Crossed nicols, field of view 0.75X0.5 mm.

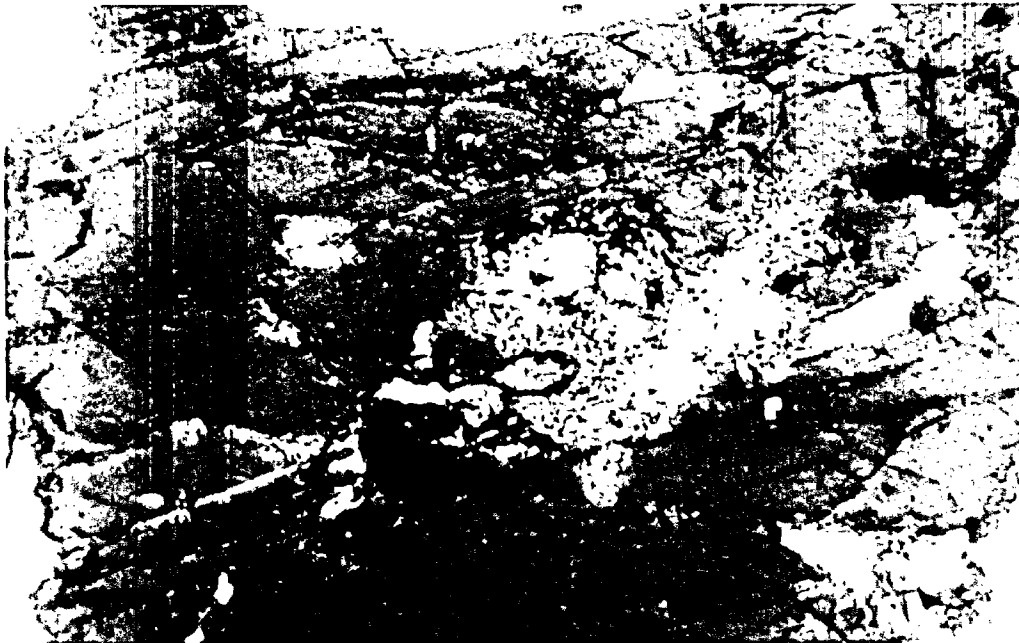


Photo 4.25: Quartz monzonite showing hornblende with clinopyroxene core and inclusions of magnetite. Plane light, field of view 1.5X1 mm.

Plagioclase ( $An_{18-10}$ ) forms subhedral to anhedral crystals, up to 3x2 mm in maximum dimensions. Twinning on the albite and Carlsbad-albite laws is common but rare on the pericline law. Most of the crystals show normal to oscillatory zoning ( $An_{20}$  to  $An_{10}$ ). Myrmekitic intergrowth of quartz in places at the boundaries of K-feldspars and plagioclase is rare and occurs in small, 0.2x0.1 mm, lobes (Photo 4.24). Alteration to sericite with occasional grains of clinozoisite occurs in patches, maximum 0.2x0.1 mm, in the more calcic zones of zoned plagioclase crystals.

Microcline, maximum 4x3 mm, occurs in subhedral to anhedral crystals. It rarely shows perthitic intergrowth. Twinning on the Carlsbad law is present in a few grains. Inclusions of anhedral plagioclase (maximum 0.5x0.2 mm), and minute prismatic apatite are occasionally present. Most of the microcline is fresh and alteration to sericite is rare.

Hornblende occurs in subhedral to anhedral crystals (maximum 1x0.5 mm) and is pleochroic from pale-green to dark-green. Twinning parallel to (100) is present in a few crystals. Biotite flakes often surround the hornblende crystals partially or completely. Alteration to epidote at crystal boundaries occurs in minute, less than 0.1 mm, grains.

Biotite, maximum 1x0.5 mm, occurs in anhedral individual flakes and randomly oriented flake aggregates. It is pleochroic from light yellowish-green to dark-green. Inclusions of prismatic apatite and zircons with pleochroic haloes are fairly common. Alteration to chlorite is rare and only occurs in minute areas near flake margins.

Anhedral quartz, maximum 2x1.5 mm, occurs in anhedral crystals which occupy interstitial zones between the feldspars and mafic minerals. Most of the crystals show an undulating extinction. Inclusions of other minerals were not observed. The anhedral magnetite, maximum 0.1 mm in diameter, and euhedral to subhedral sphene (0.2x0.1 mm) occupy the interstitial positions together with quartz.

#### 4.4.3 PARAGENESIS:

Euhedral plagioclase, although most of it has been modified by the additions of late rim material, and prismatic hornblende, are the earliest phases to crystallize. Subhedral microcline also joined these phases, at a later stage. Biotite which contains inclusions of apatite, zircon and magnetite is comparatively late in the crystallization sequence.

The occurrence of quartz in the interstitial positions implies a late crystallization of this mineral. The myrmekitic growth of plagioclase and quartz suggests that the latter continued crystallization over a considerable period of time after most of the other minerals had crystallized.

#### 4.5 QUARTZ MONZONITE

The quartz monzonite is a coarse-grained (maximum 4x2 mm), microporphyritic to hypidiomorphic granular rock. It has a heterogeneous distribution of its constituent minerals. The quartz monzonite consists of 44 to 49% microcline, 35 to 41% plagioclase, 1 to 3% hornblende, 3 to 7% biotite, 4 to 7% quartz, and minor variable amounts of magnetite, apatite, zircon, monazite and sphene.

Microcline forms subhedral to anhedral tabular crystals (maximum 4x2 mm). Carlsbad twinning is present in a number of subhedral crystals. Inclusions of anhedral plagioclase (0.5x0.3 mm), anhedral magnetite (0.1 mm in diameter), and prismatic apatite (0.1x0.05 mm) independently occur in microcline.

Plagioclase (An<sub>15-10</sub>) forms subhedral to anhedral crystals up to a maximum of 2.5x2 mm in size.



Twinning is common on the albite law. A weak, normal to oscillatory zoning ( $An_{20}$  to  $An_{10}$ ) is present in a number of crystals. Inclusions of minute apatite in plagioclase are rare. Alteration to saussurite occurs in irregular patches less than 0.5 mm in diameter.

Subhedral to anhedral hornblende forms prismatic crystals (maximum  $1 \times 0.5$  mm). It is pleochroic from yellowish-green through green to dark greenish-blue. Cores of neutral to light green pleochroic clinopyroxene are present in a few hornblende crystals (Photo 4.25). Mostly these cores show various degrees of alteration to secondary light-green tremolite-actinolite amphibole and magnetite. Minute inclusions of prismatic apatite, monazite and anhedral magnetite often occur in hornblende. Alteration to chlorite in small areas, less than 0.1 mm in diameter, occurs near crystal margins.

Biotite occurs in isolated anhedral crystals (maximum  $0.5 \times 0.2$  mm) which occupy interstitial positions between the feldspars and hornblende. Aggregates of randomly oriented biotite flakes are maximum  $3 \times 2$  mm in dimension. The boundaries of biotite flakes in these aggregates are usually marked by minute apatite and monazite grains. Biotite is pleochroic from light-yellow to dark brownish-green.

Inclusions of magnetite, apatite, monazite and zircon are common in biotite. Zircon and monazite inclusions contain pleochroic dark haloes around them in biotite. Alteration of biotite to chlorite occurs in small areas less than 0.1x0.05 mm in dimension at the crystal margins.

Anhedral quartz (maximum 3x0.5 mm), occupies the interstices between major mineral phases. Myrmekitic intergrowth at the boundaries of quartz and oligoclase is occasionally present in small areas of 0.2x0.1 mm in dimension. Micrographic intergrowth of microcline and quartz often occurs in small areas, up to 0.3x0.2 mm in maximum dimensions, inside the microcline crystals.

Anhedral magnetite, less than 0.1 mm in diameter, occupies interstitial positions together with quartz.

#### 4.5.1 PARAGENESIS:

Plagioclase, which is often included in microcline, and clinopyroxene cores in hornblende are the early formed phases. Hornblende, together with biotite, later took over the clinopyroxene. Microcline which exhibits well defined faces against quartz, precedes the latter. The inclusions of

apatite in plagioclase suggest it formed before plagioclase. The magnetite, zircon and monazite inclusions in biotite suggest their crystallization after plagioclase and hornblende, but before biotite.

## CHAPTER 5

## GEOCHEMISTRY

Seventy two representative samples for major elements, and sixty one unaltered samples were analyzed for 10 trace elements by X-ray fluorescence. The analytical procedures used are summarized in Appendix C. The observed analytical data together with molecular weight percent norms is given in Table 5.1. This data was used to calculate various ratios, mafic index, felsic index, differentiation index and solidification index submitted in Table 5.2. Total iron is reported as  $\text{Fe}_2\text{O}_3$ . Variations in major and trace element concentrations between various rocks, as represented by the mean values and standard deviations of each element, are presented in Table 5.3. The major and trace element chemistry of the various rock types of the complex varies unsystematically to a certain degree. These chemical variations are of the same general character as seen in other differentiated plutonic bodies and are complemented by the mineralogical variations.

Table 5.1: Chemical composition and molecular weight percent norms of various rock groups in the Gamitagama Lake Complex.

INNER GABBROIC ROCKS								
Rock	Troctolite		Olivine Gabbronorite				AOGN*	
Type								
Sample								
No	W100	W101	W104	W103	W98	W111	W64	W65
Dry Wt. %								
SiO <sub>2</sub>	46.71	46.94	41.35	48.61	49.68	48.60	46.55	50.07
Al <sub>2</sub> O <sub>3</sub>	23.50	23.22	16.46	12.61	15.76	19.51	16.97	15.60
ΣFe <sub>2</sub> O <sub>3</sub>	7.02	7.19	18.82	13.01	10.12	9.43	10.41	10.31
MgO	8.32	8.35	8.52	13.22	10.19	8.27	11.44	8.85
CaO	10.85	10.67	8.64	9.90	10.44	10.67	10.65	10.08
Na <sub>2</sub> O	2.50	2.42	2.12	1.63	2.02	2.53	1.83	1.13
K <sub>2</sub> O	0.24	0.23	0.21	0.20	0.21	0.27	0.42	1.72
TiO <sub>2</sub>	0.26	0.28	2.01	0.61	0.49	0.54	0.62	1.13
P <sub>2</sub> O <sub>5</sub>	0.02	0.02	0.02	0.05	0.05	0.07	0.06	0.07
MnO	0.08	0.09	0.15	0.16	0.15	0.12	0.13	0.18

TRACE ELEMENT CONCENTRATIONS IN PPM								
V	33	36	677	143	94	120	124	133
Cr	45	39	140	318	228	131	134	44
Co	54	53	107	81	74	59	63	138
Ni	159	153	80	376	265	147	174	532
Rb	4	4	5	5	4	5	10	9
Sr	804	807	591	369	463	658	637	350
Y	-	1	3	11	9	6	11	6
Zr	-	-	-	2	-	-	20	32
Nb	2	3	5	3	2	3	5	4
Ba	131	138	205	131	134	172	235	180

MOLECULAR WEIGHT PERCENT NORMS								
Q	-	-	-	-	-	-	-	1.29
C	-	-	-	-	-	-	-	-
Or	1.34	1.40	1.26	1.12	1.26	1.64	2.49	10.60
Ab	20.57	21.28	16.53	13.97	17.25	21.54	15.64	9.68
An	52.17	49.76	35.40	26.77	33.60	41.38	37.19	32.67
Ne	-	-	0.92	-	-	-	-	-
Di	0.56	2.58	3.51	12.91	10.29	6.57	9.15	9.95
Hb	0.19	0.87	3.20	5.33	4.51	2.74	3.55	4.07
En	3.22	4.12	15.54	15.57	-	7.40	4.86	17.63
Fs	1.27	1.59	7.81	7.37	-	3.54	2.16	8.28
Fo	12.24	10.73	13.99	8.23	3.72	7.22	13.78	-
Fa	5.32	4.56	16.11	4.29	2.06	3.80	6.75	-
Mt	2.60	2.57	5.18	3.09	2.91	2.98	3.10	3.85
Hm	-	-	-	-	-	-	-	-
Il	0.47	0.51	3.89	1.16	0.94	1.04	1.19	2.16
Ap	0.05	0.05	0.04	0.11	0.12	0.15	0.15	0.16

\* Amphibole Olivine Gabbronorite

Table 5.1 (cont'd).

INNER GABBROIC ROCKS (CONT'D)									
Rock	Gabbronorite								
Type									
Sample									
No	W105	W6	W147	W8	W151	W112	W146	W150	W109*
Dry Wt. %									
SiO <sub>2</sub>	45.47	46.81	46.96	47.56	49.05	49.56	49.99	51.75	51.96
Al <sub>2</sub> O <sub>3</sub>	17.81	14.65	16.12	17.15	14.84	21.06	17.43	18.08	26.14
ΣFe <sub>2</sub> O <sub>3</sub>	14.40	13.45	15.35	13.11	18.32	8.36	10.37	9.18	4.45
MgO	6.14	9.17	6.12	5.99	6.51	5.93	6.48	7.89	1.44
CaO	10.10	12.09	10.43	9.97	9.51	10.61	11.32	9.80	10.77
Na <sub>2</sub> O	2.13	1.66	2.61	2.31	2.31	3.00	2.72	2.17	4.12
K <sub>2</sub> O	0.31	0.29	0.25	0.25	0.29	0.38	0.24	0.39	0.41
TiO <sub>2</sub>	2.26	1.30	1.92	2.46	3.02	0.90	1.20	0.60	0.60
P <sub>2</sub> O <sub>5</sub>	0.06	0.01	0.08	1.05	-	0.10	0.12	0.01	0.12
MnO	0.14	0.15	0.16	0.16	0.16	0.10	0.14	0.13	0.04
<u>TRACE ELEMENT CONCENTRATIONS IN PPM</u>									
V			450		796	139	230		94
Cr			55		134	80	238		37
Co			61		74	34	37		19
Ni			35		57	115	44		27
Rb	ND**	ND	5	ND	13	12	4	ND	6
Sr			467		356	611	638		1028
Y			11		8	9	13		2
Zr			8		4	4	1		0
Nb			5		6	4	2		2
Ba			264		293	273	251		314
<u>MOLECULAR WEIGHT PERCENT NORMS</u>									
Q	-	-	-	3.72	-	-	0.20	2.94	1.29
C	-	-	-	-	-	-	-	-	-
Or	1.88	1.75	1.50	1.49	1.31	2.27	1.44	2.30	2.45
Ab	18.20	14.23	22.37	19.69	19.83	25.51	23.16	18.47	34.90
An	38.58	32.07	31.90	36.05	29.91	43.15	34.93	38.74	51.76
Ne	-	-	-	-	-	-	-	-	-
Di	5.55	15.28	9.13	3.84	8.35	5.30	11.53	5.82	0.46
Hb	4.09	8.02	7.32	1.80	6.46	2.06	5.42	2.38	0.14
En	8.57	7.53	6.08	13.28	8.47	8.28	10.92	17.09	3.39
Fs	7.25	4.53	5.59	7.16	7.52	3.69	5.89	8.00	1.15
Fo	3.04	5.97	3.58	-	2.88	2.88	-	-	-
Fa	2.83	3.96	3.62	-	2.82	1.42	-	-	-
Mt	5.52	4.13	5.02	5.80	6.64	3.50	3.95	3.07	3.05
Hm	-	-	-	-	-	-	-	-	-
Il	4.35	2.50	3.69	4.72	5.81	1.72	2.30	1.15	1.14
Ap	0.14	2.02	0.18	2.45	-	0.24	0.27	0.03	0.27

\* Sample from plagioclase rich band in banded gabbronorite

\*\* Not determined

Table 5.1 (cont'd).

INNER GABBROIC ROCKS (CONT'D)						
Rock	Norite				Andesine	
Type					Anorthosite	
Sample						
No	W96	W144	W149	W138	W148	W143
Dry Wt. %						
SiO <sub>2</sub>	47.86	48.08	50.33	51.82	50.16	51.88
Al <sub>2</sub> O <sub>3</sub>	19.58	20.15	15.98	20.89	22.93	25.80
ΣFe <sub>2</sub> O <sub>3</sub>	10.56	11.94	12.87	7.01	8.52	5.96
MgO	4.04	3.98	6.39	6.31	2.31	1.72
CaO	9.79	8.77	9.84	10.08	9.27	9.31
Na <sub>2</sub> O	3.47	3.66	2.89	2.96	4.09	3.72
K <sub>2</sub> O	0.26	0.28	0.22	0.35	0.34	0.31
TiO <sub>2</sub>	2.46	2.39	1.30	0.47	1.87	1.18
P <sub>2</sub> O <sub>5</sub>	0.79	0.61	0.01	0.01	0.42	0.07
MnO	0.13	0.13	0.17	0.10	0.09	0.05
<u>TRACE ELEMENT CONCENTRATIONS IN PPM</u>						
V	208	161	230	96	68	49
Cr	31	32	129	88	56	34
Co	35	38	52	32	24	18
Ni	15	10	104	68	7	8
Rb	3	4	4	10	8	5
Sr	621	640	322	606	850	868
Y	16	9	9	5	9	0
Zr	0	0	3	0	0	0
Nb	4	5	3	3	4	1
Ba	310	345	175	152	449	302
<u>MOLECULAR WEIGHT PERCENT NORMS</u>						
Q	0.74	0.19	0.48	1.10	1.66	6.15
C	-	-	-	-	-	2.60
Or	1.57	1.69	1.29	2.06	2.03	1.86
Ab	29.58	31.26	24.69	25.15	34.80	31.55
An	37.37	38.00	30.31	42.92	43.41	45.87
Ne	-	-	-	-	-	-
Di	3.48	0.95	9.25	4.38	0.03	-
Hb	1.68	0.53	6.32	1.49	0.01	-
En	8.52	9.55	11.80	13.77	5.78	4.29
Fs	4.73	6.14	9.25	5.36	2.81	1.39
Fo	-	-	-	-	-	-
Fa	-	-	-	-	-	-
Mt	5.78	5.69	4.11	2.87	4.91	3.89
Hm	-	-	-	-	-	-
Il	4.70	4.58	2.50	0.89	3.57	2.24
Ap	1.85	1.43	0.01	0.03	0.98	0.17

Table 5.1 (cont'd).

OUTER GABBROIC ROCKS								
Rock	Amphibole							
Type	Norite		Gabbronorite			Gabbronorite		
Sample								
No	W95	W94	W32	W30	W90	W92	W17	W12
Dry Wt. %								
SiO <sub>2</sub>	49.49	54.35	44.63	45.02	49.53	52.14	47.51	50.11
Al <sub>2</sub> O <sub>3</sub>	15.75	17.05	16.95	16.29	15.25	18.91	17.16	18.43
ΣFe <sub>2</sub> O <sub>3</sub>	12.90	9.62	16.98	16.22	10.04	8.29	14.90	10.03
MgO	7.49	7.33	6.44	5.07	8.02	6.51	5.12	6.34
CaO	8.72	7.45	9.45	9.86	13.53	9.50	8.80	10.17
Na <sub>2</sub> O	2.59	2.40	2.03	3.08	1.57	2.89	3.22	2.74
K <sub>2</sub> O	0.35	0.25	1.13	0.32	0.18	0.31	0.57	0.79
TiO <sub>2</sub>	1.28	0.50	1.99	2.44	0.87	0.56	2.01	1.01
P <sub>2</sub> O <sub>5</sub>	0.14	0.05	0.25	1.58	0.00	0.05	0.54	0.23
MnO	0.16	0.17	0.15	0.19	0.16	0.14	0.16	0.16
TRACE ELEMENT CONCENTRATIONS IN PPM								
V	352	159		305		129	275	174
Cr	152	185		33		102	48	133
Co	57	45		32		33	44	39
Ni	52	86		8		70	42	50
Rb	6	6	ND*		ND*	6	4	13
Sr	581	340		748		561	747	661
Y	12	8		47		8	55	30
Zr	8	23		19		3	99	87
Nb	7	3		6		2	14	7
Ba	256	144		525		204	536	541
MOLECULAR WEIGHT PERCENT NORMS								
Q	-	7.73	-	-	0.91	2.06	-	-
C	-	-	-	-	-	-	-	-
Or	2.09	1.48	6.78	1.93	1.04	1.87	3.50	4.68
Ab	22.16	20.46	17.45	26.41	13.43	24.60	29.68	24.77
An	30.67	35.32	34.25	30.01	34.32	37.97	31.54	35.98
Ne	-	-	-	-	-	-	-	-
Di	5.99	0.85	5.09	4.08	18.30	4.99	4.38	7.45
Hb	4.05	0.48	4.54	3.77	8.80	2.44	3.37	3.23
En	15.31	18.01	3.09	5.99	11.65	14.02	7.58	12.26
Fs	11.87	11.67	3.16	6.33	6.42	7.86	5.84	5.31
Fo	0.54	-	7.57	3.44	-	-	3.57	1.24
Fa	0.46	-	8.54	4.01	-	-	2.75	0.54
Mt	4.08	2.93	5.13	5.78	3.46	3.00	3.77	2.64
Hm	-	-	-	-	-	-	-	-
Il	2.46	0.96	3.83	4.69	1.66	1.07	2.88	1.41
Ap	0.32	0.12	0.58	3.56	-	0.12	1.17	0.49

\*Not determined



Table 5.1 (cont'd).

OUTER GABBROIC ROCKS (CONT'D)								
Rock	Amphibole							
Type	Gabbronorite (Cont'd)			Pyroxene Diorite				
Sample								
No	W113	W27	W152	W29	W25	W16	W145	W57
Dry Wt. %								
SiO <sub>2</sub>	46.22	50.17	50.91	49.26	51.79	50.21	50.46	51.91
Al <sub>2</sub> O <sub>3</sub>	16.61	15.72	17.88	16.91	17.80	15.30	16.90	15.46
ΣFe <sub>2</sub> O <sub>3</sub>	16.24	13.11	10.46	13.79	10.41	13.45	13.13	9.71
MgO	5.40	5.70	5.95	5.41	4.91	5.88	5.23	6.81
CaO	10.03	8.97	10.20	6.14	8.85	9.68	8.44	9.84
Na <sub>2</sub> O	2.91	3.38	2.72	3.05	3.73	3.14	2.75	2.42
K <sub>2</sub> O	0.38	0.74	0.40	1.20	1.19	0.34	1.14	1.55
TiO <sub>2</sub>	1.86	1.78	1.08	1.79	1.34	1.56	1.54	1.02
P <sub>2</sub> O <sub>5</sub>	0.19	0.27	0.26	0.26	0.13	0.25	0.22	0.34
MnO	0.17	0.17	0.15	0.18	0.13	0.21	0.18	0.15
TRACE ELEMENT CONCENTRATIONS IN PPM								
V	440	174	191	219	212		229	
Cr	60	94	143	36	46		104	
Co	59	42	53	52	40		42	
Ni	29	52	53	114	48		64	
Rb	5	14	15	30	23	ND*	25	ND*
Sr	693	476	668	567	521		445	
Y	31	33	29	22	52		29	
Zr	28	173	44	106	64		74	
Nb	7	13	8	21	13		8	
Ba	509	734	743	1859	1518		2492	
MOLECULAR WEIGHT PERCENT NORMS								
Q	-	-	2.24	-	-	0.43	1.53	1.52
C	-	-	-	-	-	-	-	-
Or	2.30	4.45	2.36	7.16	7.09	2.06	6.82	9.22
Ab	24.93	30.93	23.19	26.11	33.76	28.80	23.54	20.61
An	31.54	26.07	35.70	29.21	28.51	27.26	30.69	27.00
Ne	-	-	-	-	-	-	-	-
Di	7.24	8.86	7.16	4.57	8.03	9.82	4.68	10.82
Hb	7.39	5.18	3.94	3.56	3.88	6.35	3.74	5.42
En	2.08	10.38	11.63	9.05	7.79	11.70	11.00	12.08
Fs	2.44	6.07	7.34	8.08	3.76	7.56	10.09	6.94
Fc	5.73	0.92	-	1.71	1.38	-	-	-
Fa	7.39	0.54	-	1.69	0.67	-	-	-
Mt	4.94	3.50	3.78	4.82	2.99	3.27	4.45	3.68
Hm	-	-	-	-	-	-	-	-
Il	5.58	2.53	2.07	3.43	1.88	2.22	2.95	1.95
Ap	0.45	0.57	0.60	0.62	0.27	0.53	0.50	0.79

\*Not determined

Table 5.1 (cont'd).

DIORITIC ROCKS										
Rock	Hornblende		Diorite				Quartz Diorite			
Type	Gabbro									
Sample										
No	W40	W40A	W22	W132*	W20	W21	W115	W117	W124	W140
Dry Wt. %										
SiO <sub>2</sub>	50.52	50.19	48.99	51.43	52.88	56.63	55.11	55.36	55.42	55.45
Al <sub>2</sub> O <sub>3</sub>	15.77	15.74	14.77	14.92	21.08	16.94	17.72	16.50	17.72	17.76
Σ Fe <sub>2</sub> O <sub>3</sub>	10.01	10.91	15.23	12.90	8.35	8.03	9.21	11.50	8.89	10.34
MgO	6.55	6.63	6.97	6.65	2.76	5.81	3.69	3.38	3.90	3.07
CaO	10.62	10.37	7.20	8.87	7.98	7.40	7.78	6.58	7.38	6.15
Na <sub>2</sub> O	2.20	2.12	3.97	2.98	4.12	2.81	3.44	2.82	3.69	3.55
K <sub>2</sub> O	1.71	1.77	0.78	0.97	0.74	1.55	0.95	1.70	1.08	1.79
TiO <sub>2</sub>	1.11	1.41	1.64	0.99	1.58	0.71	1.56	1.65	1.43	1.35
P <sub>2</sub> O <sub>5</sub>	0.33	0.36	0.25	0.10	0.41	0.10	0.40	0.35	0.39	0.41
MnO	0.18	0.17	0.19	0.18	0.11	0.12	0.15	0.16	0.13	0.13

## TRACE ELEMENT CONCENTRATION IN PPM

V	299	297	250	237	116	121		171	203	150
Cr	72	113	50	261	32	75		67	91	57
Co	37	39	56	50	18	35		30	31	25
Ni	51	49	65	108	21	123		14	53	23
Rb	63	61	20	27	15	70		59	41	64
Sr	557	567	417	208	684	365		402	473	440
Y	32	36	27	27	14	18		26	25	24
Zr	108	125	121	89	35	84		116	52	376
Nb	9	10	19	8	10	7		9	10	9
Ba	892	925	357	242	401	453		779	340	715

## MOLECULAR WEIGHT PERCENT NORMS

Q	-	-	-	-	3.90	7.85	9.33	11.01	8.09	7.89
C	-	-	-	-	-	-	-	-	-	-
Or	10.18	10.53	4.65	5.81	4.39	9.22	5.63	10.14	6.41	10.69
Ab	18.77	18.09	36.26	25.50	37.18	25.36	29.30	24.11	31.44	30.24
An	28.38	28.51	20.50	24.70	37.06	29.23	30.28	27.54	28.75	27.43
Ne	-	-	-	-	-	-	-	-	-	-
Di	11.69	10.57	6.83	9.08	0.07	4.17	3.18	1.34	3.02	0.26
Hb	6.78	6.67	4.49	6.62	0.03	1.50	1.61	1.21	1.44	0.24
En	9.01	10.62	2.41	11.51	7.63	14.08	7.77	7.88	8.37	7.58
Fs	5.99	7.69	1.59	9.62	3.43	5.07	4.53	8.20	4.57	7.96
Fo	1.43	0.23	10.30	0.72	-	-	-	-	-	-
Fa	1.05	0.18	6.77	0.66	-	-	-	-	-	-
Mt	3.82	3.87	3.34	3.65	3.24	2.32	4.46	4.60	4.27	4.16
Hm	-	-	-	-	-	-	-	-	-	-
Il	2.13	2.19	2.33	1.90	2.21	0.99	2.98	3.15	2.73	2.58
Ap	0.78	0.85	2.53	0.24	0.85	0.21	0.94	0.22	0.92	0.97

\* Fine grained rock

Table 5.1 (cont'd).

DIORITIC ROCKS									
Rock	Quartz								
Type	Quartz Diorite (cont'd)			Monzodiorite			Tonalite		
Sample									
No	W88	W116	W55	W129	W128	W134*	W153*	W35	W33
Dry Wt. %									
SiO <sub>2</sub>	56.62	56.54	57.59	60.07	60.40	60.44	57.90	61.99	66.17
Al <sub>2</sub> O <sub>3</sub>	17.22	16.29	15.97	16.28	16.02	15.06	16.23	16.85	15.87
ΣFe <sub>2</sub> O <sub>3</sub>	8.48	11.21	7.57	8.14	8.28	7.52	9.47	7.26	5.14
MgO	3.87	3.32	5.42	2.95	2.70	3.64	3.78	2.32	1.79
CaO	7.12	6.21	6.94	5.30	5.09	5.18	6.05	4.00	4.23
Na <sub>2</sub> O	3.34	3.00	2.87	3.39	3.62	4.54	3.84	4.60	4.57
K <sub>2</sub> O	1.05	1.35	2.15	2.55	2.71	2.46	1.30	1.54	1.26
TiO <sub>2</sub>	1.23	1.59	0.69	1.03	1.06	0.89	1.14	0.99	0.60
P <sub>2</sub> O <sub>5</sub>	0.31	0.33	0.08	0.18	0.18	0.16	0.17	0.30	0.30
MnO	0.12	0.17	0.14	0.10	0.12	0.11	0.13	0.15	0.06

## TRACE ELEMENTS CONCENTRATION IN PPM

V	177	100		135	140	140	156		75
Cr	89	65		63	54	139	40		21
Co	27	35		22	25	26	69		11
Ni	61	16		20	30	76	46		18
Rb	33	49		82	81	92	47		31
Sr	455	321		346	354	299	312		269
Y	38	31		25	26	20	27		20
Zr	103	48		229	197	223	147		172
Nb	8	9		11	10	11	11		6
Ba	406	508		930	910	749	395		481

## MOLECULAR WEIGHT PERCENT NORMS

Q	11.06	13.18	8.85	12.92	14.48	14.01	10.38	16.20	22.83
C	-	-	-	-	-	4.03	-	1.06	-
Or	6.24	8.03	12.67	15.15	21.52	3.73	7.72	9.16	7.49
Ab	28.48	25.55	24.44	30.53	22.99	26.27	32.72	39.08	38.82
An	29.07	27.24	24.56	20.92	20.93	28.11	23.37	18.00	19.09
Ne	-	-	-	-	-	-	-	-	-
Di	2.30	0.72	5.28	1.59	1.52	-	2.79	-	-
Hb	1.35	0.65	2.45	1.14	1.13	-	1.93	-	-
En	8.63	8.01	11.13	6.41	6.07	5.94	8.18	5.80	4.47
Fs	5.83	8.29	5.93	5.25	5.20	9.24	6.50	4.47	2.40
Fo	-	-	-	-	-	-	-	-	-
Fa	-	-	-	-	-	-	-	-	-
Mt	3.98	4.51	3.19	3.73	4.27	4.64	3.85	3.64	3.06
Hm	-	-	-	-	-	-	-	-	-
Il	2.35	3.04	1.32	2.02	2.73	3.20	2.18	1.90	1.15
Ap	0.72	0.78	0.19	0.42	0.92	0.83	0.39	0.61	0.70

\* Fine grained rock

Table 5.1 (cont'd).

GRANITIC ROCKS								
Rock	Grano-							
Type	diorite	Granite						
Sample								
No	W46	W142	W118	W121	W41A	W408	W141	W55G
Dry Wt. %								
SiO <sub>2</sub>	67.09	71.08	71.23	71.52	71.98	72.12	72.14	72.28
Al <sub>2</sub> O <sub>3</sub>	15.96	14.90	14.55	15.00	14.72	14.50	14.13	14.41
ΣFe <sub>2</sub> O <sub>3</sub>	4.59	3.00	3.51	2.37	2.76	2.60	3.07	2.70
MgO	1.51	0.68	0.76	0.81	0.42	0.56	0.67	0.51
CaO	2.88	1.97	1.92	2.03	1.69	1.48	1.77	1.67
Na <sub>2</sub> O	3.47	3.76	3.56	3.59	3.73	3.85	3.34	3.65
K <sub>2</sub> O	3.75	4.08	4.37	4.14	4.19	4.42	4.36	4.30
TiO <sub>2</sub>	0.61	0.40	0.42	0.41	0.40	0.34	0.41	0.37
P <sub>2</sub> O <sub>5</sub>	0.14	0.08	0.08	0.08	0.07	0.06	0.08	0.07
MnO	0.06	0.05	0.05	0.04	0.04	0.05	0.05	0.04
<u>TRACE ELEMENT CONCENTRATIONS IN PPM</u>								
V	53	29	25	25	20	16	27	21
Cr	30	61	40	45	15	15	39	23
Co	10	4	5	4	4	5	6	1
Ni	24	18	18	16	18	18	13	15
Rb	93	135	153	140	163	202	109	161
Sr	271	219	205	214	201	160	208	186
Y	29	17	20	19	20	25	11	7
Zr	266	159	167	153	161	154	167	123
Nb	13	9	4	10	9	13	5	8
Ba	990	819	728	729	739	638	867	644
<u>MOLECULAR WEIGHT PERCENT NORMS</u>								
Q	22.38	28.64	28.48	29.50	30.23	28.98	31.55	30.45
C	1.44	0.92	0.67	1.13	1.14	0.83	0.91	0.88
Or	22.41	24.13	25.78	24.46	24.80	26.16	25.78	25.44
Ab	31.49	31.83	30.02	30.37	31.55	32.64	28.26	30.95
An	13.51	9.24	8.96	9.56	7.96	6.95	8.22	7.83
Ne	-	-	-	-	-	-	-	-
Di	-	-	-	-	-	-	-	-
Hb	-	-	-	-	-	-	-	-
En	4.21	1.70	1.90	2.03	1.06	1.39	1.67	1.27
Fs	1.20	-	0.44	-	-	-	-	-
Fo	-	-	-	-	-	-	-	-
Fa	-	-	-	-	-	-	-	-
Mt	2.23	2.17	2.77	0.28	1.50	1.38	2.35	1.49
Hm	-	0.41	-	1.72	0.86	0.89	0.29	0.84
Il	0.85	0.77	0.79	0.78	0.75	0.64	0.77	0.70
Ap	0.29	0.19	0.19	0.19	0.16	0.14	0.19	0.16

Table 5.1 (cont'd).

QUARTZ MONZONITE DIKE				
Rock				
Type	Quartz Monzonite			
Sample				
No	W62	W51	W50	W60
Dry Wt. %				
SiO <sub>2</sub>	61.41	62.64	62.72	64.25
Al <sub>2</sub> O <sub>3</sub>	18.16	18.04	18.51	14.74
Σ Fe <sub>2</sub> O <sub>3</sub>	5.54	5.17	4.57	6.18
MgO	1.03	0.39	0.88	0.74
CaO	1.74	1.56	2.13	2.07
Na <sub>2</sub> O	4.08	3.97	3.88	3.85
K <sub>2</sub> O	6.93	7.31	6.36	6.07
TiO <sub>2</sub>	0.84	0.68	0.70	0.79
P <sub>2</sub> O <sub>5</sub>	0.17	0.11	0.17	0.18
MnO	0.12	0.13	0.09	0.13
<u>TRACE ELEMENT CONCENTRATION IN PPM</u>				
V	0	0	5	4
Cr	32	10	9	44
Co	8	4	5	2
Ni	14	10	8	8
Rb	70	73	104	87
Sr	65	45	240	86
Y	21	17	33	23
Zr	1025	900	776	1204
Nb	7	6	14	7
Ba	382	193	2525	475
<u>MOLECULAR WEIGHT PERCENT NORMS</u>				
Q	5.44	6.96	9.97	9.73
C	1.22	1.03	1.79	-
Or	41.05	43.32	37.67	41.97
Ab	34.61	33.69	32.88	32.70
An	7.51	7.02	9.47	2.05
Ne	-	-	-	-
Di	-	-	-	2.25
Hb	-	-	-	3.73
En	2.57	0.97	2.19	0.80
Fs	2.21	2.29	1.12	1.52
Fo	-	-	-	-
Fa	-	-	-	-
Mt	3.40	3.16	3.19	3.33
Hm	-	-	-	-
Il	1.59	1.29	1.33	1.50
Ap	0.40	0.26	0.40	0.42

Table 5.2 The calculated indices and ratios for the analyzed rock samples.

	D.I	S.I	F.I	H.I	FeO/HgO	Ti(ppm)	K(ppm)	Ba/Sr	K/Rb	Rb/Sr	Y/Sr	Sr/Zr
INTER GABBROIC ROCKS												
W100	22.82	46.61	19.85	46.25	0.83	1680	18.76	0.17	469.06	0.00	0.00	804.00
W101	23.58	44.41	20.13	46.03	0.83	1590	19.59	0.16	489.82	0.00	0.00	807.00
W64	18.90	43.68	17.43	47.64	0.96	3728	34.70	0.36	347.02	0.03	0.02	10.98
W65	22.38	39.21	22.06	53.47	1.11	6774	14387	0.51	1587.53	0.02	0.02	31.85
W98	19.44	43.45	17.61	49.83	0.97	2946	1751	0.28	437.930	0.01	0.02	463.00
W103	15.92	44.11	15.65	47.42	0.88	3630	1685	0.35	336.06	0.01	0.03	184.50
W104	20.43	27.45	21.23	67.84	2.13	12072	1735	0.34	347.02	0.00	0.01	591.00
W111	24.30	40.32	20.80	51.23	1.02	3252	2283	0.26	456.61	0.01	0.01	658.00
W6	17.00	37.32	13.19	57.81	1.32	7606	X	X	X	X	X	X
W8	26.34	27.66	20.40	67.04	1.97	14784	2067	X	X	X	X	X
W105	21.69	25.74	19.46	70.11	2.28	13560	2606	X	X	X	X	X
W109	40.15	13.83	29.71	74.48	2.78	3606	3628	0.35	571.45	0.01	0.00	1028.00
W112	29.17	33.52	24.16	56.71	1.27	5394	3171	0.44	266.28	0.02	0.02	152.75
W146	26.29	32.71	20.72	59.71	1.44	7224	20091	0.39	502.27	0.01	0.02	638.00
W147	25.66	25.15	21.54	69.82	2.26	11533	2083	0.56	416.76	0.01	0.02	58.38
W150	24.54	40.19	20.67	51.77	1.05	3618	3212	X	X	X	X	X
W151	23.43	23.73	21.00	72.24	1.05	18096	2415	0.82	185.84	0.04	0.02	89.00
W96	34.00	20.79	27.60	72.90	2.60	14736	2183	0.48	727.809	0.01	0.03	621.00
W138	29.48	37.94	24.67	50.76	1.00	2808	2872	0.25	287.25	0.02	0.01	606.00
W144	35.39	20.03	31.05	73.67	2.70	1434	2349	0.53	587.37	0.01	0.01	640.00
W149	28.21	28.57	23.98	64.94	1.81	7818	1793	0.54	448.31	0.01	0.03	107.33
W143	40.93	14.69	30.20	76.63	3.10	7050	2598	0.34	519.71	0.01	0.00	868.80
W148	40.54	15.14	32.36	77.66	3.32	11226	2839	0.52	354.91	0.01	0.01	850.00
OUTER GABBROIC ROCKS												
W94	30.48	35.91	26.22	56.76	1.28	3000	2067	0.42	344.53	0.02	0.02	14.78
W95	25.88	30.87	25.18	63.28	1.66	7680	2905	0.44	484.28	0.01	0.02	72.62
W30	30.61	20.54	25.67	74.72	2.88	14634	6273	0.70	1336.52	0.00	0.01	39.37
W32	25.74	29.21	25.09	70.83	2.37	11928	9389	X	X	X	X	X
W90	16.31	38.91	11.45	55.61	1.11	5208	1452	X	X	X	X	X
W92	29.82	34.90	25.21	56.01	1.23	3342	2606	0.36	435.47	0.01	0.02	187.00
W12	29.50	31.86	25.73	59.43	1.47	3600	6525	0.81	501.95	0.02	0.05	7.59
W17	33.17	21.95	30.12	72.87	2.59	12054	4765	0.71	1191.34	0.01	0.07	7.54
W27	35.41	24.86	31.46	68.03	2.07	10692	6135	1.54	438.23	0.03	0.07	2.75
W113	29.28	21.66	24.72	73.47	2.71	11178	3188	0.73	637.59	0.01	0.04	24.75
W152	29.20	30.47	23.40	61.80	1.57	6400	3295	1.11	219.73	0.02	0.04	15.18
W16	48.37	17.59	26.43	67.84	3.35	9355	2831	X	X	X	X	X
W29	40.82	24.59	35.74	65.72	1.85	8034	9887	2.91	429.90	0.05	0.10	8.14
W25	35.28	27.07	35.31	70.20	2.29	10716	9954	3.27	331.80	0.05	0.04	5.35
W145	33.71	23.51	31.59	69.85	2.25	9228	9489	5.60	379.57	0.06	0.07	6.01
W57	32.70	32.02	28.72	58.79	1.42	6096	12843	X	X	X	X	X

Table 5.2 (cont'd).

	D.I	S.I	F.I	H.I	FeO/HgO	Tl(ppm)	K(ppm)	Ba/Sr	K/Rb	Rb/Sr	V/Sr	Sr/Zr
DIORITIC ROCKS												
W40	30.40	30.20	26.88	61.60	1.54	6660	14179	1.60	225.08	0.11	0.06	5.30
W40A	30.01	28.65	27.23	63.29	1.69	6846	14643	1.63	240.21	0.11	0.06	4.54
W20	45.65	17.29	37.82	74.32	2.73	9468	6135	0.58	409.09	0.02	0.02	19.54
W21	42.46	31.91	37.05	56.15	1.24	4234	12876	1.24	183.95	0.19	0.05	4.35
W22	40.99	25.85	39.74	66.79	1.96	9864	6434	0.85	321.70	0.05	0.06	3.44
W55	47.01	29.23	41.90	58.29	1.39	4134	17859	X	X	X	X	X
W68	62.77	20.04	57.45	65.79	1.66	3832	11116	X	X	X	X	X
W69	40.33	31.64	30.7	56.95	1.28	10140	X	X	X	X	X	X
W88	47.25	22.41	38.15	68.69	2.09	7380	8708	0.89	263.90	0.07	0.08	4.41
W115	45.81	21.39	36.07	69.97	2.25	9343	7853	X	X	X	X	X
W116	48.37	17.59	41.13	75.77	3.09	9516	11191	1.58	228.39	0.15	0.10	6.68
W117	46.90	17.41	40.75	75.92	3.06	9882	14130	1.93	239.49	0.15	0.06	3.46
W124	47.52	22.22	39.29	68.02	2.05	8562	8949	0.71	218.28	0.09	0.05	9.10
W128	60.31	15.69	55.45	76.02	2.73	6360	30111	2.57	337.17	0.23	0.07	1.80
W129	60.06	16.54	54.62	72.90	2.59	6180	2161	2.68	258.07	0.24	0.07	1.51
W132	33.05	28.30	30.84	64.06	1.74	5934	8077	1.16	299.18	0.13	0.13	2.33
W140	50.66	16.37	46.47	75.75	2.25	8100	14902	1.62	232.85	0.15	0.05	1.20
W153	52.42	20.56	45.92	69.92	3.03	6828	10767	1.26	229.10	0.15	0.09	2.12
W134	63.44	20.04	57.83	82.17	1.86	5328	20431	2.50	222.08	0.31	0.07	1.34
W33	70.10	14.03	57.98	73.01	2.58	3624	10485	1.78	338.24	0.12	0.08	1.56
W35	65.87	14.75	60.55	76.57	2.82	5964	12810	X	X	X	X	X
GRANITIC ROCKS												
W46	76.26	11.39	71.52	74.01	3.29	3630	31140	3.65	334.85	0.34	0.10	1.02
W40B	88.28	4.90	84.86	81.92	4.17	2034	36711	3.98	181.74	1.26	0.16	1.03
W41A	87.12	3.78	82.38	86.34	5.88	2374	34840	3.67	213.56	0.81	0.10	1.25
W55C	87.34	4.57	82.69	83.70	4.76	2208	35706	3.46	221.78	0.87	0.03	1.51
W118	85.38	6.47	80.52	81.45	3.62	2502	36320	3.55	238.45	0.75	0.10	1.23
W121	84.70	7.51	79.18	74.00	2.58	2472	36345	3.40	245.32	0.65	0.09	1.40
W141	86.09	5.86	81.34	81.52	4.1	2436	36180	4.16	331.93	0.52	0.05	1.24
W142	85.16	5.90	79.92	80.97	3.97	2424	33863	3.73	250.84	0.62	0.08	1.38
QUARTZ HORIZONITE												
W50	81.61	5.61	82.78	81.15	4.68	4182	52800	10.52	507.70	1.08	0.32	0.06
W51	85.40	2.32	87.86	92.59	11.97	4056	60679	4.28	831.22	1.62	0.38	0.05
W60	86.15	4.15	84.08	88.71	7.56	4712	58728	5.52	675.04	0.43	0.14	0.31
W62	82.52	5.86	86.38	88.53	4.85	5016	57491	5.87	821.30	0.01	0.26	0.07

## 5.1 INNER GABBROIC SERIES

### 5.1.1 MAJOR ELEMENT VARIATIONS:

In the Inner Gabbroic Series the troctolite contains the highest contents of CaO together with high  $\text{Al}_2\text{O}_3$  and MgO (Table 5.2). Fractionation of plagioclase and olivine controls the chemistry of the rock. The CaO and  $\text{Al}_2\text{O}_3$  are essentially concentrated in the plagioclase. Olivine contains almost all of the MgO. Most of the iron oxide and  $\text{TiO}_2$  are contained by titaniferous magnetite, though some of the iron (in the ferrous state) has probably entered the fayalitic molecule of the olivine.

The olivine gabbronorite has the highest iron oxide and MgO. The rock has lower values for CaO,  $\text{Al}_2\text{O}_3$ , and MgO. Although most of the iron oxide is concentrated in titaniferous magnetite, some of it must be contained in the olivine and pyroxenes. The clinopyroxene, a new cumulative phase in this rock, and orthopyroxene, an intercumulus phase, exert some control over the CaO, MgO and iron oxide contents.

The amphibole olivine gabbronorite is characterized by high MgO, CaO, iron oxide and  $\text{Al}_2\text{O}_3$ . Cumulus plagioclase, olivine, clinopyroxene, and intercumulus



Table 5.3 Average chemical composition of various rock types encountered in the Gamitagama Lake Complex.

INNER GABBROIC SERIES

Rock Type	Troctolite		Olivine Gabbronorite		Amphibole Ol. Gabbronorite		Gabbronorite		Norite		Andesine Anorthosite	
	$\bar{x}$	s	$\bar{x}$	s	$\bar{x}$	s	$\bar{x}$	s	$\bar{x}$	s	$\bar{x}$	s
Wt%												
SiO <sub>2</sub>	46.83	0.16	47.06	3.84	48.31	2.49	47.89	2.34	49.52	1.90	51.02	1.22
Al <sub>2</sub> O <sub>3</sub>	23.36	0.20	16.08	2.83	16.28	0.97	17.14	2.05	19.15	2.08	24.36	2.03
ΣFe <sub>2</sub> O <sub>3</sub>	7.10	0.12	12.84	4.27	10.36	0.07	12.82	3.35	10.60	2.57	7.24	1.81
MgO	8.29	0.09	10.15	2.28	10.14	1.83	6.78	1.15	5.18	1.35	2.02	0.42
CaO	10.76	0.13	9.91	0.91	10.37	0.40	10.48	0.85	9.62	0.58	9.29	0.03
Na <sub>2</sub> O	2.46	0.06	2.07	0.37	1.48	0.49	2.36	0.41	3.24	0.38	3.90	0.26
K <sub>2</sub> O	0.23	0.01	0.22	0.03	1.07	0.92	0.30	0.06	0.28	0.05	0.33	0.02
TiO <sub>2</sub>	0.27	0.01	0.91	0.73	0.87	0.36	1.71	0.84	1.66	0.95	1.53	0.49
P <sub>2</sub> O <sub>5</sub>	0.02	0.001	0.05	0.02	0.07	0.00	0.18	0.35	0.36	0.41	0.25	0.24
MnO	0.08	0.005	0.15	0.02	0.16	0.04	0.15	0.02	0.13	0.03	0.07	0.02
(PPM)							4 samples					
V	34.50	2.12	258.50	279.72	128.50	6.36	403.75	292.28	173.75	59.29	58.50	13.43
Cr	42.00	4.24	204.25	87.55	89.00	63.64	126.75	81.16	70.00	47.50	45.00	15.56
Co	53.50	0.71	80.25	20.05	100.50	53.03	51.50	19.26	39.30	8.85	21.00	4.24
Ni	156.00	4.24	217.00	130.71	353.00	253.14	62.75	35.98	49.30	44.95	7.50	0.71
Pb	4.00	0.00	4.75	0.50	9.50	0.71	8.50	4.65	5.30	3.20	6.50	2.12
Sr	805.50	2.12	520.25	129.27	493.50	202.94	518.00	131.52	547.30	150.81	859.00	12.73
Y	0.50	0.70	7.25	3.50	8.50	3.54	10.25	2.22	9.80	4.57	4.50	6.36
Zr	0.00	0.00	0.50	1.00	26.00	8.48	4.25	2.87	0.80	1.50	0.00	-
Nb	2.5	0.71	3.25	1.26	4.50	0.71	4.25	1.71	3.80	0.96	2.50	2.12
Bd	134.50	4.95	160.50	35.05	207.50	38.89	270.25	17.65	243.30	94.29	375.50	103.94

$\bar{x}$  mean  
s standard deviation

Table 5.3 (cont'd).

Rock Type	OUTER GABBROIC SERIES						DIORITIC ROCKS					
	Norite 2 samples		Gabbronorite 3 samples		Amphibole Gabbronorite 6 samples		Pyroxene Diorite 4 samples		Hornblende Gabbro 2 samples		Diorite 3 samples	
	$\bar{x}$	s	$\bar{x}$	s	$\bar{x}$	s	$\bar{x}$	s	$\bar{x}$	s	$\bar{x}$	s
Wt%												
SiO <sub>2</sub>	51.91	3.43	46.39	2.73	49.51	2.21	50.79	1.28	50.15	0.05	52.80	3.77
Al <sub>2</sub> O <sub>3</sub>	16.34	0.92	16.16	0.86	17.48	1.18	16.37	1.20	15.76	0.02	17.59	3.20
ΣFe <sub>2</sub> O <sub>3</sub>	11.26	2.32	14.41	3.80	12.17	3.08	11.77	2.14	10.71	0.29	10.54	4.07
MgO	7.41	0.11	6.51	1.47	5.84	0.54	5.75	0.81	6.43	0.18	5.18	2.18
CaO	8.08	0.90	10.95	2.25	9.61	0.62	9.13	0.79	10.50	0.18	7.53	0.41
Na <sub>2</sub> O	2.49	0.14	2.23	0.77	2.97	0.26	3.08	0.53	2.16	0.58	3.63	0.72
K <sub>2</sub> O	0.30	0.07	0.54	0.51	0.53	0.20	1.07	0.51	1.73	0.04	1.02	0.46
TiO <sub>2</sub>	0.89	0.55	1.76	0.81	1.38	0.58	1.42	0.33	1.13	0.02	1.13	0.52
P <sub>2</sub> O <sub>5</sub>	0.09	0.06	0.59	0.81	0.26	0.16	0.24	0.09	0.35	0.02	0.25	0.15
MnO	0.16	0.01	0.17	0.02	0.16	0.01	0.17	0.02	0.18	0.00	0.14	0.04
PPM												
V	258.50	140.71	305.00	-	230.50	113.24	215.50	4.95	298.00	1.41	162.30	75.96
Cr	168.50	23.33	33.00	-	96.67	37.99	41.00	7.07	92.50	28.99	52.30	21.59
Co	51.00	8.48	32.00	-	45.00	9.48	46.00	8.48	38.00	1.41	36.30	19.03
Ni	69.00	24.04	8.00	-	49.33	13.53	81.00	46.67	50.00	1.41	69.70	51.16
Rb	6.00	0.00	2.00	-	9.50	5.01	26.00	4.95	62.00	1.41	35.00	30.41
Sr	460.50	170.41	748.00	-	634.33	98.41	544.00	32.53	562.00	7.07	488.70	171.15
Y	10.00	2.83	47.00	-	31.00	14.93	37.00	21.21	34.00	2.82	19.70	6.65
Zr	15.50	10.61	19.00	-	72.33	61.05	85.00	29.70	116.50	12.02	80.00	43.14
Nb	5.00	2.82	6.00	-	8.50	4.12	17.00	5.66	9.50	0.71	12.00	6.24
Bd	200.00	79.20	525.00	-	554.00	196.26	1688.50	241.12	908.50	23.33	403.00	48.05

$\bar{x}$  mean  
s standard deviation

Table 5.3 (cont'd).

Rock Type	DIORITIC ROCKS				GRANITIC ROCKS			
	Quartz Diorite 7 samples $\bar{x}$ s	Quartz Monzodiorite 3 samples $\bar{x}$ s	Tonalite 2 samples $\bar{x}$ s	Granodiorite 1 sample	Granite 7 samples $\bar{x}$ s	Quartz Monzonite 4 samples $\bar{x}$ s		
Wt%								
SiO <sub>2</sub>	56.01	60.30	64.08	67.08	71.76	62.75		
Al <sub>2</sub> O <sub>3</sub>	17.02	15.78	16.35	15.96	14.60	17.36		
ΣFe <sub>2</sub> O <sub>3</sub>	9.60	8.01	6.20	4.54	2.85	5.36		
MgO	3.80	3.06	2.05	1.50	0.63	0.75		
CaO	6.88	5.12	4.11	2.87	1.78	1.87		
Na <sub>2</sub> O	3.24	3.61	4.58	3.46	3.63	3.94		
K <sub>2</sub> O	1.43	2.87	1.40	3.75	4.26	6.91		
TiO <sub>2</sub>	1.35	0.99	0.79	0.60	0.39	0.74		
P <sub>2</sub> O <sub>5</sub>	0.32	0.17	0.29	0.13	0.07	0.15		
MnO	0.14	0.10	0.10	0.06	0.04	0.11		
PPM	5 samples	1 sample						
V	160.20	138.33	75.00	53.00	23.28	2.25		
Cr	73.80	85.33	21.00	30.00	34.00	23.75		
Co	29.60	24.33	11.00	10.00	4.14	4.75		
Ni	33.40	42.00	18.00	24.00	16.57	10.00		
Rb	49.20	85.00	31.00	93.00	151.85	83.50		
Sr	418.20	333.00	269.00	271.00	199.00	109.00		
Y	28.80	23.66	20.00	29.00	17.00	23.50		
Zr	138.80	216.33	172.00	266.00	154.85	976.25		
Nb	9.00	10.66	6.00	13.00	8.28	8.50		
Ba	549.60	863.33	481.00	990.00	737.71	893.75		
$\bar{x}$	mean							
s	standard deviation							

orthopyroxene and amphibole control the bulk of the above elements. The amphibole and phlogopite should contain  $K_2O$  and part of the  $MgO$ .

The gabbronorite contains high amounts of  $CaO$ , iron oxide and  $Al_2O_3$ . The  $MgO$  is low in comparison to the olivine gabbronorite. Again plagioclase controls most of the  $CaO$  and  $Al_2O_3$  while clinopyroxene and orthopyroxene contain  $MgO$ , a part of the  $CaO$  and iron oxide. The  $TiO_2$  and a part of the iron oxide has entered the titaniferous magnetite.

The norite shows a marked decrease in the  $MgO$ , iron oxide,  $Al_2O_3$  and  $CaO$ , compared to the gabbronorite. This is probably due to decrease and disappearance of the clinopyroxene in the norite rock. Most of the  $CaO$ ,  $Al_2O_3$ , and all of the  $Na_2O$  is probably controlled by the cumulus plagioclase while  $MgO$  and a part of iron oxide is controlled by the orthopyroxene. The  $TiO_2$  (x 1.66%) and left over iron oxide is contained in titaniferous magnetite.

The andesine anorthosite contains the highest  $Al_2O_3$ , high  $CaO$  and  $Na_2O$  which are controlled by plagioclase. The orthopyroxene controls the  $MgO$  and part of the iron oxide. The bulk of the iron oxide and  $TiO_2$  is contained in titaniferous magnetite.

The inner gabbroic series show a successive general increase in  $\text{SiO}_2$  with each rock type from troctolite to andesine anorthosite.

#### 5.1.2 TRACE ELEMENT VARIATIONS:

The distribution of trace elements in the cumulate rocks depends on the independent behavior of the individual elements, whether compatible or incompatible, during fractionation. The compatible elements concentrate in the cumulus phases while the incompatible ones are segregated in the liquid and are concentrated in the intercumulate phases or last differentiates of the magma.

The troctolite in the inner gabbroic series, contains high Sr and low Ba. The  $\text{Sr}^{+2}$  and  $\text{Ba}^{+2}$  commonly substitute for Ca in the plagioclase framework and are controlled by the crystallization of plagioclase. Troctolite has comparatively low Ni, Co and Cr. These elements, Ni, Co, and Cr substitute for Fe in the olivine structure. The titaniferous magnetite contains V and part of the Cr where they probably substitute for  $\text{Fe}^{+3}$ .

In the olivine gabbroite Sr decreases while Ba, Co, Cr and V show a rapid increase. The slight

decrease in Sr can be related to the modal decrease in plagioclase. The increase in the Ni, Co, Cr and V is probably due to an increase in the modal olivine and titaniferous magnetite.

The amphibole olivine gabbronorite contains the lowest Sr but the highest Ni in comparison to the other rocks of the inner gabbroic series. There is a decrease in the amount of Cr and an increase in the Ba and Co. Modal abundances of the respective host mineral phases control the concentrations of these elements. The increase in Zr could be related to the modal abundances of both intercumulus amphibole and phlogopite.

The gabbronorite contains high amounts of Cr and V which relate directly to an increase in iron oxide and modal titaniferous magnetite. There is a marked increase in Ba which could be related to a modal increase in plagioclase. Both Ni and Co show a sudden decrease due to the disappearance of olivine.

The trace elements show a further decrease in the norite except for Sr and Ba. The decrease could be related to the decrease and disappearance of clinopyroxene.

The andesine anorthosite contains the highest amounts of Sr and Ba which relate directly to modal

abundance of plagioclase. There is a further decrease in the other trace elements due to the decrease and then disappearance of modal orthopyroxene.

## 5.2 OUTER GABBROIC SERIES

### 5.2.1 MAJOR ELEMENT VARIATIONS:

In the outer gabbroic series, the norite has high MgO, Al<sub>2</sub>O<sub>3</sub>, iron oxide and CaO. The Na<sub>2</sub>O and TiO<sub>2</sub> are low. Cumulate plagioclase controls most of CaO, Al<sub>2</sub>O<sub>3</sub>, and Na<sub>2</sub>O. Orthopyroxene contains MgO and some of the Iron oxide while the bulk of the latter, together with TiO<sub>2</sub>, is concentrated in titaniferous magnetite.

The gabbronorite contains the highest amounts of CaO, iron oxide and TiO<sub>2</sub>. It also has a high Al<sub>2</sub>O<sub>3</sub>, MgO and Na<sub>2</sub>O though some of the CaO and Al<sub>2</sub>O<sub>3</sub> is shared by the clinopyroxene. Orthopyroxene together with clinopyroxene controls MgO and a part of iron oxide. The rest of the iron oxide and TiO<sub>2</sub> are concentrated in titaniferous magnetite.

The amphibole gabbronorite is characterized by high Al<sub>2</sub>O<sub>3</sub>, iron oxide, CaO, Na<sub>2</sub>O and TiO<sub>2</sub>. Plagioclase contains most of the CaO, Na<sub>2</sub>O and Al<sub>2</sub>O<sub>3</sub>.

Pyroxenes and amphibole control the MgO, iron oxide and probably a part of CaO, Al<sub>2</sub>O<sub>3</sub> and Na<sub>2</sub>O. Amphibole and phlogopite contain all the K<sub>2</sub>O. TiO<sub>2</sub> and iron oxide are concentrated in titaniferous magnetite.

The pyroxene diorite is somewhat similar to amphibole gabbonorite in chemical composition. It is slightly low in iron oxide, Al<sub>2</sub>O<sub>3</sub>, MgO and CaO, but shows marked increase in Na<sub>2</sub>O, K<sub>2</sub>O and TiO<sub>2</sub> in comparison to the amphibole gabbonorite. The mineralogical control over chemistry is similar to the amphibole gabbonorite.

#### 5.2.2 TRACE ELEMENT VARIATIONS:

The trace element abundances in the outer gabbroic series also vary with the modal abundances of cumulus phases. The norite contains high Sr, Ba, Cr and V. Sr and Ba substitute for Ca in plagioclase. Titaniferous magnetite controls V and probably a part of Cr. Low amounts of Ni and Co should be concentrated in the pyroxenes.

The gabbonorite has comparatively higher amounts of Sr, Ba and V but low amounts of Cr, Co and Ni. The observed trends are due to high modal plagioclase, titaniferous magnetite and low modal pyroxenes.



The amphibole gabbronorite is characterized by a further increase in Sr and Ba in comparison to norite. The rock shows a marked decrease in Cr but only a slight decrease in Co, Ni and V. There is a marked increase in Rb, Y, Zr and Nb in this rock.

The pyroxene diorite shows a further increase or decrease in trace elements similar to the amphibole gabbronorite except for Ni and Sr. Distribution of Sr, Ba, V, Cr, Ni and Co in the cumulate mineral phases is similar to that observed in the norite. The increase in Y, Zr and Nb is related to a corresponding increase in intercumulus phases, the amphibole and phlogopite.

### 5.3 DIORITIC ROCKS

The dioritic rocks show roughly continuous systematic variations in chemistry. In major elements the hornblende gabbro contains the highest amounts of CaO, MgO, Fe<sub>2</sub>O<sub>3</sub>, TiO<sub>2</sub> and MnO. Silica, Al<sub>2</sub>O<sub>3</sub>, Na<sub>2</sub>O and K<sub>2</sub>O are the lowest of the dioritic rocks.

The diorite shows a decrease in Ca, MgO, Fe<sub>2</sub>O<sub>3</sub>, TiO<sub>2</sub>, MnO and an increase in silica, Al<sub>2</sub>O<sub>3</sub> and Na<sub>2</sub>O. Instead of increasing, K<sub>2</sub>O shows a considerable decrease.

There is a further decrease in CaO, MgO, Fe<sub>2</sub>O<sub>3</sub> and MnO in the quartz diorite, but SiO<sub>2</sub>, Al<sub>2</sub>O<sub>3</sub>, Na<sub>2</sub>O, K<sub>2</sub>O and TiO<sub>2</sub> show an increase. Similar trends are noted in the tonalite.

The hornblende gabbro is characterized by the highest content of V, Cr, Co, Rb, Sr, Ba and Y. There is a general decrease in V, Co and Sr from hornblende gabbro, through diorite and quartz diorite to tonalite.

Quartz diorite is enriched in Cr, Rb, Y, and Zr, but depleted in Ni and Nb in comparison to diorite. The tonalite is characterized by the lowest amounts of Cr, Rb, Y, Nb and Ba, except for Zr which is the highest in the dioritic rocks.

The quartz monzodiorite of the northern satellite intrusion is intermediate in chemical composition between the quartz diorite and tonalite of the main complex but has a distinctive, very high K<sub>2</sub>O content. The rock also shows a relative enrichment in Ba, Zr and Rb.

The fine-grained equivalent of diorite (W132) is poor in SiO<sub>2</sub>, Al<sub>2</sub>O<sub>3</sub>, Na<sub>2</sub>O and MnO but contains higher amounts of Fe<sub>2</sub>O<sub>3</sub>, MgO, CaO and TiO<sub>2</sub> compared to diorite. The rock contains more mafic minerals than is general for the dioritic rocks.

The fine-grained equivalent of the tonalite (W153) of the southern satellitic intrusion is similar to the quartz diorite in chemistry rather than the tonalite. However, it does contain less CaO and more Na<sub>2</sub>O.

#### 5.4 GRANITIC ROCKS

In the granitic rocks the granodiorite is characterized by higher CaO, Fe<sub>2</sub>O<sub>3</sub>, MgO, Al<sub>2</sub>O<sub>3</sub> and TiO<sub>2</sub>, but contains lower SiO<sub>2</sub>, Na<sub>2</sub>O and K<sub>2</sub>O in comparison to granite. The latter contains a significantly higher amount of SiO<sub>2</sub>, and a slightly higher Na<sub>2</sub>O and K<sub>2</sub>O content. A decrease is shown by Fe<sub>2</sub>O<sub>3</sub>, MgO, CaO and TiO<sub>2</sub> in granite.

There is a general decrease in all the trace elements from granodiorite to granite except for Rb which shows a marked increase. Ni is approximately constant in both granodiorite and granite.

#### 5.5 QUARTZ MONZONITE

The quartz monzonite is characterized by low SiO<sub>2</sub>, high Al<sub>2</sub>O<sub>3</sub>, and markedly higher amounts of Fe<sub>2</sub>O<sub>3</sub> and K<sub>2</sub>O relative to the granitic rocks. In

Figure 5.1 Plot of various oxides and indices vs differentiation index.

THE INNER GABBROIC SERIES

- (\*) Troctolite
- (◆) Olivine gabbronorite
- (▼) Amphibole olivine gabbronorite
- (■) Gabbronorite
- (▲) Norite
- (\* ) Andesine anorthosite

THE OUTER GABBROIC SERIES

- (△) Norite
- (▽) Gabbronorite
- (◇) Amphibole gabbronorite
- (□) Pyroxene diorite

THE DIORITIC ROCKS

- (●) Hornblende gabbro
- (⊙) Diorite
- (⊕) Quartz diorite
- (⊖) Quartz monzodiorite
- (⊗) Tonalite

THE GRANITIC ROCKS

- (\*) Granodiorite
- (+) Granite

- (\* ) Quartz monzonite

Arrows point to fine-grained rocks

Figure 5.1

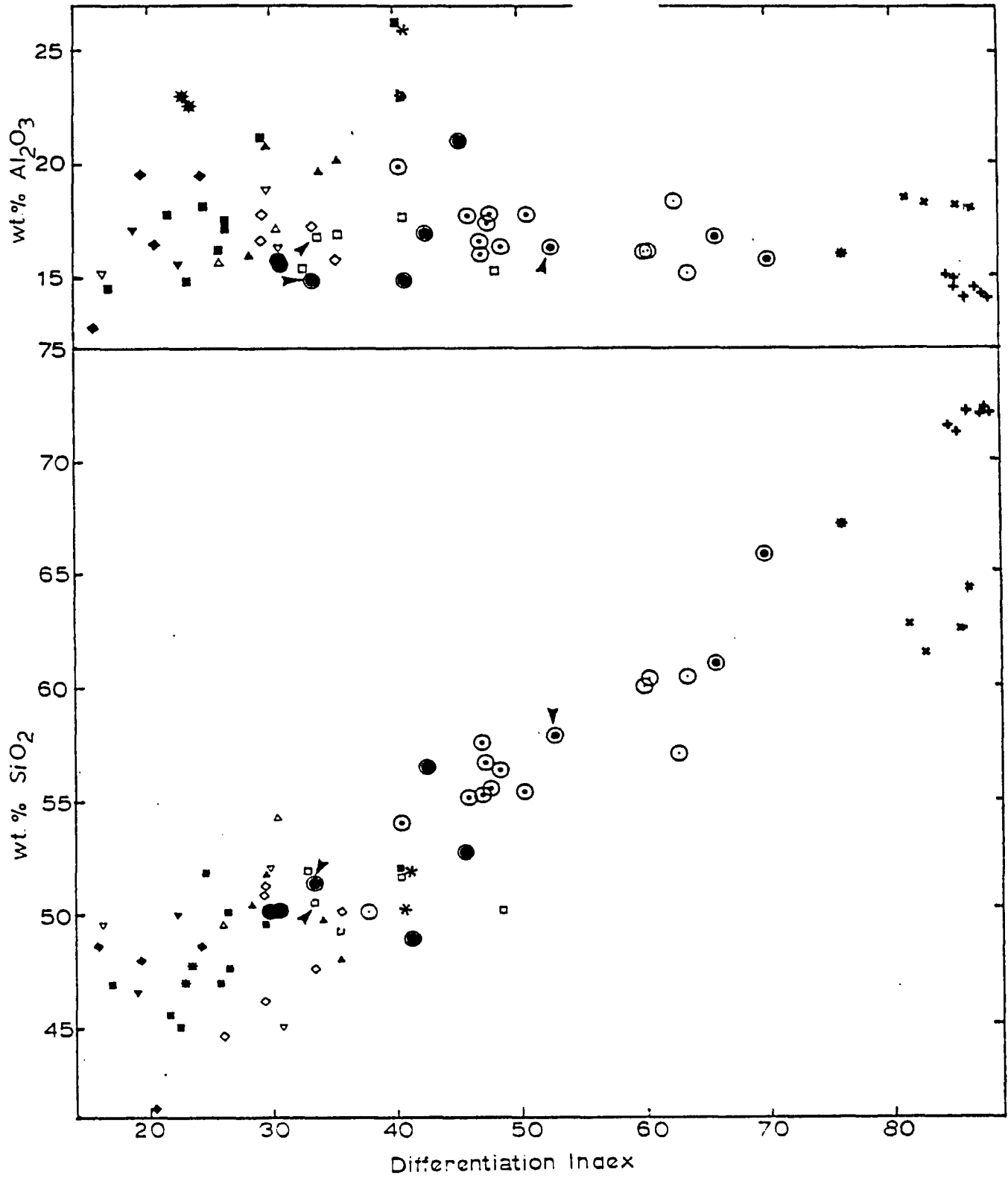


Figure 5.1 (cont'd)

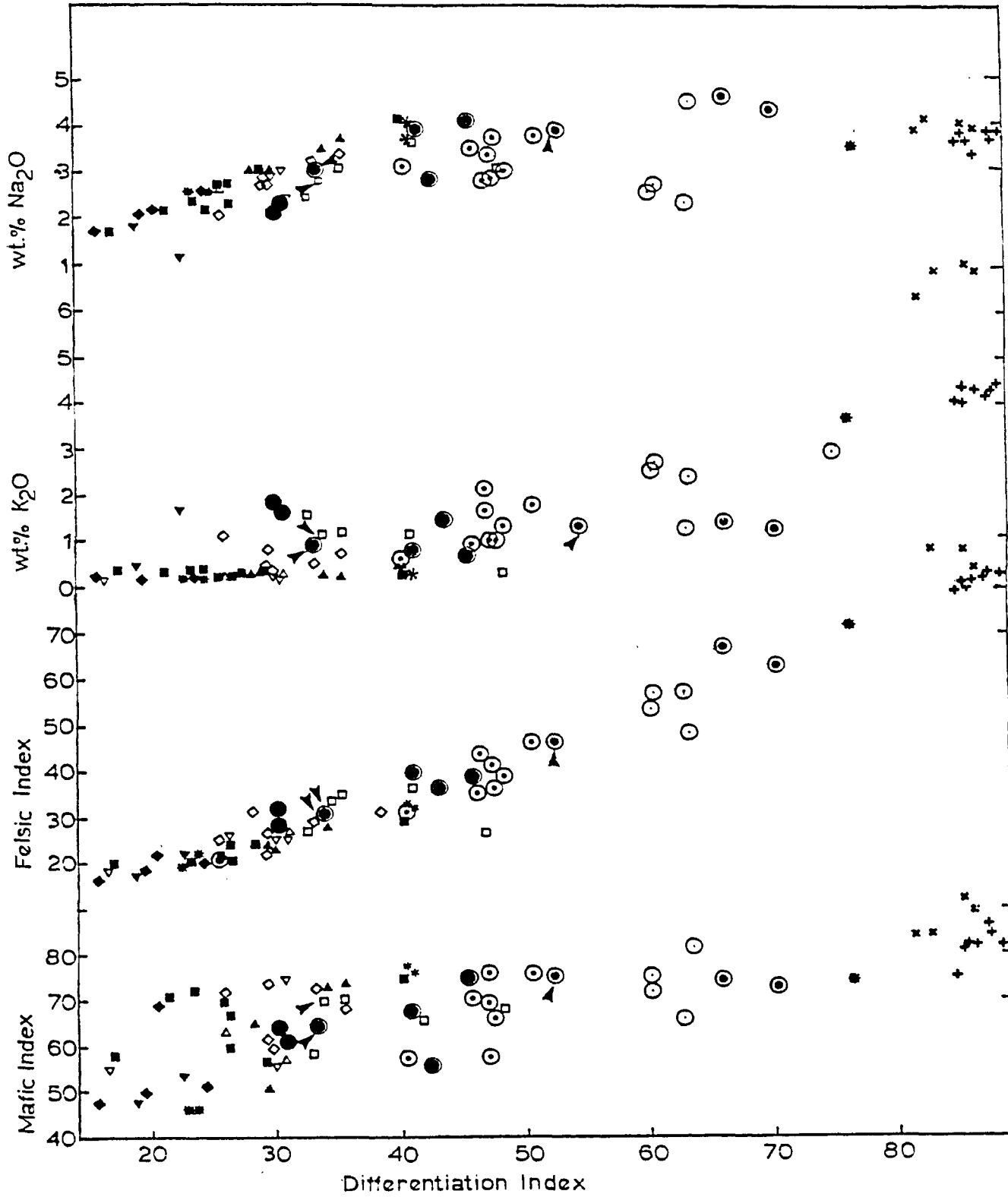
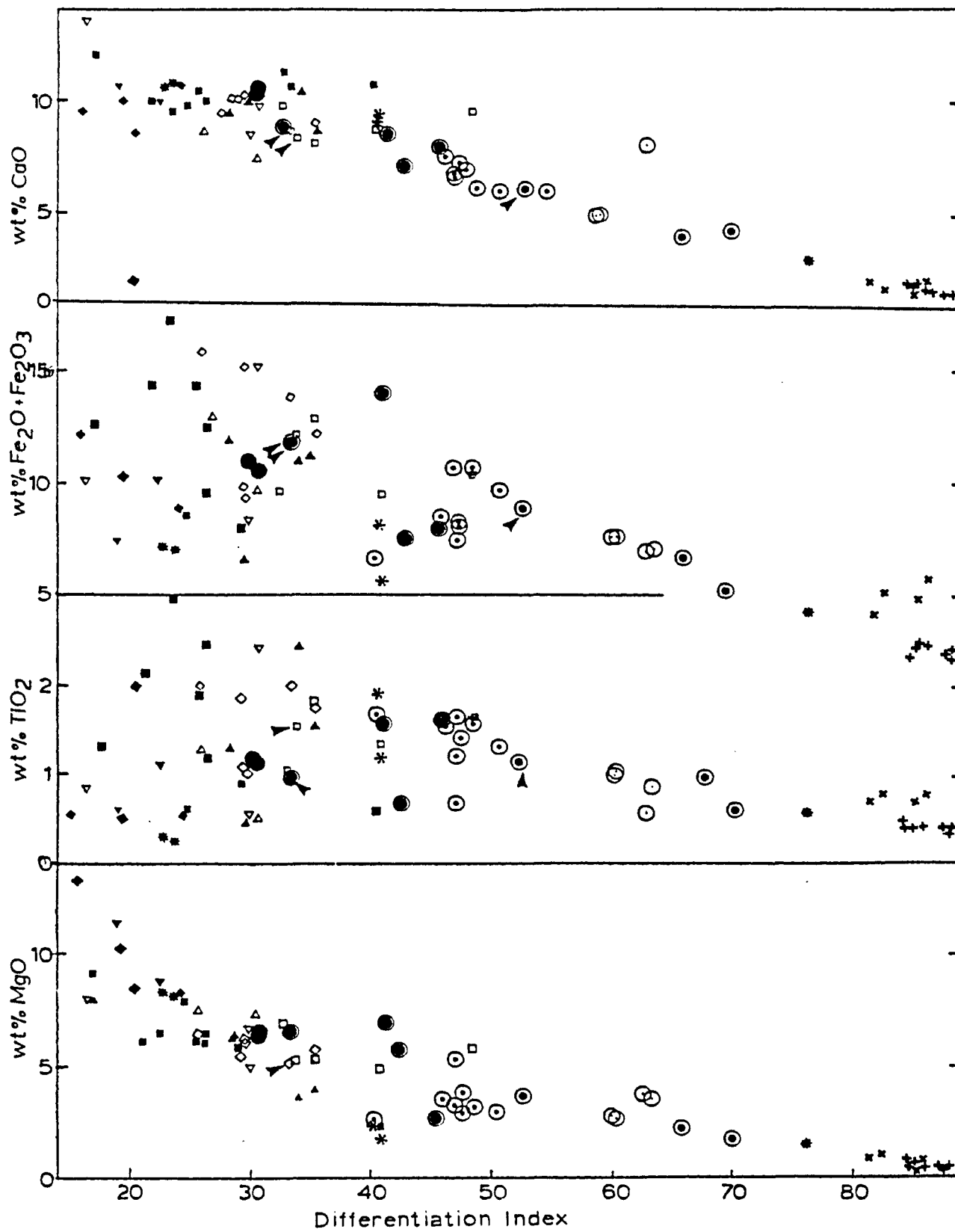


Figure 5.1 (cont'd).



trace elements it has a quite distinct low Sr and very high Zr contents.

## 5.6 GENERAL CHEMICAL VARIATIONS IN ROCK GROUPS

The major element chemistry and abundances of trace elements, as observed in the inner gabbroic rocks, varies with the modal abundances of the cumulus phases. The overall chemical trend is from highly magnesian basic rocks to intermediate anorthositic rocks, low in MgO and rich in Na<sub>2</sub>O and Al<sub>2</sub>O<sub>3</sub>. Plots of various oxides versus calculated indices reveal more or less systematic relationships. With an increasing differentiation index (normative % Q + Ab + Or + Ne + Kp + Lc, Figure 5.1) there is a general decrease in MgO, Fe<sub>2</sub>O<sub>3</sub>, CaO, TiO<sub>2</sub> and an increase in SiO<sub>2</sub>, Al<sub>2</sub>O<sub>3</sub>, Na<sub>2</sub>O, the felsic index  $((Na + K) 100 / Ca + Na + K)$  and the mafic index  $((Fe + Mn) 100 / Fe + Mn + Mg)$ . Silica, Al<sub>2</sub>O<sub>3</sub>, Na<sub>2</sub>O, mafic index (M.I.), and felsic index (F.I.) increase as MgO and CaO decrease with the decreasing solidification index  $(MgO \times 100 / MgO + Fe_2O_3 + FeO + NaO + K_2O)$  (Figure 5.2)). Fe<sub>2</sub>O<sub>3</sub> and TiO<sub>2</sub> show an early increase and then a rapid decrease with the decreasing solidification index (S.I.).



Figure 5.2 The plots of various oxides and indices vs solidification index (symbols same as in figure 5.1).

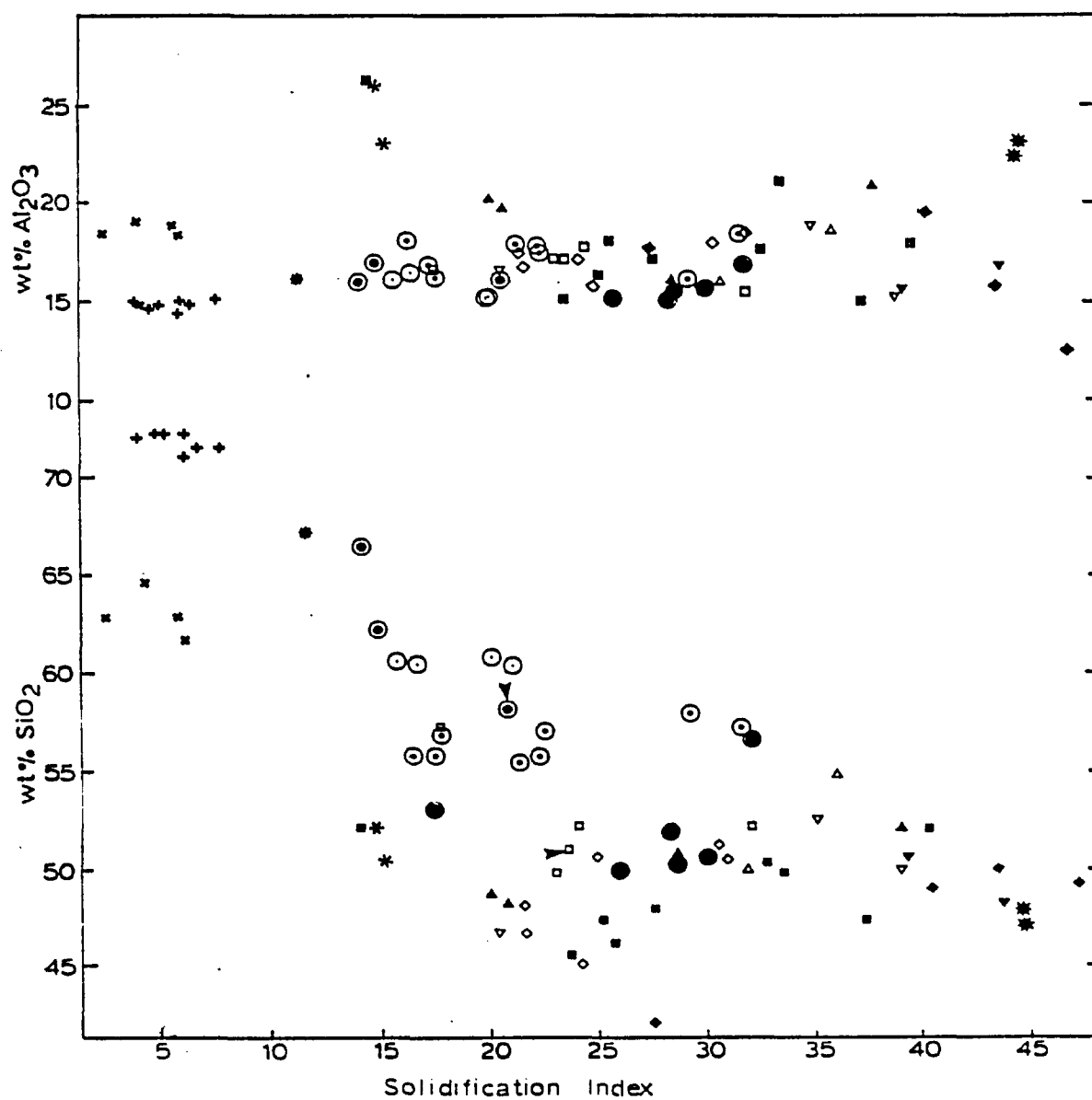


Figure 5.2 (cont'd).

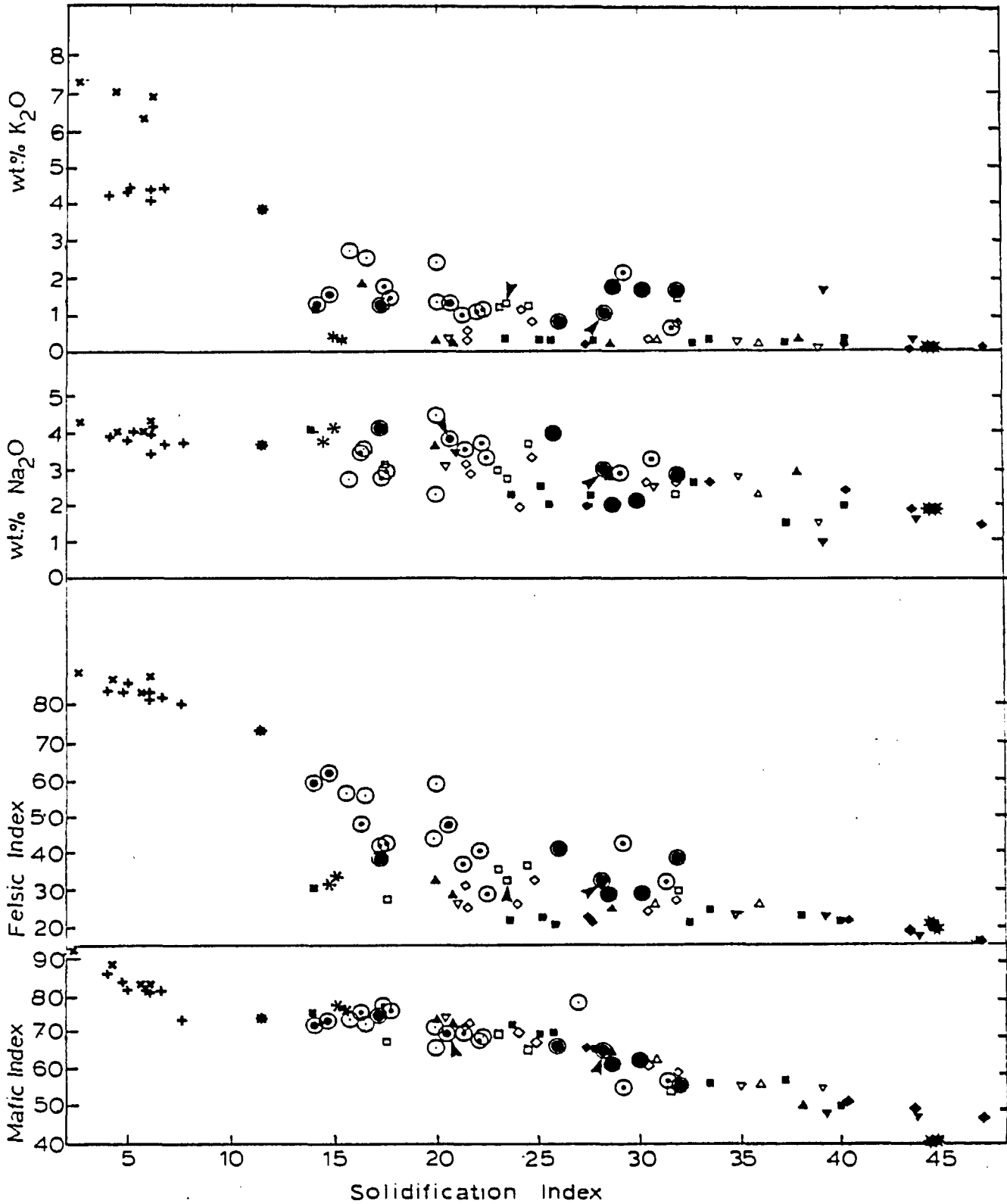
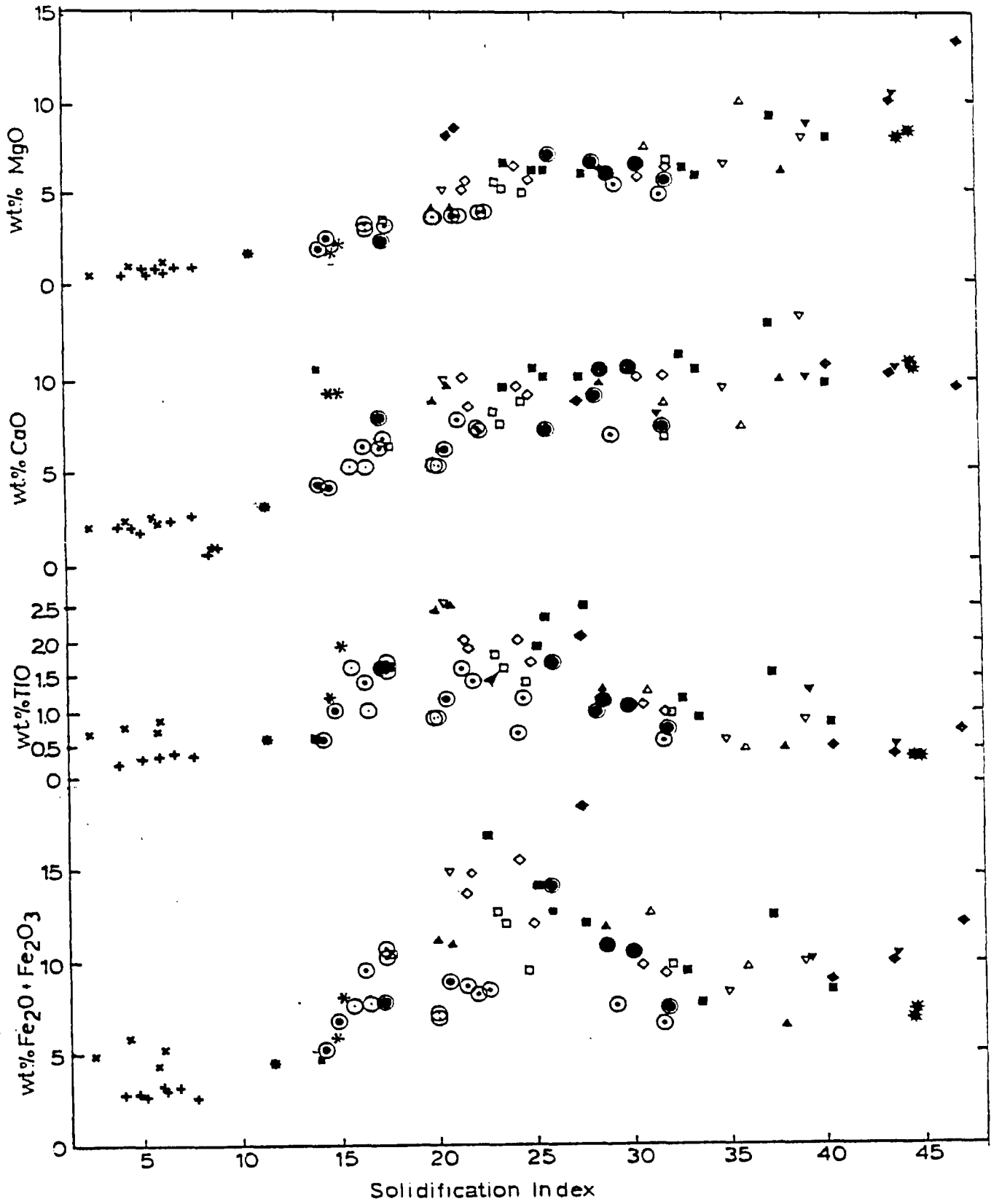


Figure 5.2 (cont'd).



Trace elements also show a strong relationship with the cumulus phases and their modal abundances: Ni, Co, Cr show a rapid decrease, V, Ti increase and then rapidly decrease with the increasing M.I. (Figure 5.3). There exists a strong positive relationship between Sr and CaO (Figure 5.4).

The inner gabbroic rocks (except for amphibole olivine gabbro norite) have a very low level of LIL (large-ion-lithophiles i.e. K, Rb, Ba) and other incompatible elements (Ti, Zr, Nb, Y). This is consistent with the petrographic observations that the cumulates contain very little intercumulus material. Flat patterns are seen for Rb, Zr, Y and Nb when plotted against the F.I., except for Ba which shows a slight increase (Figure 5.5).

The major and trace element abundances in the outer gabbroic series also vary with the modal abundances of cumulus phases. Concentrations of  $\text{SiO}_2$ ,  $\text{Na}_2\text{O}$ , the M.I. and F.I. increase as  $\text{Fe}_2\text{O}_3$ , CaO, and MgO decrease with progressive increase in the D.I. (Figure 5.1). Concentrations of CaO and MgO decrease as  $\text{SiO}_2$ ,  $\text{Na}_2\text{O}$ ,  $\text{Fe}_2\text{O}_3$ ,  $\text{TiO}_2$ , the M.I. and F.I. increase with the decreasing S.I. (Figure 5.2). A flat pattern is observed for  $\text{Al}_2\text{O}_3$  when plotted against both the D.I. and S.I.

Figure 5.3 Plots of Co, Cr, V, Ni, and Ti vs mafic index (symbols same as in figure 5.1).

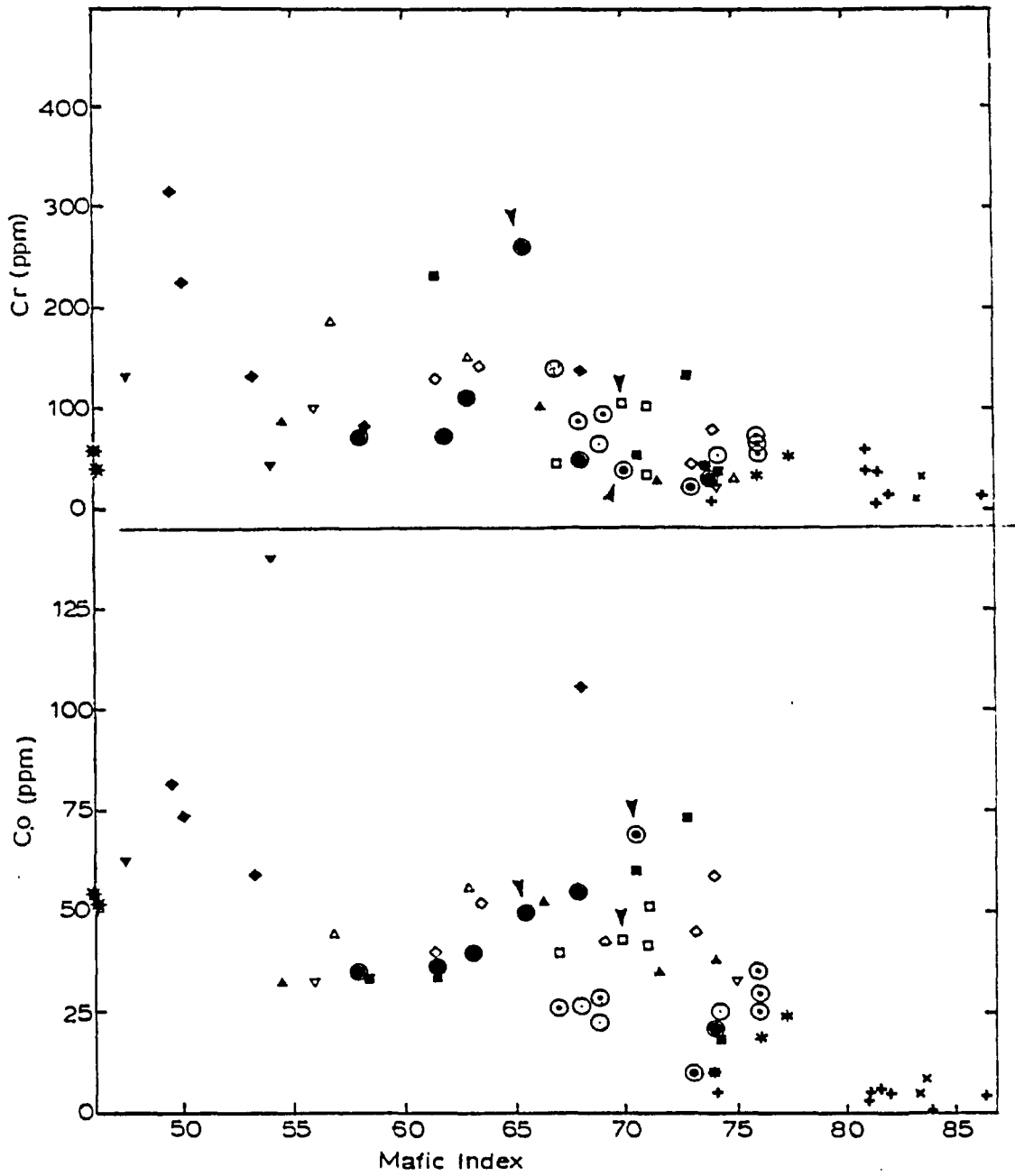
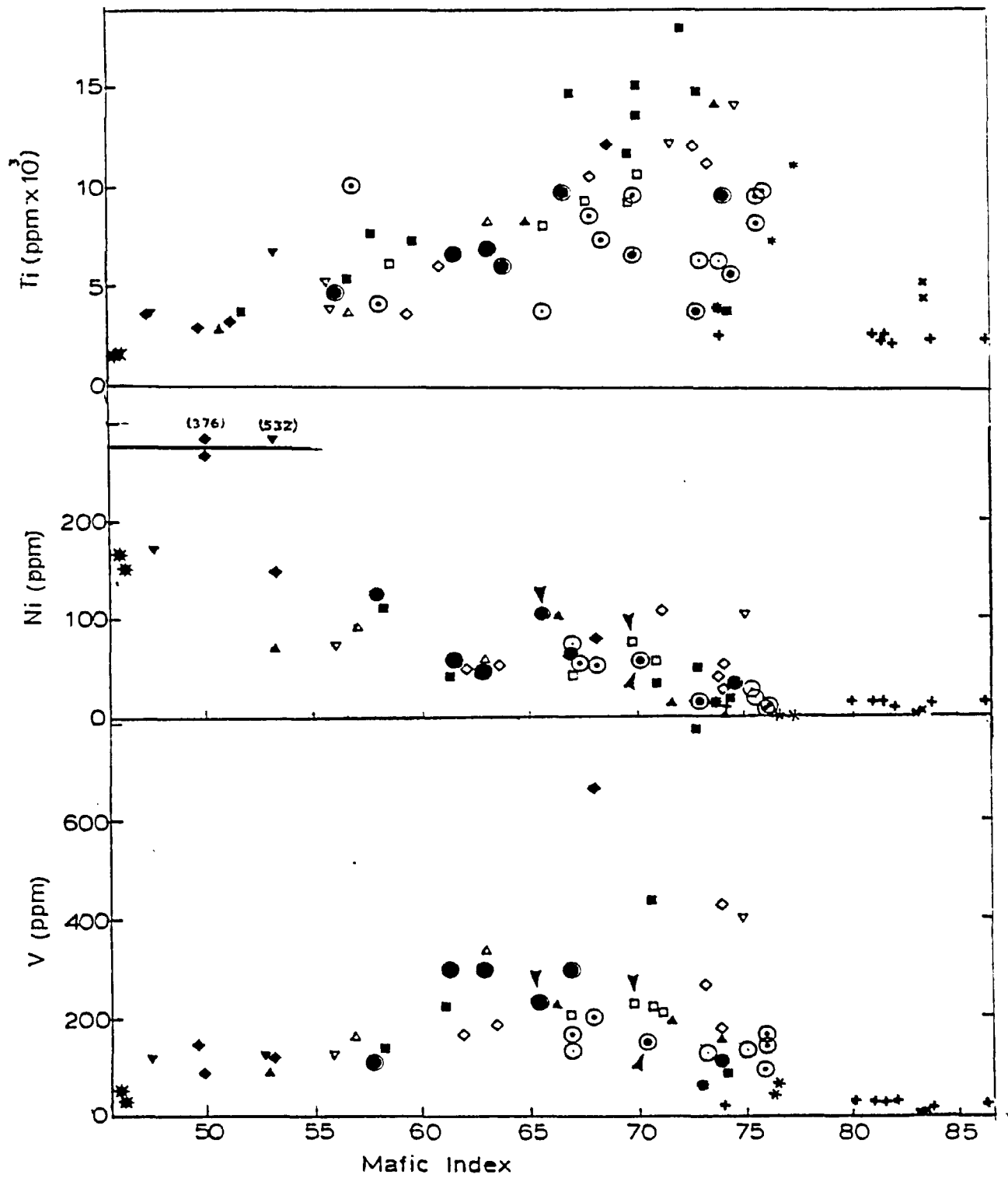


Figure 5.3 (cont'd).



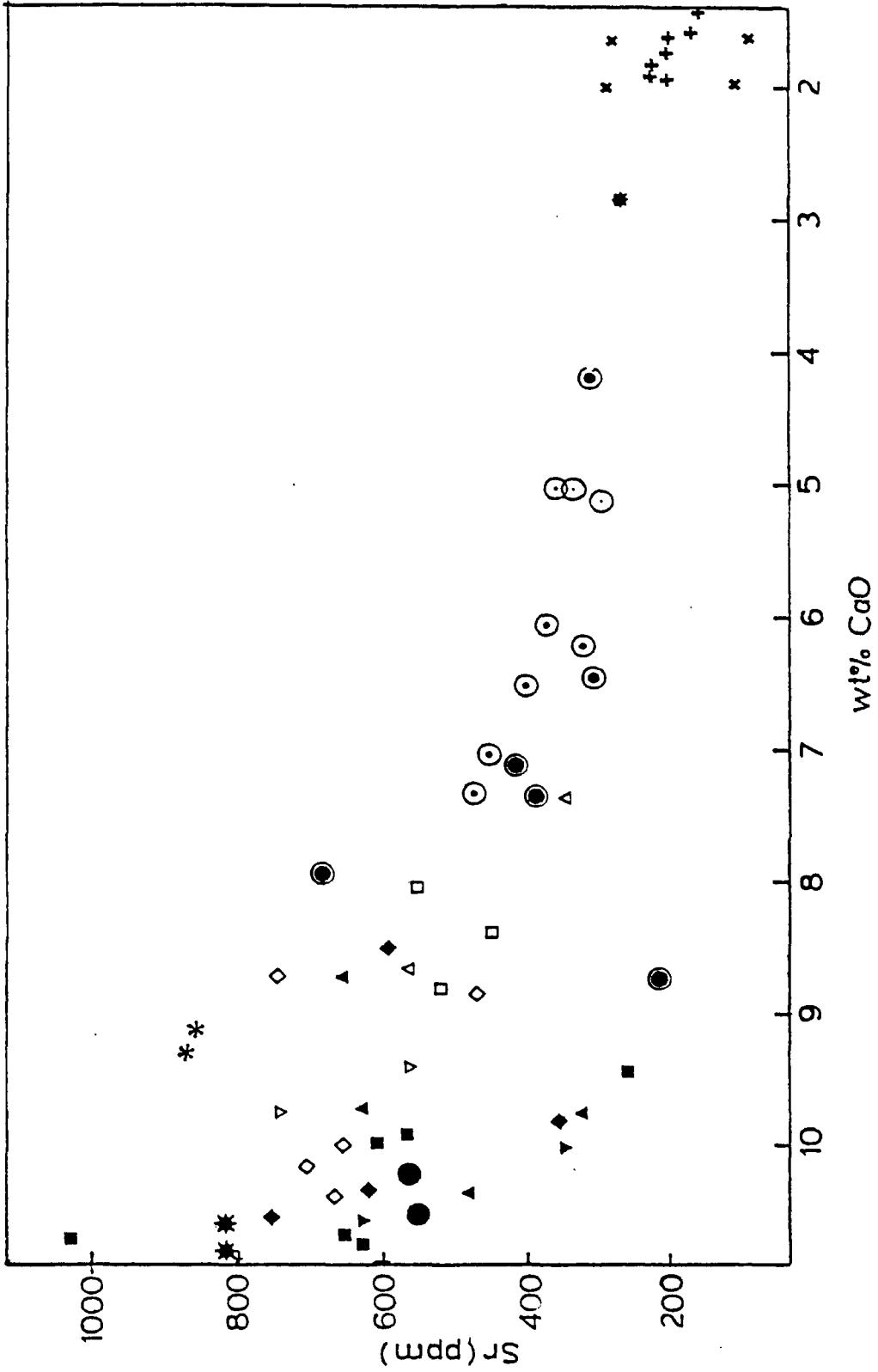


Figure 5.4 Plot of Sr (ppm) vs wt.% CaO.

In trace elements, Ni and Co have a constant level; V and  $\text{TiO}_2$  increase as Cr decreases with the progressive increase in M.I. (Figure 5.3). Concentrations of Nb, Y, Zr and Ba increase rapidly; Rb shows a slight increase and Sr decreases with increasing F.I. (Figure 5.5). Similar to the inner gabbroic series, Sr and CaO in the outer gabbroic series also show a positive relationship (Figure 5.5).

In the dioritic rocks,  $\text{SiO}_2$ ,  $\text{Na}_2\text{O}$ ,  $\text{K}_2\text{O}$ , the F.I. and M.I. increase as  $\text{Al}_2\text{O}_3$ , CaO,  $\text{Fe}_2\text{O}_3$ , MgO and  $\text{TiO}_2$  decrease with the increasing D.I. and decreasing S.I. (Figures 5.1 and 5.2). Similar relationships are revealed when various oxides are plotted against the D.I. and S.I. in the granitic rocks (Figures 5.1 and 5.2).

In trace elements, Ni, Co, Cr, V and Sr all show a decrease with an increasing M.I. of both dioritic and granitic rocks (Figure 5.3). Concentrations of Nb, Zr, Rb and Ba increase and of Y and Sr decrease with the increasing M.I. of the dioritic rocks. In the granitic rocks, however, Nb, Y, Zr, Sr and Ba decrease while Rb increases with an increasing F.I. (Figure 5.4.).

The concentrations of  $\text{SiO}_2$ ,  $\text{Fe}_2\text{O}_3$ ,  $\text{TiO}_2$ ,  $\text{Na}_2\text{O}$ ,  $\text{K}_2\text{O}$ , the F.I. and M.I. in the quartz monzonite



Figure 5.5 Plots of Rb, Ba, Sr, Y, Nb, and Zr vs felsic index.

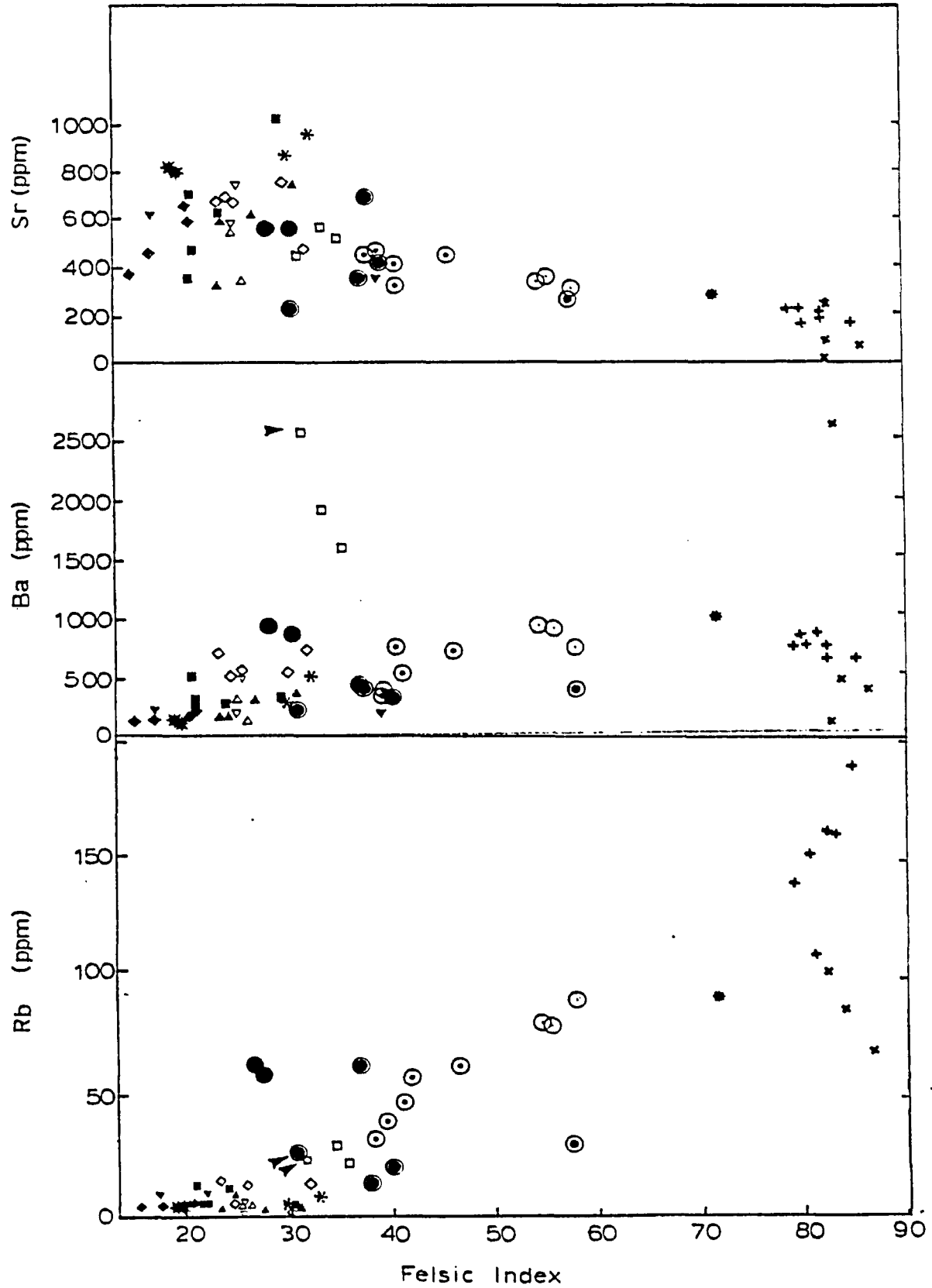
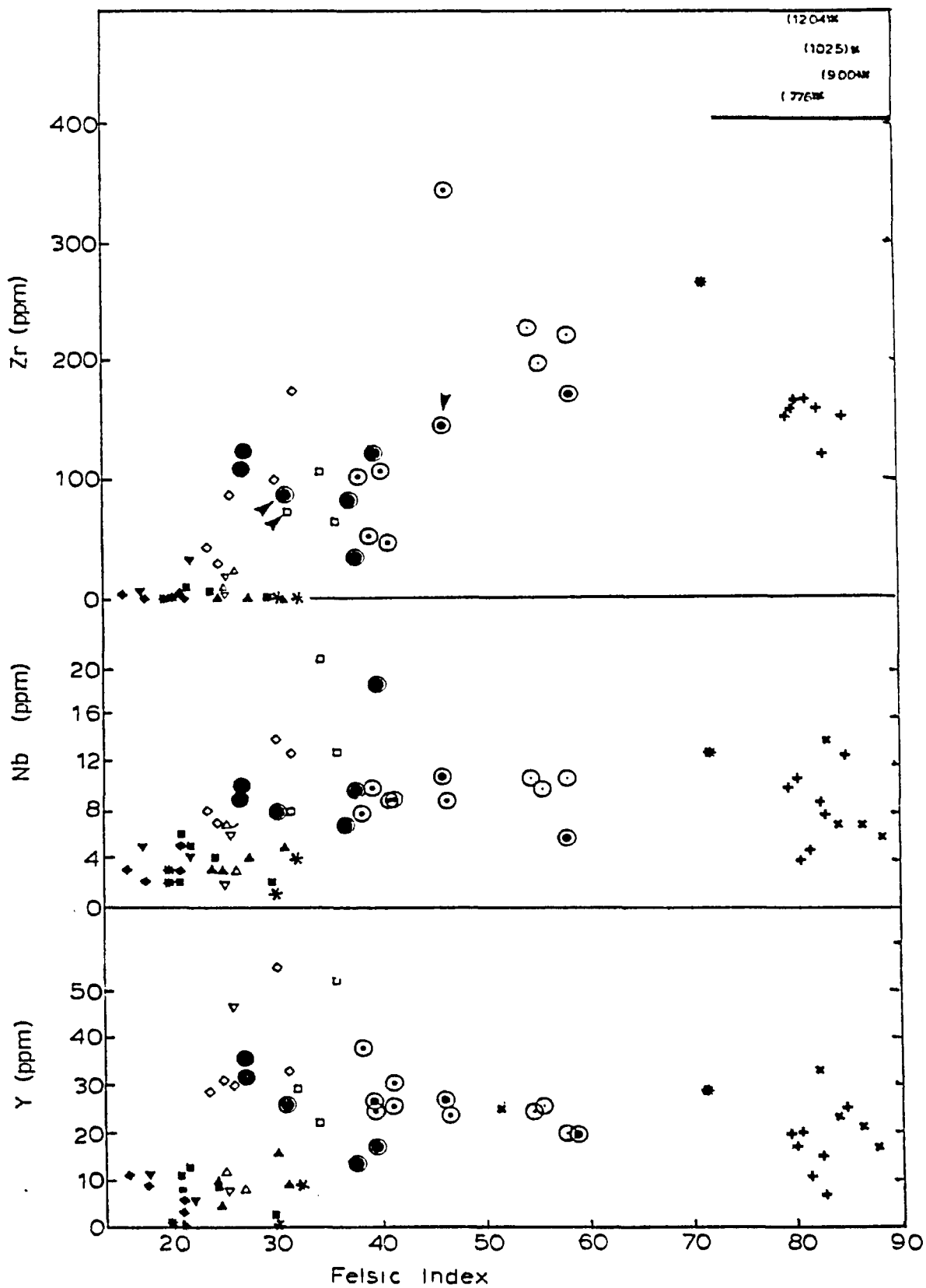


Figure 5.5 (cont'd).



increase as  $\text{Al}_2\text{O}_3$ ,  $\text{CaO}$  and  $\text{MgO}$  decrease with the increasing D.I. Also the major elements, when plotted against the S.I., show a trend similar to that of granitic rocks (Figures 5.1 and 5.2). Concentrations of Ni, V, Cr, Sr, and  $\text{TiO}_2$  plotted against the M.I. show almost a flat pattern (Figure 5.3). Nb, Y and Ba decrease while Y and Rb increase with increasing F.I. (Figure 5.4).

#### 5.7 OVERALL CHEMICAL VARIATIONS IN THE COMPLEX

In the overall chemistry of the complex,  $\text{SiO}_2$ ,  $\text{Na}_2\text{O}$  and  $\text{K}_2\text{O}$  increase as  $\text{MgO}$ ,  $\text{CaO}$ ,  $\text{Fe}_2\text{O}_3$ ,  $\text{TiO}_2$ , and  $\text{Al}_2\text{O}_3$  decrease with the increasing D.I. and increasing S.I. (Figures 5.1 and 5.2). There is a strong overlap between various rock groups except for the quartz monzonite where concentrations of  $\text{SiO}_2$ ,  $\text{Al}_2\text{O}_3$ ,  $\text{Fe}_2\text{O}_3$ ,  $\text{K}_2\text{O}$ , and  $\text{TiO}_2$  do not fit in the general sequence of variations.

Plots of Ni, Co, Cr and V show a successive and rapid decrease in each rock group with the increasing M.I. (Figure 5.3). There is a continuous increase in the concentrations of Ba and Rb with the increasing F.I., except for the quartz monzonite (Figure 5.5). A similar successive increase is noticed in Zr, Nb, and

Y in the basic and intermediate rocks when plotted against the F.I. However, in the granitic rocks, these elements decrease except for Zr which increases. The Zr is exceptionally high in the quartz monzonite (Figure 5.5).

The LIL (Rb, Ba) and other incompatible trace elements (Nb, Y, Zr) in the quartz monzonite significantly differ in behavior when compared to their more or less continuous variation in the other basic to acidic rock groups of the complex. These, together with the major element differences noted above, indicate that the quartz monzonite is different from and not related chemically to the other, overlapping rock groups.

The behaviour of major and trace elements in the Gamitagama Lake Complex is of the same general nature as is observed in other highly differentiated intrusions, particularly the Guadalupe Igneous Complex of California (Best, 1963).

## CHAPTER 6

## PETROGENESIS

One big problem which arises when dealing with differentiated suites is determining nature and composition of parent magma. In instances where homogeneous chilled margins exist, the problem is greatly diminished. As previously discussed, the chill margins were not observed in the field for the inner gabbroic or the outer gabbroic series. The fine-grain porphyritic rocks, intrusive in the inner as well as outer gabbroic series represents the last intrusive phase of gabbroic nature.

Another common problem of many composite plutons containing several intrusive phases is whether such intrusions have been formed from a single parent magma. To understand whether such a relationship exists in the different intrusive phases of the Gamitagama Lake Complex, an attempt has been made to evaluate the nature and physical conditions of crystallization (pressure and temperature) in the light of its mineralogical, chemical and field characteristics.

## 6.1 MINERALOGICAL FEATURES

The absence of sodic pyroxenes and amphiboles in rocks of the Gamitagama Lake Complex preclude the alkaline basaltic magma parentage.

Apart from other physical and chemical characteristics crystallization of orthopyroxene (hypersthene; Kuno, 1950, 1959), hydrous silicates (amphibole and biotite; Best, 1963) abundance of plagioclase (Yoder, 1969, Nishimori, 1976), and degree of iron enrichment (crystallization of magnetite; Kennedy, 1955; Kuno, 1960) may control the differentiation trends in the sub-alkaline basaltic magma.

### 6.1.1 SIGNIFICANCE OF ORTHOPYROXENE:

Kuno (1950,1959) classified sub-alkaline volcanic rocks into the hypersthentic and pigeonitic rock series. The former series contains both orthopyroxene and clinopyroxene in ground mass whereas in the latter both the pyroxenes are monoclinic (augite to ferroaugite and pigeonite. He further emphasized that hornblende and biotite is characteristic of hypersthentic series. Kuno (1959, 1968 a,b) regarded his hypersthentic and pigeonitic series as representative of the

calc-alkaline and tholeiitic volcanic rock suites respectively.

Kuno (1965), Best and Mercy (1967) suggested that the crystallization of hypersthene rather than pigeonite in the calc-alkaline magmas is due to elevated water pressure at the time of crystallization. Elevated water pressure depresses the pyroxene solvus such that pigeonite is precluded from crystallization (Muir, 1954; Best and Mercy, 1967).

In the Gamitagama Lake Complex, orthopyroxene (probably hypersthene) is a primary cumulus mineral in both the inner gabbroic series and the outer gabbroic series and crystallized directly from the parent liquids. Pigeonite or inverted pigeonite were not encountered.

#### 6.1.2 ABUNDANCE OF PLAGIOCLASE

The general feldspathic nature of the gabbroic rocks in the Gamitagama Lake Complex and their high  $\text{Al}_2\text{O}_3$  and normative plagioclase contents indicate that their parent liquids were probably rich in alumina. Nishimori (1976), observing a similar feldspathic nature, proposed the high alumina basalt as parent magma for the gabbroic rocks of Peninsular Range of

Southern California. Yoder (1969) after studying the system diopside-anorthite-water concluded that increase in water pressure can increase the amount of plagioclase crystallizing from magma. This partially explains the abundance of plagioclase as noted in the early and late differentiates of the inner gabbroic series. It also indicates that parent magma was probably rich in  $Al_2O_3$ . Many authors have recognized the high alumina nature of anorthositic rocks belonging to calc-alkaline suites (Hamilton, 1964; Taylor, 1969; Best 1969).

### 6.1.3 AMPHIBOLE AND PHLOGOPITE

The amphibole and phlogopite, as noted in petrography, are intercumulus minerals in the inner gabbroic series and early stages of the outer gabbroic series. The amphibole starts as a primary phase in the outer gabbroic series and from there on continues as a primary phase in the dioritic and the granitic rocks. Similarly, phlogopite appears as a primary phase in the last stages of outer gabbroic rocks; biotite is a primary phase in the dioritic and the granitic rocks.



Fine-grained rocks (W113 and W145) with porphyritic amphibole and phlogopite crystals represent independent intrusive phases in the complex. Kuno (1950,1959) emphasized that hornblende and biotite phenocrysts are characteristic only of his hypsitheric series (calc-alkaline series). Best (1963) suggested that the abundance of hydrous mineral in gabbroic rocks of the Guadalupe Complex indicate a high water pressure, and they are characteristic of calc-alkaline suites of rocks found in the orogenic zones.

#### 6.1.4 MAGNETITE AND OXYGEN FUGACITY

Magnetite varies from 1% to 7% of the inner gabbroic series of the complex. Although one of the earliest fractionates in the inner gabbroic series, it always occupies the interstices between major phases. In the outer gabbroic series, it is more or less constant in volume and persists till last differentiates of the series. The dioritic and the granitic rock contain only minor (less than 1 volume percent) magnetite.

Osborn (1959, 1969) suggested that high constant oxygen fugacity in basaltic magmas would cause

co-precipitation of magnetite + olivine + pyroxenes and would result in differentiation of the basalt to calcalkaline andesite.

Magnetite fractionation may be controlling process limiting iron enrichment in calc-alkaline magmas. Textural evidence indicate that magnetite is an early phase in calc-alkaline magmas (Garcia and Jacobson, 1979).

## 6.2 CHEMICAL FEATURES

### 6.2.1. MAJOR ELEMENT

Different rock groups in the Gamitagama Lake Complex show a steady increase in the  $\text{SiO}_2$ ,  $\text{Na}_2\text{O}$  and  $\text{K}_2\text{O}$ . A plot of  $\text{SiO}_2$  and alkalis shows a strong positive relationship between these elements. This trend is typical of calc-alkaline suites and is quite distinct than that of tholeiitic trend in which  $\text{SiO}_2$  content remains nearly constant or increases slightly (Kuno, 1959; Miyashiro, 1972; Wager and Brown, 1967). The calc-alkalic series show more rapid increases of  $\text{SiO}_2$  contents with fractional crystallization.

The degree of advance in the fractional crystallization of basaltic magma may be measured by increase

in its FeO/MgO ratio (Total iron as FeO; Kuno, 1973). The FeO/MgO ratio of residual magma increases in the early and middle stages of fractional crystallization in practically all igneous rocks series, but unlike the Skaergaard trend, the absolute Fe content of residual liquids decreases with increasing differentiation in the calc-alkaline trend. Rocks from the Gamitagama Lake Complex show a considerable scatter when their FeO/MgO ratio is plotted against FeO and SiO<sub>2</sub> (Figure 6.2), but most of the rocks occupy calc-alkaline fields (except those which contain abundant magnetite). A general increase in SiO<sub>2</sub> and a rapid decrease in FeO in various rock groups with increasing FeO/MgO are evident from these plots.

The AFM diagram (Figure 6.3) shows an early increase in FeO/MgO ratio due to iron enrichment in the inner gabbroic series and in the outer gabbroic series. The trend of the inner gabbroic series approximately overlaps the boundary between the tholeiitic and calc-alkaline fields; the outer gabbroic series and dioritic rocks are within the calc-alkaline field. The Gamitagama Lake Complex is slightly more enriched in iron compared to the Guadalupe Complex, and like other highly differentiated intrusions, shows extreme variation in felsic

Figure 6.1 Plot of  $\text{Si}_2\text{O}$  vs alkalis.  
 (symbols are similar to figure 6.3)

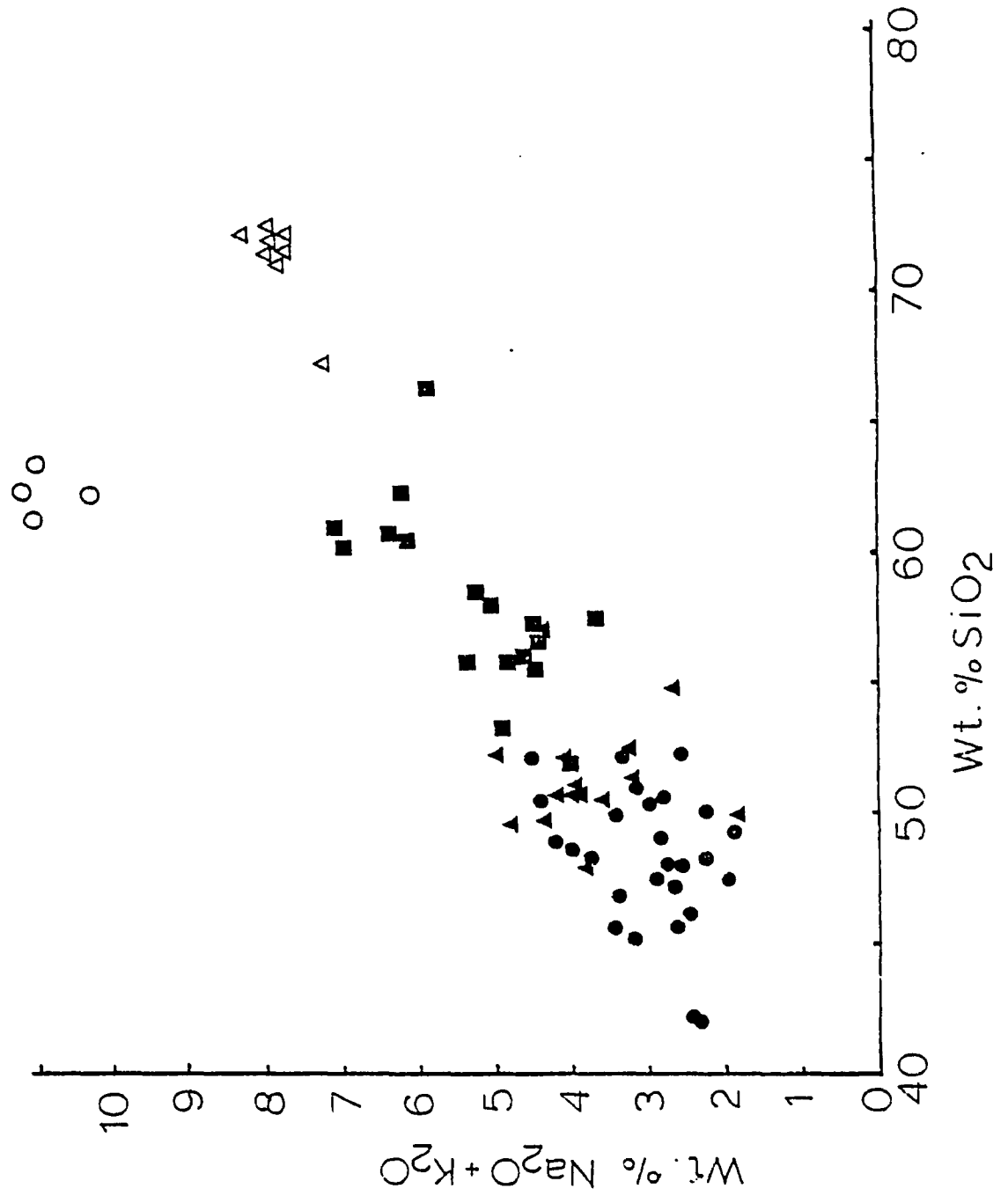
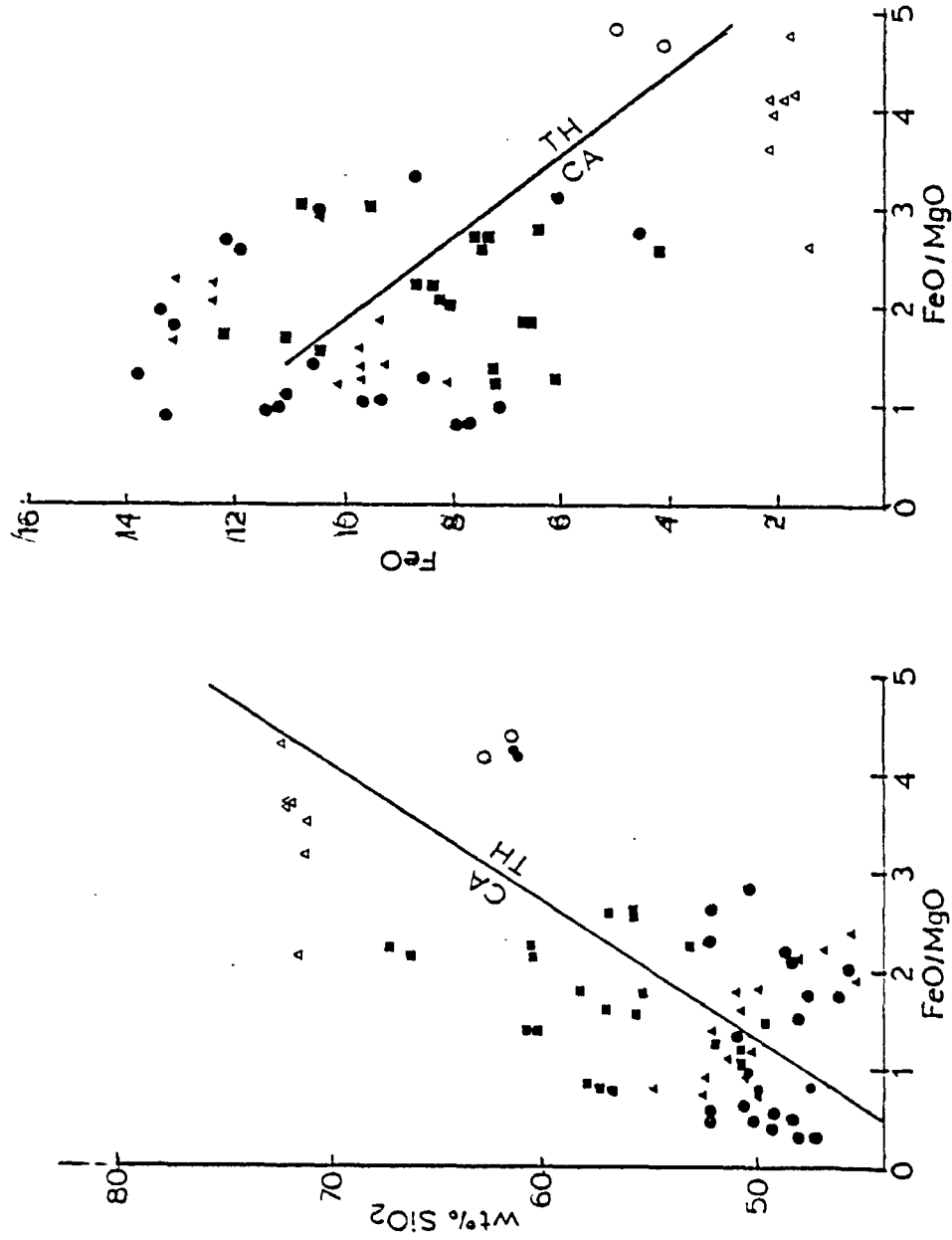


Figure 6.2 Plots of  $\text{SiO}_2$  and FeO vs FeO/MgO.  
 (symbols are similar to figure 6.3)



index (Figure 6.4). The  $\text{Na}_2\text{O} - \text{K}_2\text{O} - \text{CaO}$  plot shows a typical of calc-alkaline trend. There is a successive increase in  $\text{K}_2\text{O} + \text{Na}_2\text{O}$  emphasized by (Figure 6.5), with each intrusive phase from the inner gabbroic series to granite starts to crystallize and then drop rapidly. The soda/potash ratio maintains a relatively high level until granite starts to crystallize and then drop rapidly. This is related to initial low level of potash in the original liquids.

#### 6.2.2 TRACE ELEMENTS

In trace element behavior the Gamitagama Lake Complex is similar in nature to other highly differentiated calc-alkaline plutonic volcanic suites. The inner gabbroic series in the complex shows a rapid decrease in Ni, Co and Cr. These elements are comparatively low in the outer gabbroic rocks where they show a further decrease. Ti and V show an increase and then a rapid decrease in the inner as well as in the outer gabbroic series. The decrease in Ni, Co and Cr indicate fractionation of olivine and pyroxene. The depletion of V and Ti in the middle stages is due to fractionation of titaniferous magnetite. The systematic successive depletion of these elements in the outer gabbroic series, in the dioritic rocks and

Figure 6.3 AFM diagram showing chemical trends of  
of plutonic rocks from the Gamitagama  
Lake Complex and calc-alkaline suites of  
Guadalupe and Idaho, Southern California.

P—P Pinensular Range Gabbro (Nishimori, 1976).

- 1 Solid circles : Inner gabbroic series.
- 2 Solid Triangles: Outer gabbroic series.
- 3 Solid squares : Dioritic rocks.
- 4 Open Triangles: Granitic rocks.
- 5 Open Circles : Quartz monzonite.

Arrows refer to fine grained rocks.

Figure 6.4 Plot of felsic index vs mafic index.

1. Inner gabbroic series.
2. Outer gabbroic series.
3. Dioritic rocks.
4. Granitic rocks.
5. quartz monzonite.

The Skaergaard and Guadalupe trends are marked  
in broken lines.

Figure 6.3

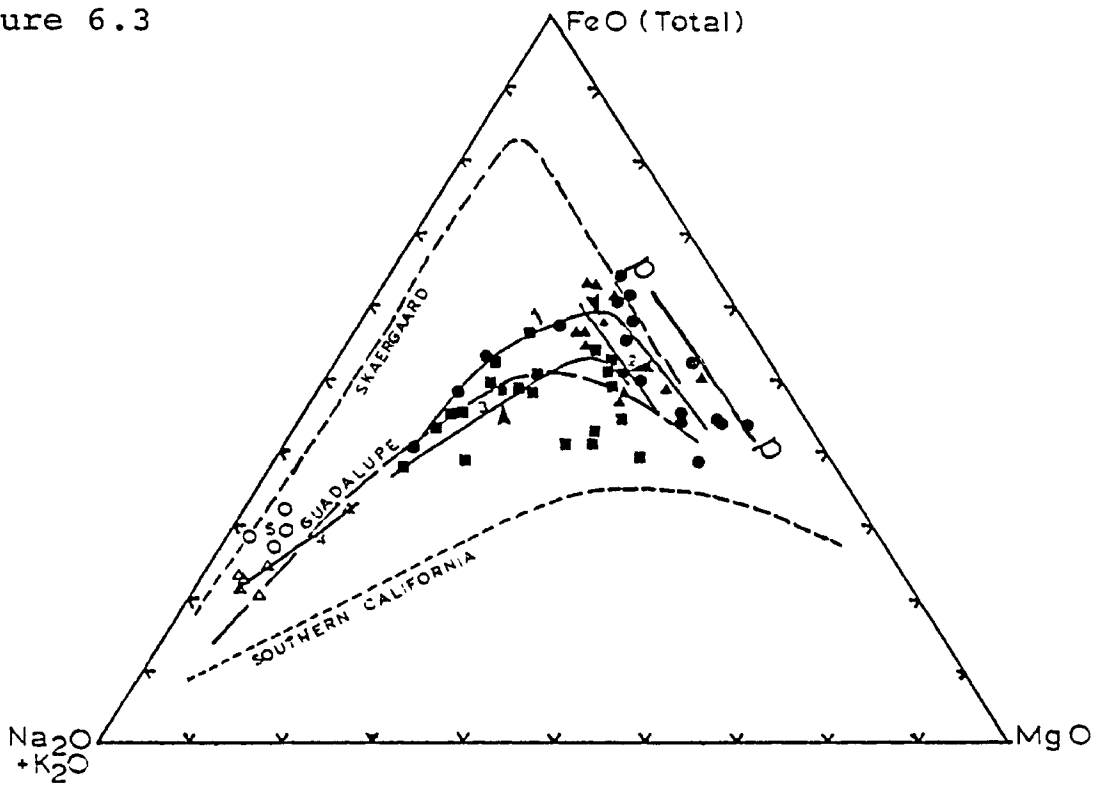


Figure 6.4

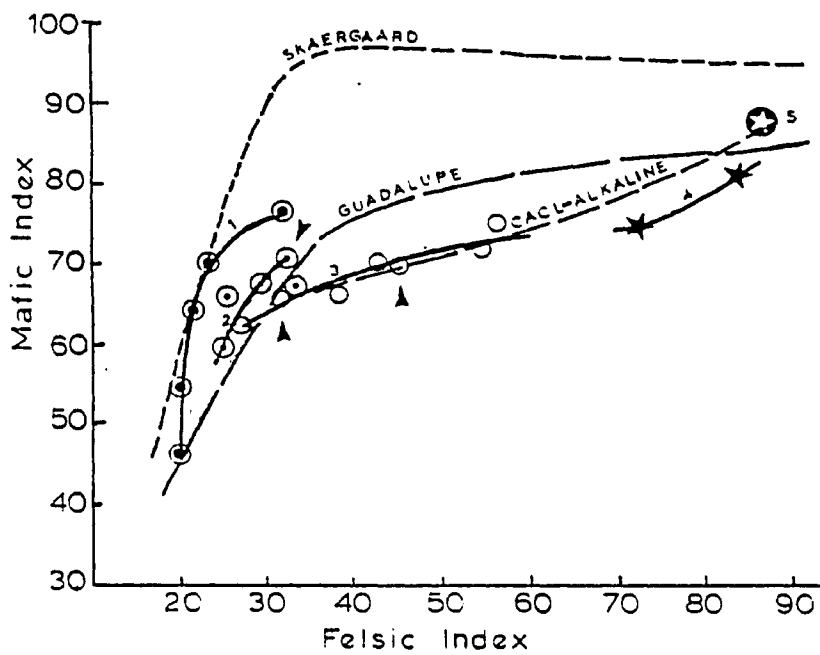




Figure 6.5 Plot of CaO vs Na O vs K O showing increase in soda/potash ratio with each rock group.

(Symbols are similar to figure 6.3)

Figure 6.6 Plot of Ba/Sr vs Sr (ppm).  
(symbols are similar to figure 6.3)

Figure 6.5

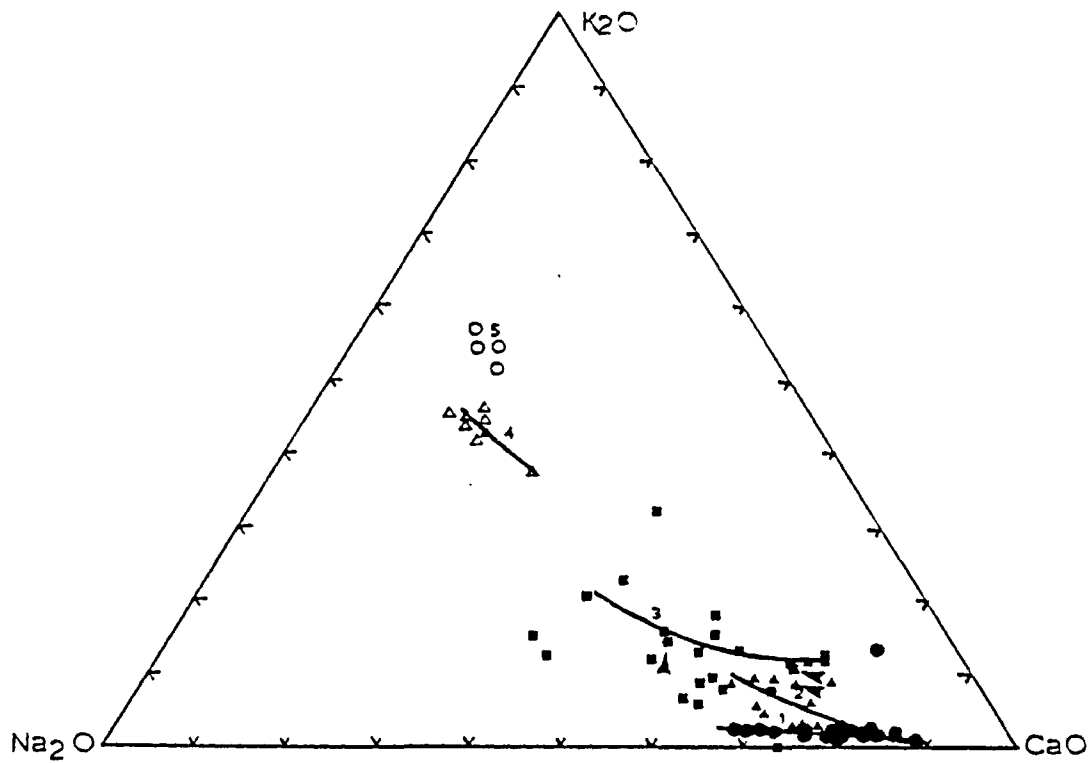
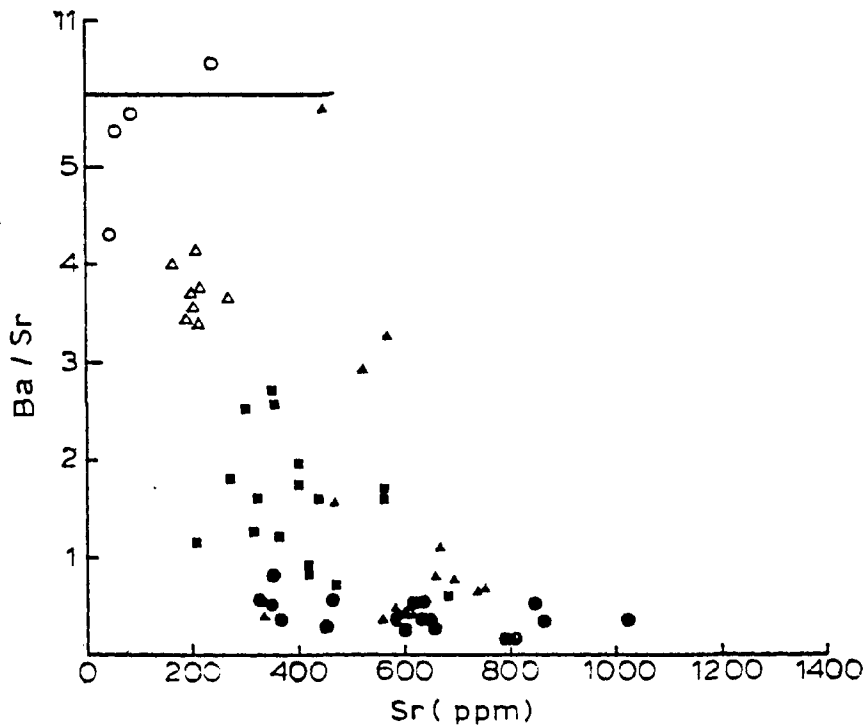


Figure 6.6



granitic rocks indicate that these rock groups are genetically related.

Nockolds and Allens (1953) showed that Cr, Ni and Co decreases in concentration with the degree of solidification in calc-alkaline rocks. They further noted that Sr and Ba have the same behavior in calc-alkaline and tholeiitic rocks. Jakes and White (1972A) and Miyashiro and Shido (1975) showed that in calc-alkaline volcanic rocks Ni, Co, and Cr abundances decrease from basalt to andesite to dacite due to fractionation.

The low levels of Y and Nb in the inner gabbroic series as well as in the early fractionates of the outer gabbroic series. Their slight increase in the former and rapid increase in the latter indicated that they are excluded from the early liquidus phases and enriched in the intercumulus phases. The successive increase of these elements in the outer gabbroic series and diorite until they become stabilized in the granitic rocks further emphasizes their genetic relation to the inner gabbroic rocks.

The abundance of large cations - Rb, Ba, Sr and K are within the range of measured values of these elements in the calc-alkaline Aleutian basalts to rhyolites. Inverse correlation between Sr and Rb can

be attributed to the fractionation of plagioclase. Progressive increase in the Ba/Sr with decreasing Sr (Figure 6.6), and a nearly flat pattern of K/Rb with increasing K indicate that both K and Rb were enriched in the gabbroic series at nearly constant rates (Figure 6.7). Plots of Y, Rb, Zr versus Ba show a positive relationship and different rock groups appear to be geochemically overlapping one another (Figure 6.8).

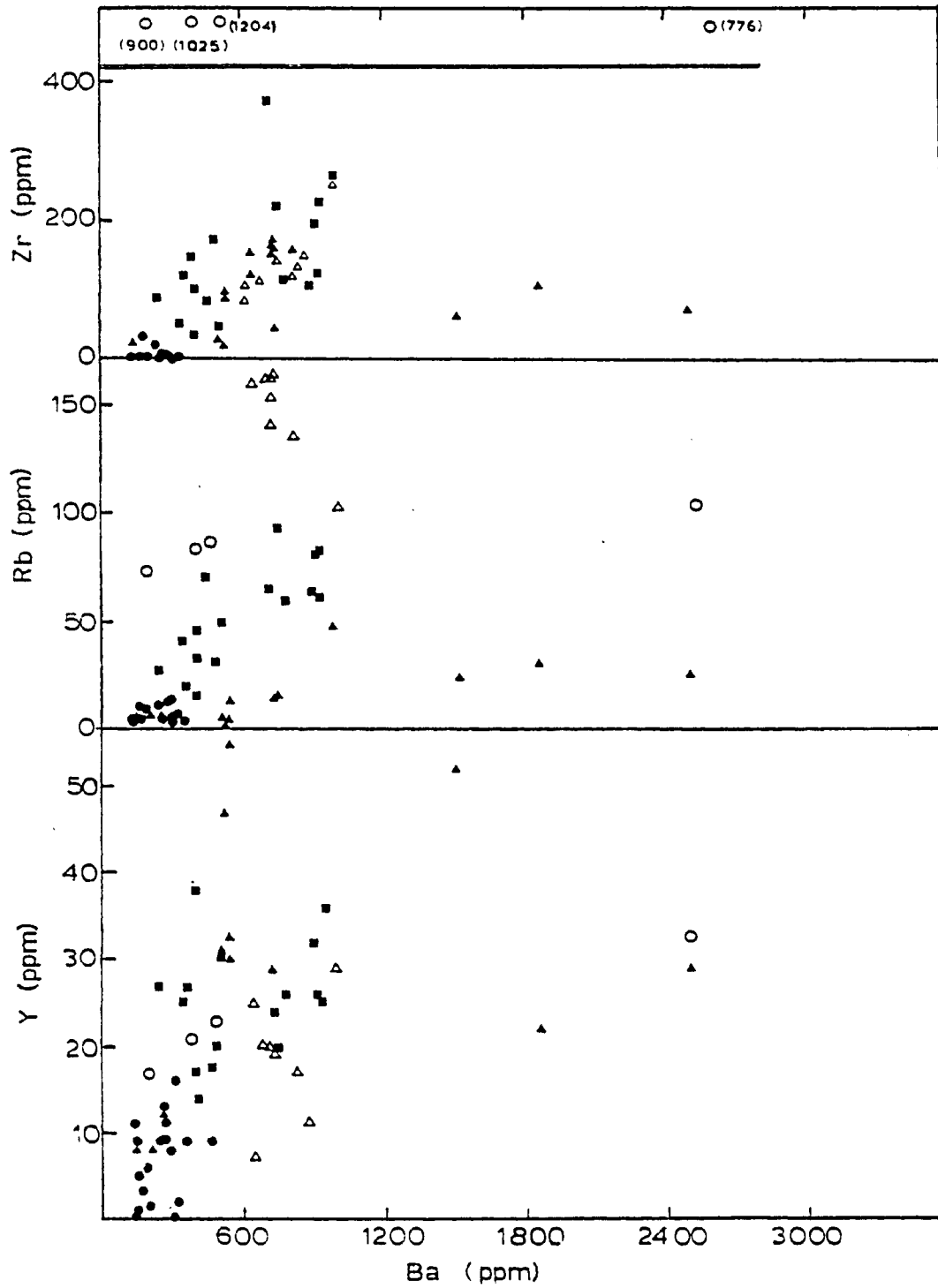
Zircon can be used as an index of magmatic differentiation because it is effectively excluded from the liquidus phases in basaltic suites (Saunders and Tarnery, 1979). The Zr in the Gamitagama Lake Complex, where it increases from the inner gabbroic series through outer gabbroic series to dioritic rocks, but sharply decreases in the granitic rock, is consistent with the differentiated calc-alkaline basaltic suites.

### 6.3 DISCUSSION

The spatial, petrographic, and geochemical characteristics of the Gamitagama Lake intrusive series (excluding the quartz monzonite) suggest that it has evolved by fractional crystallization of



Figure 6.8 Plots of Y, Rb, and Zr vs Ba.  
 (symbols are similar to figure 6.3)



ascending residual magma. The main argument for this modal includes systematic changes in minerals and their host rocks which occur throughout the intrusive series, and intrusive phases become increasingly less basic with increasing age. This implies that the parent magma in the deep seated chamber followed the chemical trend characteristic of the calc-alkaline suite.

#### 6.3.1 PROPOSED PARENT MAGMA

The fine-grained porphyritic rocks intrusive in the inner as well as outer gabbroic series represent the last intrusive phases of gabbroic nature. Although classified as equivalent to the pyroxene diorite of the outer gabbroic series, these rocks are basic enough to be called porphyritic basalt in chemical and normative classification. The fine-grained dioritic rock W132 closely resembles the porphyritic gabbroic rocks, and the medium-grained W153 is equivalent to andesite in chemical composition. These residual liquid fractions removed from the differentiating parent magma should be comparatively less basic than the original magma. The rocks of the inner gabbroic series, the outer gabbroic

series, and the chilled fine to medium-grained porphyritic gabbroic rocks are very close to the composition of high alumina basalt as defined by Irvine and Barager (1971). The high alumina basalt is proposed as the parent magma for the complex. This could have been derived from a multistage event involving partial melting of the mantle.

### 6.3.2 CRYSTALLIZATION OF THE INNER GABBROIC SERIES

The observed fractional crystallization sequence plagioclase + olivine + clinopyroxene + orthopyroxene + titaniferous magnetite in the inner gabbroic series is similar to liquidus diagram of high alumina basalt of the Medicine Highlands (Yoder and Tilley, 1962; Figure 6.9A). Plagioclase and the olivine are the liquidus minerals at  $P_{H_2O}$  of 1 kb at about 1175° C. Clinopyroxene is the near liquidus pyroxene. With the changing composition of coexisting liquid to intermediate between high alumina basalt and andesite, olivine disappears as crystallizing phase and its place is taken by clinopyroxene (Eggler and Burnham, 1973; Figure 6.9B). Orthopyroxene replaces clinopyroxene as next liquidus phase. Crystal fractionation contains increased orthopyroxene relative to



clinopyroxene. Plagioclase is the liquidus mineral in these cumulates. Amphibole is the last phase to crystallize according to the experimental work.

Quantitatively increasing Rb/Sr, Y/Sr, Ba and decreasing Sr/Zr are in agreement that plagioclase and olivine with lesser amounts of pyroxene were the principal mineral phases precipitating during crystallization of the inner gabbroic series. Decreasing abundances of Ni, Cr and Co attest to the role of olivine and clinopyroxene fractionation.

### 6.3.3 CRYSTALLIZATION OF THE OUTER GABBROIC SERIES

The observed crystallization sequence plagioclase + orthopyroxene + clinopyroxene + titaniferous magnetite + amphibole + phlogopite of the outer gabbroic series are best explained by the liquidus diagram of the Paricutin Lava (Eggler, 1972; Figure 6.10).

Plagioclase is the liquidus phase at about 1150° when water content in the liquid is less than 2.5%. When more water is present orthopyroxene is a liquidus phase. Olivine appears with the orthopyroxene on the liquidus but quickly disappears by reaction. Clinopyroxene appears near the orthopyroxene liquidus with the increasing water (about 5%). Magnetite appears

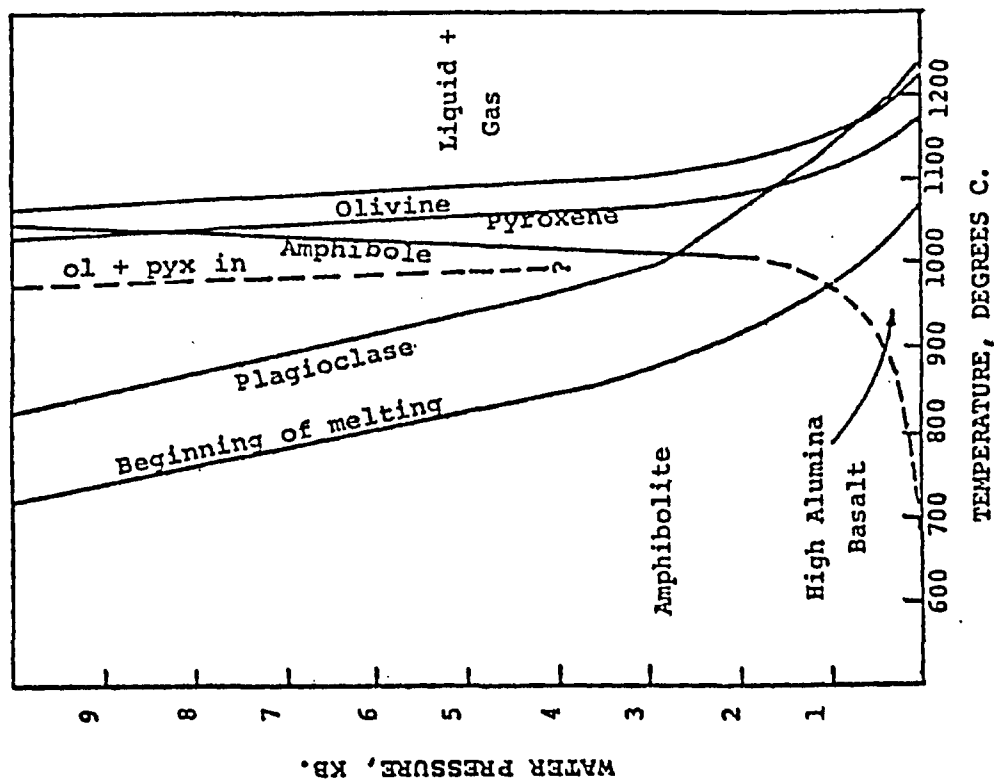


Figure 6.9A. Liquidus diagram for a Medicine Lake Highlands high alumina basalt (after Yoder and Tilley, 1962).

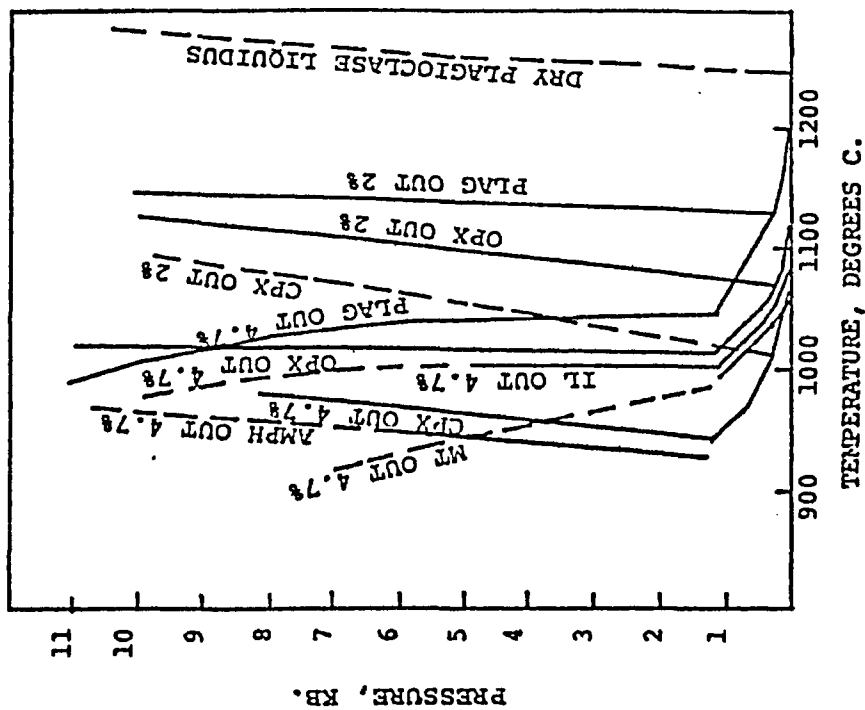


Figure 6.9B. Liquidus diagram for a Mt. Hood andesite (after Egglar and Burnham, 1973).

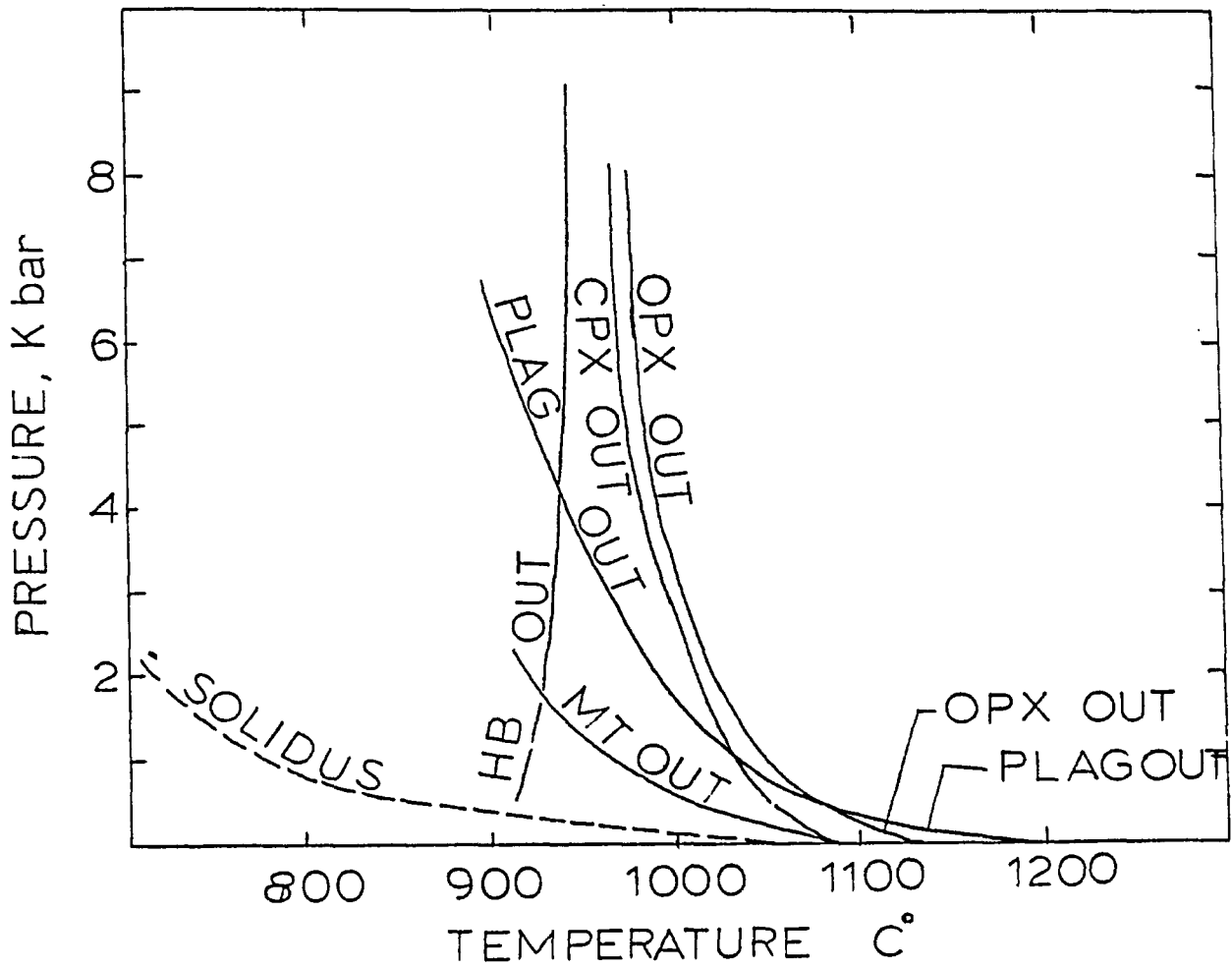


Figure 6.10 Liquidus diagram for a Paricutin lava (after Egger, 1972).

80° to 100° C below the silicate liquidus. With further increase of H<sub>2</sub>O pressure (about 5 kb) at about 950° amphibole stabilizes.

The increasing Rb/Sr, Y/Sr, Ba and decreasing Sr/Zr in the outer gabbroic series are in agreement with the plagioclase and pyroxene fractionations. The low amounts of Ni, Co, and Cr in the outer gabbroic rocks, in comparison to the inner gabbroic series, indicate that these trace elements were removed from the parent liquid by the fractionation of the olivine in the magma chamber. The K/Rb values in the inner gabbroic series and the outer gabbroic series are not significantly different. This together with the increasing Rb/Sr and Ba in the outer gabbroic series implies that amphibole and biotite were not fractionating in the magma chamber. However, the next two residual liquids which crystallized as porphyritic rocks have phenocrysts of amphibole and phlogopite respectively. These phenocrysts are in various stages of recrystallization to plagioclase + orthopyroxene + clinopyroxene + magnetite under low pressure.

#### 6.3.4 CRYSTALLIZATION OF THE DIORITIC ROCKS

In the dioritic rocks plagioclase + clinopyroxene + hornblende + biotite are the early fractionates (Figure 6.10). Plagioclase and clinopyroxene are liquidus minerals at about 1000° C when the H<sub>2</sub>O contents in the melts are greater than 5%. At lower temperatures (less than 950°) with the increase in water contents amphibole (hornblende) becomes stable (Eggler 1972).

The increasing Rb/Sr, Y/Sr and decreasing Sr/Zr and K/Rb are consistent with the fractionation of plagioclase, hornblende and biotite. A significant decrease in K/Rb in the dioritic rocks, in comparison to the outer gabbroic series, indicates fractionation of amphibole + biotite in the magma chamber. This is consistent with the observed fine-grained gabbroic rocks with amphibole and phlogopite phenocrysts. A similar significant decrease K/Rb is obvious in fine-grained rocks W145, W132 and W153.

#### 6.3.5 CRYSTALLIZATION OF THE GRANITIC ROCKS

The continued increase in Rb/Sr, Y/Sr and further decrease in Sr/Zr and K/Rb indicate that the fraction-

ation of plagioclase together with amphibole and biotite occurred both in the granitic rocks in the complex and deeper down in the magma chamber.

#### 6.4 GENESIS OF PLUTONIC SERIES

The above discussed variations in the residual liquids of the plutonic series of the complex suggest that the fractionation was initially controlled by the subtraction of olivine but with the falling temperature and increasing water pressure in the magma chamber changed to removal of dominantly amphibole and phlogopite. In the hydrous basaltic and andesitic melts amphibole can crystallize at pressures between 10-20 kb provided  $P_{H_2O}$  is greater than  $P_{Total}$ . At lower pressures (less than 6 kb if  $P_{H_2O}$  is less than  $0.2 P_{Total}$ ; less than 2 kb if  $P_{H_2O}$  is more than  $0.5 P_{Total}$ ) amphibole is unstable and is replaced by plagioclase  $\pm$  orthopyroxene  $\pm$  clinopyroxene  $\pm$  olivine + magnetite as was observed in the porphyritic chilled gabbroic rocks of the complex (Green, 1972; Helz, 1972; Allen et al., 1975; Cawthorn and O'Hara, 1976; Wyllie et al., 1976; Stewart et al., 1976). The stability of the amphibole suggests that the fractionation of the liquid phases in the magma chamber occurred

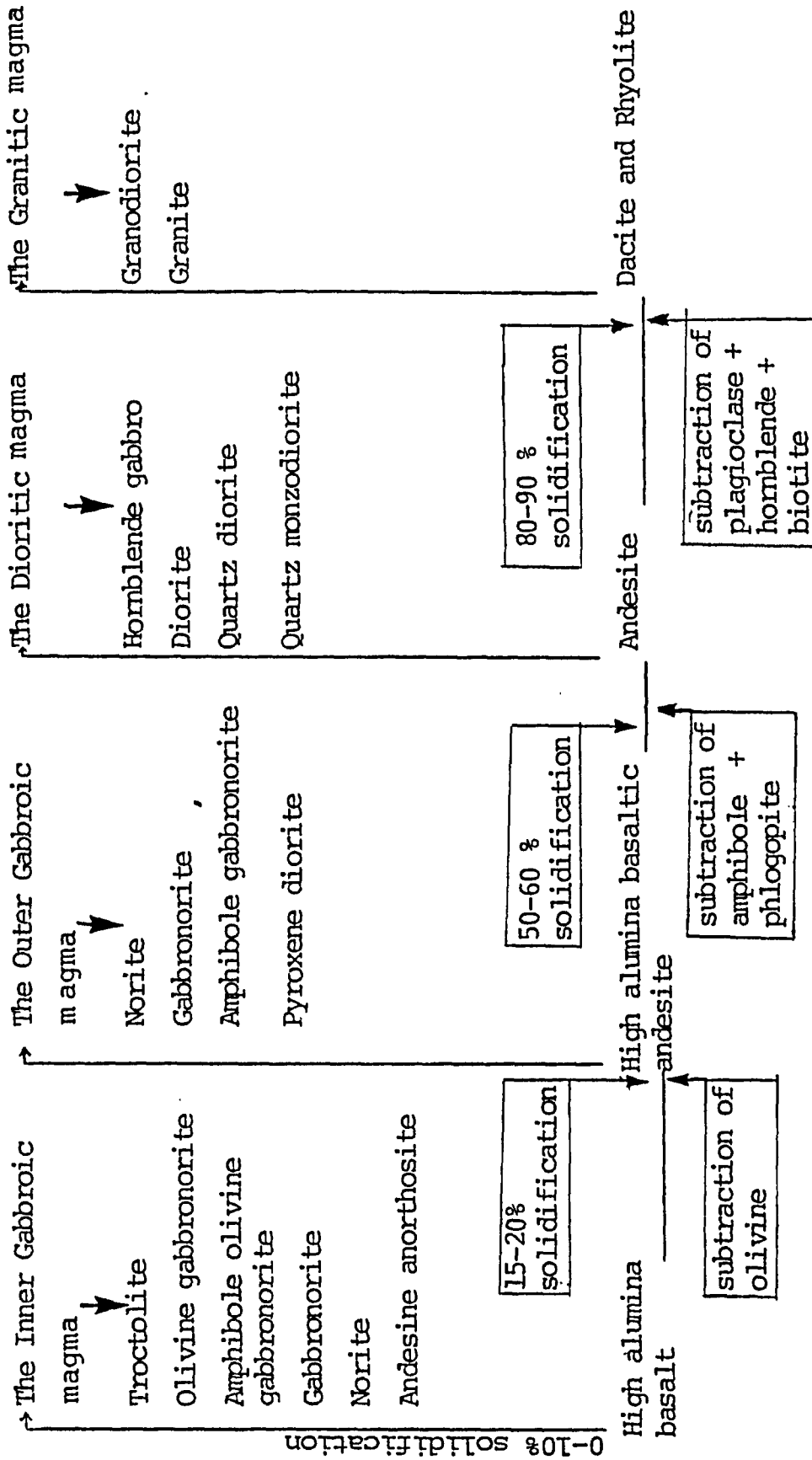


Figure 6.11 The intrusive series of the Gamitagama Lake Complex and the proposed liquid line of descent assuming a high alumina basalt as a parental magma in the magma chamber.

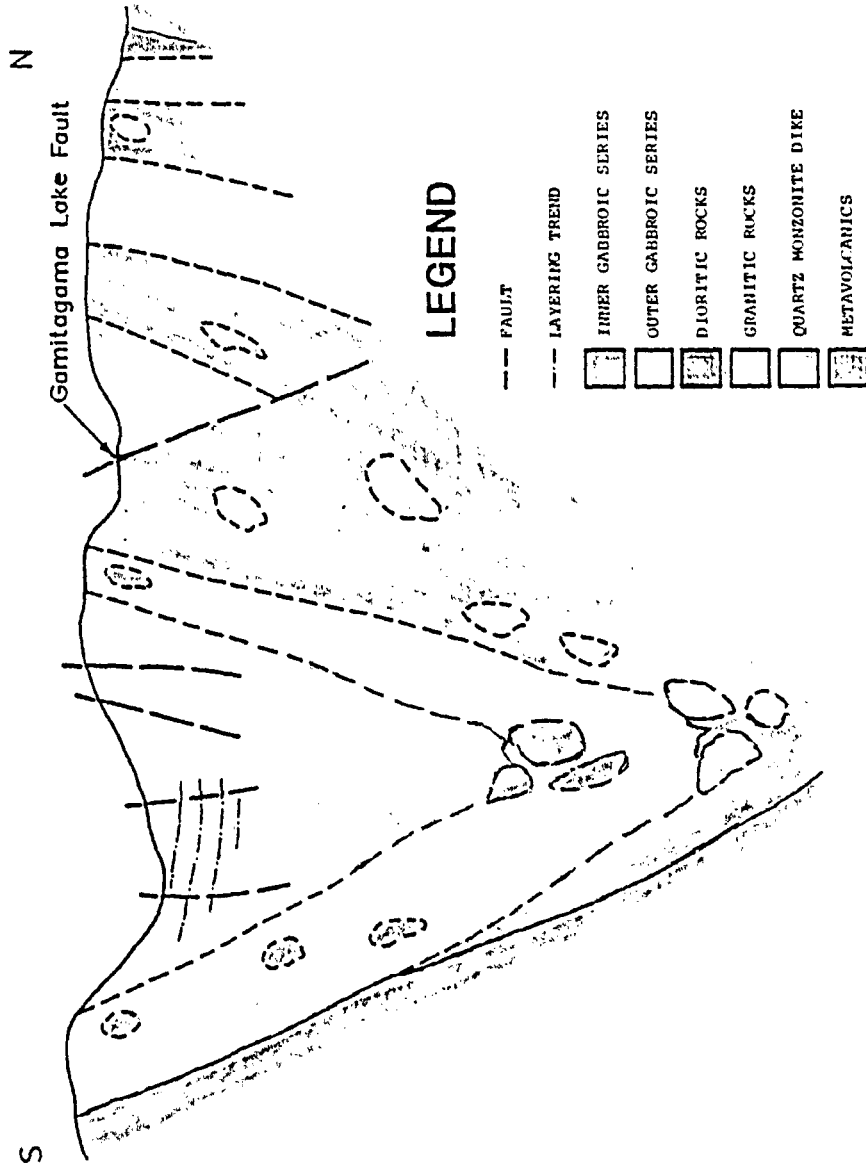
at deeper level, more than 35 km, down in the crust under conditions of increasing water fugacity. A hypothetical estimate of the solidification of the magma chamber at the various stages of tapping is presented in Figure 6.11.

#### 6.5 EMPLACEMENT AND STRUCTURE OF THE COMPLEX

The evolution of the complex took place by the initial emplacement of single batch of high alumina magma at depth less than 8 km followed by crystal settling to produce observed layering and variation of the rock types (Figure 6.12). The fractionation within a deeper magma chamber produced a series of residual liquids, successively less basic in composition, which moved upward invading the contact between the inner gabbroic rocks and the metavolcanic and metasedimentary sequence. The force of intrusion fractured and faulted the inner gabbroic rocks. Small scale intrusions of less basic gabbroic rocks invaded the inner and outer gabbroic series. Further fractionation and removal of amphibole and phlogopite from the magma chamber produced the residual magma of dioritic composition which invaded the contact between the outer gabbroic series and the metavolcanics. The



Figure 6.12 Schematic diagram illustrating the structure of the Gamitagama Lake Complex.



continued fractionation of amphibole and phlogopite (probably replaced by biotite at this stage) in the magma chamber produced the residual granitic magma which intruded the dioritic rocks of the complex. The quartz monzodiorite was probably produced by the partial melting of the crust at a later date and is not a part of the complex.

The analyses of structure within the complex is based on the data obtained from the orientation of foliation, banding, and inclusions in the plutonic rocks.

The Gamitagama Lake Complex is structurally independent of the regional pattern. The gneissosity within the metavolcanic sequence has a subvertical dip, towards the complex. An approximately similar pattern in the foliation of the dioritic rock near the outer margin of the complex is observed. The foliation pattern indicates that the contact of dioritic and metavolcanics dips inward, and the complex is almost plug-shaped.

## 6.6 TECTONIC SETTING

The calc-alkaline trend observed in the complex is characteristic of island arcs and continental

margins, that is, in the convergent margins of plates (Miyashiro, 1972). Moreover, titanium concentrations are low to moderate in the plutonic rocks of the complex which is also a characteristic of island arc suites in general (Pearce and Cann, 1973).

The metavolcanic-metasedimentary sequence in the surrounding areas of the complex documents the evolution of a volcanic island within the early Precambrian Abitibi Island Arc (Ayres, 1969).

The intrusion of high alumina basalt (which differentiated to calc-alkaline Gamitagama Lake Complex) in the Island arc suggests that it could have been derived from a multistage event involving partial melting and dehydration of the subducted slab and subsequent partial melting of the contaminated mantle underlying the arc (Key, 1977). This implies that the tectonic regime in the Late Archean was not significantly different than that of the modern day.

## CHAPTER 7

## CONCLUSION

The Gamitagama Lake Complex is similar to many zoned plutons that intrude the island arc and calc-alkaline intrusive bodies emplaced around the active continental margins of the Pacific. It consists of 4 major concentric and other minor intrusive phases. The oldest and the most basic intrusive phase occupies the center and the youngest, most acidic, occurs near the margin. Mineralogical and chemical variations in each intrusive phase indicate that they were formed by in situ fractional crystallization of liquids emplaced at shallow levels. In the gabbroic series plagioclase + olivine + clinopyroxene + orthopyroxene + titaniferous magnetite and in the dioritic and granitic rocks plagioclase + clinopyroxene + hornblende + biotite fractionated out of the respective parent liquids at pressures less than 5 kb to give calc-alkaline differentiation trends within each series.

Major and trace element characteristics and the field observations that most basic phases of each discrete intrusive event are successively less basic in composition with the decreasing age support the hypothesis that the Gamitagama Lake intrusive series

are derived by the fractional crystallization of parent high alumina basaltic magma in the source magma chamber. The chemical data are consistent with a model where fractionation was initially controlled by the subtraction of olivine but with the falling temperature and increasing water pressure shifted to removal of amphibole and/or phlogopite. The occurrence of minor porphyritic intrusive phases verify this model. The presence of amphibole and phlogopite phenocrysts in the basaltic magma indicate the existence of a more than 35 km thick solid crust (?) at the end of Archean. The intrusion of high alumina basalt (characteristic orogenic belts) in the metavolcanic-metasedimentary sequence (which represent island-arc-like deposits) suggests that the parent magma for the complex was derived by the partial melting of the mantle above converging plate and intruded into the overlying island arc deposits. This implies that the tectonic regime in the Late Archean was not significantly different than that of the modern day.

## REFERENCE

- Allegre, C.J., Treml, M., Minster J.F., Minster B., & Albarede, F., 1977. Systematic use of trace element in igneous process, Part 1: fractional crystallization processes in volcanic suite. *Contr. Mineral. Petrol.* Vol.60, 57-75.
- Anderson, A.T. and Gottfried, D., 1971. Contrasting behavior of P, Ti and Nb in a differentiated high-alumina olivine tholeiite and a calc-alkaline andesitic suite. *Geol. Soc. America Bull.* Vol.82, 1929-1942.
- Anderson, A.T., Jr., 1980. Significance of hornblende in calc-alkaline andesites and basalts. *Am. Min.*, Vol.65, 837-851.
- Arth, J.G., 1976. Behavior of trace elements during magmatic processes - a summary of theoretical models and their applications. *Jour. Research U.S. Geol. Survey* 4, 41-47.
- Ayres, L.D., 1969. *Geology of Townships 31 and 30, Ranges 20 and 19, District of Algoma. Geological Report 69, Ontario Department of Mines, 1-90.*
- Ayres, L.D., 1969. Unpublished Ph.D. Thesis. Princeton University 1969.
- Bell, R., and Dawson, G.M., 1899. Summary report on

the operations of the geological survey for the year 1898: Geol. Surv. Canada, Ann. Rept., V.11, pt.A, 99-106.

Best, M.G., 1963. Petrology of the Guadalupe Igneous Complex South-western Sierra Nevada Foothills California. J. Petrol. Vol.4, part 2, 223-259.

Best, M.G., 1969. Differentiation of calc-alkaline magmas: Oregon Dept. of Geol. and Mineral. Ind. Bull., Vol.65, 65-73.

Best, M.G., and Mercy, E.L.P., 1967. Composition and crystallization of mafic minerals in Guadaupe Igneous Complex, California. Am. Mineralogist, Vol. 52, 436-476.

Cawthron, R.G., and O'Hara, M.J., 1976. Amphibole Fractionation in calc-alkaline magma genesis. Am. J. Sci. Vol.276, 309-329.

DeLong, S.E., 1974. Distribution of Rb, Sr, and Ni in igneous rocks, Central and Western Aleutian Islands, Alaska. Geochim. Cosmochim. Acta 38, 254-266.

Eggler, D.H., 1972. Water saturated and undersaturated melting relations in a Paricutin Andesite and an estimate of water content in the natural magma., Cont. Mineral. and Petrol., Vol.34, 261-271.

- Eggler, D.H., 1972. Amphibole stability in H<sub>2</sub>O-undersaturated calc-alkaline melt. *Earth Planet Sci. Lett.*, Vol.15, 28-34.
- Eggler, D.H. and Burnham, C.W., 1973. Crystallization and fractionation trends in the system andesite-H<sub>2</sub>O-CO<sub>2</sub>-O<sub>2</sub> at pressures to 10 kb. *Geol. Soc. Amer. Bull.* Vol.84, 2517-2532.
- Emslie, R.F., 1973. Some chemical characteristics of Anorthositic suites and their significance. *Can. J. Earth Sci.*, Vol.10, 54-69.
- Erikson, E.H. Jr., 1977. Petrology and petrogenesis of the Mount Stuart Batholith - Plutonic equivalent of the high alumina basalt Association. *Contrib. Mineral. petrol.*, Vol.60, 183-207.
- Ewart, A. and Taylor, S.R., 1969. Trace element geochemistry of the rhyolitic volcanic rocks. Central North Island New Zealand. Phenocryst data. *Cont. Mineral. and Petrol.*, Vol.22, 127-146.
- Fudali, R.F., 1965. Oxygen fugacities of basaltic and andesitic magmas. *Geochim. Cosmochim. Acta*, Vol.29, 1063-1075.



- Furnes, H., Sturt, B.A. and Griffin, W.L., 1980. Trace element geochemistry of metabasalts from the Karmoy Ophiolite, Southwest Norwegian Caledonides. *Earth Planet. Sci. Lett.*, Vol.50, 75-91.
- Garcia, M.O., and Jacobson, S.S., 1979. Crystal clots, amphibole fractionation and the evolution of calc-alkaline magmas. *Cont. Mineral. Petrol.*, Vol.69, 319-327.
- Gast, P.W., 1968. Trace element fractionations and origin of tholeiitic and alkaline magma types. *Geochim. Cosmochim. Acta*, Vol.32, 1057-1086.
- Gill, J.B., 1978. Role of trace element partition coefficients in modal of andesite genesis. *Geochim. Cosmochim. Acta*, Vol.42, 709-724.
- Green, T.H., 1972. Crystallization of Calc-alkaline andesite under controlled high pressure hydrous conditions. *Contrib. Mineral. Petrol.* Vol.34, 150-166.
- Helz, R.T., 1973. Phase relations of basalts in their melting range at  $P_{H_2O}=5$  kb as a function of Oxygen Fugacity. Part I. Mafic Phases. *J. Petrol.*, Vol.14, 249-302.
- Hermes, O.D., 1968. Petrology of the Mecklenburg

- Gabbro-Metagabbro Complex, North Caroline.  
Cont. Mineral. Petrol., Vol.18, 270-294.
- Goodwin, A.M., Ridler, R.H. and Ridler, R.H., 1972.  
Ultramafic and Gabbroic Bodies in "The Superior  
Province" in: 'Variations in the Tectonic Style  
in Canada'. Edited by R.A. Price and R.J.  
Douglas, G.A.S. Special Paper No. II, 553-575.
- Holloway, J.R., and Burnham, C.W., 1972. Melting  
relations of basalt with equilibrium water  
pressure less than total pressure. J. Petrol.  
Vol.13, 1-29.
- Irvine, T.N., 1974. Petrology of Duke Island  
Ultramafic Complex, Alaska. Geol. Soc. of Am.  
Inc. Memoir 138, 1-25.
- Irvine, T.N., 1979. Rock whose composition is  
determined by crystal accumulation and  
sorting. in: The 'Evolution of Igneous  
rocks'. Edited by Yoder, H.S., 245-299,  
Princeton University Press, New Jersey.
- Irvine, T.N., and Barager, W.R.A., 1971. A guide to  
the chemical classification of the common  
volcanic rocks. Can. J. Earth Sci. Vol.8,  
523-48.
- Irving, A.J., 1978. A review of experimental studies

- on Crystal/liquid trace element partitioning. *Geochim. Cosmochim. Acta*, Vol.42, 743-771.
- Jackson, E.D., 1961. Primary textures and mineral associations in the ultramafic zone of the Stillwater Complex, Montana, U.S.: *Geol. Surv., Prof. Pap.*, 385, 1-106.
- Jackson, E.D., 1971. Hornblende from Calc-alkaline Volcanic rock of Island Arcs and continental margins. *Am. Mineral.* 57, 887-902.
- James, O.B., 1971. Origin and emplacement of the ultramafic rocks of the Emigrant Gap area, California. *J. Petrol.*, Vol.12, part 3, 523-560.
- Jaques, A.L., and Chappell, B.W., 1980. Petrology and trace element geochemistry of the Papuan Ultramafic Belt. *Contrib. Mineral. Petrol.*, Vol.75, 55-70.
- Jekes, P., and White, A.J.R., 1972. Major and trace element abundances in volcanic rocks of orogenic belts. *Geol. Soc. Amer. Bull.*, Vol.83, 29-42.
- Kennedy, G.C., 1955. Some aspects of the role of water in rock melts. *Geol. Soc. Amer.*, Spacial Paper No. 62, 489-504.

- Key, R.W., 1977. Geochemical constraints on the origin of Aleutian magmas. In: Island arcs Deep Sea Trenches and Back arc Basins (M. Talwani and W.C. Pitman III eds.) 229-242. Washington D.C. Am. Geophys. Union 1977.
- Korringa, M.K., and Noble, D.C. Sr and Ba distribution in feldspar and igneous melt. Earth Planet. Sci. Lett., Vol.11, 150.
- Kuno, H., 1950. Petrology of Hakone Volcano and the adjacent areas, Japan: Geol. Soc. Am. Bull., Vol.61, 37-76.
- Kuno, H., 1959. Origin of Cenozoic petrographic Provinces of Japan and surrounding area. Bull. Volcan. Ser. 2, Vol.20, 37-76.
- Kuno, H., 1960. High-alumina basalt. J. Petrol. Vol.1, 121-45.
- Kuno, H., 1965. Fractionation trends of basalt magmas in lava flows: J. Petrol., Vol.6, 302-321.
- Kuno, H., 1968a. Differentiation of basaltic magmas: in Hess, H.H., and Poldervaart, Basalts, V.2: New York, Intersci. Publishers, 623-688.
- Kuno, H., 1968b. Origin of andesite and its bearing on the Island arc structure: Bull. Volcanol., Ser.2, V.32, 141-176.

- Kushiro, I., 1969. Stability of phlogopite at high pressure. *Earth. Planet. Sci. Lett.*, Vol.3, 197-203.
- Kushiro, I., 1972. Effect of water on the compositions of magmas formed at high pressures. *J. Petrol.* Vol.46, 29-47.
- Kushiro, I., Yoder, H.S. Jr., and Mysen, B.O., 1976. Viscosities of basalt and andesite melts at high pressures. *J. Geophys. Res.* Vol.81, 6351-6356.
- McIntire, W.L., 1963. Trace elements partition coefficients. *Geochim. et Cosmochim. Acta*, Vol.27, 1252-1255.
- Miyashiro, A., 1972. Metamorphism and related magmatism in plate tectonics: *Am. J. Sci.* Vol.272, 629-656.
- Miyashiro, A., 1973. The Troodos Ophiolitic Complex was probably formed in an island arc. *Earth. Planet. Sci. Lett.*, Vol.19, 218-224.
- Miyashiro, A., 1974. Volcanic rock series in island arcs and active continental margins. *Am. J. Sci.* 321-355.
- Miyashiro, A., and Shido, F., 1975. Tholeiitic and calc-alkaline series in relation to the

- behaviors of Titanium, Vanadium, Chromium, and nickel. *Am. J. Sci.*, Vol.275, 265-277.
- Muir, I.D., 1954. Crystallization of Pyroxenes in an iron rich diabase from Minnesota: *Mineral. Mag.*, Vol.30, 376-388.
- Neumann, H., Mead, J., and Vitaliano, C.J., 1954. Trace element distribution during fractional crystallization as calculated from the distribution law. *Geochim. Cosmochim. Acta*, Vol.6, 90-99.
- Nishimori, R.K., 1976. Unpublished Ph.D. Thesis. University of California, San Diego, 1-220.
- Nockolds, S.R., and Allen, R., 1953. The geochemistry of some igneous rocks. *Geochim. cosmochim. Acta*, Vol.4, 105-142.
- Modresk, P.J., and Boettcher, A.L., 1973. Phase relationship of phlogopite in system  $K_2O-MgO-CaO-Al_2O_3-SiO_2-H_2O$  to 35 kb. A better modal for micas in the interior of earth. *Am. J. Sci.* Vol.273, 385-414.
- O'Hara, M.J., 1977. Geochemical evolution during fractional crystallization of a periodically refilled magma chamber. *Nature*, Vol.266, 503-507.

- Osborn, E.F., 1959. Role of oxygen pressure in the crystallization and differentiation of basaltic magma. *Am. J. Sci.*, Vol.257, 607-647.
- Osborn, E.F., 1969. The complimentariness of orogenic andesite and alpine peridotite *Geo. Chim. Cosmochim. Acta*, Vol.33, 307-324.
- Paster, T.P., Schauwecker, D.S., and Haskin, L.A., 1974. Some trace elements during solidification of the Skaergaard layered series. *Geochim. Cosmochim. Acta*, Vol.38, part 2, 574-76.
- Pearce, J.A. and Cann, J.R., 1973. "Tectonic setting of basic volcanic rocks determined using trace element analysis". *Earth Planet. Sci. Lett.* Vol.19, 290-300.
- Perfit, M.R., Bruechner, H., Lawrence, J.R., and Key, R.W., 1980. Trace element and isotopic variations in a zoned pluton and associated volcanic rocks, Unalaska Island, Alaska: A modal for fractionation in the Aleutian Calc-alkaline Suite. *Contrib. Mineral. Petrol.*, Vol.73, 69-87.
- Sapountzis, E.S., 1979. The Thessaloniki Gabbros. *J. Petrology*, Vol.20, part 1, 37-70.

- Saunders, A.D., and Tarney, J., 1972. The geochemistry of basalts from a back arc spreading centre in the East Scotia Sea. *Geochim. Cosmochim. Acta*, Vol.43, 555-572.
- Shimizu, N., 1974. An experimental study of the partitioning of K, Rb, Cs, Sr, and Ba between clinopyroxene and liquid high pressures. *Geochim. Cosmochim. Acta*, Vol.38, 1989-1798.
- Stewart, D.C., 1975. Crystal clots in calc-alkaline andesites as breakdown products of high alumina amphiboles. *Contrib. Mineral. Petrol.*, Vol.53, 195-204.
- Stewart, D.C., Allen, J.C., and Boettcher, A.L., 1976. Genesis of andesitic magma by amphibole fractionation: Petrographic and experimental evidence (abstr.) *EOS* 57, 334.
- Streckeisen, A., 1976. To each plutonic rock its proper name. *Earth-Sci. Rev.*, Vol.12, 1-33.
- Taylor, S.R., 1969. Trace element chemistry of andesites and associated calc-alkaline rocks: Oregon Dept. of Geol. Mineral. Ind. Bull., Vol.65, 43-63.
- Thornton, C.P. and Tuttle, O.F., 1960. Chemistry of Igneous Rocks; 1. Differentiation Index. *Am.*



- J. Sci., Vol. 258, 664-681.
- Turek, A., and Riddle, C., 1977. A geochemistry laboratory manual. (Sec. Ed.), Dept. of Geology, University of Windsor, 1-72.
- Turek, A., Krough, T.E., Smith, T.E., and Huang, C.H., 1978. Geochronology and geochemistry of the Gamitagama area, Ontario geol. Association of Canada. Abstracts 4, 83.
- Turek, A., Smith, T.E., and Huang, C.H., 1980. Rb-Sr whole-rock geochronology of the Gamitagama area, North-central Ontario. Can. J. Earth. Sci., Vol.18, 323-329.
- Vance, J.A., 1969. On Synneusis., Contrib. Mineral. Petrol., Vol.24, 7-29.
- Wager, L.R., 1967. Rhythmic and crystic layering in mafic and ultramafic plutons, 445-482 in Hess, H.H. and Poldervaart, A. (ed.). Basalts, Vol.2, Intersci. New York.
- Wager, L.R., Brown, G.M. and Walswarth, W.J., 1960. Types of Igneous cumulates: J. Petrol. Vol.1, 73-85.
- Wager, L.R., and Brown, G.M., 1967. Layered igneous rocks. Freeman, San Francisco.
- Walawender, M.J., Hoppler, H., Smith, T.E. and Riddle, C., 1979. Trace element evidence for

contamination in a gabbro-norite-quartz diorite sequence in the Pinensular Ranges Batholith.

*J. Geology*, Vol.87, 87-97.

Wones, D.R., and Dodge, F.C.W., 1977. The stability of phlogopite in presence of diopside and quartz. NATO Adv. study Inst. ser. C, Math. phys. Sci. No.30, 229-247.

Wyllie, P.J., Huang, W.L., Stern, C.R., and Maaloe, S., 1976. Granitic magmas: possible and impossible sources, water contents and Crystallization Sequences. *Can. J. Earth Sci.*, Vol.13, 1007-1019.

Yoder, H.S. and Eugster, H.P., 1954. Phlogopite synthesis and stability range. *Geochim. Cosmochim. Acta*. Vol.3, 22-48.

Yoder, H.S., and Tilley, C.E., 1962. Origin of basaltic magmas: an experimental study of natural and synthetic rock systems, *J. Petrol.*, Vol.3, 342-532.

Yoder, H.S., 1969. Calc-alkaline andesites: Experimental data bearing on the origin of their assumed characteristics, in: Proceedings of the Andesite Conference, State of Oregon, A.P. McBirney, ed. *Bull. Dept. Geol. Mineral Ind.* 65, 193.

## APPENDIX A

Ayres (1969) classified the rocks of the Gamitagama Lake Complex according to the old ODM classification outlined in Table A-1. The author has reclassified the rocks according to the IUGS classification (Streckeisen 1976). The "syenite and monzonite" and "leucocratic granodiorite" and "quartz monzonite" of Ayres were renamed as "quartz monzonite" and "leucocratic granodiorite and granite" respectively. Most of his various types of diorites are renamed as quartz diorite. "Olivine norite" changes to olivine gabbro norite; "anorthosite norite" and "anorthosite gabbro" change to gabbro norite; and "orthopyroxene diorite", "clinopyroxene diorite" and "amphibole diorite" change to pyroxene diorite according to the IUGS classification.

Quartz	Potassic Feldspar	COMPOSITION OF PLAGIOCLASE				MONOMINERALIC	LESS THAN 10% FELDSPAR
		An <sub>0-10</sub>	An <sub>10-30</sub>	An <sub>30-50</sub>	An <sub>50-100</sub>		
QUARTZ GREATER THAN 10%	> 2/3	Potassic Granite					
	1/3 - 2/3		Quartz Monzonite	Calcic Quartz Monzonite			
	1/8 - 1/3	Sodic Granite	Granodiorite	Calcic Granodiorite			
	< 1/4	Albite Granite	Trochiljenite	Tonalite	Quartz Gabbro		
← GRANITIC ROCKS →							
QUARTZ LESS THAN 10%	> 2/3	Potassic Syenite				Anorthosite	
	1/3 - 2/3		Monzonite		Calcic Monzonite	Hornblendite	
	1/8 - 1/3	Sodic Syenite	Syenodiorite			Pyroxenite	
	< 1/4	Albite Syenite	Diorite		Gabbro	Dunite	Peridotite

Table A.1: Modal Classification of non-feldspathoidal plutonic rocks used by Ayres 1969.

APPENDIX BA. Rocks and textures formed by crystal accumulation<sup>1</sup>

## I. Components of rocks formed by crystal accumulation.

- i) Cumulus crystal = settled crystal - a crystal (mineral) that originated outside of, and previously to, the magmatic sediment of which it now forms a part.
- ii) Postcumulus material - primary material that formed in the place it now occupies in the magmatic sediment.
- iii) Intercumulus liquid - the liquid that occupied the interstices between cumulus crystals before and during the growth of the post-cumulus material.
- iv) Adcumulus growth - the extension of the original cumulus crystals by material of the same composition, to give unzoned crystals. The process reduces the amount of intercumulus liquid by mechanically pushing it out.
- v) Trapped liquid - that part of the intercumulus liquid, if any, that remains after adcumulus growth.
- vi) Pore material - crystallized trapped liquid.

## II. Rocks formed by crystal accumulation

- i) Cumulate = magmatic sediment - a group name for igneous rocks formed by crystal accumulation through the action of gravity and subsequent modification during solidification.
- ii) Orthocumulate - a cumulate consisting essentially of one or more cumulus minerals, together with the products of crystallization of the intercumulus liquid, which necessarily has the composition of the contemporary magma. Adcumulus growth is absent to minor.

<sup>1</sup>modified after Jackson (1967; 1971), Wager (1967), Wager et al. (1960).

iii) Adcumulate - a cumulate modified by adcumulus growth with less than 5 percent pore material remaining.

iv) Mesocumulate - a cumulate modified by adcumulus growth intermediate in character between orthocumulate and adcumulate end-members.

B. Horizons and layers in cumulates<sup>1,2,3</sup>

---

I. Horizons<sup>1</sup>

i) Horizon - a reference plane in a cumulate that marks a former surface of deposition.

ii) Phase contact - a horizon marked by the appearance or disappearance of a cumulus mineral.

iii) Ratio contact - a horizon marked by a sharp change in the proportions of two cumulus minerals.

iv) Form contact - a horizon marked by a sharp change in the physical properties of a cumulus mineral, such as size or habit.

II. Layers<sup>1</sup>

i) Layer - a continuous sheetlike cumulate that is characterized by uniform or uniformly gradational properties.

ii) Centimeter-scale layering<sup>4</sup> - layering characterized by alternating layers about one centimeter. Analogous to "inch-scale layering" of Hess (1960).

<sup>1</sup>after Jackson (1967)

<sup>2</sup>after Wager and Deer (1939)

<sup>3</sup>modified after Wager and Brown (1968)

<sup>4</sup>after Morse (1969)

## APPENDIX C

Chemical analyses were performed on Philips PW 1410 Universal Vacuum X-Ray Spectrometer. Pressed rock powder pellets and glass discs were prepared following standard procedures described by Turek and Riddle (1977). Trace elements and Na were analysed using rock powder pellets. Glass discs were used for the analyses of other major elements.

All the major elements, excluding Mn for which a W target tube was used, were determined using a Cr target tube. The U.S.G.S. Standard rock powders, W1, BCR, AGV, GSP and G2 were used as references. Analytical conditions for the major elements are enlisted in Table C.1.

The precision of  $\text{SiO}_2$ , CaO and  $\text{Fe}_2\text{O}_3$ , for which 1,000,000 counts were fixed, is about  $\pm 0.3\%$  at the 99% confidence level. For the other major elements with fixed counts the precision is  $\pm 0.49\%$  for 400,000 counts ( $\text{TiO}_2$ ) and  $\pm 0.95\%$  for 100,000 counts ( $\text{K}_2\text{O}$ ). In those cases where the time is fixed, the number of counts varies with the percentage of the element being determined in the sample. The precision in such cases varies as follows:

TABLE C-1: OPERATING CONDITIONS FOR DETERMINATION OF MAJOR ELEMENTS BY X-RAY FLUORESCENCE.

Element	Si	Al	Fe	Mg	Ca	Na	K	Ti	P	Mn
Tube	cr	cr	cr	cr	cr	cr	cr	cr	cr	W
kV	50	50	50	50	50	50	50	50	50	50
mA	40	40	40	40	40	40	40	40	40	40
Crystal	TLAP	TLAP	LiF200	ADP	LiF200	TLAP	TLAP	LiF200	GERM	LiF200
Collimator	Fine	Fine	Fine	Fine	Fine	coarse	Fine	Fine	coarse	coarse
Counter (setting)	Fc500	Fc490	Fc470	Fc524	Fc510	Fc526	Fc490	Fc488	Fc492	Fc466
Lower Level	100	150	150	130	240	190	250	150	270	150
Window	190	250	200	350	390	260	300	180	350	300
Attenuation	3	2	3	2	3	2	2	3	2	3
Background 1*	-	36.73°	-	134.00°	-	52.75°	16.05°	85.16°	138.00°	62.20°
Peak Positions**	32.01°	37.70°	57.50°	136.87°	113.23°	54.99°	16.61°	86.18°	140.90°	62.97°
Background 2*	-	39.00°	-	139.87°	-	56.70°	18.00°	87.10°	143.40°	63.37°
Counting	4x10 <sup>5</sup> counts	100sec	1x10 <sup>6</sup> counts	100sec	1x10 <sup>6</sup> <sub>n</sub> counts	100sec	100sec	100sec	100sec	100sec

\* Time for background counting = 40 sec.

\*\* Time for Peak counting = 100 sec.



MnO	200,000-400,000 counts	$\pm 0.75 - \pm 0.49\%$
Al <sub>2</sub> O <sub>3</sub> , Na <sub>2</sub> O	50,000-100,000 counts	$\pm 1.30 - \pm 0.95\%$
P <sub>2</sub> O <sub>5</sub>	10,000- 50,000 counts	$< 2.10 - \pm 1.30\%$
MgO	5,000- 20,000 counts	$< 3.00 - \pm 2.10\%$

The count rates for the 72 rock samples analysed for major elements fall within the above ranges.

The trace elements analyses included V, Cr, Co, Ni, Rb, Sr, Y, Zr Nb and Ba. Analytical conditions for their determination are enlisted in Table C.2. Compton scatter peaks were measured for pure quartz, U.S.G.S. standards BCR, W1, AGV, GSP and G2 on Ag, W, Cr, and Mo target tubes. Mass absorption values were determined for each sample from this data. The values derived from the measurements using the Mo target tube were used to correct the mass absorption for the analyses of Ni, Rb, Sr and Zr. The values derived from the measurements using the Ag target tube were used to correct the mass absorption effects for the analyses of Nb and Y. Using the Cr target tube, the mass absorption values obtained were used to correct the mass absorption effects of Co and Ba. Similarly, the analyses of V and Cr were corrected for mass absorption effects using data obtained from the use of the W target tube. The precision of the 61 samples

TABLE C-2: OPERATING CONDITIONS FOR DETERMINATION OF TRACE ELEMENTS BY X-RAY FLUORESCENCE.

Element	V	cr	co	Ni	Rb	Sr	Y	Zr	Nb	Ba
Tube	W	Mo	Mo	Mo	Mo	Mo	Ag	Ag	Ag	Cr
kV	60	60	60	60	60	60	50	50	60	60
mA	50	50	25	25	25	25	40	40	40	40
Crystal	LiF220	LiF220	LiF220	LiF220	LiF220	LiF220	LiF220	LiF220	LiF220	LiF200
Collimator	Fine	coarse	coarse	coarse	Fine	Fine	Fine	Fine	Fine	Fine
Counter (setting)	Fe510	Fe490	Fe482	Fe488	Sc272	Sc272	Sc240	Sc240	Sc230	Fe488
Lower Level	400	310	300	292	300	300	160	160	170	150
Window	300	200	300	250	380	380	340	340	350	250
Attenuation	3	3	3	3	3	3	3	3	3	3
Campton Scatter	-	-	-	-	30.18°	30.18°	-	-	-	70.50°
Background 1*	121.00°	68.20°	77.50°	70.20°	37.10°	35.35°	32.20°	29.70°	29.90°	-
Peak position**	123.37°	69.29°	78.13°	71.46°	38.03°	35.90°	33.90°	32.11°	30.44°	87.25°
Background 2*	126.50°	71.00°	79.3°	73.00°	41.40°	37.10°	35.00°	33.2°	33.2°	90.00°

\* Time for background and campton scatter counting = 40 seconds.

\*\* Time for Peak counting = 100 sec.

analysed for trace elements should fall within the ranges of theoretical precision which is +5% for Rb, Sr, Ba, Zr, Y, Nb, V and Ni and +20% for Cr and Co.

## VITA AUCTORIS

Name: Abdul Ghafoor Choudry

Place & date  
of birth : Lahore, August 15, 1945

Education: Secondary School, Lahore, completed in 1961  
Intermediate Education, Lahore, completed in 1964  
The University of the Punjab, Lahore, B.Sc in  
Geology, completed in 1969  
The University of the Punjab, Lahore, M.Sc. in  
Mineralogy and Petrology, completed in 1970  
University of Windsor, Windsor, Canada, 1977-81

Experience:

Summer 1971 Assistant Geologist with Terbala Joint Venture,  
Terbala, Pakistan

1971-73 Geologist with Sarwar Stone Industries, Lahore,  
Pakistan

Summer 1978 Geologist with J. C. Stephen Explorations,  
Vancouver, B.C.

1979-1981 Contract Geologist with Ontario Geological Survey,  
Toronto, Ontario